Acquired resistance to HSP90 inhibition in triple-negative breast cancer



Dk Nuramalina Hafizah Pg Hj Mumin

St Edmund Hall, University of Oxford

Thesis submitted for the degree of
Doctor of Philosophy

Michaelmas Term 2016

Acquired resistance to HSP90 inhibition in triple-negative breast cancer

Dk Nuramalina Hafizah Pg Hj Mumin

St Edmund Hall, University of Oxford

Thesis submitted for the degree of Doctor of Philosophy
Michaelmas Term 2016

Abstract

Heat shock protein 90 (HSP90), a conserved molecular chaperone, has become a potential molecular target for cancer therapeutics. HSP90 inhibition (HSP90i) causes inhibition of several oncogenic pathways simultaneously and leads to anti-cancer activities in multiple cancers including in triple-negative breast cancer (TNBC). TNBC is a subtype of breast cancer with poor prognosis and lack of approved targeted therapies.

Although HSP90i has shown promising initial clinical data, resistance to HSP90i can still arise in TNBC patients and its resistance mechanisms are not yet understood. In this study, using an in vitro system, we report for the first time the isolation of TNBC cells with acquired resistance to HSP90i. Proteome and whole transcriptome profiling, and a bioactive small molecule screen were performed to identify the molecular basis of resistance to HSP90i and potential therapeutic approaches to overcome acquired resistance to HSP90i in TNBC cells.

Two independent HSP90i-resistant clones were acquired through prolonged exposure of a TNBC cell line (Hs578T) to HSP90i. The clones showed significant resistance to HSP90i, notably to resorcinol-based HSP90i. The HSP90i-resistant clones also shared genomic sequence variants, suggesting a pre-existing population of resistant cells within the parental cells. We demonstrate that upregulated expression of UGT1A9, possibly due to an increased intrinsic oxidative stress, is associated with acquired resistance to resorcinol-based HSP90i in TNBC cells, and sensitivity to HSP90i can be restored with a competitive inhibitor of UGT1A9. The HSP90i-resistant clones also exhibited slower growth and upregulated IL6-mediated JAK2-STAT3 survival signalling pathway, which might contribute to the cross-resistance to chemotherapeutics and other targeted therapies seen in the clones. Finally, we demonstrate that inhibition of JAK2-STAT3 signalling pathway is able to increase the cytotoxic effects of HSP90i to TNBC cells.

We conclude that by using in vitro assays, we are able to identify potential mechanisms of acquired resistance to HSP90i in TNBC cells. We propose that expression of UGT1A9 or STAT3 might be a potential biomarker of sensitivity to HSP90i in TNBC cells. A combined inhibition of HSP90 and JAK2 might be a potential therapeutic approach for the development of effective targeted therapies in TNBC patients.

Acknowledgements

Firstly, I would like to express my deepest gratitude and appreciation to my supervisor, Dr Anderson Ryan. His constant support, encouragement, guidance, dedication and valuable advice helped me greatly to progress and accomplish my work, especially within the last year. It definitely has been a privilege for me to work with him.

I would also like to thank my previous supervisor, Dr Anthony Kong, for giving me the opportunity to study here in Oxford. I appreciate his support and advice throughout my first year, even though the lab was going through difficult times.

I would like to express my sincere gratitude to my funding body, Universiti Brunei Darussalam (Chancellor's Scholarship) and to the Government of Brunei Darussalam for sponsoring my studies, and making it possible for me to pursue my studies here.

This DPhil journey definitely has not been easy but I am very grateful to all the wonderful people that I got to know throughout my time here as they have made it an amazing experience for me. Many thanks to all members of the lab: Agata, Yanyan, Aoife, Sivan, Anika, Luiza, Neele, Fiona, Sam, John, Marcus, Yasmin and Sureyya, for all the valuable skills, advice and exciting conversations. Thank you for making it an enjoyable workplace for me. A special thanks to Agata for her help and time, especially with my thesis. Also, special thanks to my dear friends Luiza, Neele and Fiona for always being sweet, helpful and caring, as well as for the fun times in the lab and outside. I would also like to thank Sara and Willie for being a kind friend within the department.

I would like to further thank my previous lab members for their help, especially Ashwag for her valuable advice, Siti for taking care of me when I first arrived and Kate for being a great friend that shared a similar journey. I am grateful that we both made it till the end.

I am very grateful to a special someone, Erkin for always being caring, supportive and helpful. This journey has been bearable, mainly due to him. He managed to always make me happy even when I was feeling stressed or emotional, especially during the thesis writing.

I would also like to thank my good friend, Huzaifah for all the wonderful memories that we shared and for always being there for me. Many thanks to my BOSS family in Oxford, BSUnion and BSRS family for making me feel like a part of home is always here with me.

And not forgetting, I would like to thank my family in Brunei: my parents, brothers, sister-in-laws, close relatives and friends for their support, encouragement and prayers. Also, to my adorable nieces, Adeliah and Sarah, for their regular updates that cheered me up.

Special thanks to my parents for their endless support, love, care, dedication and prayers. I am very grateful that their encouragement kept me going and I would not have been able to reach this point without them. I would like to dedicate this work to them. And lastly, most importantly, I would like to praise God, the Almighty for giving me the strength, courage, opportunities and His blessings until I have made it this far.

Table of contents

1. INTRODUCTION 1
1.1. BREAST CANCER 2
1.1.1. Clinical classification 2
1.1.2. Pathological classification 4
1.1.3. Gene expression classification 4
1.1.4. Immunohistochemical classification 6
1.2. THERAPEUTIC TARGETS FOR TNBC 8
1.2.1. Poly(ADP-ribose) polymerase (PARP) 10
1.2.2. Phosphoinositide 3-kinase (PI3K) 11
1.2.3. Epidermal growth factor receptor (EGFR) 12
1.2.4. Challenges in targeting TNBC 13
1.3. HEAT SHOCK PROTEIN 90 14
1.3.1. HSP90 structure and chaperone cycle 15
1.3.2. HSP90 as a therapeutic target 18
1.3.3. Development of HSP90 inhibitors 19
1.3.4. HSP90 inhibitors in TNBC 22
1.4. AIMS AND OBJECTIVES 24
2. MATERIALS AND METHODS 25
2.1. BUFFERS AND SOLUTIONS 26
2.2. CELL CULTURE 27
2.2.1. Maintenance of human cell lines 27
2.2.2. Routine passaging and cell seeding 28
2.2.3. Cryopreservation and thawing of cells 28
2.2.4. Mycoplasma testing 29
2.3. DRUG TREATMENT 30
2.4. GENERATION OF HSP90I-RESISTANT CLONES 30
2.5. CELL VIABILITY ASSAY 30
2.6. PREPARATION OF CELL PROTEIN LYSATES 31
2.7. WESTERN BLOTTING ANALYSIS 32
2.8. APOPTOSIS ASSAY 34
2.9. CELL CYCLE ANALYSIS 34
2.10. COLONY FORMATION ASSAY 35
2.11. DNA ISOLATION AND PURIFICATION 36

2.12. POLQ GENE SEQUENCING 36
2.13. SIRNA TRANSFECTION 37
2.14. PHOSPHO-RTK ARRAY 37
2.15. RNA ISOLATION AND PURIFICATION 39
2.16. RNA SEQUENCING (RNA-SEQ) 39
2.17. MASS SPECTROMETRY (MS) 41
2.18. BIOACTIVE SMALL MOLECULE SCREEN 42
2.18.1. Selleckchem Inhibitor Screening Library 42
2.18.2. Drug screen analysis 43
2.19. PICOGREEN® DOUBLE-STRANDED DNA ASSAY 45
2.20. JAK-STAT PATHWAY ARRAY 45
2.21. ENZYME-LINKED IMMUNOSORBENT ASSAY (ELISA) 47
2.22. STATISTICAL ANALYSIS 48

3. ESTABLISHMENT OF AN IN VITRO MODEL TO STUDY RESISTANCE MECHANISMS TO HSP90I 49
3.1. INTRODUCTION 50
3.2. THE EFFECTS OF HSP90I IN TNBC CELLS 52
3.2.1. Inhibition of cell viability 52
3.2.2. Downregulation of HSP90 client proteins 53
3.2.3. Induction of apoptosis 55
3.3. GENERATION OF HSP90I-RESISTANT CLONES 57
3.4. CHARACTERISATION OF HSP90I-RESISTANT CLONES 59
3.4.1. The effect of HSP90i on HSP90 client proteins 59
3.4.2. The effect of HSP90i on cell cycle in HSP90i-resistant clones 61
3.4.3. The effect of HSP90i on colony formation in HSP90i-resistant clones 61
3.4.4. Sequence variants in HSP90i-resistant clones 64
3.5. THE RELATIONSHIP BETWEEN HSP70 EXPRESSION AND THE SENSITIVITY OF TNBC CELLS TO HSP90I 65
3.5.1. HSP70: A pharmacodynamic marker of HSP90i 68
3.6. DISCUSSION 70

4. BIOLOGICAL BASIS OF RESISTANCE TO HSP90I 73
4.1. INTRODUCTION 74
4.2. PROTEOME PROFILING OF PRTK IN PARENTAL HS578T CELLS AND HSP90I-RESISTANT CLONES 76
4.3. WHOLE TRANSCRIPTOME PROFILING IN PARENTAL HS578T CELLS AND HSP90I-RESISTANT CLONES 80

4.3.1. Differential gene expression in parental Hs578T cells and HSP90i-resistant clones after ganetespib treatment *81*

4.3.2. Differential gene expression in Hs578T cells associated with acquired resistance to HSP90i *85*

4.4. UGT1A EXPRESSION IN HSP90I-RESISTANT CLONES 86

4.4.1. Involvement of UGT1A9 in response to ganetespib *88*

4.4.2. The effects of a competitive inhibitor of UGT1A9 on HSP90i activity *90*

4.5. AKR1C1 EXPRESSION IN HSP90I-RESISTANT CLONES 93

4.5.1. Increased levels of oxidative stress in HSP90i-resistant clones *96*

4.5.2. Pathway enrichment analysis of differential gene expression *98*

4.6. DISCUSSION 101

5. OVERCOMING ACQUIRED RESISTANCE TO HSP90I 105

5.1. INTRODUCTION 106

5.2. BIOACTIVE SMALL MOLECULE SCREEN 107

5.2.1. Identification of differentially active compounds in HSP90i-resistant clone CR3 compared with parental Hs578T cells *108*

5.2.2. Identification of differentially active compounds in HSP90i-resistant clone CR3 with the presence of ganetespib *111*

5.2.3. Validation of positive hits from bioactive small molecule screen *114*

5.3. JAK2-STAT3 SIGNALLING PATHWAY IN HSP90I-RESISTANT CLONES 119

5.3.1. Combined inhibition of JAK2 and HSP90 in HSP90i-resistant clones *121*

5.3.2. Gene expression profiling of JAK-STAT signalling pathways *123*

5.3.3. Autocrine-mediated JAK2-STAT3 signalling in HSP90i-resistant clones *125*

5.3.4. Correlation between pSTAT3 expression and sensitivity to HSP90i *126*

5.4. BIOMARKERS OF INTRINSIC AND ACQUIRED RESISTANCE TO HSP90I IN TNBC CELLS 128

5.4.1. The relationship of potential biomarkers to prognosis in breast cancer patients *131*

5.5. DISCUSSION 133

6. FINAL DISCUSSION AND CONCLUSION 137

6.1. FINAL DISCUSSION 138

6.2. LIMITATIONS OF STUDY 146

6.3. CONCLUSION 147

7. REFERENCES 149

8. APPENDIX 169

List of figures

Figure 1.1: Overall survival in breast cancer patients....5
Figure 1.2: Mutational profile of breast cancer molecular subtypes 9
Figure 1.3: HSP90 client proteins and the hallmarks of cancer....15
Figure 1.4: The dynamic HSP90 chaperone cycle.....17
Figure 2.1: Schematic of RNA-seq and analysis pipeline 40
Figure 3.1: Differential sensitivity to ganetespib in TNBC cell lines....52
Figure 3.2: The effect of ganetespib treatment on EGFR signalling pathways in TNBC cells 54
Figure 3.3: Expression of HSP90 oncogenic client protein (EGFR) in TNBC cells....55
Figure 3.4: The effect of ganetespib treatment on apoptosis in TNBC cells....56
Figure 3.5: Generation of HSP90i-resistant Hs578T clones....58
Figure 3.6: Cross-resistance to HSP90i in HSP90i-resistant clones....58
Figure 3.7 The effect of ganetespib treatment on EGFR signalling in HSP90i-resistant clones 60
Figure 3.8: G2/M cell cycle arrest seen only in parental Hs578T 62
Figure 3.9: Inhibition of colony formation after HSP90i in TNBC cells 63
Figure 3.10: Verification of stop-gain variant on the POLQ gene in HSP90i-resistant clones by Sanger DNA sequencing....64
Figure 3.11: Correlation of HSP70 expression with ganetespib sensitivity (IC_{50}) 66
Figure 3.12: HSP70 knockdown by siRNA in HCC1143 cells 67
Figure 3.13: Sensitivity to ganetespib in HCC1143 cells after siRNA knockdown of HSP70 protein expression 67
Figure 3.14 Sensitivity of TNBC cells to HSP70 inhibitor VER-15508 68
Figure 3.15 HSP70 expression as a pharmacodynamic marker of HSP90i....69
Figure 4.1: Profiling of pRTKs in Hs578T and HSP90i-resistant clones....77
Figure 4.2: Expression of EGFR and MET in Hs578T cells and HSP90i-resistant clones 78
Figure 4.3: Sensitivity of HSP90i-resistant clone CR3 to EGFR and MET inhibitors....79
Figure 4.4: Differential expression of genes associated with HSP90 and cell cycle upon ganetespib treatment 82
Figure 4.5: Overlap of significantly upregulated and downregulated genes in HSP90i-resistant clones CR2 and CR3....86
Figure 4.6: Upregulated expression of UGT1A family members in HSP90i-resistant clones 87
Figure 4.7 Combination effect of propofol on the sensitivity to ganetespib 89
Figure 4.8: The effect of propofol on the cell viability of Hs578T cells and HSP90i-resistant clones 90
Figure 4.9:The effects of propofol or/and ganetespib treatment in Hs578T, CR2 and CR3 ..91

Figure 4.10: Sensitivity to other classes of HSP90 inhibitors 92

Figure 4.11: Identification of an upregulated protein band at 37 kDa in HSP90i-resistant clones 94

Figure 4.12: Upregulated gene expression of AKR1C family members in HSP90i-resistant clones 95

Figure 4.13: Significantly upregulated expression of ARE-dependent genes in Hs578T cells and HSP90i-resistant clones 97

Figure 4.14: NQO1 and pATM expression in Hs578T cells and HSP90i-resistant clones 98

Figure 4.15: Activation of antioxidant defence system due to oxidative stress.....100

Figure 5.1: Schematic of the 96-well based bioactive small molecule screen.....107

Figure 5.2: Correlation between duplicate samples and independent runs in the screen 108

Figure 5.3: Z-scores of sensitivity to compounds comparing parental Hs578T cells and HSP90i-resistant clone CR3 109

Figure 5.4: Growth curves of Hs578T cells and HSP90i-resistant clone CR3 upon ganetespib treatment 111

Figure 5.5: Z-scores of sensitivity to compounds comparing HSP90i-resistant clone CR3 in the absence and presence of ganetespib.....112

Figure 5.6: Dose-response of compounds from the screen that were selectively cytotoxic in HSP90i-resistant clone CR3 115

Figure 5.7: The effect of Aurora Kinase inhibitors in combination with ganetespib in HSP90i-resistant clone CR3 116

Figure 5.8: The effect of LY2784544 in combination with ganetespib in HSP90i-resistant clone CR2.....117

Figure 5.9: The effect of AZD1480 in combination with ganetespib in HSP90i-resistant clones CR2 and CR3 118

Figure 5.10: Inhibition of STAT3 activity in Hs578T cells and HSP90i-resistant clones ...120

Figure 5.11: Induction of apoptosis in Hs578T cells and HSP90i-resistant clones after JAK2 and HSP90 inhibition.....121

Figure 5.12: The effect of LY2784544 on sensitivity to ganetespib 122

Figure 5.13: Expression of genes involved in JAK-STAT signalling pathways in HSP90i-resistant clone CR3 123

Figure 5.14: Differential expression of genes involved in JAK-STAT signaling pathways using RNA-seq and JAK-STAT array analysis. 124

Figure 5.15: IL6 expression in Hs578T cells and HSP90i-resistant clones CR2 and CR3 ..125

Figure 5.16: Correlation of pSTAT3 expression with ganetespib sensitivity (IC_{50}) 127

Figure 5.17: Expression of NQO1 and MCL1 in Hs578T cells and HSP90i-resistant clones 129

Figure 5.18: Correlation of NQO1 and MCL1 expression with ganetespib sensitivity.....130

Figure 5.19: UGT1A9, STAT3, NQO1 and MCL1 expression and prognosis in breast cancer 132

Figure 6.1: Proposed mechanisms of resistance to HSP90i in TNBC cells.....143

List of tables

Table 1.1: Breast cancer stages 2

Table 1.2: Choice of treatment for breast cancer patients 3

Table 1.3: Treatment option for breast cancer subtypes 6

Table 1.4: HSP90 inhibitors 19

Table 1.5: Synthetic HSP90 inhibitors in clinical trials 21

Table 2.1: Buffers and solutions prepared in this study 26

Table 2.2: Cell lines used in this study 27

Table 2.3: List of antibodies used for western blotting analysis 33

Table 2.4: Proteins detectable with Proteome Profiler^{TM} human phosho-RTK array kit 38

Table 2.5: Expression of genes detectable with TaqMan® Array Human JAK-STAT pathway 47

Table 3.1: Sensitivity to ganetespib in TNBC cell lines 53

Table 3.2: Sensitivity to HSP90i in parental Hs578T cells and HSP90i-resistant clones CR2 and CR3 59

Table 3.3: Sensitivity to ganetespib in HCC1143 cells after HSP70 siRNA treatment 68

Table 4.1: Sensitivity of Hs578T and HSP90i-resistant clone CR3 to erlotinib or gefitinib 79

Table 4.2: Differentially expressed genes in ganetespib-treated cells compared to DMSO-treated cells 81

Table 4.3 The top 20 most significantly enriched pathways associated with downregulation of gene expression in ganetespib-treated Hs578T cells 84

Table 4.4: Differentially expressed genes in HSP90i-resistant clones compared to Hs578T cells 85

Table 4.5: Differential gene expression of UGT1A family in Hs578T (30 nM ganetespib), CR2 and CR3 compared to DMSO-treated Hs578T 88

Table 4.6: Sensitivity to ganetespib alone or in combination with propofol 89

Table 4.7: The identity of the most prevalent proteins in the 37 kDa protein band in HSP90i-resistant clone CR3 when compared to Hs578T cells by MS 95

Table 4.8 The top 20 most significantly enriched pathways seen in HSP90i-resistant clones 99

Table 5.1: Compounds that were selectively cytotoxic to parental Hs578T cells compared with HSP90i-resistant clone CR3 110

Table 5.2: Compounds that were selectively cytotoxic to HSP90i-resistant clone CR3 in the absence of ganetespib 113

Table 5.3: Compounds that were selectively cytotoxic to HSP90i-resistant clone CR3 in the presence of ganetespib 113

Table 5.4: Sensitivity to compounds from the screen that were selectively cytotoxic to HSP90i-resistant clone CR3 114

Table 5.5: Sensitivity to LY2784544 in combination with 10 nM ganetespib 117

Table 5.6: Cytotoxicity of ganetespib alone and in combination with 1 μM LY2784544 122

List of supplementary tables

Supplementary Table 1: 326 compound bioactive small molecule library.....169

Supplementary Table 2: List of variants seen in both HSP90i-resistant clones 176

Supplementary Table 3: Differentially expressed genes after ganetespib treatment in Hs578T cells 179

Supplementary Table 4: The top 100 significantly upregulated genes in both HSP90i-resistant clones compared to Hs578T cells.....181

Supplementary Table 5: The top 100 significantly downregulated genes in both HSP90i-resistant clones compared to Hs578T cells.....185

Supplementary Table 6: Differential gene expression of AKR1C family members in Hs578T (30 nM ganetespib), CR2 and CR3 cells compared to DMSO-treated Hs578T cells.....188

Supplementary Table 7: Differential expression of ARE genes in Hs578T (30 nM ganetespib), CR2 and CR3 cells compared to DMSO-treated Hs578T cells 189

Supplementary Table 8: Differential gene expression of genes associated to JAK-STAT signaling pathway in HSP90i-resistant clone CR3 compared to DMSO-treated Hs578T cells 192

List of supplementary figures

Supplementary Figure 1: Sensitivity to ganetespib in HSP90i-resistant clone CR3 178

Supplementary Figure 2: ROS levels in Hs578T cells and HSP90i-resistant clones CR2 and CR3 191

Supplementary Figure 3: The effect of ganetespib treatment on JAK2-STAT3 signalling pathway in TNBC cells.....193

Supplementary Figure 4: Expression of UGT1A9 in TNBC cells 193

Abbreviations

AHA1	activator of HSP90 ATPase homologue 1
AKR1C	Aldo-keto reductase member C family
ARE	antioxidant-response element
ATCC	American type culture collection
ATM	Ataxia-Telangiectasia mutated
BL	basal-like
BRCA1	breast cancer susceptibility gene 1
BRCA2	breast cancer susceptibility gene 2
BrdU	Bromodeoxyuridine
CDK	cyclin-dependent kinase
Ct	threshold cycle
CTD	carboxyl-terminal domain
CYP40	cyclophilin 40
DMEM	Dulbecco's modified Eagle medium
DMSO	dimethyl sulfoxide
DSB	double-strand break
ECL	enhanced chemiluminescence
EGFR	epidermal growth factor receptor
ELISA	enzyme-linked immunosorbent assay
ER	oestrogen receptor
F.I	fluorescence intensity
FBS	foetal bovine serum
FC	fold change
GRP94	glucose regulated protein 94 (GRP94)
HER2	Human epidermal growth factor 2 receptor
HOP	HSP70 and HSP90-organizing protein
hr	hour(s)
HR	homologous recombination repair
HRP	horseradish peroxide
HSF1	heat shock transcription factor 1
HSP	heat shock protein
HSP90	heat shock protein 90
HSP90i	HSP90 inhibition/inhibitor(s)
IHC	immunohistochemistry
IM	immunomodulatory
ISH	in situ hybridization

JAK2	Janus kinase 2
JAK2i	JAK2 inhibition/inhibitor(s)
LAR	luminal androgen receptor
M	mesenchymal
MD	middle domain
MET	hepatocyte growth factor receptor
min	minute(s)
MS	mass spectrometry
MSL	mesenchymal stem-like
MTOR	mammalian target of rapamycin
NGS	next-generation sequencing
NQO1	NAD(P)H Quinone Dehydrogenase 1
NRF2	nuclear factor E2-related factor 2
NTD	amino-terminal domain
OGT	Oxford Gene Technology
PARP	poly(ADP-ribose) polymerase
PBS	phosphate buffered saline
PCR	polymerase chain reaction
PI	propidium iodide
PI3K	phosphoinositide 3-kinase
PR	progesterone receptor
pRTK	phosho-RTK
RNA-seq	RNA sequencing
ROS	reactive oxygen species
RPMI	Roswell Park Memorial Institute medium 1640
RT-PCR	reverse transcription PCR
RTK	receptor tyrosine kinase
siRNA	small interfering RNA
SSB	single-strand break
STAT3	signal transducer and activator of transcription 3
TBS	tris-buffered saline
TNBC	triple-negative breast cancer
TRAP	tumour necrosis factor type 1 receptor-associated protein
TPR	tetratricopeptide repeat
UGT1A	UDP Glucuronosyltransferase Family 1 Member A

1. Introduction

1.1. Breast cancer

Breast cancer is the second most common cancer worldwide and most common cancer in women with 1.67 million new cases reported in 2012 (Ferlay et al., 2015). It accounts for 12.9% of all cancer cases and 25% of cancer in women. There are 522,000 deaths per year from breast cancer globally, making it the leading cause of women cancer-related death in less developed countries and second cause in developed countries (Ferlay et al., 2015). Breast cancer is a heterogeneous disease with several classifications based on clinical, pathological, gene expression and immunohistochemical features (Viale, 2012).

1.1.1. Clinical classification

In the clinic, breast cancer is conventionally classified as early, locally advanced or metastatic disease, based on tumour size, extent of cancer spread to lymph nodes, and metastasis **(Table 1.1)**. Breast cancer staging is used as the basis for predicting survival and in the choice of initial treatment (surgery, chemotherapy and/or radiotherapy) in patients **(Table 1.2)** (Ludwig and Weinstein, 2005)(Cancer Research UK, 2014).

Table 1.1: Breast cancer stages

Stage	Description	5-year survival rate[1]
Early (Stage I or II)	Tumour size ≤ 5 cm No sign of cancer spread	99%
Locally advanced (Stage III)	Tumour size > 5 cm Cancer spreads to lymph nodes	60%
Metastatic (Stage IV)	Cancer has metastasised to other parts of the body	15%

Obtained from Cancer Research UK (cancerreasearchuk.org, Accessed December 2016) and (Carlson et al., 2011)
[1]Survival rates are from women diagnosed with breast cancer between 2002 and 2006 in England

Breast-conserving surgery is the standard treatment for early stage breast cancer patients with a curative intent. In locally advanced breast cancer patients, neoadjuvant chemotherapy is considered in patients with large tumours. After the tumour has reached an operable size, surgery can be performed to treat the patient. Palliative radiotherapy is considered in locally advanced patients with non-operable tumours after neoadjuvant chemotherapy to maximise local control (Veronesi et al., 2005, Carlson et al., 2011).

Treatment option after surgery for early and locally advanced breast cancer patients includes radiotherapy and/or adjuvant systemic therapy (chemotherapy, endocrine therapy or targeted therapy) (Carlson et al., 2011). This is to reduce the risk of cancer recurrence and increase overall survival in breast cancer patients. The decision for selecting the appropriate adjuvant therapy depends on several prognostic and predictive factors, including clinical and pathological characteristics of tumours, patient age, surgery method, presence of metastasis and biomarker status (Carlson et al., 2011). Treatment for metastatic breast cancer patients also involves radiotherapy, chemotherapy, endocrine therapy and/or targeted therapy. However, these therapies are not generally used with curative intent but to prolong survival and improve quality of life in metastatic breast cancer patients (Carlson et al., 2011).

Table 1.2: Choice of treatment for breast cancer patients

Stage	Standard treatment
Early	Surgery, radiotherapy and/or adjuvant systemic therapy (curative)
Locally advanced	Neoadjuvant chemotherapy, surgery followed by adjuvant therapy (curative) For non-operable tumour, neoadjuvant chemotherapy and radiotherapy (palliative)
Metastatic	Chemotherapy, radiotherapy and/or systemic therapy (palliative)

Adapted from (Carlson et al., 2011).

1.1.2. Pathological classification

Pathological classification is performed on breast cancer to determine the tumour type and grade (Ellis et al., 1992, Elston and Ellis, 2002). The majority of breast cancers (80%) are classified as invasive ductal carcinomas not otherwise specified (IDC-NOS) and the remaining cases include lobular, tubular or medullary carcinomas (<15%) (Weigelt and Reis-Filho, 2009). The histological tumour grade can be determined from the level of differentiation (tubule formation and nuclear pleomorphism) and the proliferative activity (mitotic index) of the tumour (Rakha et al., 2008). Grade I, II and III are considered well-differentiated, moderately differentiated and poorly differentiated tumours respectively. The tumour grade provides useful prognostic factors in breast cancer patients, where higher grade is associated with worst prognosis (relapse-free and overall survival) (Rakha et al., 2008). Since high-grade tumours have a higher risk of recurrence and death, a prompt adjuvant chemotherapy is recommended. However, breast cancer patients with low-grade tumour could be offered with endocrine therapy instead of chemotherapy as it is less toxic for the patients (Rakha et al., 2008).

1.1.3. Gene expression classification

Although it is still an emerging practice in the clinic, gene expression profiling of tumours using microarrays (Oncotype DX assay) can be determined in breast cancer patients (Carlson and Roth, 2013). The Oncotype DX assay evaluates the expression levels of 21 genes, which are associated with proliferation, invasion and oestrogen signalling. This provides useful prognostic and predictive information, where the breast cancer patients can be classified as high, intermediate or low-risk for recurrence and appropriate adjuvant systemic therapy can be recommended to the patients (either endocrine therapy and/or chemotherapy) (Carlson and Roth, 2013).

Global gene expression profiling can also be performed on breast cancer tumours through clustering analysis. Breast cancer tumours can be classified into distinct subtypes: luminal (A and B), basal-like, human epidermal growth factor 2 receptor (HER2) enriched and normal-like subtypes (Perou et al., 2000, Sorlie et al., 2001, Parker et al., 2009). The luminal subtype is characterised by high expression of genes expressed in breast luminal cells (luminal cell keratins 8/18) while the basal-like subtype is characterised based on high gene expression of keratins 5/6 and 17, laminin and fatty acid binding protein 7 (Perou et al., 2000, Sorlie et al., 2001).

The HER2-enriched subtype is characterised by high expression of several genes in the HER2 amplicon while the normal-like subtype is characterised by the expression of known genes of adipose tissue and basal epithelial cells (Perou et al., 2000, Sorlie et al., 2001). These breast tumour subtypes are biologically-distinct disease and associated with different clinical outcome, with basal and HER2-enriched subtypes having the worst clinical outcome compared to the luminal subtypes **(Figure 1.1)** (Sorlie et al., 2003, Sorlie et al., 2001).

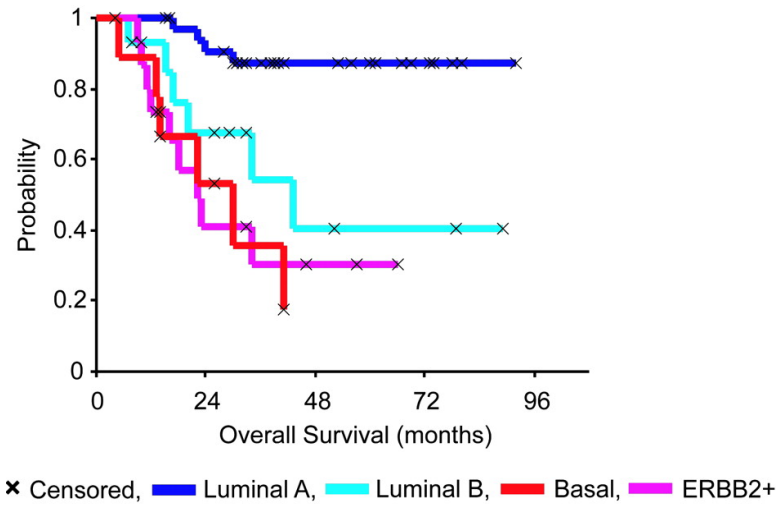


Figure 1.1: Overall survival in breast cancer patients

Kaplan-Meier analysis of overall survival for breast cancer patients based on their molecular subtypes. Luminal A, luminal B, basal and ERBB2+ (HER2+) subtypes are shown.

Adapted from (Sorlie et al., 2003). Copyright (2003) National Academy of Sciences.

1.1.4. Immunohistochemical classification

In the clinic, systemic therapy for early and advanced breast cancer patients still largely depends on the assessment of three biomarkers: the expression of oestrogen receptor (ER) and progesterone receptor (PR) by immunohistochemistry (IHC), and expression of human epidermal growth factor 2 receptor (HER2) by IHC and/or in situ hybridization (ISH) **(Table 1.3)** (Hammond et al., 2010, Wolff et al., 2013, Bianchini et al., 2016).

Table 1.3: Treatment option for breast cancer subtypes

Tumour subtype	Expression	Incidence (%)	Treatment option
ER-positive	ER and/or PR positive	75	Chemotherapy and/or endocrine therapy (tamoxifen)
HER2-positive	HER2 positive	15	Chemotherapy and/or HER2-targeted therapy (trastuzumab)
TNBC	ER, PR and HER2 negative	10	Chemotherapy

About 75% of all breast cancers are ER-positive, where tumours express ER and/or PR. The primary treatment option for ER-positive tumours is endocrine therapy, either through inhibiting oestrogen synthesis (aromatase inhibitors) or ER functions (tamoxifen) (Zhang et al., 2014). Increased ER expression in ER-positive tumours is associated with better response to endocrine therapy and longer survival in breast cancer patients (Elledge et al., 2000). Adjuvant tamoxifen (for 5 years) is greatly effective for early ER-positive breast cancer patients as it reduces the risk of recurrence and increases the overall survival for patients (Early Breast Cancer Trialists' Collaborative et al., 2011). The addition of tamoxifen to adjuvant chemotherapy also improves the overall survival for early ER-positive breast cancer patients compared to chemotherapy alone (Early Breast Cancer Trialists' Collaborative, 2005). There is also an approved targeted therapy available for advanced breast cancer patients with ER-positive and HER2-negative tumours. It is a selective cyclin-dependent kinase (CDK) 4 and 6 inhibitor (palbociclib), which inhibits the CDK-mediated signalling involved in dysregulated cell division observed in cancer (O'Leary et al., 2016).

The combination treatment of CDK4/6 inhibitor (palbociclib) and aromatase inhibitor (letrozole) significantly improves the clinical outcome of patients with advanced ER-positive and HER2-negative breast cancer tumours (Finn et al., 2015).

About 15% of breast cancers are HER2-positive, where tumours have HER2 gene amplification and/or protein overexpression. HER2-positive tumours are associated with more aggressive disease and worse prognosis in breast cancer patients (Arteaga et al., 2012, Slamon et al., 1987). Treatment with trastuzumab, a monoclonal antibody against HER2, is recommended for patients with HER2-positive tumours. Trastuzumab treatment significantly improves the clinical outcome (disease-free survival and overall survival) for patients with HER2-positive tumours (Perez et al., 2011, Romond et al., 2005). The addition of trastuzumab after neoadjuvant chemotherapy also improves the overall survival for patients with HER2-positive tumours (Marty et al., 2005, Buzdar et al., 2005).

The third breast cancer subtype is triple negative breast cancer (TNBC), which accounts for about 10% of all breast cancer cases. TNBC is associated with younger age (<50) and is more common in African-American women (Reis-Filho and Tutt, 2008, Morris et al., 2007, Rakha et al., 2007). TNBC is defined by the absence of ER and PR expression, as well as a lack of HER2 gene amplification or protein overexpression at diagnosis. The tumours are predominantly IDC-NOS (80%), larger in size, more aggressive, of higher grade and have greater lymph node involvement compared to other subtypes (Dent et al., 2007). TNBC have higher rates of distant disease recurrence and death within 5 years of diagnosis compared to other subtypes (Dent et al., 2007).

Chemotherapy is the only systemic treatment option for TNBC, with patients having significantly higher pathological complete response rate (pCR) in response to neoadjuvant chemotherapy compared to other subtypes. However, TNBC patients have lower rates of progression-free survival and overall survival within the first three years compared to other

subtypes. TNBC patients with residual disease after neoadjuvant chemotherapy have a significantly worse overall survival compared to other subtypes displaying residual disease (Liedtke et al., 2008).

1.2. Therapeutic targets for TNBC

Due to the lack of approved targeted therapies and poor prognosis in TNBC patients, there is a strong need to identify potential molecular targets for TNBC treatment. Molecular gene profiling of breast cancer tumours is a powerful approach to identify such targets as it allows identification of mutations and signalling pathways enriched in TNBC.

About 51-73% of TNBC are basal-like, and 90% of basal-like breast cancer are TNBC (Bianchini et al., 2016, Cheang et al., 2015). Basal-like tumours commonly have *TP53* mutations (80% of cases, mostly loss-of-function) and *PIK3CA* mutations (9% of cases, including activating mutations) **(Figure 1.2)**. There are also mutations in the breast cancer susceptibility gene 1 and 2 (*BRCA1* and *BRCA2)* that lead to loss-of-function in 20% of basal-like tumours (Cancer Genome Atlas, 2012, Foulkes et al., 2003). The common mutations in TNBC tumours are also *TP53* (43-62%) and *PI3KCA* (10.2%) (Shah et al., 2012). Furthermore, about 20% of TNBC tumours have *BRCA1* or *BRCA2* mutations (Gonzalez-Angulo et al., 2011).

Amplification of *KRAS* (32%), *BRAF* (30%) and *EGFR* (23%) is commonly observed in basal-like tumours, as well as increased PI3K pathway activity (Cancer Genome Atlas, 2012). EGFR overexpression is significantly associated with poor prognosis in basal-like tumours (Nielsen et al., 2004). Amplification of *KRAS*, *BRAF*, *EGFR* and *MET* (1-40%) is also observed in TNBC tumours. In addition, TNBC tumours can display enriched pathway activation of PI3K, EGFR and growth hormone signalling (Bianchini et al., 2016, Shah et al., 2012). These known genetic aberrations and enriched pathways have led to several

therapeutic targets in current clinical development for TNBC patients, including compounds targeting PARP, PI3K and EGFR (Bianchini et al., 2016). Despite this, there remains a demand for novel targets in TNBC for clinical development, ultimately leading to improved outcomes for TNBC patients.

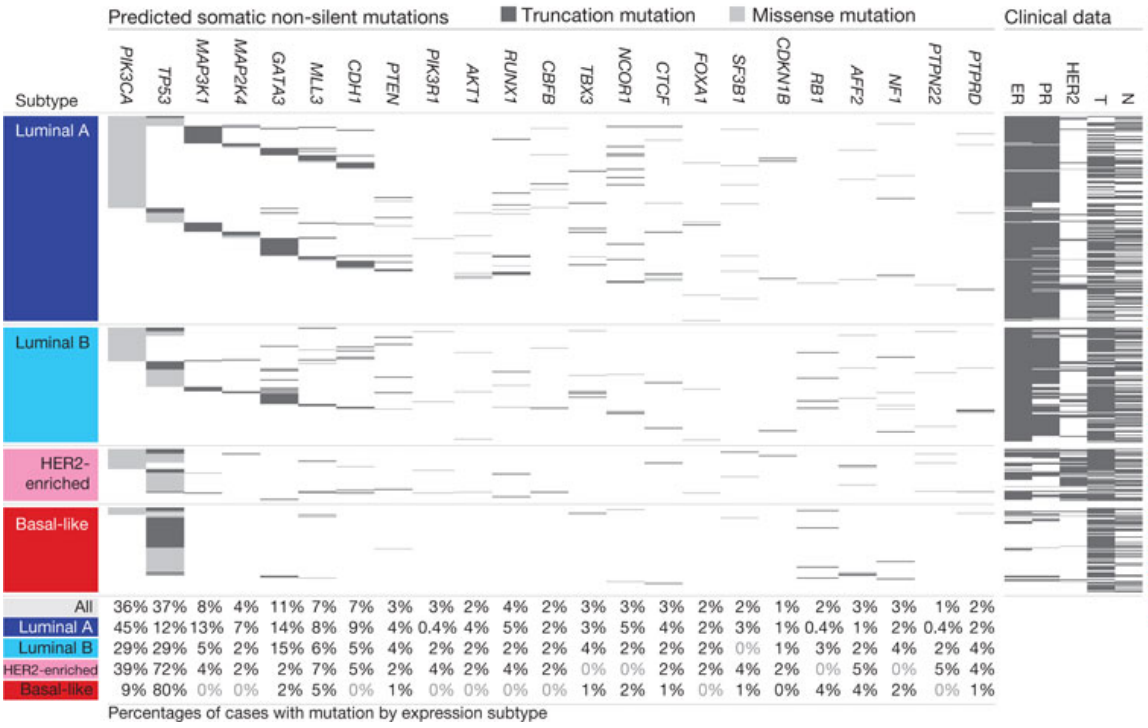


Figure 1.2: Mutational profile of breast cancer molecular subtypes

Tumour samples from breast cancer patients were grouped into intrinsic molecular subtypes based on gene expression profiles. The left-hand panel shows the molecular subtype: luminal A (blue), luminal B (light blue), HER2-enriched (pink) and basal-like (red). The middle panel represents the mutated genes identified from whole-exome sequencing, and percentage of cases with mutation in the gene. The right-hand panel shows the clinical features based on ER, PR and HER2 expression (dark grey represents positive and white represents negative).

(Adapted from (Cancer Genome Atlas, 2012))

1.2.1. Poly(ADP-ribose) polymerase (PARP)

Since 20 % of TNBC patients have *BRCA1* and *BRCA2* mutations, these patients could potentially benefit from poly(ADP-ribose) polymerase (PARP) inhibitor therapy (Comen and Robson, 2010, Gonzalez-Angulo et al., 2011). BRCA1- and BRCA2- mutant cancer cells (breast and ovarian) were shown to be selectively sensitive to PARP inhibitors (Bryant et al., 2005, Farmer et al., 2005). PARP is involved in the detection of DNA single-strand breaks (SSBs) and activation of the DNA damage repair pathway, while BRCA1 and BRCA2 are involved in homologous recombination repair (HR) of DNA double-strand breaks (DSBs).

Endogenous DNA damage occurs in every cell in the body. For example, in every cell of the body, base hydrolysis or damage by endogenous reactive oxygen species (ROS) are estimated to induce more than 10,000 base lesions per day, which are then repaired by highly specialised base-excision repair processes (Lindahl, 1993, De Bont and van Larebeke, 2004). Since PARP plays a key role in the repair of base damage in DNA, PARP inhibition results in an increased number of DNA SSBs at the DNA replication fork. This leads to stalled replication forks and the development of replication-fork associated DNA DSBs. DNA replication associated DSBs are repaired predominately by HR. Since BRCA-mutant cells are unable to perform HR repair, treatment with PARP inhibitors induces high levels of DNA replication fork collapse and subsequent cell death (Helleday, 2011, Lord and Ashworth, 2016).

There are several PARP inhibitors in clinical trials for BRCA-mutant cancer patients. Olaparib, a PARP inhibitor, showed evidence of clinical benefit with overall tumour response rates of 41% and 33% in patients with BRCA-mutant advanced breast cancer and ovarian, respectively (Tutt et al., 2010, Audeh et al., 2010). Olaparib became an FDA and

EU approved drug in 2014 for the treatment of BRCA-mutant advanced ovarian cancer (Kim et al., 2015).

In TNBC, another clinical trial (NCT00679783) showed no confirmed objective responses in BRCA-mutant advanced TNBC patients while other studies have shown evidence of clinical benefit (Fong et al., 2009, Gelmon et al., 2011). Olaparib and other PARP inhibitors such as veliparib and rucaparib are still in clinical trials for BRCA-mutant advanced TNBC patients both as monotherapies and in combination with other therapies (Livraghi and Garber, 2015). One of the challenges that can arise with PARP inhibitors is the presence of clinical resistance in BRCA-mutant tumours. Potential mechanisms of resistance to PARP inhibitors are through the restoration of HR, increased drug efflux or re-activation of the BRCA gene by secondary mutations (Barber et al., 2013, Lord and Ashworth, 2013).

1.2.2. Phosphoinositide 3-kinase (PI3K)

Phosphoinositide 3-kinase (PI3K) is a lipid kinase consisting of a catalytic subunit (p110) and regulatory subunit (p85); which is involved in the regulation of cell proliferation, survival and migration. Activation of PI3K downstream signalling pathways is mediated through AKT and mammalian target of rapamycin (MTOR) (Gordon and Banerji, 2013). The gene encoding the catalytic subunit of PI3K (*PI3KCA)* is frequently mutated (10.2%) and PI3K signalling pathway is highly activated in TNBC tumours (Shah et al., 2012). Hyperactivation of AKT or MTOR signalling is associated with poor prognosis in TNBC patients (Kalimutho et al., 2015).

There are several PI3K, AKT and MTOR inhibitors under investigation in clinical trials for TNBC patients, including BKM120 (a pan PI3K inhibitor), MK2206 (an allosteric AKT) and everolimus (an MTOR inhibitor) (clinicaltrials.gov). One TNBC patient demonstrated a partial response with BKM120 (Bendell et al., 2012). However, PI3K pathway inhibitors as

single agents have shown limited efficacy in several clinical studies, probably due to the presence of feedback pathway activation and crosstalk with other signalling pathways (Fruman and Rommel, 2014).

1.2.3. Epidermal growth factor receptor (EGFR)

Epidermal growth factor receptor (EGFR) is a member of the epidermal growth factor receptor family (ERBB/HER), which consists of four receptor tyrosine kinases (RTK): EGFR, HER2 (ERBB2), HER3 (ERBB3) and HER4 (ERBB4) (Olayioye et al., 2000). Binding of specific ligands to the extracellular domain of HER receptors causes receptor dimerization (e.g. EGFR:EGFR) and heterodimerisation (e.g. HER2:HER3) and subsequent activation of the tyrosine kinase domain located at intracellular carboxy-terminal end of the RTK.

After receptor activation, the kinase activity autophosphorylates and transphosphorylates specific tyrosine residues on the intracellular domain of the RTK, which then provide docking sites for adaptor proteins, kinases and phosphatases. These events initiate intracellular signalling cascades, including two key EGFR signalling pathways: PI3K-AKT and RAS-MAPK pathways (Yarden and Sliwkowski, 2001, Baselga and Swain, 2009). The RAS-MAPK pathway is involved primarily in the regulation of cell proliferation and migration while the activation of PI3K-AKT pathway plays a major role in promoting cell survival and growth, and together both pathways act to drive oncogenesis (Vivanco and Sawyers, 2002, Baselga and Swain, 2009).

Since amplified *EGFR* and enriched EGFR signalling pathway are observed in TNBC, TNBC patients might benefit from EGFR inhibitor therapy (Shah et al., 2012). There are already FDA approved inhibitors of EGFR for other cancers, including the small molecules erlotinib (lung cancer and pancreatic cancer), gefitinib (lung cancer) and lapatinib (HER2-

positive breast cancer), and the antibodies cetuximab (colorectal cancer and head/neck cancer) and panitumumab (colorectal cancer) (Grandis and Sok, 2004, Yewale et al., 2013). These compounds have also been tested in several clinical trials in metastatic breast cancer patients including in TNBC. However, they showed limited clinical activity or improvements in patient outcomes (Dickler et al., 2008, von Minckwitz et al., 2005, Carey et al., 2012). There was only minor inhibition of EGFR downstream signalling after cetuximab treatment in TNBC tumours, suggesting that alternative pathway activation might cause resistance to EGFR inhibition in TNBC patients (Carey et al., 2012).

1.2.4. Challenges in targeting TNBC

Despite several promising preclinical and clinical studies, it is still a challenge to develop effective targeted therapies for TNBC patients. Several of these therapeutic compounds are poorly active in tumours or acquired resistance to these therapies eventually develops in cancer patients. This might be due to the crosstalk between signalling pathways that leads to feedback activation of inhibited pathways, the acquisition of secondary mutations or intratumoural heterogeneity (Kalimutho et al., 2015). TNBC has a low frequency of single targetable molecular drivers, which could limit the activity of the targeted therapies (Le Du et al., 2015).

The heterogeneity of TNBC might contribute to the different responses to targeted therapies. TNBC can be sub-classified into six distinct subtypes based on gene expression profiles; basal-like (BL1 and BL2), immunomodulatory (IM), mesenchymal (M), mesenchymal stem-like (MSL) and luminal androgen receptor (LAR). BL1 subtype is enriched with genes in cell cycle and cell division components and BL2 subtype is enriched with growth factor signalling pathway genes. IM subtype is enriched with genes in immune cell signalling while M and ML subtypes are enriched in gene expression of biological pathways involved in

motility, differentiation and growth. LAR subtype is enriched with genes in androgen receptor signalling pathways. (Lehmann et al., 2011).

Even though cancer is a complex disease, tumours have several commonly observed characteristics or hallmarks. These include: (i) sustaining proliferative signalling, (ii) evading growth suppressors, (iii) evading apoptosis, (iv) limitless proliferative potential, (v) inducing angiogenesis, (vi) activating invasion and metastasis, (vii) deregulated cellular energetics, (viii) avoiding immune destruction, (ix) tumour-promoting inflammation, (x) genome instability and mutation (Hanahan and Weinberg, 2011). Therefore, a potential strategy to overcome or prevent the emergence of resistance to targeted therapies in TNBC patient is to target these cancer hallmarks simultaneously and maximise the anti-tumour effects of the inhibition.

1.3. Heat shock protein 90

Heat shock protein 90 (HSP90) is a conserved molecular chaperone that regulates the maturation, activation and stability of more than 200 client proteins including various oncogenic proteins; receptor tyrosine kinases (HER2, EGFR, IGF-1R, MET), transcription factors (HIF1, TP53), signalling proteins (AKT, SRC) and cell cycle regulatory proteins (CDK4, CDK6, cyclin D). HSP90 client proteins are involved in multiple hallmarks of cancer **(Figure 1.3)** (Trepel et al., 2010, Neckers and Workman, 2012, Hanahan and Weinberg, 2011, Garg et al., 2016).

HSP90 is highly abundant in the cells; constituting 1-2% of total protein levels under normal conditions. Its expression increases two fold following exposure to stress conditions, including hypoxia and a nutrient-deprived microenvironment, as commonly seen in tumours (Whitesell and Lindquist, 2005). High expression of HSP90 is associated with poor prognosis and worse recurrence-free survival in breast cancer patients, including TNBC

patients (Song et al., 2010, Pick et al., 2007, Cheng et al., 2012). Therefore, HSP90 is a potential molecular target for the development of novel cancer therapeutics for TNBC patients as it provides the opportunity to disrupt multiple pathways which simultaneously promote oncogenesis.

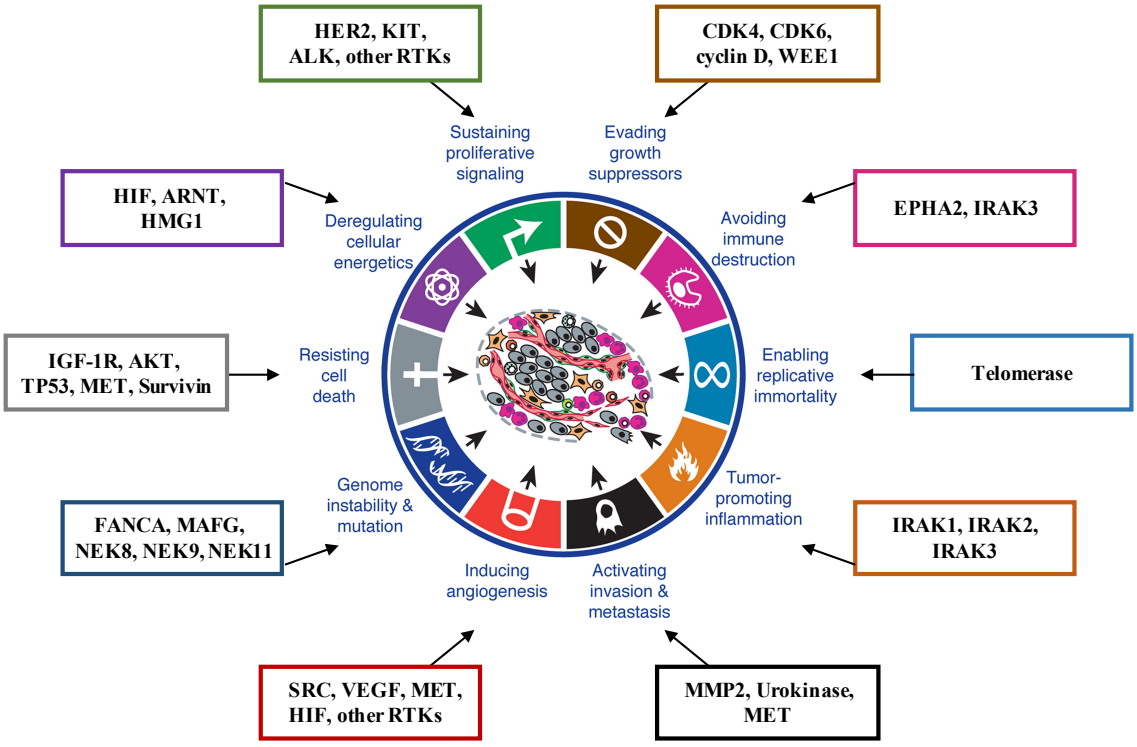


Figure 1.3: HSP90 client proteins and the hallmarks of cancer

Adapted from (Hanahan and Weinberg, 2011, Garg et al., 2016).

1.3.1. HSP90 structure and chaperone cycle

In human, HSP90 is found primarily in the cytoplasm. HSP90 subfamilies; tumour necrosis factor type 1 receptor-associated protein (TRAP1) and glucose regulated protein 94 (GRP94) are also present in mitochondria and endoplasmic reticulum, respectively (Chen et al., 2005). HSP90 is a homodimer with three highly conserved domains: amino-terminal domain (NTD), middle domain (MD) and carboxyl-terminal domain (CTD) (Taipale et al., 2010). The NTD contains a topologically distinct ATP-binding domain known as Bergerat fold; where the structural motif belongs to the GHKL superfamily (gyrase, HSP90, histidine

kinase and MutL)(Dutta and Inouye, 2000). The MD contains a hydrophobic and amphipathic protrusion for the interaction with client proteins. It also contains a catalytic arginine residue loop for efficient ATP hydrolysis (Pearl and Prodromou, 2006, Meyer et al., 2003). The CTD is responsible for HSP90 dimerisation and it contains a MEEVD sequence that makes up a conserved tetratricopeptide repeat (TPR) domain-binding motif. This motif is recognised by TPR-containing co-chaperones such as HOP (HSP70 and HSP90-organizing protein) and cyclophilin 40 (CYP40) (Minami et al., 1994, Young et al., 1998).

The activity of HSP90 involves dynamic conformational rearrangements driven by ATP hydrolysis and interactions with several co-chaperones, which inhibit or activate HSP90 ATPase activity and help in the recruitment of client proteins **(Figure 1.4)** (Taipale et al., 2010, Pearl and Prodromou, 2006, Li et al., 2012). HSP90 is usually in an open confirmation. Co-chaperone HOP binds to HSP90 at the TPR motif of CTD and forms a HSP90-HOP complex **(Figure 1.4b)**. This interaction stabilises the open confirmation and inhibits the ATPase activity of HSP90. Client protein binds to HSP40 and HSP70 to form a client protein complex. The HSP70 also contains a TPR domain-binding motif, which can be recognised by HOP. The client protein complex is recruited to the HSP90-HOP complex and this facilitates the loading of client protein onto the MD of HSP90 **(Figure 1.4c)**(Johnson et al., 1998, Cintron and Toft, 2006).

ATP binds to the nucleotide-binding pocket at the NTD and this causes the transitions of HSP90 from an open confirmation to a closed confirmation. The closed confirmation is stabilised by the binding of co-chaperone protein p23 to NTD. This binding causes HOP to dissociate from the complex and enables the conformational maturation of the client protein **(Figure 1.4d)**(McLaughlin et al., 2006, Li et al., 2012). Co-chaperone AHA1, activator of HSP90 ATPase homologue 1, binds to the NTD and facilitates the interaction of NTD to the catalytic arginine residue loop in the MD. This interaction stimulates the ATPase activity of

HSP90. (Retzlaff et al., 2010). Co-chaperone CYP40 also binds to CTD at the TPR motif and it helps to regulate the activity of the client protein (Taipale et al., 2010). After ATP hydrolysis, the mature client protein is released from HSP90 **(Figure 1.4e)**. The co-chaperone p23 also gets released from the complex and the open confirmation of HSP90 is restored.

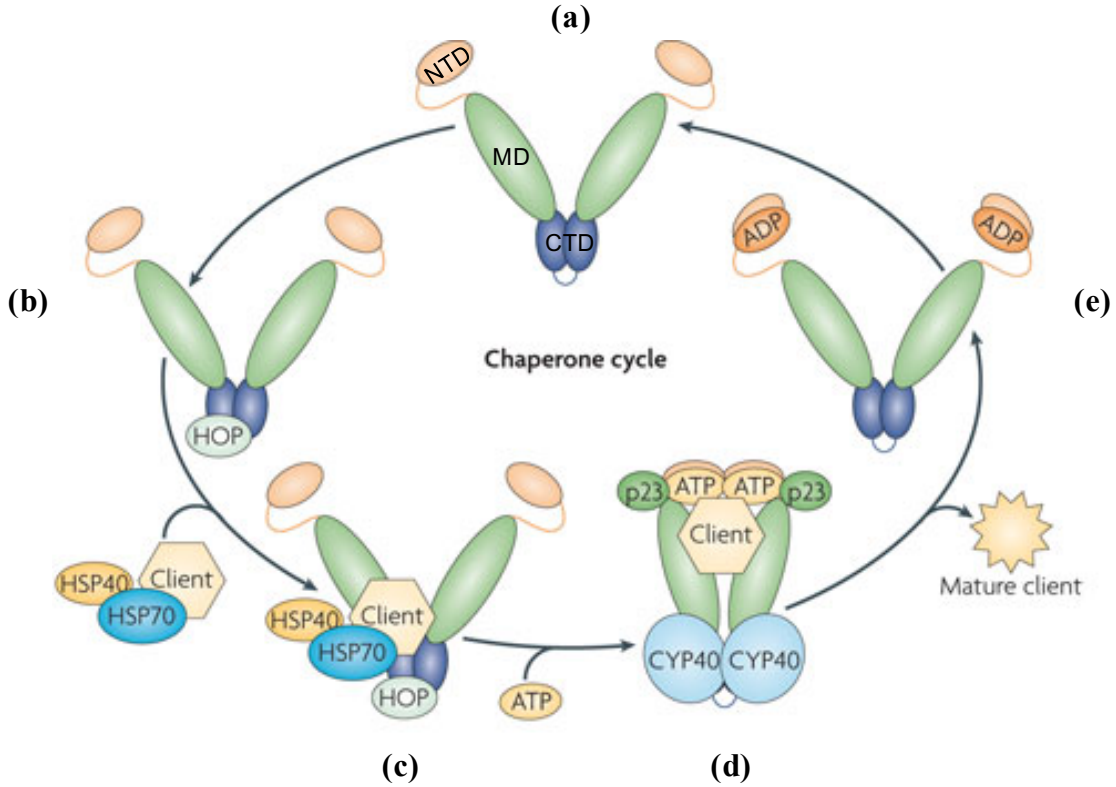


Figure 1.4: The dynamic HSP90 chaperone cycle.

(a) Open conformation of HSP90 consists of amino-terminal domain (NTD, orange), middle domain (MD, green) and carboxyl-terminal domain (CTD, blue).

(b) Co-chaperone HOP to CTD. This interaction stabilizes the open confirmation and inhibits the ATPase activity of HSP90.

(c) Client protein binds to HSP40 and HSP70 to form a client protein complex. The complex gets recruited to the HSP90-HOP complex. The client protein gets loaded onto the MD.

(d) ATP binds to the nucleotide-binding pocket at NTD and HSP90 adopts a closed confirmation. Co-chaperone p23 also binds to NTD. This stabilises the closed confirmation and facilitates the dissociation of HOP and maturation of client protein. Co-chaperone CYP40 also binds to CTD and regulates the activity of client protein.

(e) Hydrolysis of ATP to ADP causes the release of mature client protein. Dissociation of p23 and ADP from HSP90 restores HSP90 to an open confirmation.

(Adapted from (Taipale et al., 2010, Neckers and Workman, 2012))

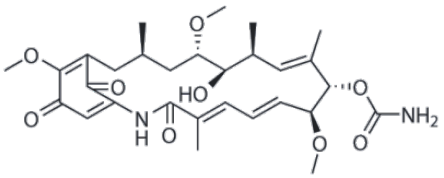
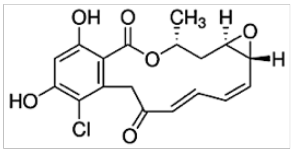
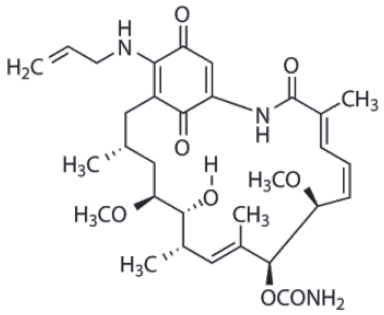
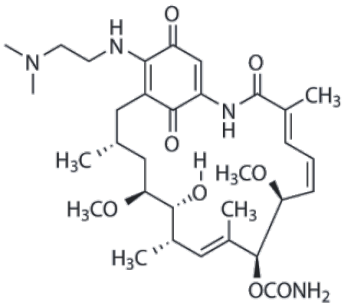
1.3.2. HSP90 as a therapeutic target

HSP90 was first identified as a therapeutic target when treatment with natural product compounds, geldanamycin and radicicol, decreased the levels of oncogenic client protein (SRC, HER2). The compounds destabilised the HSP90-client protein complex and this caused the client protein to be directed for ubiquitin-mediated proteosomal degradation (Whitesell et al., 1994, Schulte et al., 1998, Mimnaugh et al., 1996).

Geldanamycin and radicicol are not structurally related **(Table 1.4)**. However, x-ray crystallographic studies demonstrate that they bind selectively to the nucleotide-binding pocket at the NTD of HSP90 and they also mimic the interactions of ADP/ATP to HSP90. Competitive inhibition of geldanamycin or radicicol disrupts the ATPase activity of the HSP90 chaperone cycle, which is important for its functions (Roe et al., 1999). Development and synthesis of several HSP90 inhibitors for cancer therapeutics are mostly focused on targeting the NTD of HSP90.

Several preclinical studies with HSP90 inhibitors demonstrate effective anti-cancer activities in multiple cancer models at tolerable doses, including ovarian, prostate and breast cancer. HSP90 inhibitors cause simultaneous degradation of oncogenic client proteins and inhibition of tumour growth in vivo (Solit et al., 2002, Banerji et al., 2005, Eiseman et al., 2005). They also have higher binding affinity to HSP90 from tumours compared to normal tissue. This tumour selectivity might be due to the HSP90 from tumours is mostly in an active HSP90-chaperone complex compared to the non-chaperone complex of HSP90 in normal tissues (Kamal et al., 2003). This selectivity is also seen in vivo, where HSP90 inhibitors accumulate in tumours and are rapidly cleared from blood and normal tissues (Chiosis and Neckers, 2006).

Table 1.4: HSP90 inhibitors

Geldanamycin	Radicicol
	
17-AAG	**17-DMAG**
	

Compound	Stage of development in clinical trial	Tumour responses reported	Clinical progress
Geldanamycin-based derivatives			
17-AAG	Phase I-II	HER2-positive breast cancer, myeloma	Development terminated
17-DMAG	Phase I-II	HER2-positive breast cancer, ovarian cancer, prostate cancer, AML, melanoma	Development terminated

* Chemical structures obtained from Selleckchem.com and Sigmaaldrich.com, accessed September 2016
(Adapted from (Garcia-Carbonero et al., 2013) and clinicaltials.gov)

1.3.3. Development of HSP90 inhibitors

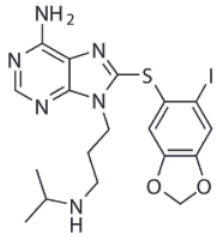
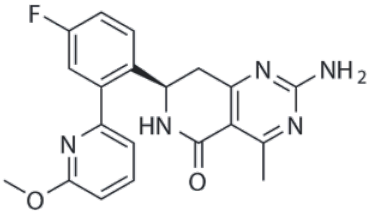
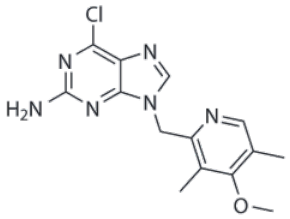
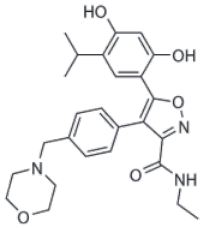
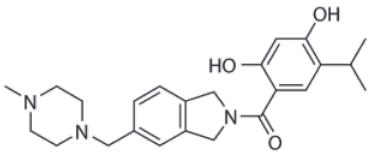
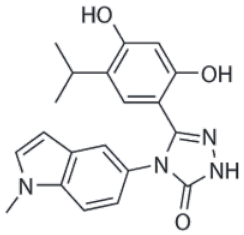
Even though geldanamycin showed potent anti-cancer activities in vitro and in vivo studies, it did not progress in the clinic due to its low chemical stability, poor solubility and hepatotoxicity in animal models. Similarly, radicicol showed anti-cancer activities in vitro but it was inactive in vivo due to its poor chemical stability (Khandelwal et al., 2016, Supko et al., 1995). Geldanamycin-based derivatives were developed with improved

pharmacological properties and tolerable toxicity by substituting the methoxy group on the quinone in geldanamycin with amine groups **(Table 1.4)** (Jhaveri et al., 2012).

17-AAG caused downregulation of oncogenic client proteins in vitro (HER2, RAF1 and p53) and inhibited tumour growth in xenograft models (An et al., 1997, Banerji et al., 2005). 17-AAG was the first HSP90 inhibitor to enter clinical studies for cancer. Several Phase II clinical studies of 17-AAG did not show significant clinical activity (complete or partial responses) in cancer patients, including prostate, renal and breast cancer. This might be due to poor solubility and oral bioavailability of the compound, which led to a lack of target inhibition in the tumours (Heath et al., 2008, Ronnen et al., 2006, Garcia-Carbonero et al., 2013). However, clinical studies of 17-AAG in combination with trastuzumab, a HER2 antibody, were well tolerated and showed tumour responses in HER2-positive breast cancer patients (Modi et al., 2007, Modi et al., 2011, Arteaga, 2011). Despite these promising studies, the clinical development of 17-AAG was terminated in 2010, possibly due to the compound was costly to manufacture with only limited patent life. Tumour responses were also reported with 17-DMAG in several cancer patients but its development was terminated in 2008 due to toxicity (Garcia-Carbonero et al., 2013).

The first generation HSP90 inhibitors have several drawbacks, including poor solubility, low oral bioavailability and unfavourable toxicity in cancer patients. In order to overcome these limitations, second-generation HSP90 inhibitors are currently being developed, including purine-based and resorcinol-based HSP90 inhibitors **(Table 1.5)** (Soga et al., 2013, Khandelwal et al., 2016). X-ray crystallographic studies demonstrate that the hydrogen bonding interactions from HSP90 to either the adenine group (purine) of ATP or the aromatic ring (resorcinol) of radicicol are important for HSP90 inhibition (Roe et al., 1999).

Table 1.5: Synthetic HSP90 inhibitors in clinical trials

PU-H71	NVP-HSP990	BIIB021
		
NVP-AUY922	**AT13387**	**Ganetespib**
		

Compound	Stage of development in clinical trial	Tumour responses reported	Clinical progress
Purine-based			
PU-H71	Phase I-II	-	Ongoing (myeloma)
NVP-HSP990	Phase I-II	-	Development terminated
BIIB021	Phase I-II	CCL, GIST, breast cancer	Development terminated
Resorcinol-based			
NVP-AUY922	Phase I-II	HER2-positive breast cancer, NSCLC	Ongoing (NSCLC, GIST)
AT13387	Phase I-II	GIST	Ongoing (NSCLC, breast cancer including TNBC)
Ganetespib	Phase I-III	Breast (including TNBC), NSCLC (terminated following futility analysis), rectal, melanoma, CML and AML	Ongoing (ovarian, esophageal, breast, ALK positive lung cancer)

* Chemical structures obtained from Selleckchem.com, accessed September 2016
(Adapted from (Garcia-Carbonero et al., 2013) and clinicaltials.gov)

1.3.4. HSP90 inhibitors in TNBC

There are several second-generation HSP90 inhibitors that demonstrate effective anti-cancer activities in TNBC. A study with a purine-based HSP90 inhibitor, PU-H71 showed that TNBC cells are also sensitive to HSP90 inhibition and sensitivity is not limited to HER2-positive breast cancer cells. PU-H71 caused the downregulation of oncogenic client proteins involved in proliferation (EGFR, IGF-1R, HER3, KIT), G2-M phase cell cycle arrest and induced apoptosis in TNBC cells. There was also significant tumour growth inhibition in TNBC xenografts (Caldas-Lopes et al., 2009). Currently, PU-H71 is in clinical trial development for myeloma only (clinicaltrials.gov).

Ganetespib, a resorcinol-based HSP90 inhibitor, also caused the downregulation of multiple client proteins (EGFR, IGF-1R, MET and CRAF), inhibition of metastasis and tumour growth in TNBC xenografts (Proia et al., 2014) (Friedland et al., 2014). Ganetespib, in combination with chemotherapy, also enhanced G2-M phase cell cycle arrest, induced apoptosis and tumour growth inhibition in TNBC xenografts (Proia et al., 2014).

Ganetespib has a unique triazolone moiety, which improves its pharmacological and biochemical properties **(Table 1.5)** (Ying et al., 2012). It lacks the benzoquinone chemical moiety, which is associated with the dose-limiting hepatotoxicity to geldanamycin derivatives. Compared to other first- or second-generation HSP90 inhibitors, ganetespib causes higher in vitro potency, greater in vivo anti-cancer activities, and more efficient distribution in tumour without causing any serious toxicity (liver, cardiac and ocular) (Ying et al., 2012, Shimamura et al., 2012, Zhou et al., 2013).

Ganetespib is one of the most advanced HSP90 inhibitors in clinical development (Proia and Bates, 2014, Jhaveri and Modi, 2015). It is being investigated in numerous clinical trials (Phase I-III) as monotherapy or in combination with other treatments (other targeted

therapies, chemotherapy and radiation) in several cancers, including breast, non-small cell lung, melanoma, rectal and oesophageal (clinicaltrials.gov). In TNBC patients, ganetespib was well tolerated and 7 of the first 11 patients treated showed tumour responses or stable disease (NCT01677455). A complete clinical response was also observed in one TNBC patient after treatment with ganetespib for 12 weeks (150 mg/m^2 twice weekly for 3 out of 4 weeks) (Awada et al., 2013).

1.4. Aims and objectives

HSP90 inhibition (HSP90i) is a promising approach for the development of novel cancer therapeutics in TNBC. In clinical studies, HSP90i showed effective tumour responses in TNBC patients. Despite this encouraging clinical responses to HSP90i, these responses were short-lived and acquired resistance to HSP90i developed in TNBC patients. In addition, not all TNBC patients responded to HSP90i, suggesting intrinsic resistance to HSP90i also exists (Awada et al., 2013).

The mechanisms of resistance to HSP90i in cancer patients are not yet fully understood. A greater understanding of how resistance to HSP90i can arise should help to identify potential predictive biomarkers for a better selection of responsive TNBC patients to HSP90i therapy and to develop alternative therapeutic strategies for non-responsive TNBC patients. There have been several successes in identifying clinically relevant intrinsic and acquired resistance to other anti-cancer targeted agents using in vitro models, including gefitinib-resistant lung cancer cell lines and trastuzumab-resistant breast cancer cell lines (Rosa et al., 2014).

We hypothesise that by using in vitro assays, we will be able to identify potential mechanisms of resistance to HSP90i in TNBC. Therefore, the overall aim of this work is to investigate the mechanisms of acquired resistance to HSP90i in TNBC cells. The specific objectives are as follows:

1. To establish an in vitro model of TNBC cells with acquired resistance to HSP90i
2. To investigate the mechanism of resistance to HSP90i by characterising the molecular phenotype of HSP90i-resistant TNBC cells
3. To identify potential therapeutic approaches to overcome acquired resistance to HSP90i in TNBC cells

2. Materials and Methods

2.1. Buffers and solutions

Table 2.1: Buffers and solutions prepared in this study

Application	Buffer	Composition
Cell viability assay	Resazurin solution (125 µg/ml)	Stock solution of 12.5 mg/ml resazurin (Sigma-Aldrich, USA) in dH_2O stored at -20 ^oC. Resazurin solution of 125 µg/ml prepared fresh on the day of experiments by 1:100 dilution in dH_2O.
Preparation of cell lysates	Lysis buffer	50 mM Tris-HCl, pH 7.6 (Promega, USA) 137 mM NaCl (Sigma-Aldrich) 10% (v/v) glycerol (VWR, USA) 0.1% (v/v) Igepal (Sigma-Aldrich) 0.1% (v/v) SDS (AppliChem GmbH, Germany) 50 mM sodium fluoride (Sigma-Aldrich) 1 mM sodium orthovanadate and cOmplete protease inhibitor cocktail (Roche, Switzerland)
Cell cultures	1x phosphate buffered saline (PBS)	1:10 of 10x PBS (Lonza, Switzerland) and dH_2O
Western blotting	1x tris-buffered saline (TBS)	1x pack OmniPur® TBS 20x Ready Pack powder (Calbiochem, Germany) dissolved in 20 litres dH_2O to make up 137 mM NaCl, 2.7 mM KCl, 25 mM Tris, pH 7.5
Western blotting	TBST	1x TBS, 0.1% (v/v) Tween-20 (Sigma-Aldrich)
Western blotting	5x sample loading buffer	25 mM Tris-Base (Sigma-Aldrich), pH 6.8 1% (v/v) SDS 1mM AccuGENE^{TM} EDTA (Lonza) 2.5% (v/v) β-mercaptoethanol (Sigma-Aldrich) 0.25 mg/ml Bromophenol blue (Acros organics, USA)
Western blotting	Running buffer	1:10 (v/v) of 10x Tris/Glycine/SDS running buffer (Bio-Rad, USA) in dH_2O
Western blotting	Transfer buffer	1:10 (v/v) of 10x Tris/Glycine buffer (Bio-Rad) in dH_2O 20% (v/v) methanol (Sigma-Aldrich)
Western blotting	Blocking buffer	For chemiluminescence: 5% (w/v) non-fat skimmed milk powder (Sigma-Aldrich) in TBS For fluorescence: 1:1 mixture of Odyssey® Blocking Buffer (LI-COR, USA) and TBS
Western blotting	Antibody buffer	For Chemiluminescence: 5% (w/v) non-fat skimmed milk powder in TBST For fluorescence: 1:1 mixture of Odyssey® Blocking Buffer (LI-COR) and TBST
Clonogenic assay	Crystal violet fixation solution	0.5% (w/v) crystal violet (Merck, Germany) 75% (v/v) methanol in dH_2O
PicoGreen assay	DNA lysis buffer	25 mM EDTA 0.1% Triton X-100 (VWR) in dH_2O, pH 8.0
PicoGreen assay	PicoGreen solution	1:200 (v/v) of Quant-iT PicoGreen dsDNA reagent (Life Technologies, USA) in PBS

Mass spectrometry	Fixing solution	93% (v/v) Methanol 7% (v/v) Acetic Acid (Sigma-Aldrich)
Mass spectrometry	Coomassie solution	2x stock solution: 0.25% (v/v) Brilliant Blue R concentrate (Sigma-Aldrich) 40% (v/v) Methanol 7% (v/v) Acetic Acid in dH_2O
Mass spectrometry	Destain solution	40% (v/v) Methanol 7% (v/v) Acetic Acid

2.2. Cell culture

2.2.1. Maintenance of human cell lines

The human cell lines used in this study are listed in **Table 2.2**. The cell lines (except BT20) were authenticated using Short Tandem Repeat (STR) analysis (LGC standards). In culture, the cells were maintained in either Dulbecco's modified Eagle medium (DMEM; Life Technologies) or Roswell Park Memorial Institute medium 1640 (RPMI-1640; Life Technologies), and supplemented with 10% (v/v) foetal bovine serum (FBS; Sigma-Aldrich), 2 mM GlutaMax^{TM} (Life Technologies) and 50 U penicillin/ 50 µg/ml streptomycin (Life Technologies). All cells were grown in a humidified incubator of 5% CO_2 at 37°C.

Table 2.2: Cell lines used in this study

Cell Line	Source	Culture medium	Mutation status[4]
MDA-MB-231	ATCC[1]	DMEM	*BRAF, CDKN2A, KRAS, NF2, TP53, PDGFRA*
MDA-MB-468	ATCC	DMEM	*PTEN, RB1, SMAD4, TP53*
MDA-MB-453	ATCC	DMEM	*PI3K3CA, CDH1, PTEN*
HCC-1937	[2]	RPMI-1640	*BRCA1, TP53, MAPK13, MDC1*
HCC-1143	[2]	RPMI-1640	*TP53*
Hs578T	[2]	DMEM	*CDKN2A, HRAS, TP53*
BT-20	[3]	DMEM	*CDKN2A, PIK3CA, TP53*

[1]ATCC= American type culture collection (Manassas, USA)
[2]Kindly provided by Dr Patricia Mc Gowan (St. Vincent's University Hospital, Ireland)
[3]Kindly provided by Professor Adrian Harris (University of Oxford, UK)
[4] List of mutations taken from (Lehmann et al., 2011)

2.2.2. Routine passaging and cell seeding

Cells were routinely passaged once they have reached sub-confluence (80-90%). After washing the cells with PBS, cells were trypsinised with 0.25% Trypsin-EDTA (Life Technologies) for 3-5 minutes (min) and the detached cells were diluted (1:10) with complete culture medium. Prior to seeding cells for any experiments, density (number/ml) of viable cells was measured using a Countess® automated cell counter (Life Technologies). A 1:1 mixture of the diluted cell suspension and 0.4% trypan blue solution (Life Technologies) was added into a Countess® cell counting chamber slide for counting. Cells were seeded according to the desired cell density for the experiment with complete culture medium; unless otherwise stated.

2.2.3. Cryopreservation and thawing of cells

For long-term storage of cell lines, the cells were trypsinised before reaching full confluency and diluted in complete culture medium. Cell suspension was then centrifuged for 5 min at 280 x g and the cell pellet was resuspended in freezing medium containing complete culture medium and 10% (v/v) dimethyl sulfoxide (DMSO; Fisher Scientific, USA). Aliquots were transferred to cryogenic tubes and frozen at -80^{o}C overnight in an isopropanol filled Mr Frosty^{TM} freezing container (Thermo Scientific, USA); before being stored in liquid nitrogen. Cells from liquid nitrogen were recovered by thawing rapidly in a 37^{o}C water bath for 2 min and transferring the cells immediately into a flask containing pre-warmed complete culture medium. The medium was replaced with fresh complete culture medium the next day.

2.2.4. Mycoplasma testing

The cell lines used in this study were tested for *Mycoplasma* infection using real-time polymerase chain reaction (PCR); as described in (Ishikawa et al., 2006). Genomic DNA was isolated from the cells as described in **(Chapter 2.11)** and a region of *Mycoplasma* 23S ribosomal RNA gene (amplifiable from eight common *Mycoplasma* species) was amplified by PCR. The primers (Sigma-Aldrich) used:

Forward: 5'- GGAAAATGTTATTTTGACGGAACCT -3'
5'- TCTGAATYTGCCGGGACCACC -3'
5'- GGAATCCCGTTTGAAGATAGGA -3'
Reverse: 5'- CTTTCCMTCACKGTACTRGTTCACT -3'

The PCR reactions were prepared in 20 µl containing SYBR Green PCR Master Mix (Applied Biosystems, UK), 0.1 µg of DNA samples, and 0.3 µM of each primer. The reactions were performed using a 7500 Fast Real-Time PCR System (Applied Biosystems) with these conditions:

Hot start	95°C	3 min	
Denaturation	95°C	15 sec	} 40 cycles
Annealing/Extension	65°C	30 sec	
Melting curve	55-95°C		
	(0.5 °C increment)	10 sec	

Genomic DNA from *Mycoplasma orale,* a common human-derived cell culture contaminant (Minerva Biolabs, Germany; *#51-0112*) was included as a positive control. A fluorescence signal is produced when SYBR Green binds to dsDNA and the level of fluorescence signal is proportional to the amount of *Mycoplasma* species DNA present in the reactions. The threshold cycle (Ct) value; where the signal appeared above the background signal was calculated for each cell line. The Ct values were compared to the positive controls to confirm that the cell lines were not positive for mycoplasma infection.

2.3. Drug treatment

Unless otherwise specified, all drugs were prepared as 10 mM stock solution in DMSO. Ganetespib, VER-11508, HSP990, PUH-71 and 326-compound bioactive small molecule library **(Supplementary Table 1)** were obtained from Selleckchem (USA). Phyleomycin (from *Streptomyces verticillus, #P9564*) was obtained from Sigma-Aldrich. Propofol (MP Biomedicals, UK) was prepared in DMSO at a concentration of 0.5 M. All stock solutions were aliquoted and stored at -20°C until used. Dilutions of drugs for treatment were made using DMSO and/or complete culture medium. Unless otherwise specified, DMSO was used as a treatment control at 0.1% final concentration (v/v).

2.4. Generation of HSP90i-resistant clones

Hs578T cells were seeded in ten 10 cm plates (1.0×10^5 cells/plate). After 3 days, the cells were treated with 30 nM (8 plates), 50 nM (1 plate) and 100 nM (1 plate) ganetespib. Fresh complete culture medium with ganetespib was replaced once a week. After several weeks, colonies started to form in the plates (0-10 colonies per plate). Independent colonies from separate plates were isolated using cloning cylinders (Sigma, #C1059) and trysinisation. Each clone was left to grow in the absence of ganetespib and later split for further selection with ganetespib (15-30 nM) after 48 hr of plating. The clones that were still able to grow well in 30 nM ganetespib were continuously maintained in culture with the presence of 30 nM ganetespib.

2.5. Cell viability assay

Cell viability was assessed using a resazurin-based cell viability assay. Cells ($0.8 - 3.0 \times 10^3$ cells) were seeded in triplicates in 96-well plate and allowed to adhere overnight. The cells were treated the next day with compound or combinations of compounds for 72 hours (hr). A range of drug concentrations was used by performing serial dilutions with complete culture

medium. After treatment, prepared resazurin solution **(Table 2.1)** was added into each well to a final concentration of 12.5 µg/ml and incubated for 2 hr. The metabolically active viable cells reduce the resazurin to highly fluorescent resorufin. The fluorescence intensity (excitation 544 nm; emission at 590 nm) was measured using a POLARstar Omega plate reader (BMG Labtech GmbH, Germany). After subtracting the average fluorescence intensity of blank (medium, no cells) from the wells, the fluorescence intensity was proportional to the number of viable cells. The percent cell viability after each treatment was normalised either to DMSO-treated control or to cells treated at the fixed concentration of compound alone for combination treatment. IC_{50} (the drug concentration that reduces cell viability to 50% of control) was calculated from three independent experiments, each with triplicates measurements, using the Origin software (OriginLab Corporation, USA).

2.6. Preparation of cell protein lysates

Cells (0.8 -1.5 x 10^6 cells) were seeded in 10 cm plates and allowed to adhere overnight. The cells were treated the next day with the compound for the times and concentrations specified, and incubated at 37°C. After completion of treatment, the medium was collected, centrifuged for 5 min at 280 x g and the cell pellet was washed twice with ice-cold PBS. In parallel, the plate with attached cells was washed twice with ice-cold PBS and left on ice with ice-cold lysis buffer **(Table 2.1)** for 10 min. The cells were scraped off from the plate and added to the cell pellet for resuspension. The cell suspension was left on ice for 30 min before brief sonication (twice for 10 sec) with a Bioruptor® Plus (Diagenode Inc., Belgium). The cells were centrifuged at 16,100 x g for 10 min at 4°C. Supernatants containing soluble proteins were used immediately for experiments or stored at -20 °C or -80°C (longer storage). The concentration of protein lysates was measured using a NanoDrop 1000 spectrophotometer at 280 nm absorption (Thermo Scientific).

2.7. Western blotting analysis

Protein lysates were prepared for western blotting analysis by normalising protein concentrations using complete lysis solution followed by the addition of 1 volume of 2x Laemmli sample loading buffer (Sigma-Aldrich) or 0.25 volumes of 5x sample loading buffer **(Table 2.1)**. The prepared samples were then heated to 95°C for 8 min. A protein ladder (Precision Plus Protein™ Dual Color ladder; Bio-Rad, USA) and 30-50 µg of protein lysates were resolved onto a 4-15% gradient precast gel either Mini-PROTEAN TGX gel (Bio-Rad) or Criterion™ TGX™ gel (Bio-Rad) with running buffer **(Table 2.1)**. Electrophoresis was set at 250 V for 25 min (mini gel, 8.6 x 6.7 cm) or 150 V for 1 hr (large gel, 13.3 x 8.7 cm). The resolved proteins were transferred to a PVDF membrane (0.45 µM pore size, Millipore) using a transfer cell containing transfer buffer **(Table 2.1)** for 45 min at 150 V (mini gel) or for 1 hr at 90 V (large gel). The membrane containing the transferred proteins was stained with Ponceau S Solution (Sigma-Aldrich), cut according to the protein of interest and washed with TBST.

The membrane was then incubated with prepared blocking buffer for 1 hr at room temperature and with primary antibody **(Table 2.3)** diluted in prepared antibody buffer at 4°C overnight. After incubation, the membrane was washed three times for 10 min with TBST and incubated with appropriate secondary antibody **(Table 2.3)** diluted in prepared antibody buffer for 1 hr at room temperature. The membrane was washed three times with TBST for 10 mins and once with TBS for 10 mins.

The proteins on the membrane were detected and visualised either by chemiluminescence or fluorescence depending on the secondary antibodies used during incubation. For membranes incubated with LI-COR secondary antibodies, the fluorescent signals from the antibodies were directly detected using the Odyssey® scanner (LI-COR). For membranes incubated with horseradish peroxide (HRP)-conjugated secondary antibodies, either Pierce® Enhanced

Chemiluminescence (ECL) Western Blotting substrate (Thermo Scientific) or Amersham ECL Prime Western Blotting detection reagent (GE Healthcare, UK) was added onto the membrane as an enzyme substrate. The chemiluminescent signals from the reaction were detected using a ChemiDoc^{TM} MP Imaging System (Bio-Rad). Quantification of protein bands was performed using the detection software and intensity (photon counts) of the band was proportional to the amount of protein. The intensity of each band was normalised to the loading control of respective lane.

Table 2.3: List of antibodies used for western blotting analysis

Name	Clonality	Species	Dilution	Manufacturer	Catalogue Number
Primary antibodies:					
β-actin[1]	Monoclonal (AC-15)	Mouse	1:5,000	Sigma-Aldrich	*#A1978*
AKR1C1	Polyclonal	Rabbit	1:1,000	Abcam	*#ab192785*
total AKT[1]	Polyclonal	Rabbit	1:1,000	Cell Signaling	*#9272*
phospho-AKT (S473)[1]	Polyclonal	Rabbit	1:500	Cell Signaling	*#9271*
total ATM	Monoclonal	Rabbit	1:5,000	Abcam	*#ab32420*
phospho-ATM (S1981)[2]	Monoclonal (EP1890Y)	Rabbit	1:10,000	Epitomic Inc.	*#2152-1*
Cyclophilin B (PPIB)	Polyclonal	Rabbit	1:5,000	Abcam	*#ab16045*
total EGFR[1]	Polyclonal	Rabbit	1:1,000	Cell Signaling	*#2232*
phospho-EGFR (Y1068)[1,2]	Polyclonal	Rabbit	1:500	Invitrogen	*#44788G*
HSP70[1,2]	Polyclonal	Rabbit	1:500	Cell Signaling	*#4876*
HSP90[1]	Monoclonal (C45G5)	Rabbit	1:1,000	Cell Signaling	*#4877*
total MET[1]	Monoclonal (D1C2)	Rabbit	1:1,000	Cell Signaling	*#8198*
phospho-MET (Y1234/1235)[1,2]	Monoclonal (D26)	Rabbit	1:1,000	Cell Signaling	*#3077*
NQO1	Monoclonal (A180)	Mouse	1:1,000	Cell Signaling	*#3187*
PARP	Polyclonal	Rabbit	1:2,000	Cell Signaling	*#9542*
phospho-STAT3 (Y705)[2]	Polyclonal	Rabbit	1:500	Cell Signaling	*#9131*
UGT1A9[2]	Polyclonal	Rabbit	1:1,000	Abcam	*#ab96214*
UGT1A[2]	Polyclonal	Rabbit	1:1,000	Cell Signaling	*#4371*

Secondary antibodies:				
Anti-mouse-HRP	Goat	1:5,000	Thermo Scientific	*#31430*
Anti-rabbit-HRP	Goat	1:5,000	Thermo Scientific	*#31460*
IRDye® 800CW	Goat	1:5,000	LI-COR	*#926-32211*
IRDye® 680RD	Goat	1:5,000	LI-COR	*#926-68070*

[1]Antibodies that were used with either LI-COR fluorescence or ECL chemiluminescence detection

[2]Antibodies that required Amersham ECL Prime Western Blotting detection reagent

2.8. Apoptosis assay

Cells (1.0 x 10^5 cells) were seeded in duplicate in 6-well plates and allowed to adhere overnight. The cells were treated the next day with the compound at indicated concentration for 72 hr. After treatment, the medium was collected and attached cells were trysinised and collected in ice-cold PBS. The cells were centrifuged at 280 x g for 5 min at 4°C. After washing the cell pellet twice with PBS, the cells were resuspended in a mixture of 1:1000 dilution Alexa Fluor® 647-Annexin V conjugate (Life Technologies) and Propidium Iodide (PI; Sigma-Aldrich) prepared in Annexin V buffer (BD Biosciences, USA). PI is a fluorescent dye that stains nucleic acids while Annexin V binds to phosphotidyl-serine on cell surface of apoptotic cells. The stained cells were assessed using CyAn™ ADP High-Performance Flow Cytometer (DakoCytomation, Denmark) and Summit® software.

2.9. Cell cycle analysis

Cells (0.8 - 1.0 x 10^6 cells) were seeded in duplicate in 10 cm plates and allowed to adhere overnight. The cells were treated the next day with the compound at indicated concentration for 24 hr. Twenty minutes before the end of treatment, cells were pulse labelled with 20 μM Bromodeoxyuridine (BrdU; Sigma-Aldrich) and protected from light. After treatment, the medium was collected and the attached cells on the plate were also collected by trypsinisation and resuspended with the collected medium. The cells were then centrifuged at

280 x g for 5 min. Cell pellets were resuspended in 100 µl of PBS and fixed by drop-wise addition of 1 ml ice-cold 70% ethanol (Sigma-Aldrich) while vortexing. Cells were incubated for at least 30 min on ice before centrifugation at 280 x g for 5 min. Cell pellets were resuspended in 2 M HCl (Fisher Scientific) containing 0.1 mg/ml pepsin (Sigma-Aldrich) and incubated at room temperature for 20 min. After centrifugation at 280 x g for 5 min, cell pellets were washed twice with PBS and once with PBS containing 2% FBS. The cell pellets were then resuspended in 100 µl of PBS containing 2% FBS and 1:100 dilution of mouse anti-BrdU antibody (BD Biosciences, *#347580*). Cells were incubated at room temperature for 90 min, vortexing every 30 min. After incubation, cells were washed once with PBS containing 2% FBS and resuspended in 100 µl of PBS containing 2% FBS and 1:200 dilution of goat anti-mouse Alexa Fluor® 488 secondary antibody (Life Technologies). After incubation at room temperature for 1 hr in the dark, cells were washed once with PBS and resuspended in 0.5 ml PBS containing 20 µg/ml of PI (Calbiochem). DNA content and BrdU incorporation were assessed using FACScan Flow Cytometer (BD Biosciences) and BD CellQuest™ Pro software. Cell cycle distributions (G0/G1-, S- and G2/M- phases) were determined using ModFit LT (Verity Software House, USA) and FlowJo software (Tree Star Inc, USA).

2.10. Colony formation assay

Cells (300-800 cells) were seeded in triplicates in 6-well plates and allowed to adhere overnight. The cells were treated the next day with the compound at indicated concentration for 24 hr. After treatment, cells were washed with PBS and fresh complete culture medium without compound added. Once the cells formed colonies with a size of at least 50 cells (7-14 days), they were fixed and stained with prepared crystal violet solution **(Table 2.1)** for at least 10 min at room temperature. Cells were washed with water and left to air dry. Images of plates were obtained with a Gelcount™ instrument (Oxford Optronix Ltd, UK) and the

number of colonies was counted manually. The number of colonies for each treatment was calculated as a percentage relative to DMSO-treated control cells.

2.11. DNA isolation and purification

Cells were seeded in 10 cm plates. When the cells reached 90% confluency, the cells were collected by trypsinisation and centrifugation. DNA was isolated and purified from the cell pellet using the MasterPure^{TM} DNA Purification Kit (Epicentre, USA); according to the manufacturer's instructions. DNA concentration of samples was measured using a NanoDrop 1000 spectrophotometer, and purified DNA was stored at -20^{o}C.

2.12. POLQ gene sequencing

To validate the presence of stop-gain variant in the POLQ gene (c.6850 G>A, p.R2241*), DNA was isolated from the cells and the region of variant was amplified using PCR. The primers (Sigma-Aldrich) used:

Forward: 5'-GATGGGACTCAGGATTCAAAACG-3'

Reverse: 5'-GTAGTGTAGCCAATTCATACATTCA-3'

The PCR reactions were prepared in 25 µl containing MyFi DNA polymerase (Bioline Reagents, UK), 0.5 µg of DNA samples, and 0.4 µM of each primer. The reactions were performed using a thermal cycler (Applied Biosystems) with these conditions:

Hot start	95°C	3 min	
Denaturation	94°C	1 min	⎫
Annealing	63°C	1 min	⎬ 35 cycles
Extension	72°C	1 min	⎭
Final extension	72°C	7 min	

An aliquot of the PCR products and a geneRuler 1kb Plus DNA ladder (Thermo Scientific) were resolved on an agarose (Sigma-Aldrich) gel in 0.5x Tris Borate-EDTA (TBE) buffer (Sigma-Aldrich) to confirm that the single PCR product was at the expected size. The PCR products were then purified using a MinElute PCR purification kit (Qiagen, Germany); according to the manufacturer's instructions. The purified PCR products were analysed by Sanger DNA Sequencing (SourceBioscience, Nottingham, UK) and the sequences visualised with FinchTV (Geospiza, US) to identify any presence of variants.

2.13. siRNA transfection

In order to knockdown the expression of HSP70 protein in the cells, transfection with predesigned and validated HSP70 (Sigma-Aldrich, *#NM_005346, siRNA ID: SASI_Hs01_00101768*) small interfering RNA (siRNA) was used. Cells (1.5 x 10^5 cells) were first seeded in 6-well plates with complete culture medium without penicillin/streptomycin and allowed to adhere overnight. The next day, cells were transfected with either 50 nM or 100 nM HSP70 siRNA using Lipofectamine® 2000 transfection reagent (1:500 final dilution; Invitrogen, USA) according to manufacturer's instruction. The mixture was prepared in serum-free Opti-MEM® (Life Technologies) medium. In parallel, cells were also transfected with Mission® siRNA Universal Negative Control #1 (Sigma-Aldrich, *#SIC001*) and transfection reagent alone for transfection negative siRNA control and mock-treated control, respectively. The cells were harvested after indicated time points and processed for western blotting analysis or cell viability assay.

2.14. Phospho-RTK Array

Simultaneous detection of relative phosphorylation of RTK was performed using a human phosho-RTK (pRTK) array. Protein lysates were first prepared as described in **(Chapter 2.6)** and normalised (400 μg/ml) using the complete lysis buffer before performing the Proteome

Profiler™ human pRTK array kit (R&D Systems, USA); according to the manufacturer's instructions. In summary, the lysates were incubated with the nitrocellulose membranes containing duplicate spots of 49 human pRTKs **(Table 2.4)** capture antibodies overnight at 4°C on a shaker. The arrays were washed three times before incubation with anti-Phospho-Tyrosine-HRP Detection Antibody for 2 hr at room temperature. After washing the arrays, they were incubated with Chemi Reagent Mix for 1 min and chemiluminescence detection of protein spots were visualised using a ChemiDoc™ Imaging System. Quantification of protein spots was performed using ImageJ software (National Institutes of Health, USA). After subtracting the average pixel intensity (photon count) of background from the spots, the intensity was proportional to the expression of pRTK. The intensity of each pRTK was normalised relative to the DMSO-treated control sample. pRTKs with more than double the intensity of the background were considered in the analysis.

Table 2.4: Proteins detectable with Proteome Profiler™ human phosho-RTK array kit

Proteins			
ALK	EPHA10	FLT3	RYK
AXL	EPHB1	MET	KIT
DDR1	EPHB2	IGF1R	TIE1
DDR2	EPHB3	INR	TIE2
DTK	EPHB4	CSFR	TRKA
EGFR	EPHB6	MER	TRKB
EPHA1	ERBB2	RON	TRKC
EPHA2	ERBB3	MUSK	VEGFR1
EPHA3	ERBB4	PDGFRA	VEGFR2
EPHA4	FGFR1	PDGFRB	VEGFR3
EPHA5	FGFR2	RET	
EPHA6	FGFR3	ROR1	
EPHA7	FGFR4	ROR2	

2.15. RNA isolation and purification

After completion of treatment, cells on the plates were collected by trypsinisation and centrifugation. RNA was then isolated and purified from the cell pellet using the RNeasy® Plus Mini Kit (Qiagen); according to the manufacturer's instructions. The purity of RNA samples was measured using a NanoDrop 1000 spectrophotometer (260/280 > 1.8, 260/230 >1.8). RNA samples were stored at -80^{o}C until used.

2.16. RNA Sequencing (RNA-seq)

Hs578T cells and HSP90i-resistant clones (0.8 - 1.0 x 10^6 cells) were seeded in 10 cm plates and allowed to adhere overnight. The cells were treated the next day with ganetespib at indicated concentration for 24 hr. DMSO was used as treatment control. After treatment, RNA was isolated from the cells as described in **(Chapter 2.15).** Duplicate samples (1 µg RNA in 30 µl) were subjected to RNA Sequencing (RNA-seq) analysis (Oxford Gene Technology) and gene expression was quantified using their analysis pipeline (Trapnell et al., 2012) **(Figure 2.1)**.

Briefly, mRNAs were first isolated from the RNA samples and libraries for sequencing were prepared using TruSeq RNA Sample Prep Kit v2 (Illumina). Paired-end sequencing was performed using HiSeq2000 platform (Illumina) and the sequencing reads were mapped onto the human genome (GRCh37) using Bowtie (http://bowtie.cbcb.umd.edu/) and splice junctions were identified using TopHat ((http://tophat.cbcb.umd.edu). The mapped reads were assembled to transcripts and aligned using Cufflinks (http://cufflinks.cbcb.umd.edu/) for differential gene expression between samples. The differential gene expressions were expressed in log2 fold change (FC) and they were considered statistical significant with q-value ≤ 0.05. Q-value is an adjusted p-value that takes into account the false discovery rate within the positive test.

Pathway enrichment analysis was performed on differentially expressed genes in the cells using MetaCore™ (https://portal.genego.com, accessed August 2016) (Thomson Reuters, USA). Mutation profiling was also performed on the sequencing reads to identify any potential sequence variants in the cells. (In collaboration with Dr Anastasia Samsonova, University of Oxford). Variant calling in the RNA-seq data was done with RNASeqmut (version 0.6 with STAR alignment support) using the recommended protocol (https://github.com/davidliwei/rnaseqmut), including raw variant calling, merging variants, genotyping and filtering with standard default parameters.

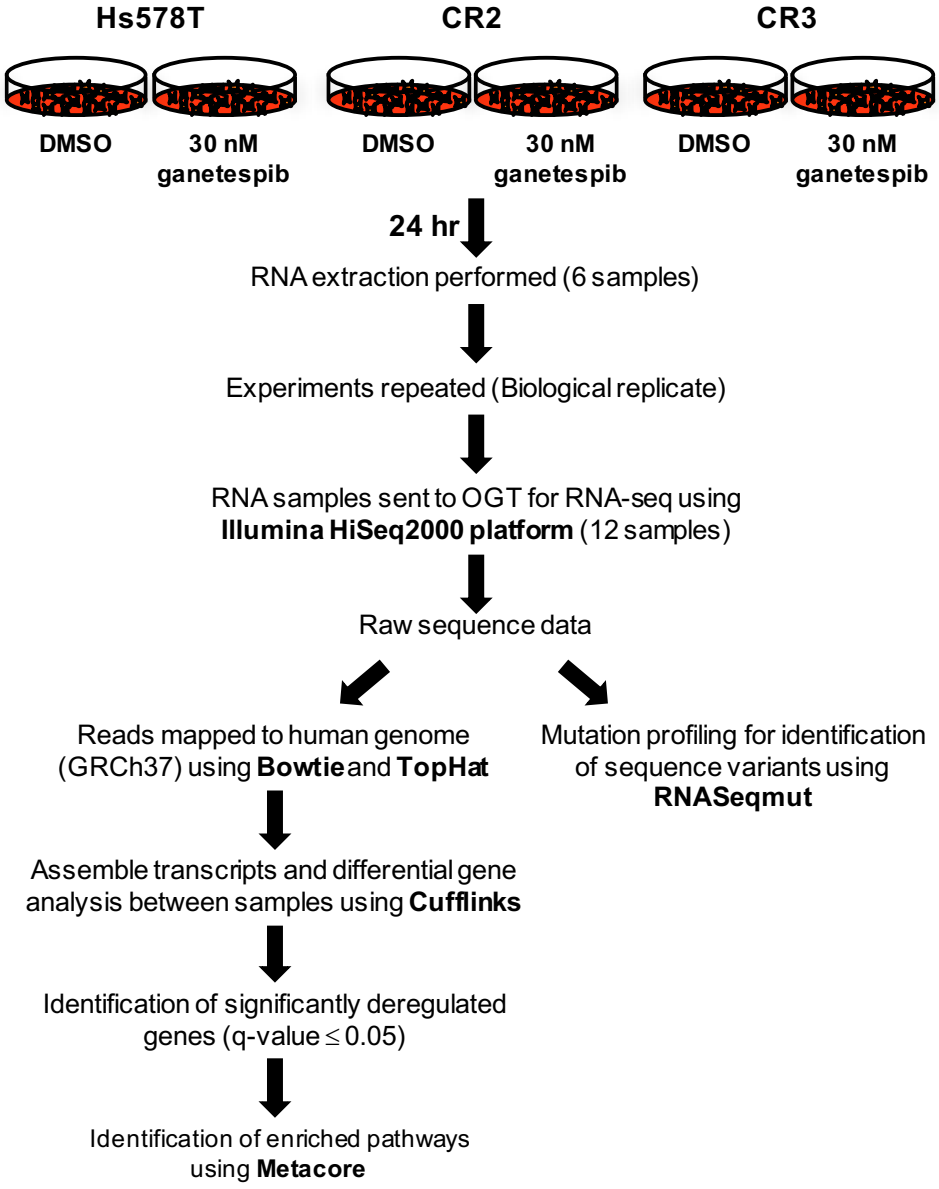


Figure 2.1: Schematic of RNA-seq and analysis pipeline

2.17. Mass spectrometry (MS)

Protein lysates of cells were obtained as described in **(Chapter 2.6)**. The protein concentrations in the lysates were normalised using sample loading buffer and they were then heated to 95°C for 8 min. 40 µg of protein lysates and a protein ladder were resolved onto a 4-15% gradient precast gel Mini-PROTEAN TGX gel and the electrophoresis was set at 250 V for 25 min. After the run was completed, the gel was fixed with prepared fixing solution **(Table 2.1)** for 30 min and proteins on the gel were stained with prepared coomassie solution for 1 hr on a shaker. Destaining solution was added for 3 hr until the protein bands were visible and fresh solution was replaced several times. Protein band of interest was cut using a scalpel and sent to Target Discovery Institute (TDI, University of Oxford) for mass spectrometry (MS). In-gel digestion and MS analysis were performed using to their pipeline (Mackeen et al., 2010, Tomlinson et al., 2015, Fischer et al., 2012).

In summary, in-gel digestion was performed on the gel protein bands using trypsin. The tryptic peptides were extracted from the gel and analysed by nano-LC_MS/MS using a LTQ Orbitrap Velos Elite (Thermo Scientific) coupled to a nano-UPLC system (Nanoacquity, Waters, UK). Full MS scans were acquired over the m/z range of 300 – 1500 at 60000 resolutions. Proteins were identified using MASCOT data search engine version 2.3 (Matrix Science, http://matrixsience.com). MS/MS data was searched against the UniProt_UPR Homo Sapiens database using the Decoy function, while selecting trypsin as enzyme (allowing 1 miscleavage), peptide charge of +2, +3, +4 ions, peptide tolerance of 10 ppm and MS/MS of 0.5 Da; #13C at 1; Carboamidomethylation as fixed modification, and Oxidation (M) and Deamidation (N) as a variable modification. MASCOT data search results were filtered using ion score cut off at 20 and a false discovery rate of 1%.

2.18. Bioactive small molecule screen

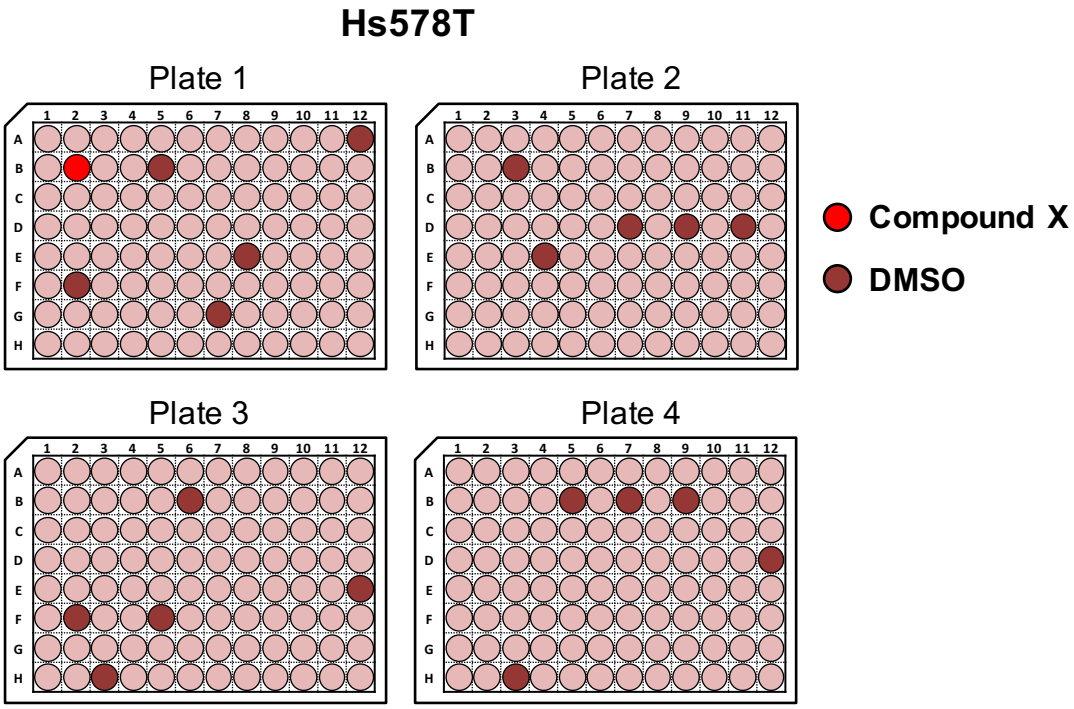
2.18.1. Selleckchem Inhibitor Screening Library

A library containing 326 bioactive small molecule compounds (Selleck, L1100), phleomycin and ganetespib was used in the screen **(Supplementary Table 1)**. The library was distributed into four 96-well plates and each plate also contained wells with DMSO. A stock concentration of each compound was prepared at 10 μM with phenol red free DMEM. Each plate was set up in duplicate and the entire screen was performed twice.

Parental HS578T cells and HSP90i-resistant clone CR3 (800 and 1000 cells respectively) were seeded in 96-well plate and allowed to adhere overnight. The cells were treated the next day with the compounds (final concentration of 1 μM). CR3 cells were also treated in the presence of 10 nM ganetespib. Resazurin-based cell viability was used as an end point **(Chapter 2.5)**. After 72 hr treatment, resazurin solution was added into each well and incubated for 2 hr before the fluorescence intensity (F.I) was measured using a plate reader. After subtracting the average F.I of blank (medium, no cells) from the wells, the F.I was proportional to the number of viable cells

2.18.2. Drug screen analysis

For respective cell line (Hs578T cells, CR3 or CR3 with 10 nM ganetespib), the percentage cell viability after each treatment of compound was first calculated and normalised relative to the average DMSO-treated control in each plate. The average percentage cell viability for each compound calculated from two independent runs performed in duplicates. The average percentage cell viability was then normalised to the overall mean percentage of cell viability from the entire screen for the respective cell line.



For example, the normalised cell viability after treatment of compound X in Hs578T cells:

1) Percentage cell viability to compound X $= \left(\frac{\mathbf{A}}{\mathbf{B}}\right) \times \mathbf{100}$

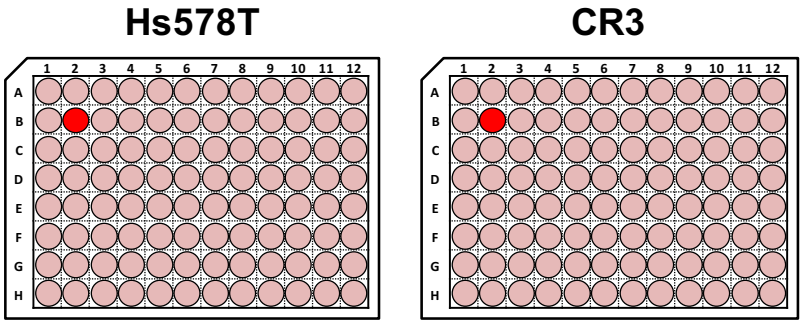
A = F.I after treatment with compound X in Hs578T cells

B = Average F.I after treatment with DMSO in Hs578T cells

2) Normalised cell viability to compound X $= \left(\frac{\mathbf{C}}{\mathbf{D}}\right)$

C = Average percentage cell viability to compound X from two independent runs

D = Mean percentage cell viability from all 328 compounds in Hs578T cells



The sensitivity of each compound were compared between two cell lines. The log value of cell viability to each compound between the cell lines was first calculated. Z-score was determined by normalising the log value of cell viability between the cell lines to the standard deviation (SD) of the entire screen. For example, comparing the sensitivity of compound X between Hs578T cells and HSP90i-resistant clone CR3:

3) log value of cell viability to compound X between cell line $= log\left(\frac{\mathbf{E}}{\mathbf{F}}\right)$

E = Normalised cell viability to compound X in HS578T cells

F = Normalised cell viability to compound X in CR3

4) Z score $= \frac{\mathbf{G}}{\mathbf{SD}}$

G = log value of cell viability to compound X between Hs578T cells and CR3

SD = Standard deviation of log values from all 328 compounds

Z-score ≥ 2 represents that the clone CR3 is sensitive to compound X compared to Hs578T cells

Z-score ≤ -2 represents that the clone CR3 is resistant to compound X compared to Hs578T cells

2.19. PicoGreen® double-stranded DNA assay

A PicoGreen® double-stranded DNA assay was used to assess relative cell growth over time. Cells were seeded in 96-well plates at a density of 300 cells/well and allowed to adhere overnight. The cells were treated the next day with the compound. Each day, cells in triplicates wells were lysed, starting at the time of treatment and continuing until 7 days after treatment. To lyse cells, media was removed and DNA lysis buffer **(Table 2.1)** added into the wells. After all the time points were completed, an equal volume of 2x PicoGreen® solution **(Table 2.1)** was added into all of the wells and incubation continued for 20 mins protected from light. PicoGreen stains double-stranded DNA and the fluorescence intensity (excitation at 480 nm, emission at 520 nm) was measured using the POLARstar Omega plate reader. After subtracting the fluorescence intensity of each well with the blank (absence of cells), the fluorescence intensity is proportional to the DNA content in each well. The PicoGreen fluorescence for each time point was normalised relative to the fluorescence at the start of treatment (0 hr).

2.20. JAK-STAT pathway array

Reverse transcription PCR (RT-PCR) with TaqMan® Array Human JAK-STAT pathway (Applied Biosystems) was used to assess the expression of 92 genes associated with JAK-STAT pathways and 4 endogenous control genes **(Table 2.5)**. Cells (0.8 - 1.0 x 10^6 cells) were seeded in 10 cm plates. The cells were treated the next day with the compound at indicated concentration for 24 hr. After treatment, RNA was isolated from the cells as described in **(Chapter 2.15)**. The RNA was then converted to cDNA using High-Capacity cDNA Reverse Transcription kit (Applied Biosystems); according to the manufacturer's instructions. A 1:1 mixture of RNA samples (100 ng/µl) and master mix reactions were prepared. The reactions were performed using a thermal cycler (Applied Biosystems) set at

25°C for 10 min, 37°C for 2 hr and 85°C for 5 min. The cDNA samples obtained were stored at -20 °C until used.

The PCR reactions for the JAK-STAT array were prepared in 20 µl containing 10 ng of the cDNA samples and TaqMan® Gene Expression Master Mix (Applied Biosystems). Quantitative real-time PCR was performed using the 7500 Fast Real-Time PCR system with these conditions:

Hot start	50°C	2 min	
	95°C	10 min	
Denaturation	63°C	15 sec	40 cycles
Annealing/Extension	72°C	1 min	

For each sample, the fluorescence signal produced by the TaqMan® probes depends on the amount of cDNA that was generated from the mRNA encoded by each gene. The increase in fluorescent signal was proportional to the amplification of cDNA with every cycle. The Ct value was calculated and compared between samples. The Ct values within each run were first normalised to an endogenous control gene (GAPDH). The relative expression of each gene between samples was done using the comparative Ct method (ΔΔCt):

$\Delta Ct_{sample} = Ct_{sample} - Ct_{GAPDH}$

$\Delta Ct_{control\ cells} = Ct_{control\ cells} - Ct_{GAPDH}$

$\Delta\Delta Ct = \Delta Ct_{sample} - \Delta Ct_{control\ cells}$

Relative expression $= 2^{-\Delta\Delta Ct}$

Table 2.5: Expression of genes detectable with TaqMan® Array Human JAK-STAT pathway

Genes			
18S*	IFNA2	MAP2K4	RAN
GAPDH*	IFNAR1	MAP2K6	SH2B1
HPRT1*	IFNB1	MAPK1	SMAD3
GUSB*	IFNG	MAPK3	SMAD4
AKT1	IFNGR1	MCM5	SOCS1
AKT2	IGF1R	MPL	SOCS2
AKT3	IL10	MYC	SOCS3
BRCA1	IL1B	NRAS	SOS1
CD4	IL1R1	PIAS1	SP1
CREBBP	IL2RA	PIK3CA	STAM
EGF	IL4R	PIK3CB	STAT1
EGFR	IL6	PIK3CD	STAT2
ELP2	IL8	PIK3R1	STAT3
EP300	IRF9	PIK3R2	STAT5B
EPO	JAK1	PRL	STAT6
EPOR	JAK2	PRLR	SUMO1
ERBB2	JAK3	PSMA3	THPO
FGF2	JUN	PSMB5	TNFRSF1A
FOS	KIT	PSMC4	TNFRSF1B
GH1	KPNA1	PSMC5	TYK2
GHR	KRAS	PSMD4	UBB
GRB2	MAP2K1	PTPN11	UBC
HRAS	MAP2K2	PTPN6	UBE2I

*endogenous control genes

2.21. Enzyme-linked immunosorbent assay (ELISA)

Cells were seeded in 96-well plate at a density of 5.0 x 10^3 cells/well and allowed to adhere overnight. The cells were treated the next day with the compound at indicated concentration for 24 hr. After treatment, the media from the wells were collected and centrifuged at 280 x g for 5 min. Supernatants were collected and stored at -20°C before performing the enzyme-linked immunosorbent assay (ELISA) using the Quantikine ELISA Human IL-6 kit (R&D Systems); according to the manufacturer's instructions.

In summary, the medium collected was added in duplicate into the strips of 8 wells that were pre-coated with monoclonal antibody specific for human IL-6. After incubating for 2 hr at

room temperature, the wells were washed four times with wash buffer and incubated with polyclonal antibody specific for human IL-6 conjugated to horseradish peroxidase for 2 hr at room temperature. After washing the wells again with wash buffer, they were incubated with substrate solution (hydrogen peroxide and chromogen) for 20 min at room temperature before stopping the reaction with a stop solution (2 N sulfuric acid). The absorbance at 450 nm for each well was measured using the POLARstar Omega plate reader. The optical density (450 nm) for each well was proportional to the IL6 concentration in the media. The concentration of IL-6 in the media after treatment was normalised relative to the DMSO-treated HS578T cells.

2.22. Statistical analysis

GraphPad Prism® 7 (GraphPad Software, USA) was used for all statistical analyses and to generate graphs including heatmaps. For data comparison between cell lines and treatment conditions, two-way analysis of variance (ANOVA) was used. For comparison between two groups, Student's t-test was used. Statistical significance of p values ≤ 0.05, ≤ 0.01, ≤ 0.001, ≤ 0.0001 were represented as *, **, ***, **** respectively.

3. Establishment of an in vitro model to study resistance mechanisms to HSP90i

3.1. Introduction

HSP90i demonstrates effective anti-cancer activities in various cancers, including TNBC. It causes degradation of several client proteins simultaneously (EGFR, IGF-1R and MET), tumour growth inhibition, induction of apoptosis and cell cycle arrest as well as clinical tumour response in patients (Solit et al., 2002, Banerji et al., 2005, Proia et al., 2014) (Friedland et al., 2014). Even though HSP90i is a promising therapeutic approach for TNBC, clinical studies showed that resistance to HSP90i can still arise in TNBC patients (Awada et al., 2013). Resistance to targeted therapies remains a major challenge in cancer patients (Groenendijk and Bernards, 2014).

Tumours can have either (i) intrinsic (de novo) resistance, where they do not respond to the therapies or (ii) acquired resistance, where they have an initial response to the therapies but subsequently become refractory and this resistance to therapies causes disease progression in cancer patients (Ellis and Hicklin, 2009). An understanding of resistance mechanisms to targeted therapies allows identification of predictive biomarkers for better selection of patients for treatment and/or alternative therapies after disease progression. For example, *KRAS* mutations cause intrinsic resistance to EGFR monoclonal antibodies in colorectal cancer and screening for *KRAS* mutations in these patients is recommended in the clinic as a predictive biomarker for the treatment (Lievre et al., 2006, Allegra et al., 2009).

There are several in vitro and in vivo models to study resistance to therapies. These include using primary cultures of cancer cells derived from patient tumours and established human immortalised cancer cell lines in vitro as well as xenografts using cancer cell lines and patient-derived tumours in immunocompromised mice in vivo studies (Rosa et al., 2014). Both approaches have advantages and disadvantages. Samples derived from cancer patients may be the most clinically relevant compared to cell lines as they maintain the characteristics of the tumours when obtained. However, patient samples are not readily available compared

to established cancer cell lines. Invasive tumour biopsies from patients are required and the obtained cells do not all effectively grow in culture or when engrafted into mice (Hidalgo et al., 2014).

In vivo models using mice provide a microenvironment that mimics the human tumour microenvironment and can be used for drug testing at multiple doses and schedules (Denayer et al., 2014). However, the assessment of treatment efficacy (growth and response) over a course of treatment can be challenging. Additionally, in vivo studies are often time-consuming and expensive (Denayer et al., 2014). In vitro studies with established cancer cell lines allow experimental manipulation, detailed mechanistic and high-throughput studies with controlled conditions, including transfections and drug screening assays (Ferreira et al., 2013, Wilding and Bodmer, 2014). Several cancer cell lines are genetically characterised and these data allow prediction of sensitivity to several anti-cancer therapies (Garnett et al., 2012, Barretina et al., 2012).

Several in vitro models have been used to successfully identify clinically relevant intrinsic and acquired resistance to other anti-cancer targeted agents, including the ones targeting EGFR, ABL, ALK, BRAF and HER2 (Rosa et al., 2014). For example, MET amplification leads to EGFR inhibitor (gefitinib) resistance in lung cancer patients. It was described in acquired gefitinib-resistant lung cancer cells derived from gefitinib-sensitive cancer cell lines after prolonged exposures to EGFR inhibitor (Engelman et al., 2007).

In this chapter, we examined the anti-cancer activities of HSP90i in TNBC cells and focused on the establishment of an in vitro model to identify potential mechanisms of resistance to HSP90i in TNBC using ganetespib as a source of HSP90i- the leading HSP90i in late stage clinical development for several cancers (Proia and Bates, 2014).

3.2. The effects of HSP90i in TNBC cells

3.2.1. Inhibition of cell viability

In order to investigate the sensitivity of TNBC cell lines to HSP90i, a panel of seven TNBC cell lines (MDA-MB-468, HCC1937, HCC1143, MDA-MB-231, Hs578T, MDA-MB-453 and BT20) was treated with increasing concentrations of ganetespib for 3 days and cell viability was assessed using a resazurin-based assay. The seven TNBC cells showed differential sensitivity to ganetespib over a 5- fold range, with Hs578T being the most sensitive cell line (IC_{50} = 4.79 ± 0.32 nM) and HCC1143 being the least sensitive cell line (IC_{50} = 22.59 ± 6.82 nM) **(Figure 3.1 and Table 3.1)**.

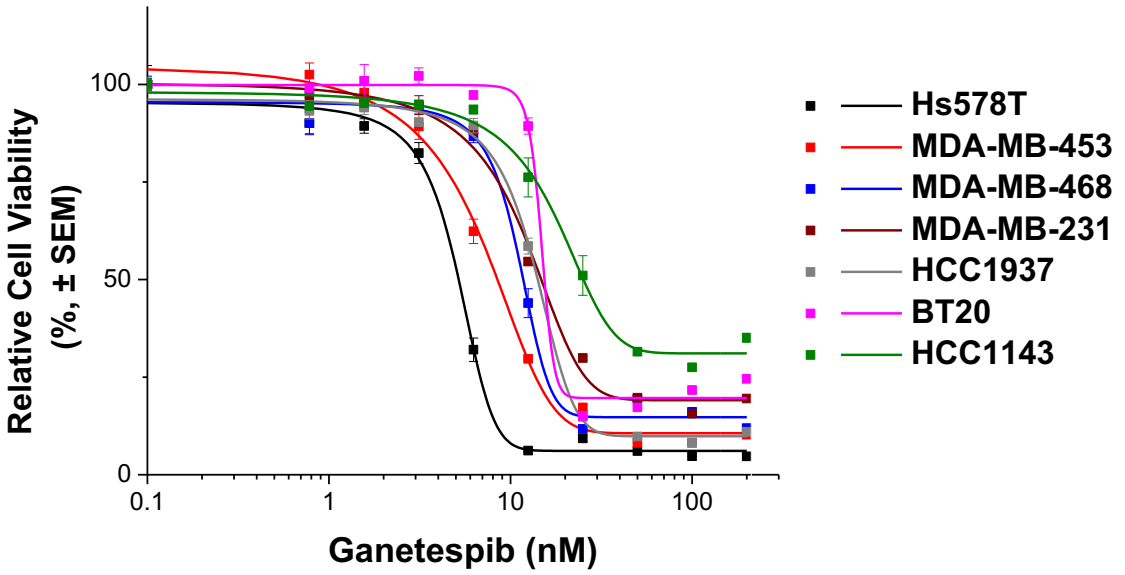


Figure 3.1: Differential sensitivity to ganetespib in TNBC cell lines

A panel of TNBC cell lines (Hs578T, MDA-MB-453, MDA-MB-468, MDA-MB-231, HCC 1937, BT20 and HCC1143) was treated with increasing concentrations of ganetespib (0 - 200 nM) for 72 hr and cell viability was assessed using a resazurin-based assay. Percentage of cell viability was expressed relative to the DMSO-treated control. Representative graph from three independent experiments each performed in triplicates. Error bars indicate SEM.

Table 3.1: Sensitivity to ganetespib in TNBC cell lines

TNBC cell lines	Ganetespib (nM) IC_{50} ± SEM
Hs578T	4.79 ± 0.32
MDA-MB-453	6.92 ± 0.73
MDA-MB-468	11.29 ± 0.71
MDA-MB-231	12.56 ± 1.05
HCC1937	12.90 ± 0.29
BT20	13.99 ± 0.74
HCC1143	22.59 ± 6.82

3.2.2. Downregulation of HSP90 client proteins

HSP90 is involved in the regulation of several client proteins, including EGFR and its downstream signalling pathway protein (AKT) (Neckers and Workman, 2012). Since EGFR is overexpressed in TNBC, the effects of HSP90i on EGFR and AKT were examined in the TNBC cell lines (Shah et al., 2012, Nielsen et al., 2004). After treatment with increasing concentrations of ganetespib for 24 hr in Hs578T cells, western blotting analysis showed a dose-dependent downregulation of EGFR and AKT as well as a decrease in their phosphorylation (pEGFR and pAKT) at Y1068 and S473 respectively **(Figure 3.2A)**. Similar effects of ganetespib treatment were also seen in other TNBC cells; MDA-MB-231 and HCC1143 **(Figure 3.2B and C)**, although there was heterogeneity in basal levels of EGFR in the cells **(Figure 3.3)**.

HSP90i activates heat shock transcription factor protein 1 (HSF1), which in turn promotes HSP70 gene expression (Elo et al., 2005). HSP70 (a co-chaperone of HSP90) protein level is used as a pharmacodynamic marker of HSP90i in several studies, including colon and ovarian cancer cells (Clarke et al., 2000, Banerji et al., 2005). As expected, dose-dependent upregulation of HSP70 was observed in Hs578T, MDA-MB-231 and HCC1143 cells after ganetespib treatment. Taking together, these data suggest that HSP90i in TNBC cells leads

to a dose-dependent inhibition of HSP90 activity and downregulation of HSP90 client proteins (EGFR and AKT).

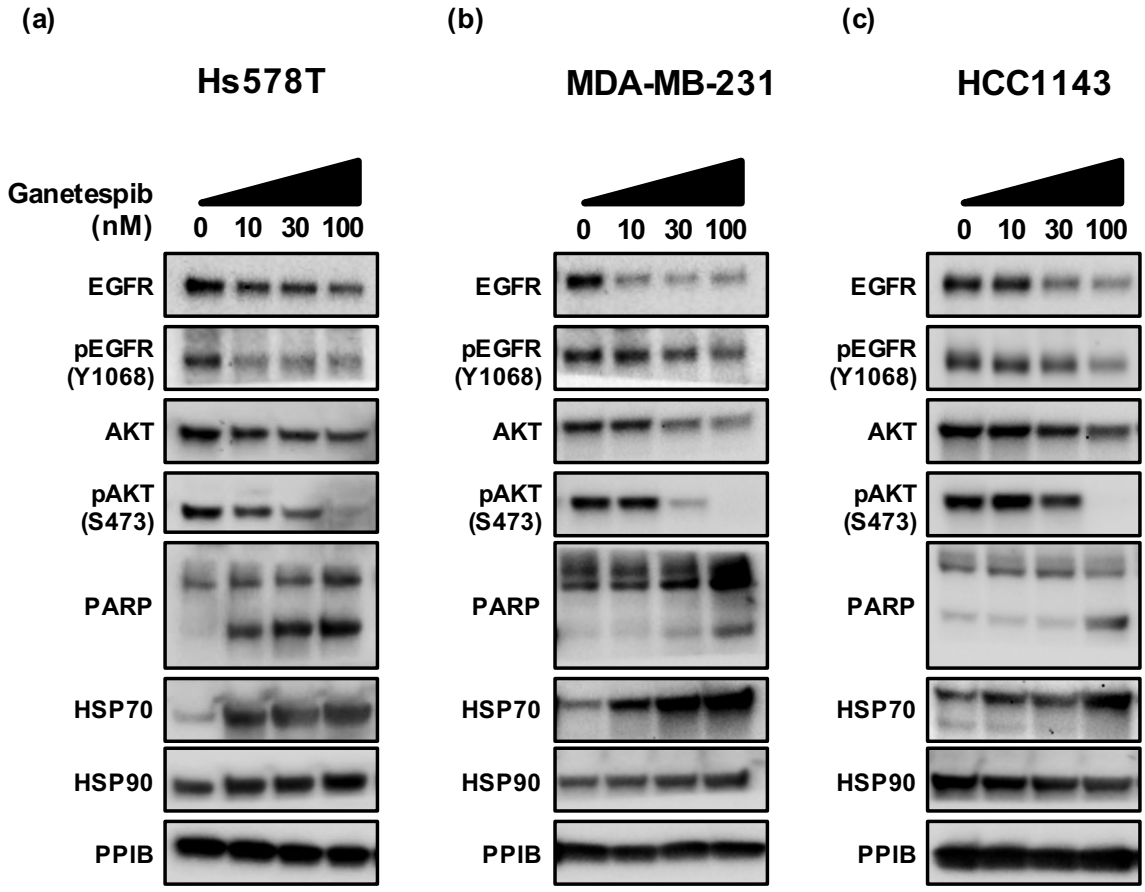


Figure 3.2: The effect of ganetespib treatment on EGFR signalling pathways in TNBC cells

(a) Hs578T, **(b)** MDA-MB-231 and **(c)** HCC1143 cells were treated with ganetespib (0 - 100 nM) for 24 hr. Protein lysates were analysed by western blotting. EGFR signalling pathways (EGFR and AKT, including their phosphorylation states) were used to assess the effect of HSP90i on client proteins. Cleaved PARP was used to assess induction of apoptosis and HSP70 was used as a pharmacodynamics marker for inhibition of HSP90 activity. PPIB was used as loading control.

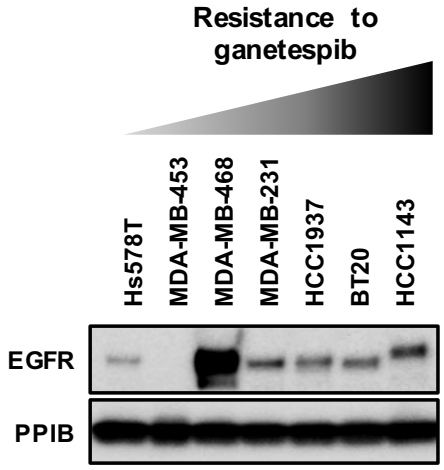


Figure 3.3: Expression of HSP90 oncogenic client protein (EGFR) in TNBC cells

Lysates of TNBC cell lines (Hs578T, MDA-MB-453, MDA-MB-468, MDA-MB-231, HCC1937, BT20 and HCC1143) were analysed by western blotting. PPIB was used as loading control.

3.2.3. Induction of apoptosis

HSP90 client proteins are involved in the regulation of cellular proliferation and survival (Garg et al., 2016). Therefore, TNBC cells were examined to determine whether the decrease in cell viability seen after ganetespib treatment was associated with increased apoptosis. To assess apoptosis, the level of cleaved-PARP after treatment with increasing concentration of ganetespib was measured in Hs578T, MDA-MB-231 and HCC1143 cells by western blotting. A dose-related increase in cleaved PARP levels was observed in the TNBC cells after ganetespib treatment **(Figure 3.2)**. Apoptosis induction was associated with ganetespib sensitivity in these cells. The most sensitive TNBC cell line, Hs578T cells, showed higher induction of apoptosis after 30 nM ganetespib treatment compared to MDA-MB-231 and HCC1143 cells.

Flow cytometry analysis with PI and Annexin V staining was performed on MDA-MB-231 and MDA-MB-468 cells as another method to assess apoptosis after ganetespib treatment. Consistent with cleaved PARP results, a dose-related increase in Annexin V positive cells was observed in both cell lines after treatment with increasing concentration of ganetespib

for 72 hr **(Figure 3.4)**. Taken together, these observations suggest that the inhibition of HSP90 activity by ganetespib in the panel of TNBC cell lines leads to inhibition of cell viability, downregulation of HSP90 client proteins, and induction of cell death by apoptosis.

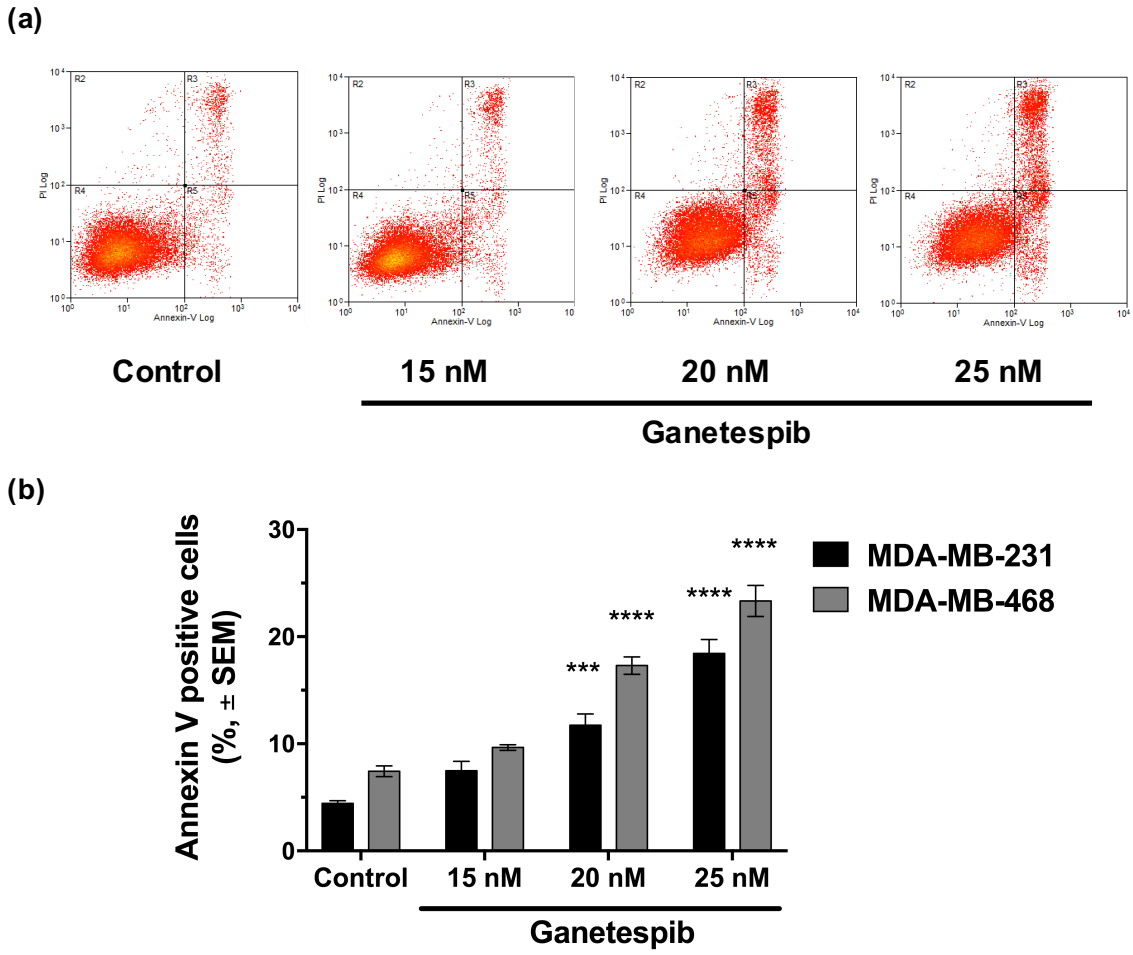


Figure 3.4: The effect of ganetespib treatment on apoptosis in TNBC cells

MDA-MB-231 and MDA-MB-468 cells were treated with ganetespib (0- 25 nM) for 72 hr and subjected to flow cytometry with PI and Annexin V staining. **(a)** Representative images of cell populations with PI staining (y-axis) and Annexin V staining (x-axis). The cell populations consisted of live cells (bottom left, double negative staining), necrotic cells (top left, Annexin V negative/ PI positive), early apoptotic cells (bottom right, Annexin V positive/PI negative) and late apoptotic cells (top right, double positive staining).

(b) The graph represents the percentage of apoptotic cells (Annexin V positive cells) in MDA-MB-231 and MDA-MB-468 cells after ganetespib treatment relative to the total number of cells analysed from three independent experiments each performed in duplicates; error bars indicate SEM. Within each cell line, ganetespib-treated cells at indicated concentrations were compared to DMSO-treated cells. ***, **** indicate p values <0.001, <0.0001 respectively; which was determined by ANOVA with cell line and dose as factors.

3.3. Generation of HSP90i-resistant clones

Hs578T was the most sensitive cell line among the panel of TNBC cells, and was used to generate HSP90i-resistant TNBC cells. Hs578T cells were exposed to ganetespib (at concentrations >IC_{50}) for selection of HSP90i-resistant clones **(Figure 3.5)**. Hs578T cells were first plated onto ten 10 cm plates (10^5 cells per plate). After three days, cells were treated with 30 nM (8 plates), 50 nM (1 plate) or 100 nM (1 plate) ganetespib. The medium was replaced by fresh media containing ganetespib once every week during the incubation.

Resistant Hs578T cells did not emerge during treatment with 50 nM or 100 nM ganetespib. However, after six weeks of 30 nM ganetespib treatment, individual colonies grew in the plates. Six independent clones were picked from different plates and sub-cultured into 6-well plates. Three out of the six clones (CR2, CR3 and CR6) grew in the presence of 30 nM ganetespib through several passages. The two best growing clones (CR2 and CR3) were selected for further studies and maintained in culture in the presence of 30 nM ganetespib.

The sensitivity of CR2 and CR3 to ganetespib was assessed using the resazurin-based cell viability assay. The dose-response curve of CR2 and CR3 showed that they were more resistant to ganetespib compared to parental Hs578T cells **(Figure 3.6a)**. The IC_{50} values of CR2 and CR3 were 15.57 ± 1.90 nM and 20.28 ± 2.75 nM respectively. They were 4 to 5-fold higher than the IC_{50} value of parental Hs578T cells (IC50 = 4.79 ± 0.32 nM) **(Table 3.2)**. Both clones also showed cross-resistance to 1st generation (17-AAG) and 2nd generation (NVP-AUY922) HSP90i, more markedly to NVP-AUY922 **(Figure 3.6b and c, Table 3.2)**. Since ganetespib and NVP-AUY922 are resorcinol-based HSP90i, the underlying mechanisms of resistance to these HSP90i might overlap. These results suggest that clones CR2 and CR3 have acquired significant resistance to HSP90i, notably to resorcinol-based HSP90i.

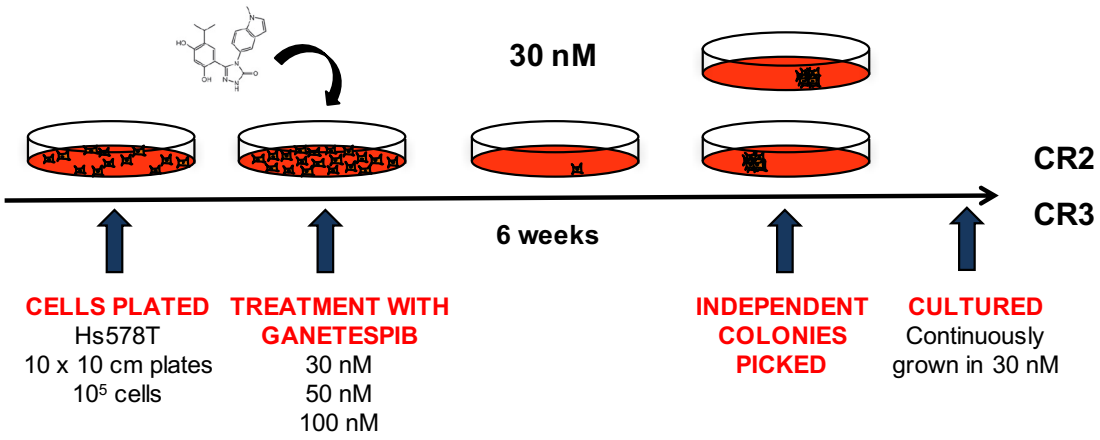


Figure 3.5: Generation of HSP90i-resistant Hs578T clones

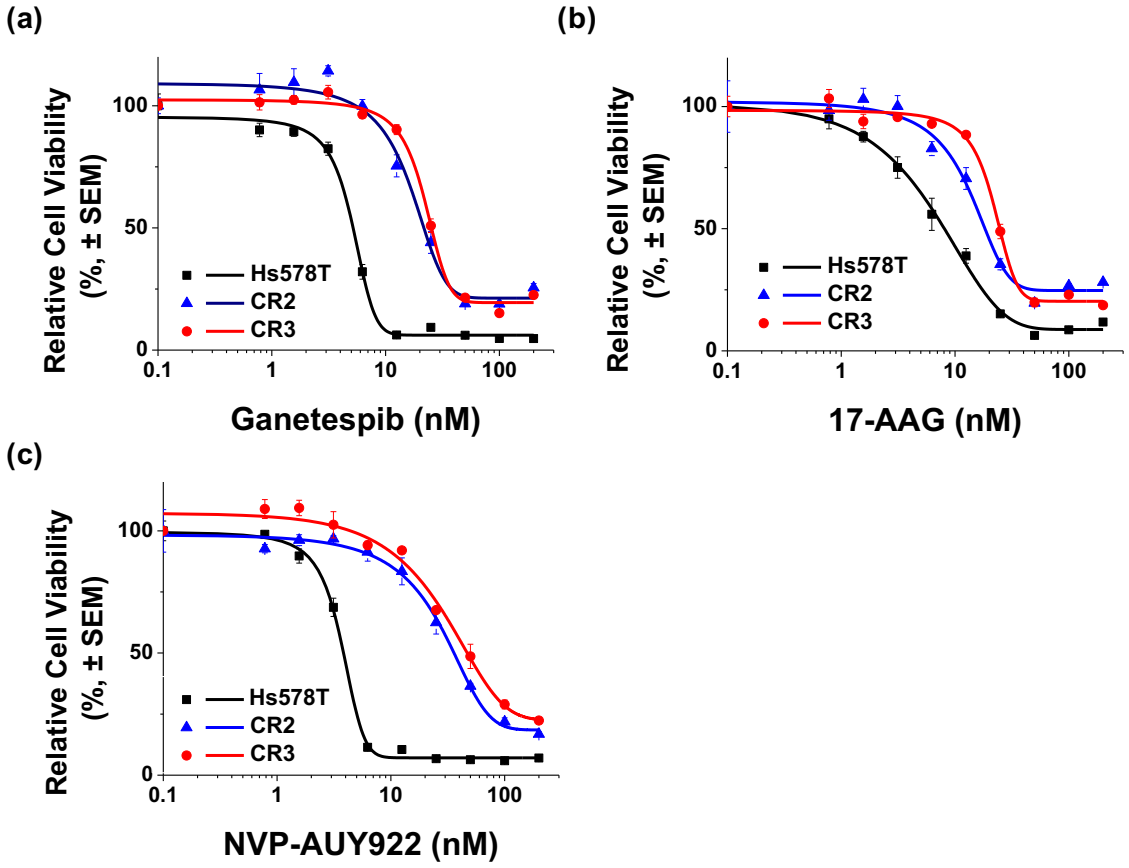


Figure 3.6: Cross-resistance to HSP90i in HSP90i-resistant clones

Hs578T, CR2 and CR3 cells were treated with increasing concentrations (0 - 200 nM) of HSP90i for 72 hr, **(a)** ganetespib **(b)** 17-AAG and **(c)** NVP-AUY922. Cell viability was assessed using a resazurin-based assay. Cell viability (%) for each treatment was expressed relative to the DMSO-treated control. Representative graphs from three independent experiments, each performed in triplicates. Error bars indicate SEM.

Table 3.2: Sensitivity to HSP90i in parental Hs578T cells and HSP90i-resistant clones CR2 and CR3

Cell line	Ganetespib (nM) IC_{50} ± SEM	17-AAG (nM) IC_{50} ± SEM	NVP-AUY922 (nM) IC_{50} ± SEM
Hs578T	4.79 ± 0.32	8.60 ± 1.80	3.64 ± 1.80
CR2	15.57 ± 1.90	15.23 ± 1.24	29.12 ± 1.24
CR3	20.28 ± 2.75	21.92 ± 5.93	34.04 ± 5.93

3.4. Characterisation of HSP90i-resistant clones

3.4.1. The effect of HSP90i on HSP90 client proteins

After successful generation of HSP90i-resistant clones, the cytotoxic effects of HSP90i including the effect on HSP90 client proteins (EGFR and AKT) and induction of apoptosis in the clones were assessed and compared with parental Hs578T cells. Total and phosphorylated EGFR and AKT protein levels were not downregulated after 30 nM ganetespib treatment in either CR2 or CR3 **(Figure 3.7a)**. Ganetespib treatment also did not induce cleaved PARP in CR2 and CR3 **(Figure 3.7b)**. However, upregulation of HSP70 was observed after ganetespib treatment in CR2 and CR3 suggesting that the compound was pharmacologically active in these cells **(Figure 3.7a)**. Interestingly, basal levels of HSP70 in CR2 and CR3 were higher than in parental Hs578T cells, suggesting that increased HSP70 expression might be associated with the resistance to HSP90i. These observations also suggest that, although ganetespib is still pharmacologically active in the HSP90i-resistant clones, the cells are able to escape the downregulation of client proteins and induction of apoptosis.

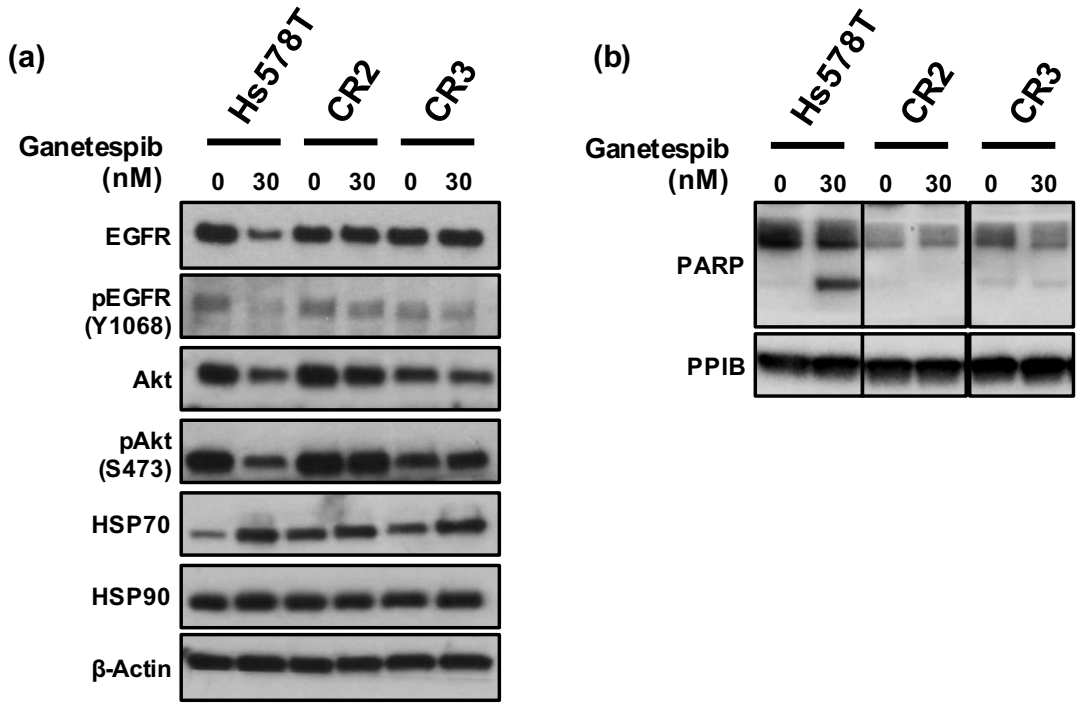


Figure 3.7 The effect of ganetespib treatment on EGFR signalling in HSP90i-resistant clones

Parental Hs578T cells and HSP90i-resistant clones CR2 and CR3 were first plated in the absence of ganetespib. The next day, cells were treated with 30 nM ganetespib for 24 hr. Lysates were subjected to western blotting analysis. **(a)** EGFR signalling pathways (EGFR and AKT, including their phosphorylation states) were used to assess the effect of HSP90i on client proteins. HSP70 was used as a pharmacodynamic marker for inhibition of HSP90 activity. **(b)** Levels of cleaved PARP were also determined to assess induction of apoptosis. PPIB and β-actin were used as loading controls. Representative images from two experiments are shown.

3.4.2. The effect of HSP90i on cell cycle in HSP90i-resistant clones

Proteins involved in the regulation of cell cycle are HSP90 client proteins and HSP90i causes disruption of cell cycle in several cancers (Burrows et al., 2004). In this study, the effect of HSP90i on cell cycle was assessed in parental Hs578T cells and HSP90i-resistant clones using flow cytometry with PI and BrdU staining. Flow cytometry analysis demonstrated that ganetespib treatment (30 nM ganetespib, 24 hr) reduced the proportion of BrdU-labelled S-phase cells and led to an accumulation of cells in the G2/M-phase in Hs578T cells **(Figure 3.8a)**. However, the level of BrdU-labelled cells in each cell cycle phase was unaffected in both CR2 and CR3 clones after ganetespib treatment **(Figure 3.8b and c)**. These observations indicate that HSP90i causes a G2/M cell cycle arrest in TNBC cells. However, HSP90i-resistant clones are able to escape this cell cycle arrest.

3.4.3. The effect of HSP90i on colony formation in HSP90i-resistant clones

We showed that HSP90i did not induce apoptosis in the HSP90i-resistant clones. The HSP90i-resistant clones CR2 and CR3 were also tested in colony forming assay to assess whether their proliferative ability upon HSP90i was affected compared to parental Hs578T cells. A dose-dependent decrease in colony forming ability was observed in parental Hs578T, CR2 and CR3 cells after treatment with increasing concentrations of ganetespib for 24 hr **(Figure 3.9a)**. However, parental Hs578T cells had significantly greater inhibition of colony formation ability compared to CR2 and CR3 after ganetespib treatment **(Figure 3.9b)**. These data suggest that the effect on the inhibition of colony formation is reduced in the HSP90i-resistant clones when compared to parental Hs578T cells.

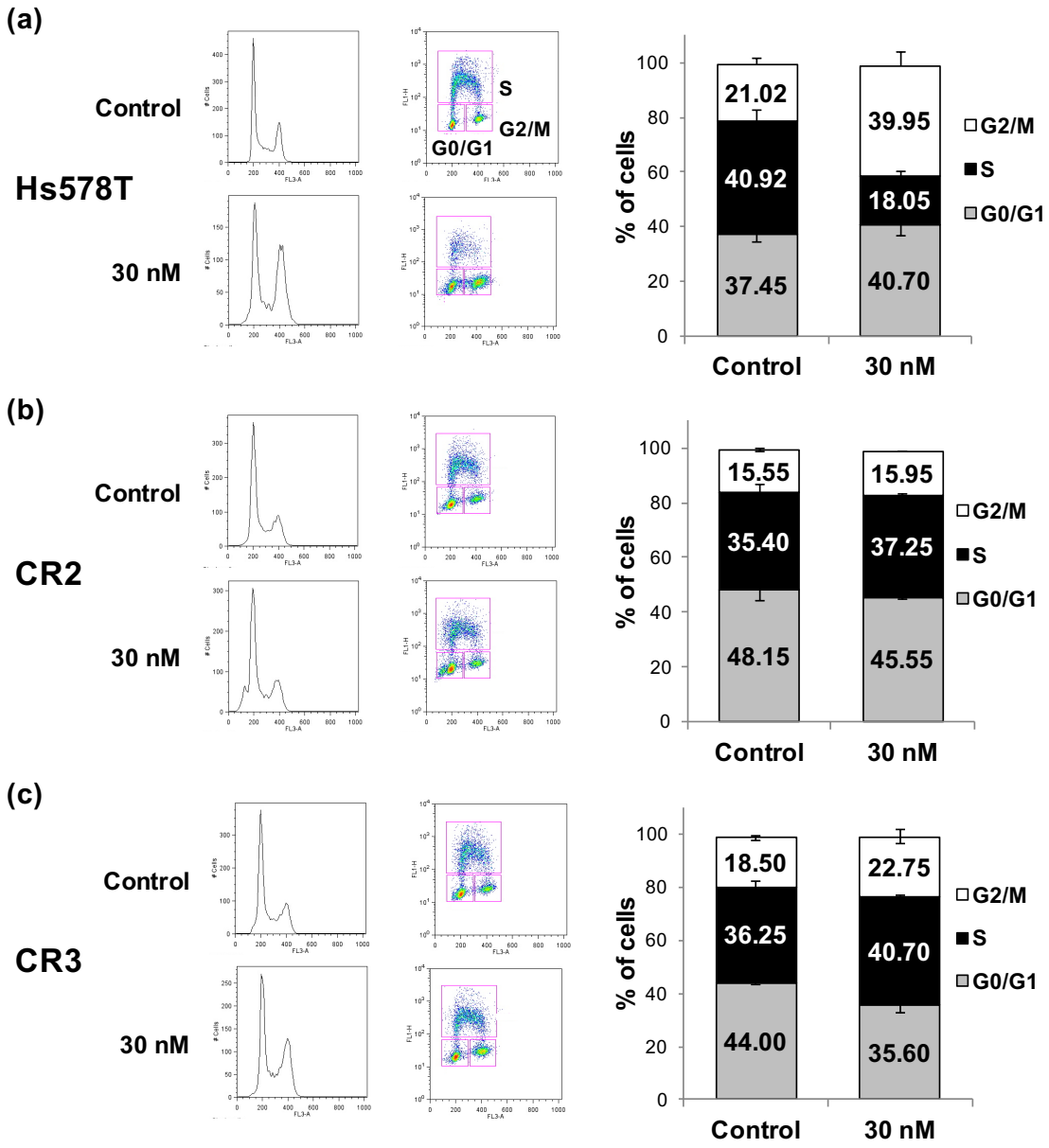


Figure 3.8: G2/M cell cycle arrest seen only in parental Hs578T

(a) Parental Hs578T, **(b)** HSP90i-resistant Hs578T clones CR2 and **(c)** CR3 were treated with 30 nM ganetespib for 24 hr and pulse labelled with BrdU for 20 min prior to analysis to label cells in S-phase. Cells were stained with PI and anti-BrdU antibody and analysed by flow cytometry. The images in the left panels represent the DNA content from PI staining (FL3-A) and the central panels represent the cell population with BrdU staining (FL1-H, y-axis) and PI staining (FL3-A, x-axis). The cell populations consisted of G0/G1- (bottom left), G2/M- (bottom right) and S-phase. The graphs on the right represent the mean percentage of cell population in each phase of cell cycle from two independent experiments, each performed in duplicates. Error bars indicate SEM.

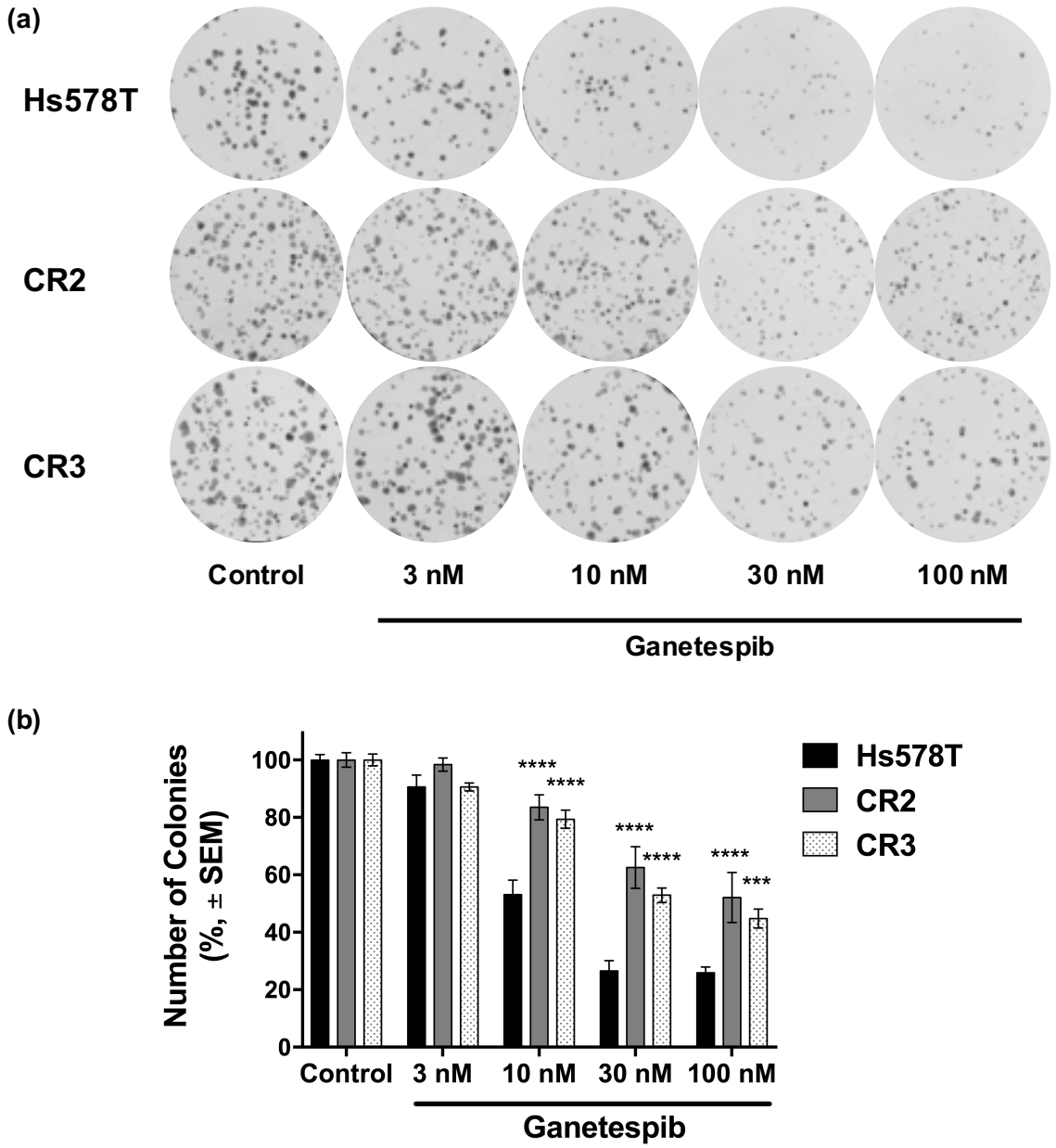


Figure 3.9: Inhibition of colony formation after HSP90i in TNBC cells

Parental Hs578T (300 cells/well) and HSP90i-resistant clones CR2 and CR3 cells (800 cells/well) were plated onto 6 well plates and treated with the indicated concentration of ganetespib for 24 hr. After replacing the media with fresh media without ganetespib, their colony forming abilities were assessed. **(a)** Representative images of colonies for the treated cells. **(b)** Colony formation expressed as mean number of colonies (%) relative to DMSO-treated control from three independent experiments each performed in triplicates. Error bars indicate SEM (n=3). The HSP90i-resistant clones CR2 and CR3 were compared to parental Hs578T cells treated with same concentration of ganetespib. ***, **** indicate p values <0.001, <0.0001 respectively; which was determined by ANOVA with cell line and dose as factors.

3.4.4. Sequence variants in HSP90i-resistant clones

Whole transcriptome sequences of HSP90i-resistant clones CR2 and CR3 were obtained from RNA sequencing (RNA-seq, refer to Chapter 4.3). Genomic profiling was performed on these clones by comparing their sequences with parental Hs578T cells to identify any sequence variants that might affect sensitivity to HSP90i. Thirty-five sequence variants were observed in CR2 and CR3 when compared to Hs578T cells **(Supplementary Table 2)**. No mutations in the HSP90 gene were detected in either of the HSP90i-resistant clones. However, CR2 and CR3 shared 32 missense variants and one stop-gain variant. A heterozygous stop-gain variant on the POLQ gene (c.6850 G>A, p.R2241*) was seen in both clones CR2 and CR3 and was validated on genomic DNA using Sanger DNA sequencing with POLQ primers **(Figure 3.10)**. Since HSP90i-resistant clones CR2 and CR3 are independent clones, arising on different selection plates, these results suggest that both clones may have been derived from a pre-existing, genetically distinct, subpopulation of cells within the parental Hs578T cell line.

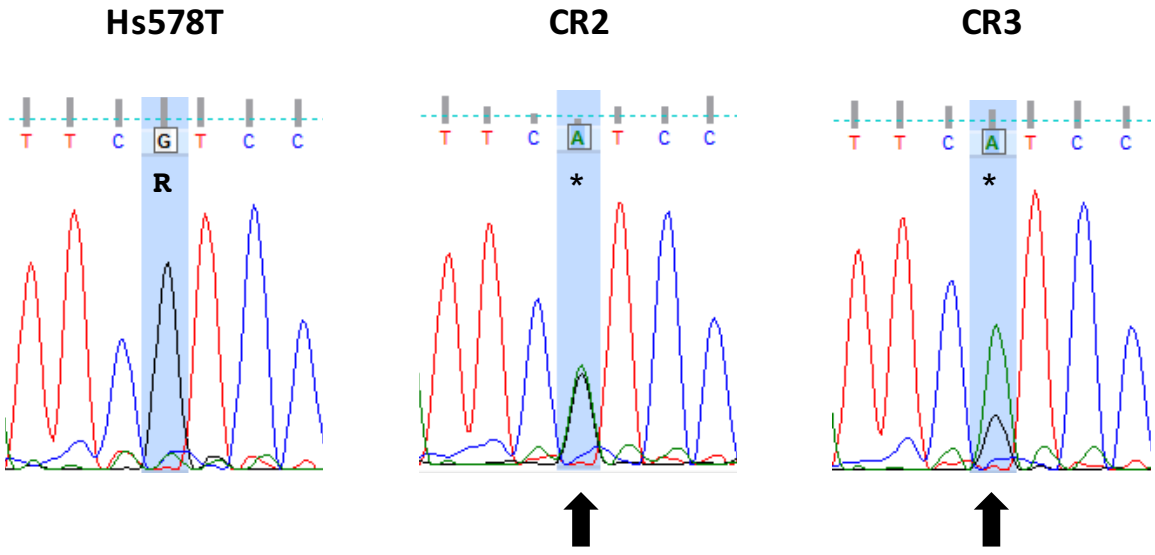


Figure 3.10: Verification of stop-gain variant on the POLQ gene in HSP90i-resistant clones by Sanger DNA sequencing

DNA from parental Hs578T, CR2 and CR3 cell lines was isolated and the POLQ gene amplified by PCR and analysed by Sanger DNA sequencing. The chromatogram shows the presence of a heterozygous stop-gain variant on the POLQ gene (c.6850 G>A, p.R2241*) in HSP90i-resistant clones CR2 and CR3. Arrows indicate the position of sequence variant.

3.5. The relationship between HSP70 expression and the sensitivity of TNBC cells to HSP90i

HSP70 protein expression might be associated with resistance to HSP90i in TNBC cells. Increased HSP70 protein levels were seen in the HSP90i-resistant clones when compared with parental Hs578T cells **(Figure 3.7a)**. The relationship between HSP70 expression and ganetespib sensitivity in TNBC cells was investigated. HCC1143 cells expressed the highest level of HSP70 and MDA-MB-231 cells expressed the lowest level **(Figure 3.11a)**. There was a positive correlation between ganetespib IC_{50} values and HSP70 protein levels ($r = 0.6380$), but it was not statistical significant ($p = 0.1231$), possibly due to the small sample size ($n=7$). Nevertheless, the positive trend suggested that higher HSP70 expression in HCC1143 cells might contribute to ganetespib resistance **(Figure 3.11b)**. The effect of HSP70 expression on ganetespib sensitivity in HCC1143 cells was further investigated.

siRNA knockdown of HSP70 expression was optimised in HCC1143 cells **(Figure 3.12).** However, reduced HSP70 expression did not significantly affect sensitivity to ganetespib **(Figure 3.13 and Table 3.3)**. The sensitivity of a small molecule HSP70 inhibitor (VER-11508) was determined in HCC1143 cells, parental Hs578T cells and one of the HSP90i-resistant clones (CR3). There was no apparent difference in sensitivity to VER-11508 between the different cell lines (IC_{50}>10 μM) **(Figure 3.14)**. Together, these data suggest that HSP70 expression levels are not a major determinant of resistance to HSP90i in TNBC cells.

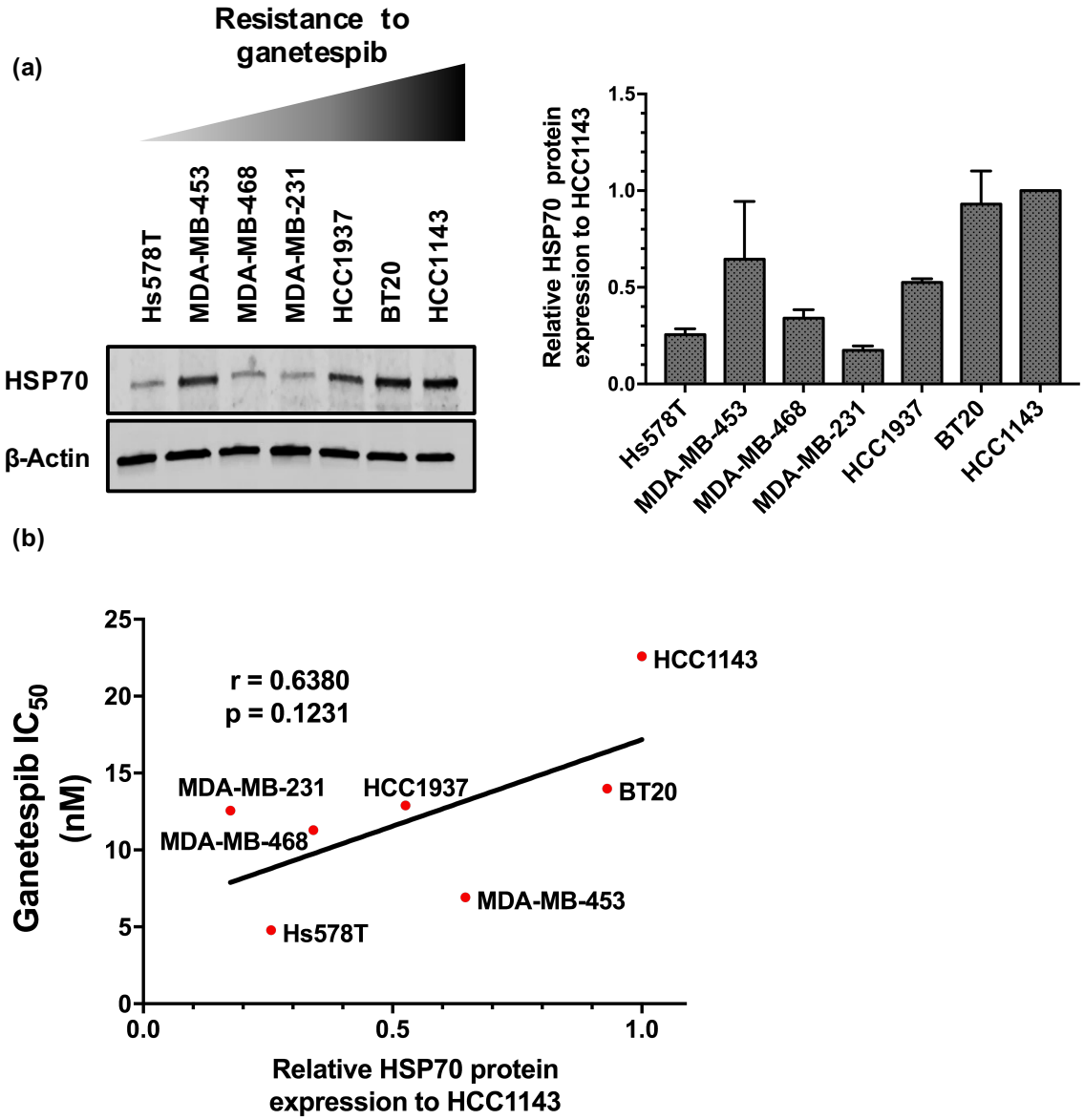


Figure 3.11: Correlation of HSP70 expression with ganetespib sensitivity (IC_{50})

(a) TNBC cell lines (Hs578T, MDA-MB-453, MDA-MB-468, MDA-MB-231, HCC 1937, BT20 and HCC1143) were analysed by western blotting. β-actin was used as loading control. Densitometric quantification of HSP70 protein band for each cell line was calculated after normalisation to its respective loading control and expressed relative to the protein band intensity in HCC1143 cells. The graph represents the mean relative HSP70 protein expression of TNBC cell lines from three independent experiments. Error bars indicate SEM (n=3).

(b) The scatter plot displays the relationship between ganetespib sensitivity (IC_{50}) and mean relative HSP70 protein expression of TNBC cell lines compared to HCC1143 cells, which was determined by Pearson's correlation (r).

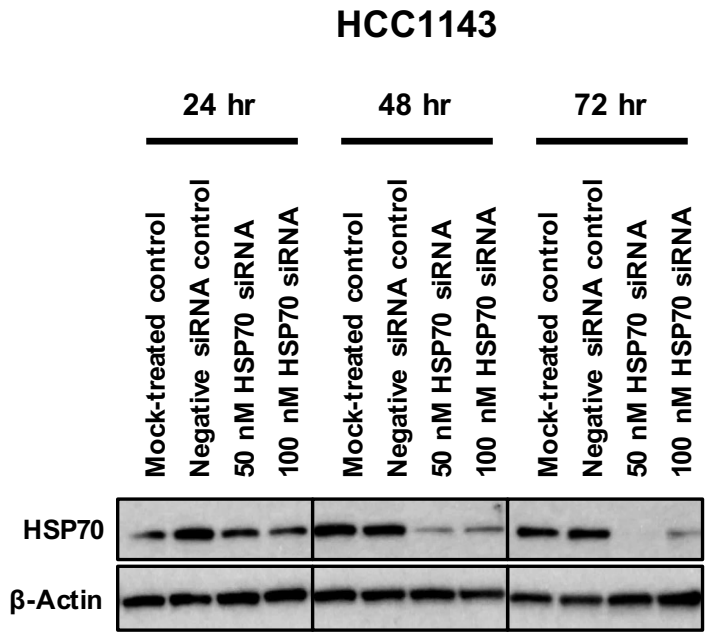


Figure 3.12: HSP70 knockdown by siRNA in HCC1143 cells

HCC1143 cells were transfected with indicated concentration of HSP70 siRNA. Mock-treated and negative siRNA were used as transfection controls. Cell lysates obtained at indicated time after transfection were analysed by western blotting. β-actin was used as loading control.

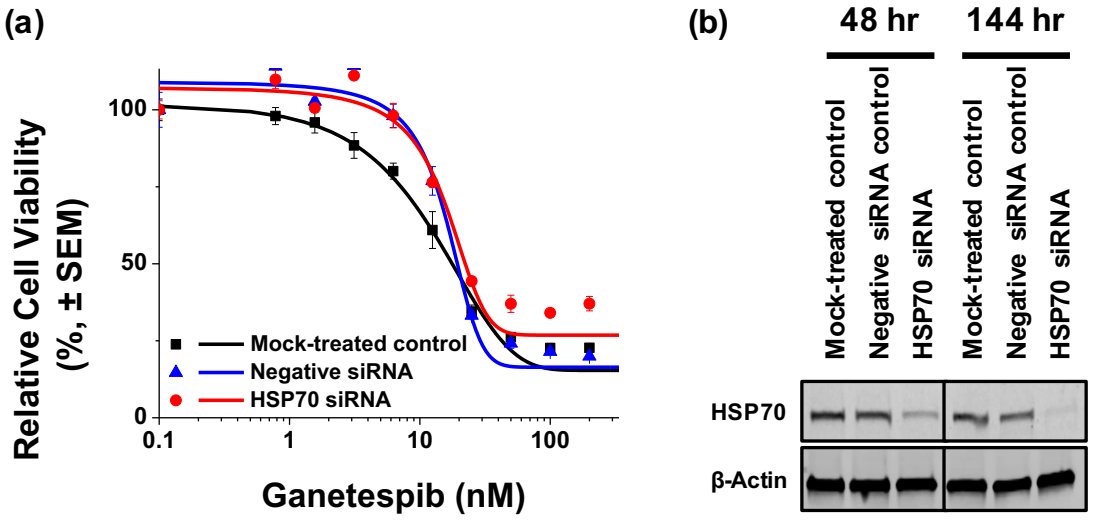


Figure 3.13: Sensitivity to ganetespib in HCC1143 cells after siRNA knockdown of HSP70 protein expression

(a) After transfection of HCC1143 cells with 50 nM HSP70 siRNA for 48 hr, cells were replated into 96-well plates. The next day, cells were treated with ganetespib (0 - 200 nM) for 72 hr and cell viability was assessed using a resazurin-based assay. Mean cell viability (%) for each treatment was quantified relative to the DMSO-treated control. Representative graph from two independent experiments performed in triplicates. Error bars indicate SEM.

(b) To validate successful knockdown of HSP70, lysates were collected before replating for cell viability assay and after completion of treatment (48 hr and 144 hr from the start of transfection). Lysates were analysed for western blotting and β-actin was used as a loading control.

Table 3.3: Sensitivity to ganetespib in HCC1143 cells after HSP70 siRNA treatment

siRNA	Ganetespib (nM) IC_{50} ± SEM
None (Mock-treated)	24.11 ± 5.95
Negative control	16.74 ± 0.81
HSP70	22.34 ± 2.46

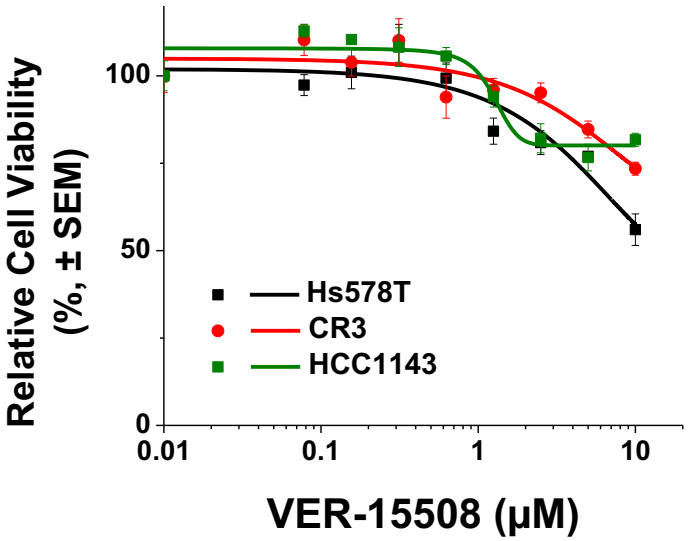


Figure 3.14 Sensitivity of TNBC cells to HSP70 inhibitor VER-15508

Hs578T, HSP90i-resistant CR3 and HCC1143 cells were treated with increasing concentrations of a HSP70 inhibitor (VER-11508, 0 - 10 μM) for 72 hr. Cell viability was assessed using a resazurin-based assay. Cell viability (%) for each treatment was quantified relative to the DMSO-treated control. Representative graph from two independent experiments performed in triplicates. Error bars indicate SEM.

3.5.1. HSP70: A pharmacodynamic marker of HSP90i

Transcription factor HSF1 exists as an inactive monomer or in a multi-protein complex which includes HSP70 and HSP90. In response to stress, or in the presence of HSP90i, HSF1 is released from the complex whereupon it trimerises and binds to the promoter of HSP genes, and activates transcription (Elo et al., 2005, Zou et al., 1998). HSF1-dependent HSP70 expression frequently occurs in response to HSP90i and an increase in HSP70

protein expression levels is considered a pharmacodynamic marker of HSP90i in both preclinical and clinical studies (Modi et al., 2007, Mahalingam et al., 2009).

The effect of ganetespib treatment on HSP70 protein expression in parental Hs578T cells and HSP90i-resistant clone CR3 was examined after continuous exposure to ganetespib, as well as treatment withdrawal after 48 hr of ganetespib exposure. A time-dependent increase in HSP70 protein expression was seen in both cell lines after treatment with 30 nM ganetespib **(Figure 3.15a)**. Additionally, a time-dependent decrease in HSP70 protein expression was seen after withdrawal of ganetespib **(Figure 3.15b)**. Indeed, in line with previous studies, HSP70 expression appears to be a pharmacodynamic marker of HSP90i in TNBC cells.

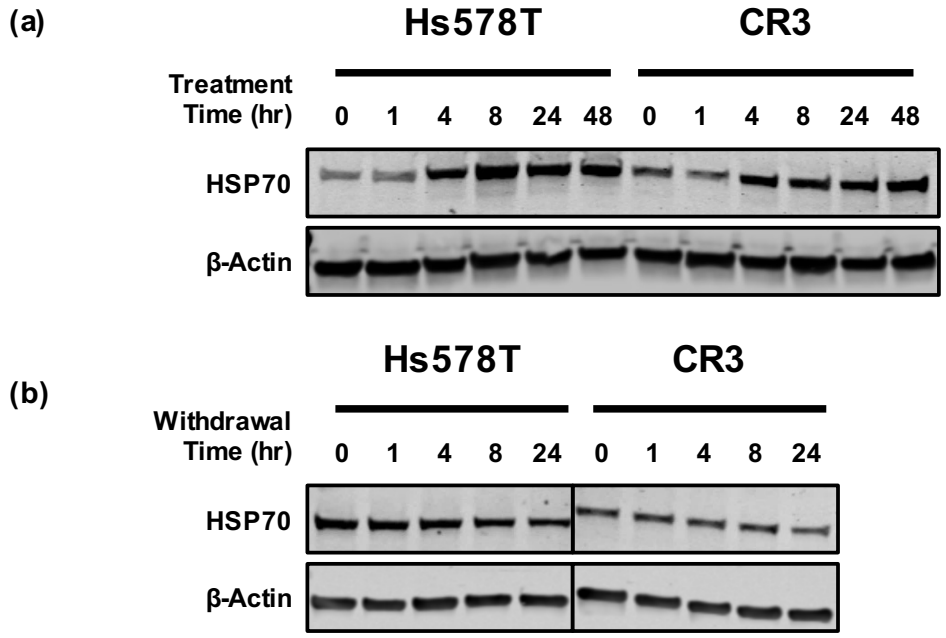


Figure 3.15 HSP70 expression as a pharmacodynamic marker of HSP90i

(a) Parental Hs578T and HSP90i-resistant CR3 cells were plated in the absence of ganetespib. The cells were treated the next day with 30 nM ganetespib for up to 48 hr. Cell lysates were prepared and analysed by western blotting.

(b) Parental Hs578T and HSP90i-resistant CR3 cells were treated with 30 nM ganetespib for 48 hr. After treatment, the media was removed, cells were washed twice with PBS and allowed to grow with drug-free media for up to 24 hr. Cell lysates were also analysed by western blotting. β-actin was used as loading control.

3.6. Discussion

HSP90 is an interesting cancer therapeutic target as HSP90i shows effective anti-cancer activities in various cancers, including TNBC (Proia et al., 2014, Caldas-Lopes et al., 2009, Mehta et al., 2011). In line with these studies, we demonstrate that HSP90i with ganetespib causes inhibition of cell viability, downregulation of client proteins (EGFR and AKT), induction of apoptosis, G2/M cell cycle arrest and inhibition of colony formation ability in TNBC cells.

Since clinical studies showed that resistance to HSP90i can arise in TNBC patients, we established an in vitro model to investigate the resistance mechanism to HSP90i in TNBC cells. Independent HSP90i-resistant clones were successfully generated after prolonged exposure to ganetespib in one of the TNBC cell lines (Hs578T cells). The two independent HSP90i-resistant clones CR2 and CR3 showed significant increase in resistance to HSP90i compared to parental Hs578T cells. We observed an increase in cell viability (IC_{50}) and colony formation ability as well as a decrease in induction of apoptosis and G2/M cell cycle arrest after ganetespib treatment in the clones. The HSP90i-resistant clones CR2 and CR3 also showed significant cross-resistant to other HSP90i; most notably to the chemically-related compound NVP-AUY922 (Garcia-Carbonero et al., 2013). HSP90i-resistant clone CR3 maintained its resistance to HSP90i even after drug withdrawal for two weeks **(Supplementary Figure 1).**

Tumours have a high level of intra-tumour heterogeneity and exposure to therapy causes positive selection pressure. This leads to the enrichment of pre-existing population with resistance-conferring mutations (Burrell and Swanton, 2014). As an example, the presence of a pre-existing population with secondary gatekeeper mutation in EGFR (T790M) causes resistance to tyrosine kinase inhibitors and is associated with reduced progression-free survival in non-small cell lung cancer (Inukai et al., 2006, Su et al., 2012). In our studies, the

two independently isolated HSP90-resistant clones showed a high degree of similarity in sequence variants, suggesting that the resistant clones may have arisen from a pre-existing population of cells. The clones may have had a pre-existing resistance to HSP90i, rather than acquiring de novo resistance but there is currently no other evidence to support this.

Among the sequence variants present in both HSP90i-resistant clones, 10 variants were predicted with deleterious effects on protein function (PolyPhen score ≥0.5, **Supplementary Table 2**) (Ramensky et al., 2002). However, they were heterozygous with wild-type gene sequences still present. It is not yet known whether any of these genetic variants, either alone or in combination, contributed to the HSP90 resistance. Since RNA-seq only identifies variants in expressed regions, whole genome DNA sequencing with higher sensitivity and specificity can be carried out on the HSP90i-resistant clones (Schneeberger, 2014). Other genetic variants including mutations in regulatory elements and non-expressed regions that may contribute to the resistant phenotype can be identified in the cells.

An increase in HSP70 protein expression levels is considered a pharmacodynamic marker of HSP90i in both preclinical and clinical studies (Modi et al., 2007, Mahalingam et al., 2009). In our study, HSP90i caused a dose-dependent upregulation of HSP70 protein levels in several TNBC cell lines (Hs578T, MDA-MB-231 and HCC1143 cells). A time-dependent upregulation of HSP70 protein levels was observed in TNBC cells upon addition of HSP90i, which was reversed upon its removal. Consistent with the previous studies, we demonstrate that an upregulation of HSP70 protein levels is also a pharmacodynamic marker of HSP90i in TNBC cells.

Upregulation of HSP70 has been suggested to have an underlying resistance mechanism by reducing the apoptotic effects of HSP90i (Powers et al., 2008, Guo et al., 2005, Piper and Millson, 2011). In our study, the HSP90i-resistant clones expressed higher basal levels of HSP70 protein expression compared to parental cells. There was also a positive correlation

between basal HSP70 protein expression and sensitivity to ganetespib in the panel of TNBC cells, although it did not reach statistical significance. However, reduction of HSP70 expression by siRNA treatment did not cause any change in sensitivity to ganetespib in the TNBC cells (HCC1143 cells). There was also no evidence of increased sensitivity to a small molecule inhibitor of HSP70 in the HSP90i-resistant cells when compared with parental cells. Taken together, these data suggest that HSP70 expression is only a pharmacodynamic marker of HSP90i and it does not have an underlying mechanism of resistance to HSP90i in our experimental setting.

In this chapter, we demonstrate the isolation and phenotypic characterisation of the two independent HSP90i-resistant clones CR2 and CR3 from the parental Hs578T cells. These clones represent an in vitro model of TNBC cells with acquired resistance to HSP90i.

4. Biological basis of resistance to HSP90i

4.1. Introduction

The biological basis of resistance to HSP90i in the HSP90i-resistant clones was not yet determined, but it did not appear to be associated with HSP70 expression. Several studies have performed transcriptome and proteome profiling on HSP90i in several cancer types (including breast, ovarian, pancreas and colon) to understand the molecular mechanism of action and to identify potential biomarkers to HSP90i (Song et al., 2008, Clarke et al., 2000, Zajac et al., 2010, Maloney et al., 2007).

Quantitative proteomic studies post HSP90i treatment demonstrate that HSP90i affects a high portion of protein kinases especially tyrosine kinases and the downregulation of phosphorylation events (Sharma et al., 2012). Feedback loops and cross-talk signalling through activation of receptor tyrosine kinases (RTKs) have been associated with resistance to targeted therapies in cancer (Engelman et al., 2007, Yonesaka et al., 2011, Logue and Morrison, 2012, Niederst and Engelman, 2013). As an example, MET activation causes resistance to EGFR inhibition in lung cancer by driving the activation of the PI3K signalling pathway. Initial indication of persistent MET activation after EGFR inhibition in resistant lung cancer cells in vitro was observed using a phospho-RTK array (Engelman et al., 2007). A phospho-RTK array allows for the simultaneous screening of several pRTKs in different cancer cell lines and is a useful approach to identify activated RTKs which could be potential targets for cancer therapeutics (Morishita et al., 2010).

Transcriptome profiling has also been used to provide insights to the mechanisms of drug resistance in cancer as well as to predict the sensitivity to cancer therapies (von der Heyde et al., 2015, Chang et al., 2003, Zhang and Luo, 2016). Transcriptome profiling including hybridisation- or sequence-based approaches, using microarray or RNA-sequencing (RNA-seq) respectively allows for the quantitative assessment of expression levels of transcripts under different conditions (Wang et al., 2009). When compared to microarray, RNA-seq is

highly robust due to increased sensitivity and higher reproducibility. It also has a broader coverage across the transcripts and allows the identification of transcript and sequence variants including single nucleotide polymorphisms (Zhao et al., 2014).

In this chapter, we performed proteome and whole transcriptome profiling using a phospho-RTK array and RNA-seq on the parental Hs578T cells as well as the two independent HSP90i-resistant clones to identify the potential mechanisms of resistance to HSP90i in TNBC cells.

4.2. Proteome profiling of pRTK in parental Hs578T cells and HSP90i-resistant clones

In order to obtain a global profiling of the phosphorylation state of RTKs in the HSP90i-resistant clones, a pRTK array analysis was performed on parental Hs578T cells, as well as CR2 and CR3 clones. In this assay, antibodies against 49 human RTKs are spotted onto nitrocellulose membranes and an anti-phospho-tyrosine antibody conjugated to horseradish peroxidase with chemiluminescence detection is used to quantify levels of pRTKs.

The quantification of 49 pRTKs from both HSP90i-resistant clones (CR2 and CR3) was compared to parental Hs578T cells in the absence and presence of ganetespib (30 nM, 24 hr). Using this technique, only two pRTKs were consistently detectable in both clones (pEGFR and pMET) (**Figure 4.1a and b**). Ganetespib treatment in parental Hs578T cells caused a marked decrease in the phosphorylation state of EGFR (pEGFR) and hepatocyte growth factor receptor (pMET) **(Figure 4.1c)**, consistent with the anticipated effects of HSP90i on the maturation of client proteins. However, there was an increase in the pEGFR and pMET levels in both CR2 and CR3 when compared to treated or untreated Hs578T cells. Compared to the untreated parental Hs578T cells, the expression of pEGFR was 3.04 and 2.68-fold greater, and the expression of pMET was 1.36 and 2.30-fold greater in the CR2 and CR3 **(Figure 4.1c)**.

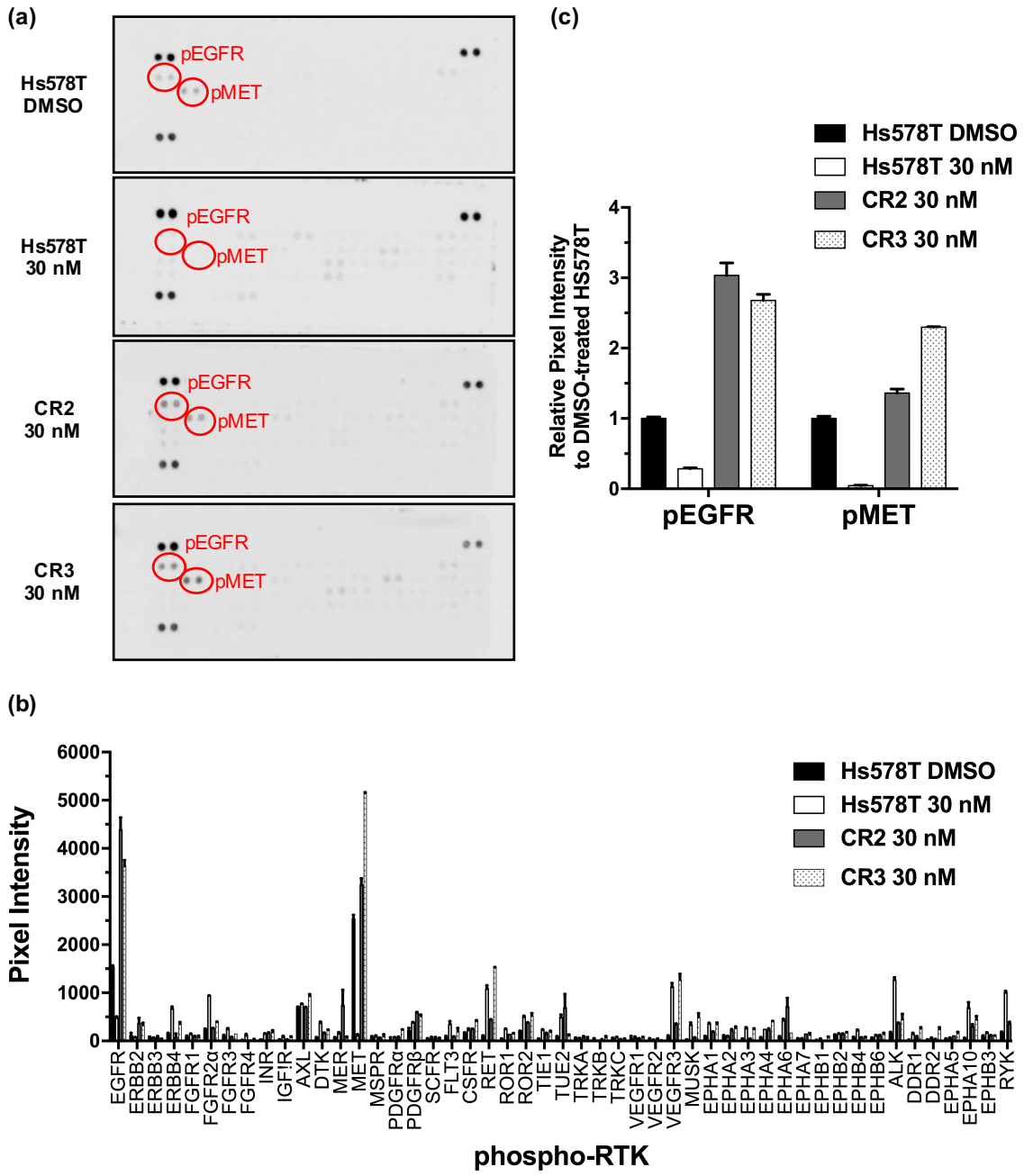


Figure 4.1: Profiling of pRTKs in Hs578T and HSP90i-resistant clones

(a) Parental Hs578T cells and HSP90i-resistant clones CR2 and CR3 were plated in the absence of ganetespib. The next day, the cells were treated with 30 nM ganetespib for 24 hr. After completion of treatment, cell lysates were obtained and analysed by pRTK array analysis. DMSO-treated Hs578T cells were used as a control. The spots represent the expression of different pRTKs (n=49) and reference controls, each performed in duplicate.

(b) Quantification of each spot was calculated based on photon counts (pixel intensity) after normalisation to the reference spot from the respective array. pEGFR and pMET were the only high intensity spots consistent between the two resistant clones.

(c) The pixel intensiy for pEGFR and pMET in each cell line was expressed as relative to DMSO-treated Hs578T cells. The graph represents the mean relative pEGFR and pMET protein expression from duplicate spots in one experiment and error bars indicate range.

Western blotting analysis also showed that there was higher expression of pEGFR and pMET in both HSP90i-resistant clones compared to parental Hs578T cells, more prominently in CR3 **(Figure 4.2)**. We hypothesised that the HSP90i-resistant clones might be more sensitive to EGFR or MET inhibitors due to increased activation of these signalling pathways. Therefore, we examined the sensitivity of HSP90i-resistant clone CR3 to growth inhibition by specific inhibitors of EGFR (erlotinib) and MET (crizotinib), but found no significant difference in sensitivity compared with parental Hs578T cells **(Figure 4.3 and Table 4.1)**. These results suggest that upregulation of activated EGFR and MET are not the major cell survival signalling pathways in the HSP90i-resistant clones.

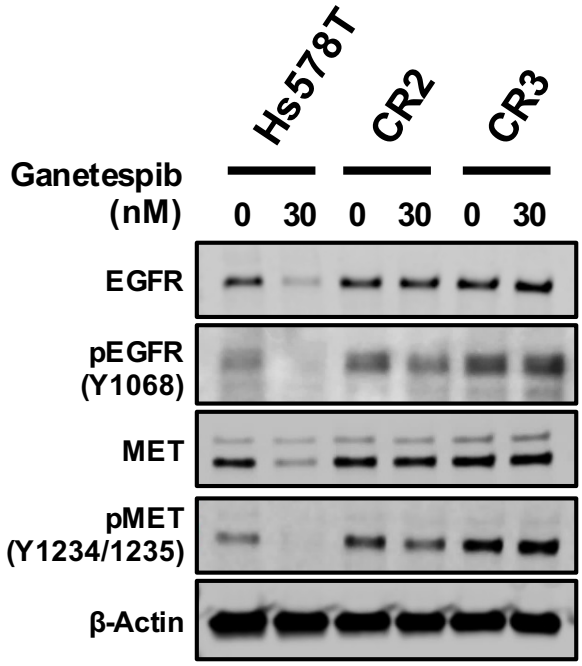


Figure 4.2: Expression of EGFR and MET in Hs578T cells and HSP90i-resistant clones

Lysates obtained from parental Hs578T cells and HSP90i-resistant clones CR2 and CR3 after treatment with ganetespib (0, 30 nM) for 24 hr were analysed by western blotting. β-actin was used as loading control.

Table 4.1: Sensitivity of Hs578T and HSP90i-resistant clone CR3 to erlotinib or gefitinib

Cells	Erlotinib (μM) IC_{50} ± SEM	Crizotinib (μM) IC_{50} ± SEM
Hs578T	2.32 ± 0.47	1.12 ± 0.19
CR3	5.58 ± 0.74	0.97 ± 0.03

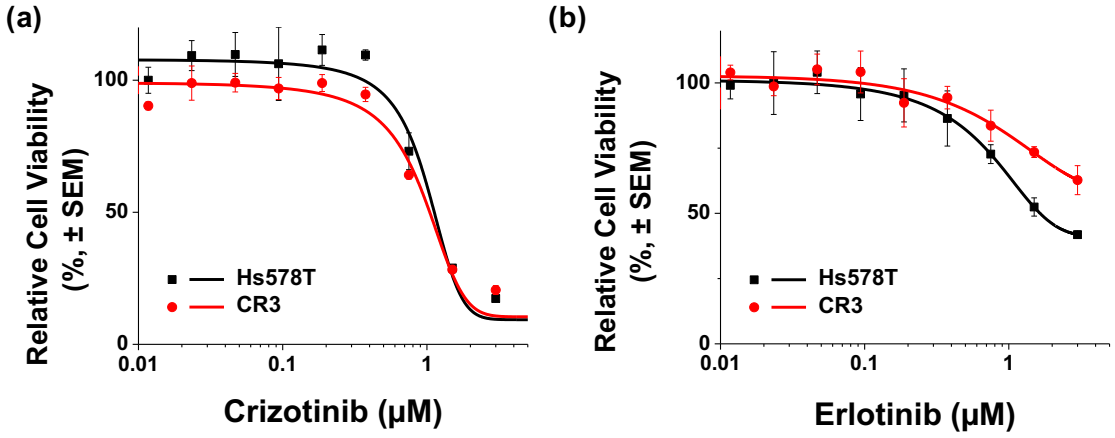


Figure 4.3: Sensitivity of HSP90i-resistant clone CR3 to EGFR and MET inhibitors

Parental Hs578T cells and HSP90i-resistant clone CR3 were treated with increasing concentration (0 - 3 μM) of (a) crizotinib (MET inhibitor) and (b) erlotinib (EGFR inhibitor) for 72 hr and cell viability assessed by a resazurin-based assay. The cell viability (%) for each treatment was expressed relative to the DMSO-treated control. Representative graphs from three independent experiments each performed in triplicates. Error bars indicate SEM.

4.3. Whole transcriptome profiling in parental Hs578T cells and HSP90i-resistant clones

Whole transcriptome profiling with RNA-seq was used to obtain a global signature of differentially expressed genes from TNBC cells after acquiring resistance to HSP90i as seen in HSP90i-resistant clones CR2 and CR3. RNA-seq uses next-generation sequencing (NGS) to measure the quantity of mRNA in a biological sample. RNA samples from control and ganetespib-treated Hs578T, CR2 and CR3 cells were analysed for RNA-seq by Oxford Gene Technology (OGT) using an Illumina HiSeq2000 platform.

An average of 28,851,396 paired end reads from the 12 samples were mapped onto the human genome (GRCh37) and assembled to transcripts. For each sample, transcripts were measurable for >14000 genes. Transcripts for some genes were not quantifiable where the expression level was below the level of detection, or the genes were not transcribed in the cells. The transcripts between samples were compared to identify any significant gene expression changes (q-value ≤ 0.05). The RNA-seq analysis appeared reproducible as there were absence of significant gene expression changes in any of the duplicates.

4.3.1. Differential gene expression in parental Hs578T cells and HSP90i-resistant clones after ganetespib treatment

Differential gene expression analysis was examined between DMSO-treated and ganetespib-treated cells to determine the transcriptome response to ganetespib treatment. A significant deregulation of 2562 genes (18.3%) was seen in parental Hs578T cells after ganetespib treatment, with transcripts from 1068 genes (7.6%) being upregulated and 1494 (10.7%) genes being downregulated **(Table 4.2)**. Importantly, there were no significant changes in gene expression seen in both HSP90i-resistant clones CR2 and CR3 after treatment with ganetespib. This observation further suggests that both clones have acquired resistance to HSP90i through a mechanism that does not require an induced change in gene expression on exposure to the drug.

Table 4.2: Differentially expressed genes in ganetespib-treated cells compared to DMSO-treated cells

	Deregulated genes	Upregulated genes	Downregulated genes
Ganetespib-treated Hs578T	2562 (18.3%)	1068 (7.6%)	1494 (10.7%)
Ganetespib-treated CR2	0	0	0
Ganetespib-treated CR3	0	0	0

Previous studies showed that HSP90 inhibition caused an upregulation of several HSP genes in various cancer models including ovarian and breast cancers (Maloney et al., 2007, Zajac et al., 2010). As expected, significant gene upregulation of HSP90 (HSP90α and HSP90β), HSP70 (HSC70 and HSP72), HSP27, HSPA4L, HSPA1L, HSP40 (DNAJA1 and DNAJA4), HSP47, HSP60 and AHSA1 were also seen in Hs578T cells after ganetespib treatment **(Figure 4.4 and Supplementary Table 3)**.

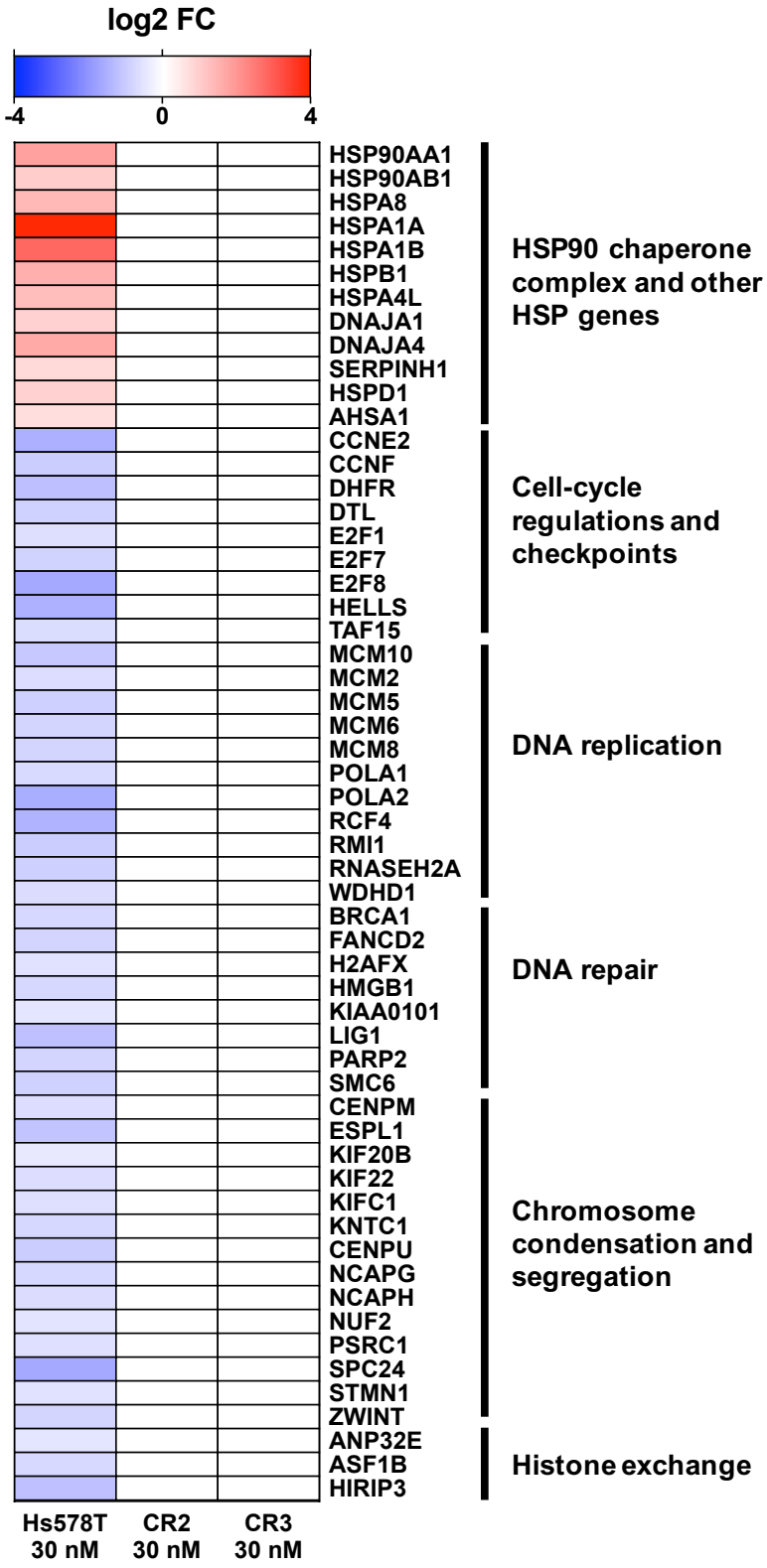


Figure 4.4: Differential expression of genes associated with HSP90 and cell cycle upon ganetespib treatment

Heatmap representing the effect on gene expression of HSP90 chaperone complex and other HSP-related genes, as well as cell cycle related proteins after ganetespib treatment (24 hr) in Hs578T cells and HSP90i-resistant clones (CR2 and CR3). The colour scale indicates log2 fold change (FC) in gene expression for individual ganetespib-treated cells when compared to DMSO-treated cells from blue (-4) to red (+4) for significantly altered genes (q-value ≤ 0.05).

Among the 147 genes previously reported to be downregulated in erythroleukemia cells after ganetespib treatment (Proia et al., 2011), 66 genes were also significantly downregulated in Hs578T cells after 24 hr treatment of 30 nM ganetespib. These genes mostly consisted of cell cycle related genes involved in cell cycle regulation or checkpoints (CCNE2, E2F1), DNA replication (MCM10, RFC2), DNA repair (BRCA1, LIG1), chromosome condensation or segregation (KIF22, CENPU) and histone exchange (ANP32E) **(Figure 4.4 and Supplementary Table 3).**

Additionally, in order to identify pathways that were affected due to the downregulation of HSP90 client proteins after HSP90i exposure, pathway enrichment analysis using MetaCore™ (https://portal.genego.com, accessed August 2016) was performed on significantly downregulated gene expression in ganetespib-treated Hs578T cells. As a result, cell cycle related pathways were among the top most significantly enriched pathways with altered gene expression **(Table 4.3)**. Consistent with our previous findings **(Figure 3.8)**, HSP90i causes changes in gene expression that leads to the activation of cell cycle checkpoint arrest in TNBC cells.

Table 4.3 The top 20 most significantly enriched pathways associated with downregulation of gene expression in ganetespib-treated Hs578T cells

Pathway maps	Fraction of genes	FDR
Development: Regulation of epithelial-to-mesenchymal transition (EMT)	19/64	5.57E-07
Development: TGF-beta-dependent induction of EMT via MAPK	16/47	6.65E-07
Cell adhesion: ECM remodelling	16/52	2.36E-06
Development: TGF-beta-dependent induction of EMT via SMADs	13/35	3.43E-06
Cell cycle: Start of DNA replication in early S phase	12/32	8.72E-06
Cell adhesion: Chemokines and adhesion	21/100	1.05E-05
Cytoskeleton remodelling: TGF, WNT and cytoskeletal remodelling	22/111	1.31E-05
Immune response: Histamine H1 receptor signalling in immune response	14/48	1.44E-05
Stimulation of TGF-beta signalling in lung cancer	14/48	1.44E-05
DNA damage: Brca1 as a transcription regulator	11/30	2.08E-05
DNA damage: ATM/ATR regulation of G1/S checkpoint	11/32	4.04E-05
Immune response: C5a signalling	13/50	1.29E-04
Cell cycle: The metaphase checkpoint	11/36	1.29E-04
dCTP/dUTP metabolism	16/75	1.29E-04
Transcription: Ligand-dependent activation of the ESR1/SP pathway	10/30	1.36E-04
Immune response: IL-1 signalling pathway	12/44	1.39E-04
Cell cycle: Regulation of G1/S transition	11/38	1.80E-04
Immune response: MIF-induced cell adhesion, migration and angiogenesis	12/46	2.02E-04
Glucocorticoid-induced elevation of intraocular pressure as glaucoma risk factor	14/62	2.02E-04
Immune response: IL-6 signalling pathway via JAK/STAT	15/72	2.56E-04

4.3.2. Differential gene expression in Hs578T cells associated with acquired resistance to HSP90i

Differential gene expression analysis comparing DMSO-treated parental Hs578T cells with DMSO-treated HSP90i-resistant clone CR2 or CR3 was performed to identify potential molecular signature(s) associated with acquired resistance to HSP90i in TNBC cells. Compared to parental Hs578T cells, HSP90i-resistant clones CR2 and CR3 showed significant changes in the expression of more than 20% of transcribed genes; 3268 genes (23.3%) and 4244 genes (30.3%) respectively **(Table 4.4)**.

Interestingly, most of the affected genes were overlapping between the clones suggesting similar mechanism of resistance to HSP90i. There were 1223 upregulated genes and 1250 downregulated genes overlapping between CR2 and CR3 **(Figure 4.5)**. The 100 most significantly upregulated and downregulated genes shared between CR2 and CR3 are listed in **Supplementary Table 4 and 5**. Further investigation was focused on the significantly upregulated genes as they might identify activation of signalling pathways that could be directly involved in the resistance mechanisms to HSP90i in CR2 and CR3, and therefore be potentially considered as targets for overcoming resistance to HSP90i.

Table 4.4: Differentially expressed genes in HSP90i-resistant clones compared to Hs578T cells

	Deregulated genes	Upregulated genes	Downregulated genes
CR2	3268 (23.3%)	1581 (11.3%)	1687 (12%)
CR3	4244 (30.3%)	2005 (14.3%)	2239 (16%)

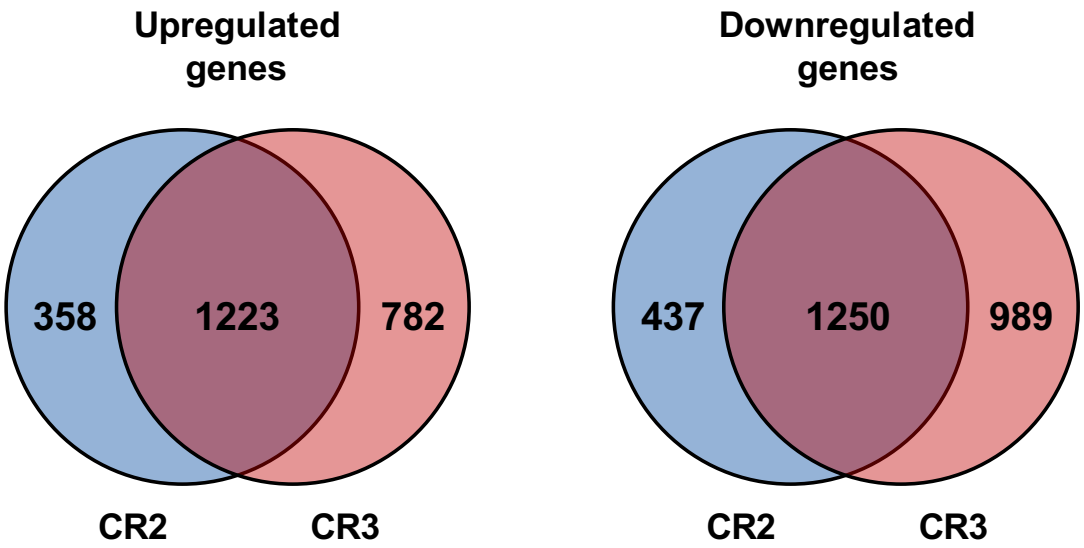


Figure 4.5: Overlap of significantly upregulated and downregulated genes in HSP90i-resistant clones CR2 and CR3

4.4. UGT1A expression in HSP90i-resistant clones

UGT1A9, UDP Glucuronosyltransferase Family 1 Member A9 was found among the most significantly upregulated genes in both HSP90i-resistant clones CR2 and CR3 with log2 fold change (FC) values of >7 **(Supplementary Table 4)**. Other UGT1A family members were also significantly upregulated in both clones when compared to Hs578T cells **(Figure 4.6a and Table 4.5)**. The RNA expression of UGT1A family members was not significantly affected upon ganetespib treatment in parental Hs578T cells. Western blotting analysis confirmed a higher UGT1A and UGT1A9 protein expression in CR2 and CR3 when compared to parental Hs578T cells, in the absence or presence of ganetespib **(Figure 4.6b)**. The involvement of UGT1A9 on ganetespib activity in CR2 and CR3 was further investigated.

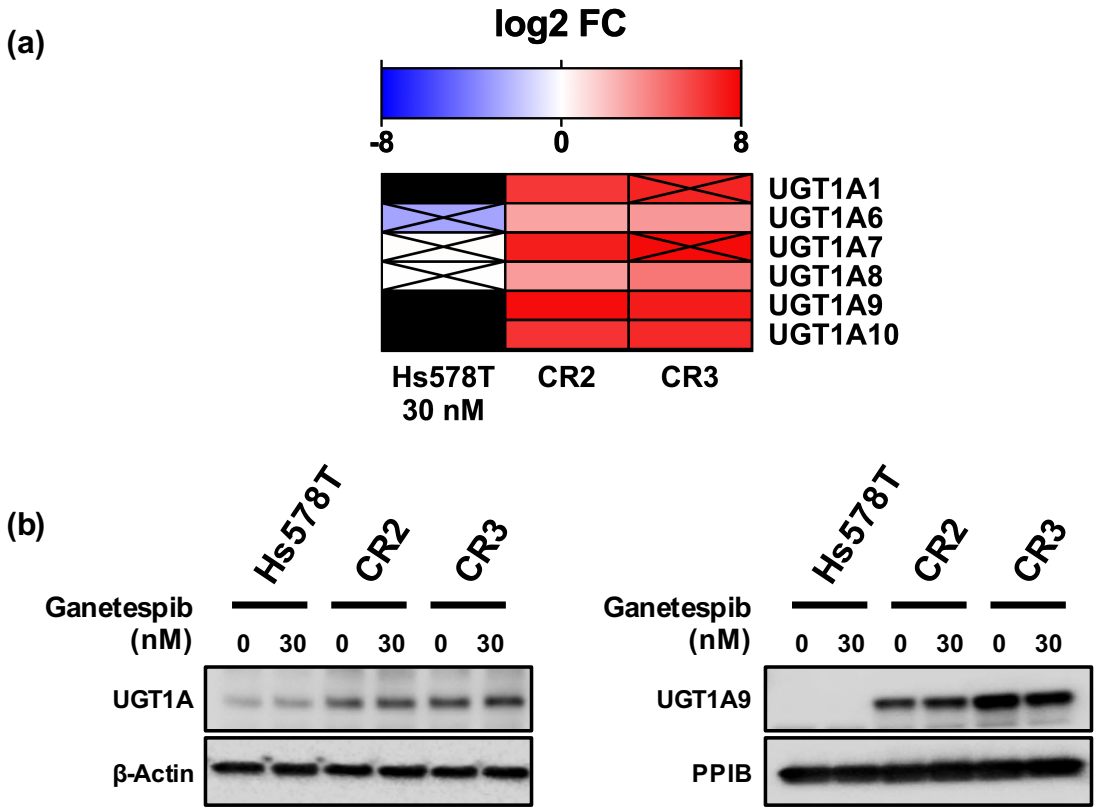


Figure 4.6: Upregulated expression of UGT1A family members in HSP90i-resistant clones

(a) Heatmap representing the gene expression of UGT1A family members in ganetespib-treated Hs578T cells (30 nM, 24 hr) and in DMSO-treated HSP90i-resistant clones CR2 and CR3 when compared to DMSO-treated Hs578T cells. The colour scale indicates log2 FC in gene expression for individual cells when compared to DMSO-treated Hs578T cells from blue (-8, downregulation) to red (+8, upregulation). Unless indicated, the log2 FC data are statistically significant (q-value ≤ 0.05). A black bar indicates that the gene expression level was below the detectable limit for that gene/cell line, and a cross indicates that the differential expression was not statistically significant (q-value >0.05).

(b) Lysates obtained from Hs578T cells, CR2 and CR3 in the absence and presence of ganetespib (30 nM, 24 hr) were analysed by western blotting. PPIB and β-actin were used as loading controls. Representative images from two independent experiments are shown.

Table 4.5: Differential gene expression of UGT1A family in Hs578T (30 nM ganetespib), CR2 and CR3 compared to DMSO-treated Hs578T

Genes		Hs578T 30 nM		CR2		CR3	
		log2 FC	q-value	log2 FC	q-value	log2 FC	q-value
UGT1A1	UDP Glucuronosyltransferase Family 1 Member A1	NA	NA	6.27	0.106 (ns)	6.88	0.085 (ns)
UGT1A6	UDP Glucuronosyltransferase Family 1 Member A6	-2.86	0.099 (ns)	2.86	0.078 (ns)	3.25	3.21E-02
UGT1A7	UDP Glucuronosyltransferase Family 1 Member A7	0.06	0.975 (ns)	7.06	0.083 (ns)	7.77	0.063 (ns)
UGT1A8	UDP Glucuronosyltransferase Family 1 Member A8	0.01	0.993 (ns)	3.13	5.58E-04	4.30	4.10E-04
UGT1A9	UDP Glucuronosyltransferase Family 1 Member A9	NA	NA	7.63	3.04E-02	7.16	1.98E-02
UGT1A10	UDP Glucuronosyltransferase Family 1 Member A10	NA	NA	6.40	5.58E-04	6.73	4.10E-04

Note: UGT1A3-5 genes were investigated but the expression values were below the detection limit. NA indicates that the expression values were below the detection limit for that cell line.

4.4.1. Involvement of UGT1A9 in response to ganetespib

Ganetespib can be glucuronidated by UGT1A family members; most notably UGT1A9 and this leads to the formation of water-soluble metabolites that can be exported from the cells (Landmann et al., 2014, Acquaviva et al., 2014a). Therefore, the high level of UGT1A9 expression seen in HSP90i-resistant clones CR2 and CR3 might partly explain their decreased sensitivity to ganetespib. Sensitivity to ganetespib in combination with a competitive inhibitor of UGT1A9 (propofol) was assessed in the parental Hs578T cells and HSP90i-resistant clones (Cummings et al., 2003, Court, 2005). The sensitivity to ganetespib in parental Hs578T cells was not greatly affected by combination treatment with propofol (300 μM). However, there was a significant combination effect of propofol on the sensitivity of CR2 and CR3 to ganetespib **(Figure 4.7)**. The IC_{50} values of ganetespib in CR2 and CR3 decreased by two-fold with the presence of propofol; 6.27 ± 0.50 nM and 5.03 ± 0.35 nM respectively **(Table 4.6)**. The sensitivity to propofol alone (300 μM) was not toxic in these cells **(Figure 4.8)**. These data suggest that the inhibitory activity of ganetespib in HSP90i-resistant clones can be largely restored using a competitive inhibitor of UGT1A9.

Table 4.6: Sensitivity to ganetespib alone or in combination with propofol

Cell line	Ganetespib IC_{50} ± SEM (nM)	Ganetespib in the presence of 300 µM propofol IC50 ± SEM (nM)
Hs578T	4.93 ± 0.05	4.39 ± 0.39
CR2	11.23 ± 0.65	6.27 ± 0.49
CR3	10.48 ± 1.06	5.03 ± 0.35

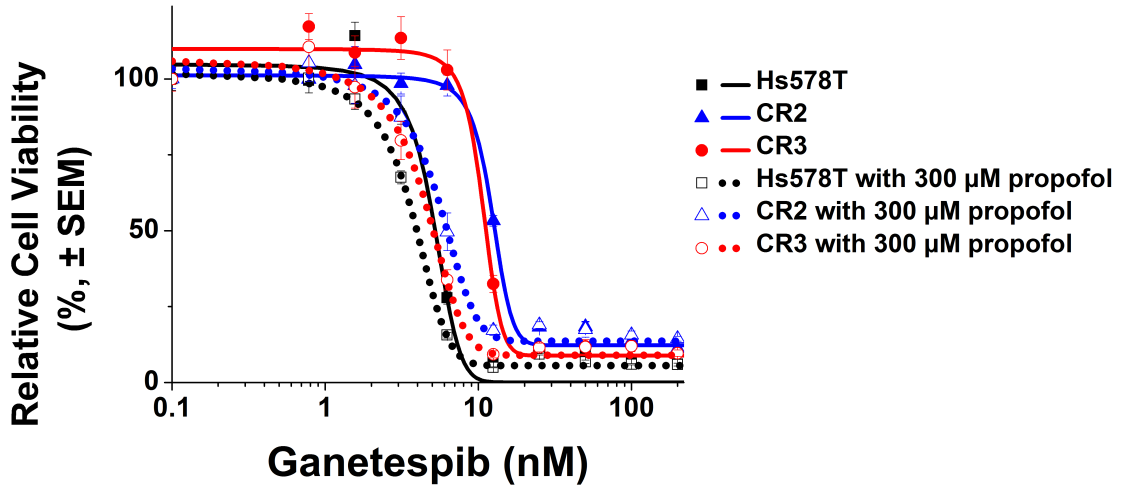


Figure 4.7 Combination effect of propofol on the sensitivity to ganetespib

Parental Hs578T cells and HSP90i-resistant clones CR2 and CR3 cells were treated with increasing concentration (0 - 200 nM) of ganetespib alone or in combination with 300 µM propofol for 72 hr and cell viability was analysed by a resazurin-based assay. Cell viability (%) for each treatment was expressed relative to either DMSO-treated or propofol-treated controls. Representative graph from three independent experiments each performed in triplicates and error bars indicate SEM.

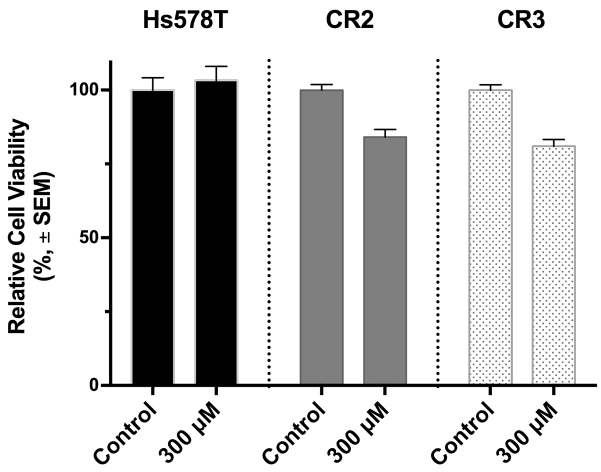


Figure 4.8: The effect of propofol on the cell viability of Hs578T cells and HSP90i-resistant clones

Hs578T cells and HSP90i-resistant clones CR2 and CR3 were treated with increasing 300 μM propofol for 72 hr. Cell viability was assessed by a resazurin-based assay. Cell viability (%) for each treatment was expressed relative to DMSO-treated control. The graph represents the mean cell viability from three independent experiments, each performed in triplicates. Error bars indicate SEM.

4.4.2. The effects of a competitive inhibitor of UGT1A9 on HSP90i activity

The effects on HSP90 client protein and induction of apoptosis after the combination treatment of ganetespib and propofol were investigated in parental Hs578T cells and HSP90i-resistant clones. Western blotting analysis was performed on Hs578T, CR2 and CR3 after treatment with propofol (100 and 300 μM), ganetespib (30 nM) or in combination for 24 hr. As seen previously, ganetespib alone caused an effective downregulation of HSP90 client protein EGFR expression and an upregulation of cleaved PARP in parental Hs578T cells only, while both HSP90i-resistant clones were unaffected **(Figure 4.9)**.

Treatment with propofol alone increased EGFR protein expression in parental Hs578T cells and HSP90i-resistant clones. However, only in combination with propofol, ganetestpib treatment reduced EGFR protein expression in HSP90i-resistant clones, CR2 and CR3 **(Figure 4.9a and b)**. This was associated with increased levels in cleaved PARP **(Figure 4.9c)** and a dose dependent increase of HSP70 expression **(Figure 4.9a and b)**. These

observations indicate that HSP90 activity in HSP90i-resistant clones CR2 and CR3 was effectively inhibited by ganetespib treatment, in the presence of propofol. Therefore, competitive inhibition of UGT1A9 successfully restored the inhibitory activity of ganetespib in HSP90i-resistant clones.

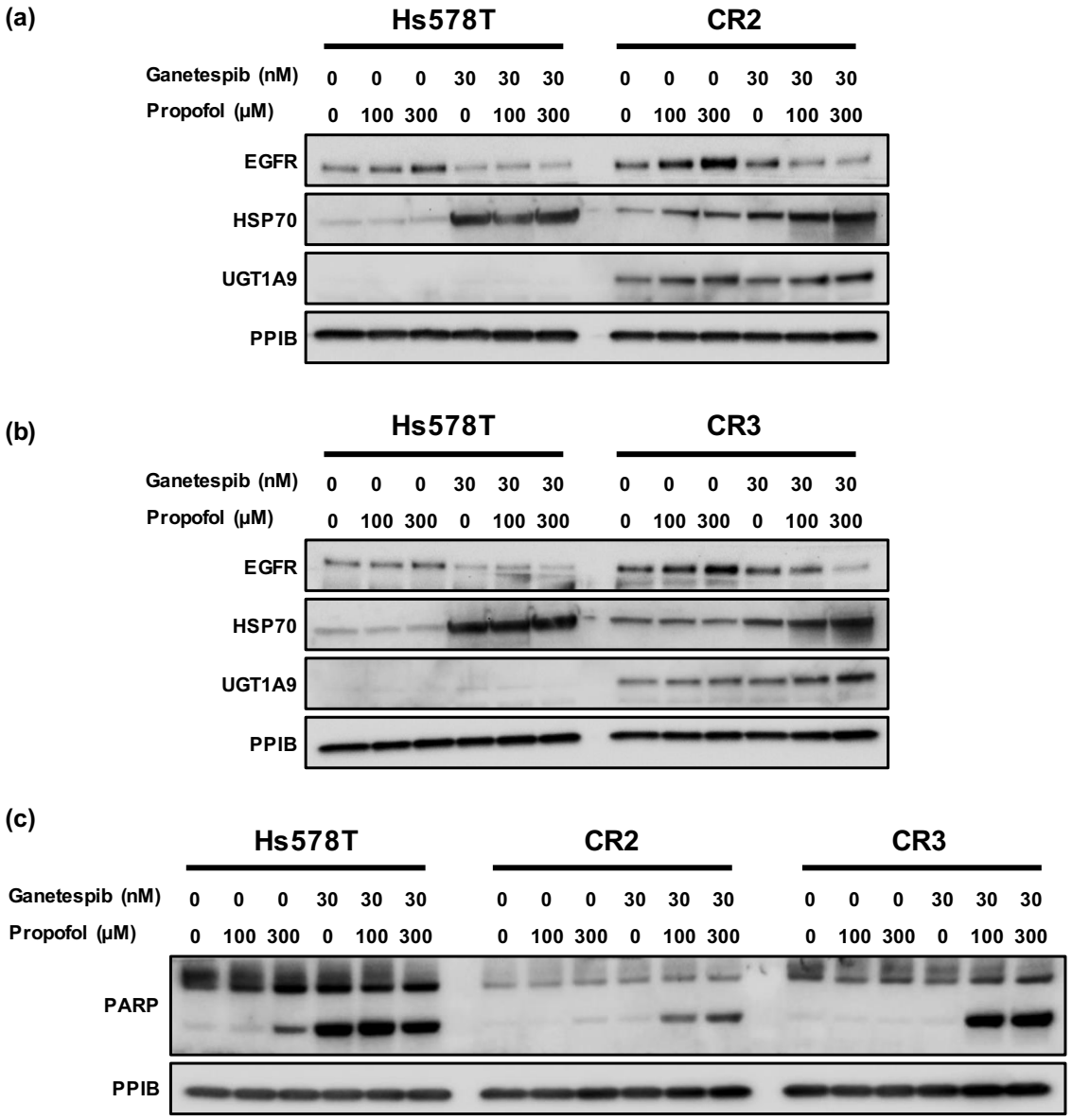


Figure 4.9:The effects of propofol or/and ganetespib treatment in Hs578T, CR2 and CR3

Hs578T cells and HSP90i-resistant clones CR2 and CR3 were treated with propofol (100 and 300 μM), ganetespib (30 nM) or in combination for 24 hr. Lysates of the parental Hs578T cells and HSP90i-resistant clones **(a)** CR2 and **(b)** CR3 were analysed for western blotting. Hsp70 was used as a pharmacodynamic marker for inhibition of Hsp90 activity. **(c)** Levels of cleaved PARP were also determined to assess induction of apoptosis. PPIB was used as a loading control. Representative images from two experiments are shown.

Interestingly, NVP-AUY922 can also be glucuronidated by UGT1A family members and they are both resorcinol-based HSP90i (Acquaviva et al., 2014a). As reported in Chapter 3.3, the HSP90i-resistant clones also showed greater cross-resistance to NVP-AUY922 compared to 17-AAG, a geldanamycin-based HSP90i. Therefore, the sensitivity of the clones to another class of HSP90i (purine-based HSP90i) was assessed (Soga et al., 2013, Garcia-Carbonero et al., 2013). Interestingly, CR2 and CR3 did not show greater resistance to purine-based HSP90i compared to the resorcinol-based HSP90i **(Figure 4.10)**. These data suggest that resistance to HSP90i in CR2 and CR3 might be limited to certain classes of HSP90i and that the underlying mechanisms of resistance in these clones might be due to rapid metabolism of structurally related drugs.

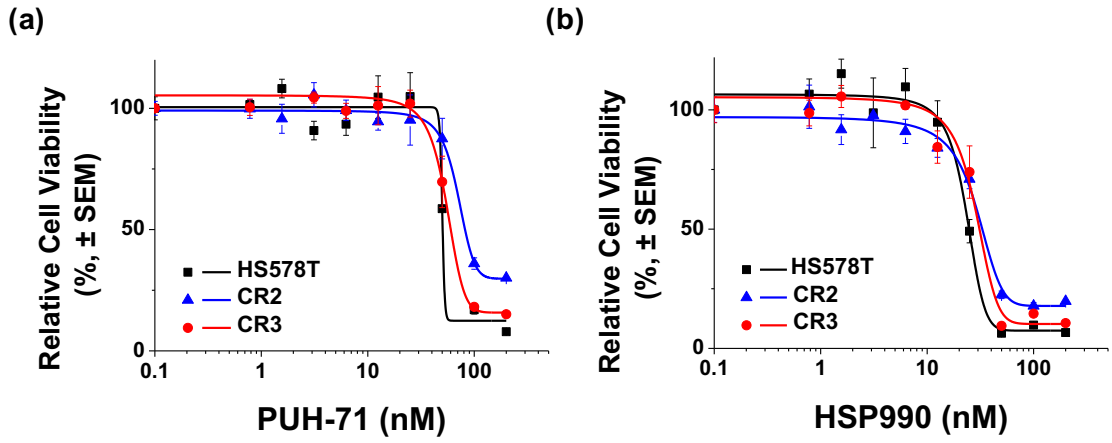


Figure 4.10: Sensitivity to other classes of HSP90 inhibitors

Parental Hs578T cells and HSP90i-resistant clones CR2 and CR3 were treated with increasing concentration of HSP90i; (a) PUH-71 and (b) HSP990 (0 - 200 nM) for 72 hr and cell viability was assessed by a resazurin-based assay. Cell viability (%) for each treatment was expressed relative to either DMSO-treated control. Representative graph from three independent experiments each performed in triplicates. Error bars indicate SEM.

4.5. AKR1C1 expression in HSP90i-resistant clones

The expression of Aldo-keto reductase member C family members (AKR1C) was another interesting hit seen in the HSP90i-resistant clones when compared to parental Hs578T cells. While performing ponceau staining during western blotting analysis of Hs578T, CR2 and CR3 lysates, a protein band at 37 kDa was present in both HSP90i-resistant clones, more prominently in CR3 but not in parental Hs578T cells **(Figure 4.11a)**. The band at 37 kDa from Hs578T and CR3 was analysed by Mass Spectrometry (MS) **(Figure 4.11b)**. The AKRIC family members were the top hits that emerged from the MS analysis **(Table 4.7)**.

Expression of AKR1C family members was also significantly higher in CR2 and CR3 compared to Hs578T cells in RNA-seq data **(Figure 4.12a and Supplementary Table 6)** with AKR1C1 among the top 20 upregulated genes in both HSP90i-resistant clones (log2 FC >5). Ganetespib treatment in Hs578T also caused a significant upregulation of AKR1C family but to a lesser extent (log2 FC <3). Western blotting confirmed that CR2 and CR3 expressed higher AKR1C1 protein level compared to Hs578T cells and that ganetespib treatment induced AKR1C1 expression in Hs578T cells **(Figure 4.12b)**. The upregulated AKR1C1 expression in the HSP90i-resistant clones was further investigated.

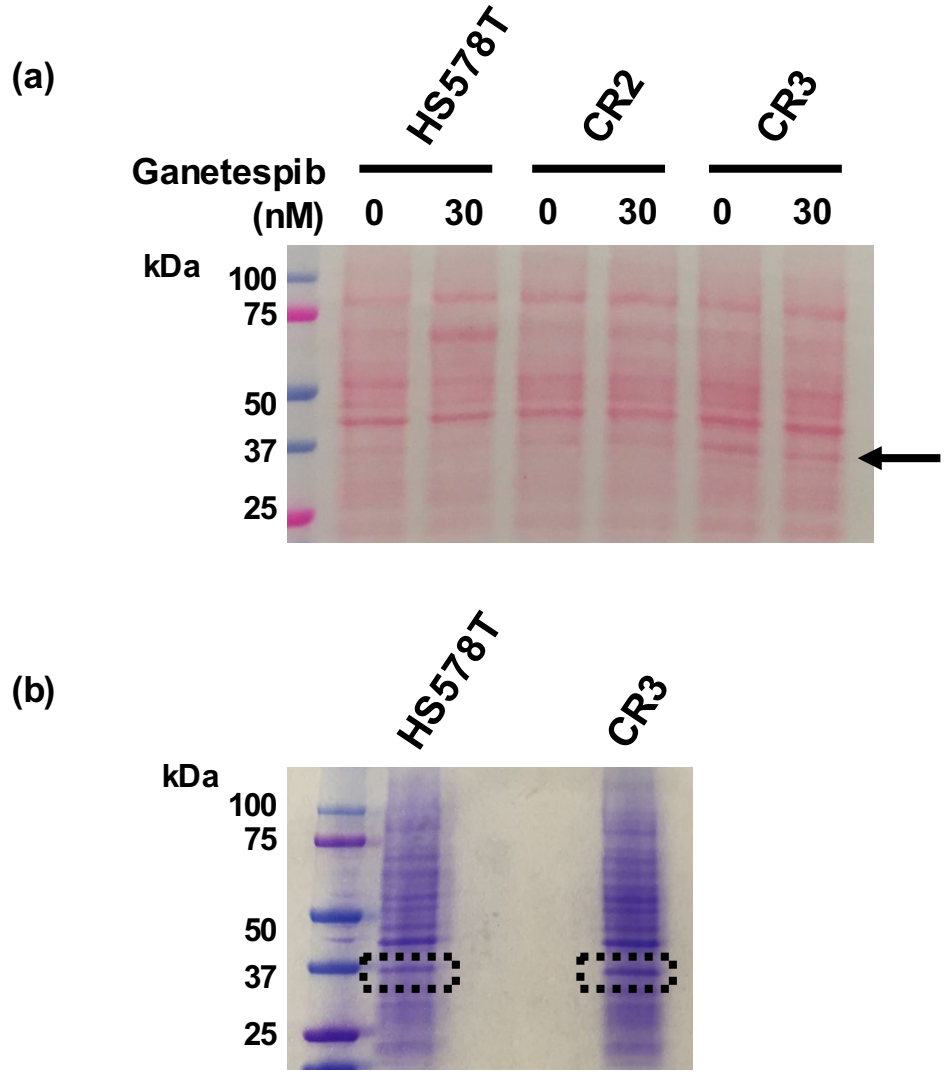


Figure 4.11: Identification of an upregulated protein band at 37 kDa in HSP90i-resistant clones

Parental Hs578T cells and HSP90i-resistant clones CR2 and CR3 were treated with ganetespib (30 nM) for 24 hr. **(a)** Cell lysates were analysed for western blotting and the PVDF membrane was ponceau stained. The arrow indicates the presence of a prominent protein band in HSP90i-resistant clones, more in CR3 compared to Hs578T cells. **(b)** The DMSO-treated Hs578T and CR3 lysates were run on an SDS-PAGE gel and the band at approximately 37 kDa (dotted area) was excised after staining with coomassie blue, and analysed by mass spectrometry.

Table 4.7: The identity of the most prevalent proteins in the 37 kDa protein band in HSP90i-resistant clone CR3 when compared to Hs578T cells by MS

Protein		Mass	Score
AKR1C3	Aldo-keto reductase family 1 member C3	37229	952
AKR1C1	Aldo-keto reductase family 1 member C1	37221	919
AKR1C2	Aldo-keto reductase family 1 member C2	37111	570
AKR1C4	Aldo-keto reductase family 1 member C4	37442	203

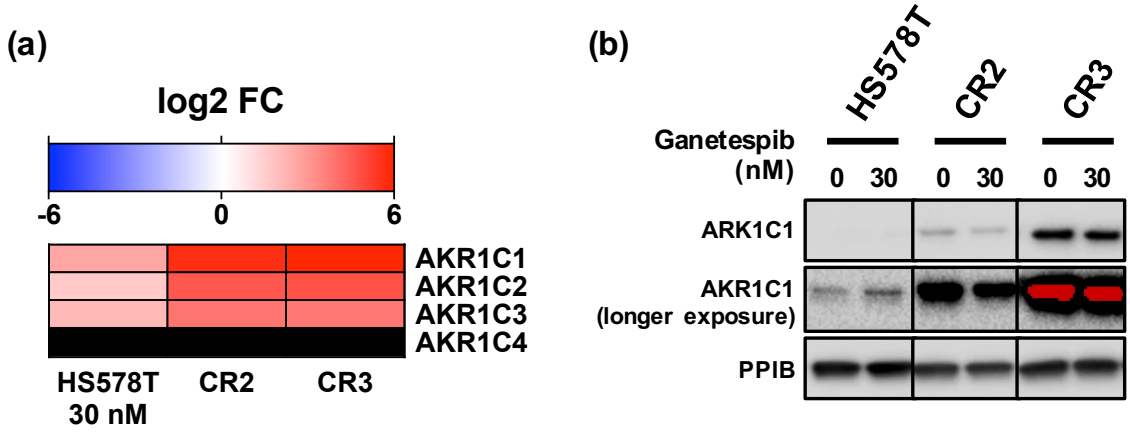


Figure 4.12: Upregulated gene expression of AKR1C family members in HSP90i-resistant clones

(a) Heatmap representing the gene expression of AKR1C family members in ganetespib-treated Hs578T cells (30 nM, 24 hr) and in HSP90i-resistant clones CR2 and CR3 compared to DMSO-treated Hs578T cells. The colour scale indicates the significant log2 FC (q-value ≤ 0.05) in gene expression for individual cells compared to DMSO-treated Hs578T cells from blue (-6, downregulation) to red (+6, upregulation). Black bar indicates that the gene expression level was below the detectable limit for that gene/cell line.

(b) Lysates obtained from Hs578T, CR2 and CR3 cells after ganetespib treatment (30 nM) for 24 hr were analysed by western blotting. PPIB was used as loading control. AKR1C1 was only detected at longer exposure times in Hs578T cells.

4.5.1. Increased levels of oxidative stress in HSP90i-resistant clones

The transcription of both UGT1A and AKR1C family genes can be induced by a transcription factor called nuclear factor E2-related factor 2 (NRF2) through the antioxidant-response element (ARE) (Jung et al., 2013, Motohashi and Yamamoto, 2004). Exposure to oxidative and electrophilic stress activates the NRF2-ARE signalling pathway, and the protein products of ARE-dependent genes play key role in detoxification and elimination of the reactive oxidants and electrophiles (Nguyen et al., 2009).

The expression of 47 ARE-dependent genes which have been reported to be positively induced by NRF2 in humans was investigated in the parental Hs578T cells and HSP90i-resistant clones (Hayes and Dinkova-Kostova, 2014). RNA-seq analysis showed that 25 out of the 47 ARE-dependent genes were significantly upregulated in one or more cell lines. Ganetespib treatment in Hs578T cells induced a significant upregulation of 10 ARE genes, overall to a lesser level than the basal expression levels of these genes in CR2 and CR3 **(Figure 4.13, Supplementary Table 7)**. Compared to parental Hs578T cells, CR2 and CR3 expressed significantly higher levels of 21 ARE genes; including genes that are involved in detoxification (ABCC3, NQO1), anti-oxidants (GCLC, TXNRD1), NADPH regeneration (G6PD) and iron metabolism (HMOX1) **(Figure 4.13, Supplementary Table 7)**. Western blotting analysis also showed that higher NAD(P)H Quinone Dehydrogenase 1 (NQO1) protein levels were expressed in CR2 and CR3 compared to Hs578T cells **(Figure 4.14a)**. The increased expression of AKR1C1, UGT1A9 and other ARE genes in CR2 and CR3 suggests that there might be reactive oxidants present in the cells that causes the activation of the NRF2-ARE signalling pathway and the transcription of genes involved in eliminating the oxidants from the cells.

Since Ataxia-Telangiectasia mutated (ATM) protein kinase is a sensor of reactive oxygen species (ROS) and can be activated by exposure to oxidative stress (Guo et al., 2010a, Guo

et al., 2010b), the expression of ATM in HSP90i-resistant clones was investigated. Indeed, the phosphorylation of ATM (S1981) was seen in CR2 and CR3, even in the absence of ganetespib **(Figure 4.14b)**. This observation further suggests that both clones might have higher intrinsic levels of oxidative stress compared to parental Hs578T cells.

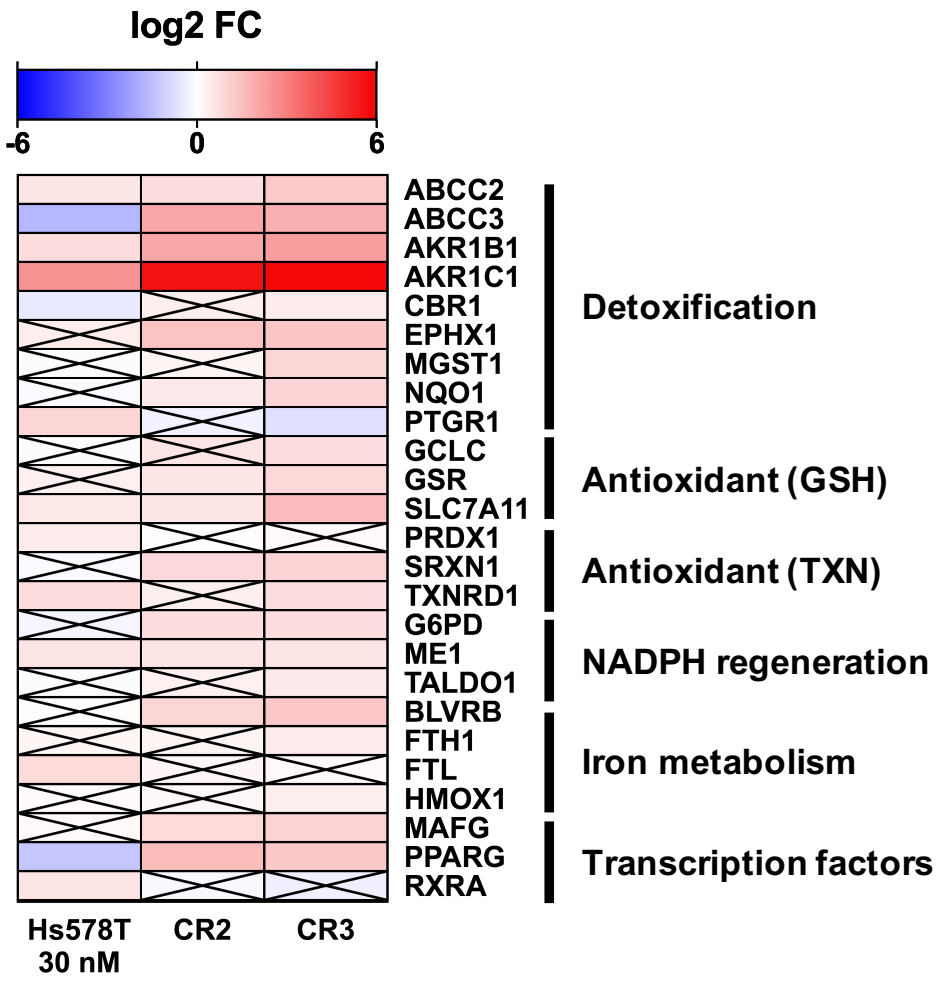


Figure 4.13: Significantly upregulated expression of ARE-dependent genes in Hs578T cells and HSP90i-resistant clones

Heatmap representing the gene expression of ARE-dependent genes in parental Hs578T cells (30 nM ganetespib) and HSP90i-resistant clones CR2 and CR3 when compared to DMSO-treated Hs578T cells. The colour scale indicates log2 FC in gene expression for individual cells when compared to DMSO-treated Hs578T cells from blue (-6, downregulation) to red (+6, upregulation). Unless indicated, the log2 FC data are statistically significant (q-value ≤ 0.05). A cross indicates that the differential expression was not statistically significant (q-value >0.05).

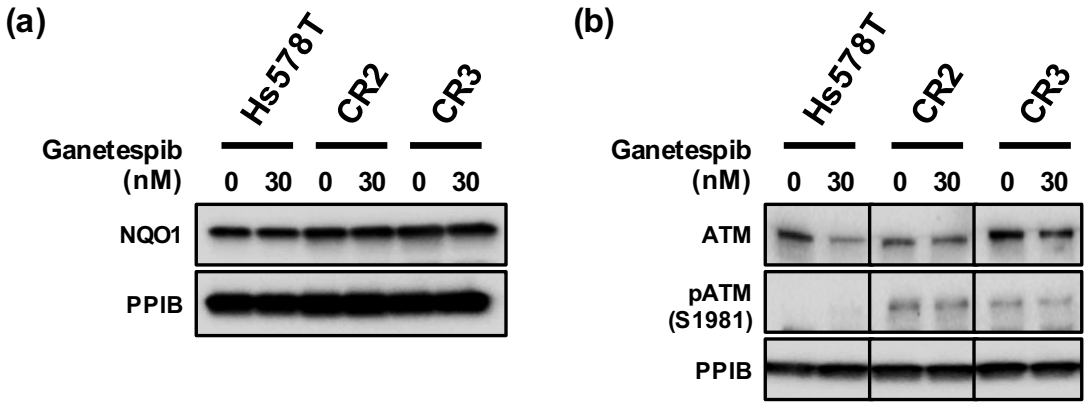


Figure 4.14: NQO1 and pATM expression in Hs578T cells and HSP90i-resistant clones

Cell lysates obtained from Hs578T, CR2 and CR3 cells after ganetespib treatment (30 nM, 24 hr) were analysed by western blotting of **(a)** NQO1, **(b)** ATM and pATM (S1981) expression. PPIB was used as loading control. Representative images from two experiments are shown.

4.5.2. Pathway enrichment analysis of differential gene expression

In order to identify any activation of signalling pathways that could be potential targets for overcoming the resistance to HSP90i, pathway enrichment analysis using Metacore^{TM} was performed on significantly upregulated genes observed in both HSP90i-resistant clones CR2 and CR3 when compared to Hs578T cells. Pathway analysis revealed a diverse activation of pathways including the JAK-STAT signalling pathway, IGF signalling pathway and NF-kB signalling pathways **(Table 4.8)**. Interestingly, and consistent with our previous observations, an activation of antioxidant defence system due to oxidative stress was among the most enriched pathways (p-value ≤ 0.05) in CR2 and CR3 **(Figure 4.15)**.

Table 4.8 The top 20 most significantly enriched pathways seen in HSP90i-resistant clones

Pathway maps	Fraction of genes	FDR
Apoptosis and survival: Anti-apoptotic TNFs/NF-kB/Bcl-2 pathway	10/42	5.15E-03
Immune response: Oncostatin M signalling via JAK-STAT in human cells	7/20	5.15E-03
Role of IL-23/ T17 pathogenic axis in psoriasis	11/54	5.15E-03
Development: PEDF signalling	10/49	7.27E-03
IGF family signalling in colorectal cancer	11/60	7.27E-03
Immune response: IL-3 signalling via JAK-STAT, p38, JNK and NF-kB	14/93	7.27E-03
Signal transduction: NF-kB activation pathways	51/10	7.45E-03
Cell adhesion: ECM remodelling	10/52	7.76E-03
Development: WNT signalling pathway	10/53	7.88E-03
Cell adhesion: Endothelial cell contacts by junctional mechanisms	7/26	7.88E-03
Immune response: CCL2 signalling	10/54	7.88E-03
Development: YAP/TAZ-mediated co-regulation of transcription	10/56	9.93E-03
Oxidative stress: Role of Sirtuin1 and PGC1-alpha in activation of antioxidant defence system	10/60	1.66E-02
NETosis in SLE	7/31	1.81E-02
Androgen receptor activation and downstream signalling in Prostate cancer	14/110	1.81E-02
Development: Activation of ERK by ACM1, ACM3 and ACM5	8/44	3.00E-02
Development: TGF-beta-dependent induction of EMT via SMADs	7/35	3.34E-02
Immune response: IL-5 signalling via JAK-STAT	9/57	3.34E-02
Immune response: MIF - the neuroendocrine-macrophage connector	8/46	3.34E-02
Immune response: Oncostatin M signalling via JAK-STAT in mouse cells	5/18	3.34E-02

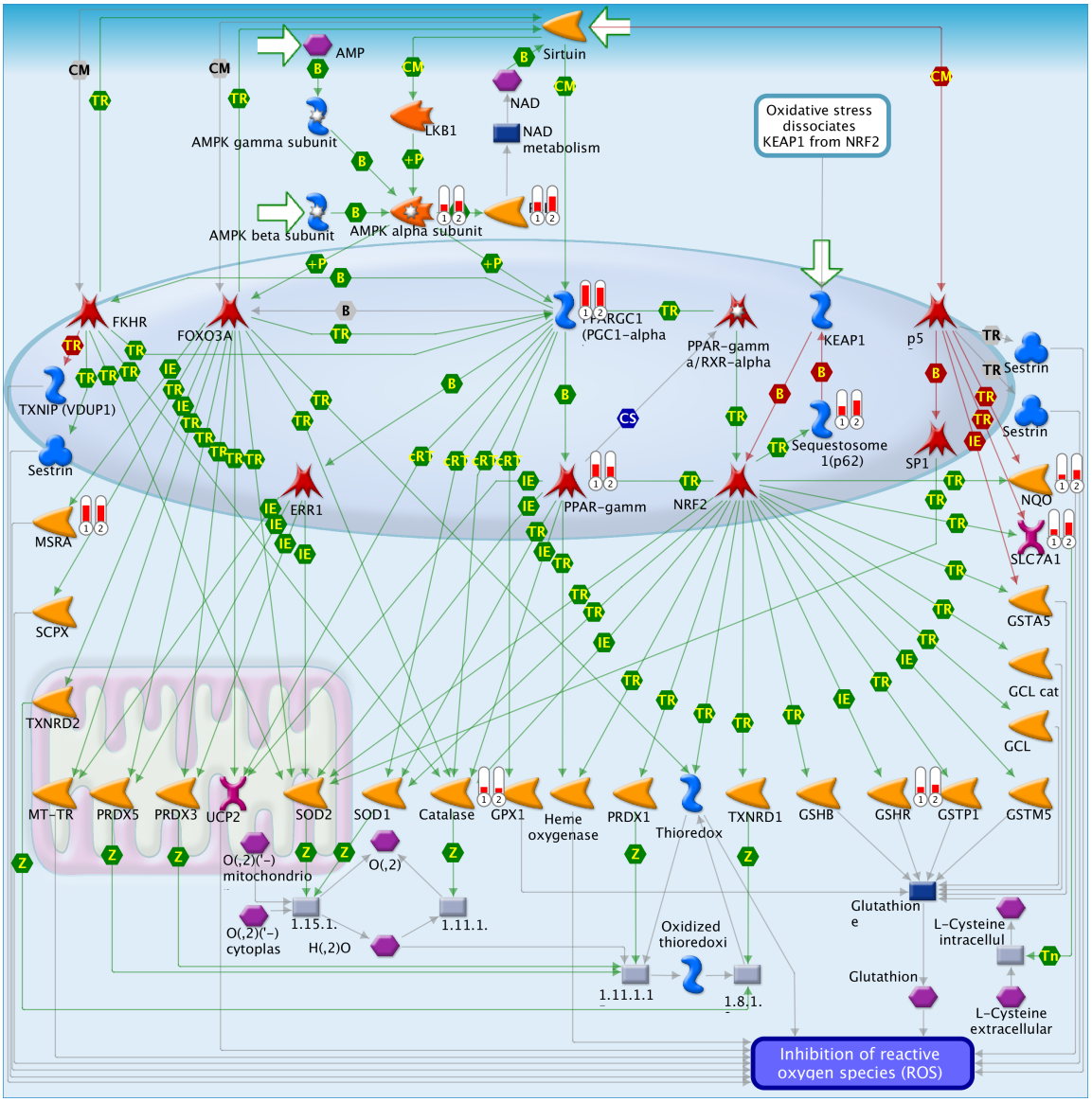


Figure 4.15: Activation of antioxidant defence system due to oxidative stress

One of the pathway obtained after pathway enrichment analysis using Metacore on upregulated genes in CR2 and CR3. The two bars next to the proteins indicate the level of upregulated genes in CR2 (1) and CR3 (2). Green arrows indicate activation and red arrows indicate inhibition. TR indicates transcription regulation. IE indicates influence on expression.

4.6. Discussion

Resistance to targeted cancer therapies has been associated with activation of RTKs and downstream compensatory signalling pathways (Logue and Morrison, 2012). However, in this study, proteomic profiling on parental Hs578T cells and independent HSP90i-resistant clones using a phospho-RTK array did not provide enough evidence for upregulation of RTK signalling. The only activation of RTKs seen in HSP90i-resistant clones were EGFR and MET. However, they might not be the major survival signalling pathway in these cells due to the lack of increased sensitivity to EGFR and MET inhibitors.

MET activation causes resistance to EGFR inhibitor through a persistent activation of its downstream signalling pathways in lung cancer cells. The combination of MET and EGFR inhibitors is required to inhibit the downstream signalling pathway and induce anti-tumour effects in the cells (Niederst and Engelman, 2013, Engelman et al., 2007). There might be a potential cross talk activation of the downstream signalling pathways of EGFR and MET (PI3K-AKT and RAS-MAPK pathways) in the HSP90i-resistant clones, even after successful inhibition of either target (EGFR or MET). Combined inhibition of EGFR and MET might also be necessary to increase the sensitivity of both inhibitors in HSP90i-resistant clones.

We also performed whole transcriptome profiling using RNA-seq on the parental Hs578T cells and HSP90i-resistant clones in order to identify differential expression of genes that can provide insights into the mechanisms of response and resistance to HSP90i in TNBC cells. HSP90i with ganetespib treatment induced differential expression of several genes in TNBC cells. HSP-related and HSP90 co-chaperones genes were among the upregulated genes in the cells after ganetespib treatment. This is consistent with studies reported in various cancers, including breast and ovarian cancers (Maloney et al., 2007, Zajac et al.,

2010). HSP90i activates transcription factor HSF1 and initiates the transcription of several HSP genes including HSP70 (Elo et al., 2005, Zou et al., 1998).

In terms of downregulated genes, HSP90i induced a downregulation of several cell cycle related genes in the TNBC cells. Cell cycle related pathways were also among the most significantly enriched pathways with downregulated gene expression in the cells. Since proteins involved in the regulation of cell cycle phases directly or indirectly (cyclins, CDKs and Survivin) are client proteins of HSP90, HSP90i causes downregulation of cell cycle related genes and proteins that leads to the induction of cell cycle arrest in several cancer cells including breast cancer (Proia et al., 2011, Burrows et al., 2004, Caldas-Lopes et al., 2009, Karkoulis et al., 2010). Flow cytometry analysis described in the previous chapter **(Figure 3.8)** also demonstrates that ganetespib treatment causes a G2/M cell cycle arrest in TNBC cells (Hs578T cells). Our study supports the inhibitory effect of ganetespib treatment on cell cycle reported in another cancer model (erythroleukemia cells)(Proia et al., 2011).

In our study, there was no significant changes in gene expression observed in both HSP90i-resistant clones CR2 and CR3 after ganetespib treatment. This further indicates that both clones have acquired resistance to HSP90i. However, several genes were significantly differentially expressed in the HSP90i-resistant clones when compared with parental Hs578T cells and these genes were mostly overlapping in both clones. This further suggests that the two independent HSP90i-resistant clones CR2 and CR3 might have similar mechanisms of resistance to HSP90i. Among the most significantly upregulated genes in both HSP90i-resistant clones were UGT1A family members, most notably UGT1A9.

In human, the UGT1A family is involved in the metabolism of lipophilic substrates including hormones, drugs and toxicants through glucuronidation. UGT1A catalyses the linkage of glucuronic acid to the functional group on the substrates (hydroxyl, carboxy or amino) and converts them to hydrophilic glucuronides that can be eliminated from the cells

(Rowland et al., 2013, Tukey and Strassburg, 2000). Glucuronidation contributes to the intrinsic drug resistance mechanism including topoisomerase inhibitors in colon cancer cells (Cummings et al., 2003). Ganetespib can also undergo glucuronidation by UGT1A family members (UGT1A9) and this rapid metabolism affects their sensitivity to HSP90i in colorectal cancer cell lines (Landmann et al., 2014, Acquaviva et al., 2014a).

Both HSP90i-resistant clones CR2 and CR3 expressed high level of UGT1A9 protein expression. Combination treatment with a competitive inhibitor of UGT1A9 (propofol) in the HSP90i-resistant clones caused a decrease in cell viability (IC_{50}), downregulation of HSP90 client protein (EGFR) as well as an induction of apoptosis and upregulation of HSP70 expression. The HSP90i-resistant clones were mostly resistant to resorcinol-based HSP90i but not cross-resistant across all chemical classes of HSP90i. These observations suggest that propofol prevents glucuronidation of a resorcinol-based HSP90i (ganetespib) by UGT1A9 and largely restores the cytotoxic effects of the HSP90i in HSP90i-resistant clones. Our study is consistent with the studies in colorectal cancer cells, where the mechanism of resistance to resorcinol-based HSP90i is due to its glucuronidation by UGT1A family members (Acquaviva et al., 2014a).

Other than UGT1A family members, our RNA-seq data analysis showed that there was an upregulated expression of several NRF2 ARE-dependent genes in the HSP90i-resistant clones. NRF2 is usually found in the cytoplasm in a complex with a repressor protein, Kelch ECH associating protein 1 (KEAP1) that promotes its proteosomal degradation. However, upon exposure to oxidative and/or electrophilic stress (ROS), NRF2 gets released from KEAP1 and is translocated to the nucleus, where it induces the transcription of several ARE-dependent genes that enhance the detoxification and antioxidant capacity of the cells as part of the cellular survival defence mechanisms to stresses (Kensler et al., 2007, Nguyen et al., 2009).

Intrinsic ROS is generated in cancer cells, due to increased oncogenic signals and metabolic processes (Pelicano et al., 2004). Excessive increase in ROS levels can cause damage (DNA, lipids and proteins) that leads to cell death (Ott et al., 2007). A moderate increase in ROS levels has potential roles in the regulation of proliferation, differentiation and migration in cancer progression (Wu, 2006). Cancer cells can adapt to the increased levels of intrinsic ROS through the upregulation of their antioxidant defence capacity (Trachootham et al., 2009).

In our study, an activation of antioxidant defence was among the most significantly enriched pathways with altered gene expression in the HSP90i-resistant clones. There was also an activation of ATM observed in these clones. ATM acts as a ROS sensor and can be activated by exposure to oxidative stress (Guo et al., 2010a, Guo et al., 2010b). Our data suggest that there might be a higher intrinsic level of ROS in the HSP90i-resistant clones compared to parental Hs578T cells. Analysis with a luminescence-based ROS assay suggested higher ROS levels in HSP90i-resistant clones compared to parental Hs578T cells, but it did not reach statistical significance **(Supplementary Figure 2).** Further experiments with more sensitive quantification of ROS still need to be done to explore these findings including using ROS-scavenger enzymes, fluorescence imaging or flow cytometry.

In this chapter, we demonstrate that the increased expression of UGT1A9, possibly due to the presence of higher intrinsic oxidative stress, is associated with the mechanism of acquired resistance to resorcinol-based HSP90i in TNBC cells and this resistance can be overcome using a competitive inhibitor of UGT1A9.

5. Overcoming acquired resistance to HSP90i

5.1. Introduction

In the previous chapter, we described that the acquired resistance to resorcinol-based HSP90i can be overcome by co-administration of a competitive inhibitor of UGT1A9, propofol. However, propofol is a potent intravenous medication for anaesthesia initiation used in intensive medical care. Its effects on patients, including unconsciousness and circulatory collapse, limits its potential as a therapeutic option in cancer patients (Marik, 2004). Regardless of the properties of a UGT1A9 inhibitor, the UGT1A family members are unlikely to make a good target for preventing or overcoming resistance to resorcinol-based HSP90i in cancer patients, as they are associated with the metabolism of a wide range of substrates in human, including steroids and bilirubin metabolism (Tukey and Strassburg, 2000).

Our pathway enrichment analysis from RNA-seq data revealed that, in addition to the activation of antioxidant defence, genes in several key biological processes were also upregulated in the HSP90i-resistant clones, most notably pro-survival and JAK-STAT signalling pathways **(Table 4.8)**. These pathways might also be associated with resistance to HSP90i and could potentially provide novel targets for overcoming this resistance in TNBC cells.

Drug screenings are part of cancer drug discovery as it allows identification of molecular mechanisms and compounds with selective effects on growth inhibition or toxicity in particular cancers (Shoemaker, 2006). Therefore, in this chapter, we utilised a 328-compound bioactive small molecule library and screened for compounds that selectively inhibit the cell viability of HSP90i-resistant clones to identify potential novel targets for overcoming resistance to HSP90i.

5.2. Bioactive small molecule screen

A screen with a 328-compound bioactive small molecule library was performed on parental Hs578T cells and the HSP90i-resistant clone CR3 **(Figure 5.1)**. The library (n=328) consists of 326 compounds (Selleck, L1100) **(Supplementary Table 1)**, phleomycin and ganetespib, which covers a broad range of established targets in cancer therapy. Many of the compounds are approved for clinical use, or in late stage clinical or preclinical development. The screen with CR3 cells was carried out, in the absence or presence of ganetespib (10 nM), to identify compounds with selective combination effects. The screen was reproducible with cell viability from both duplicate and independent experiments being highly correlated ($r > 0.8$, $p < 0.001$) **(Figure 5.2)**.

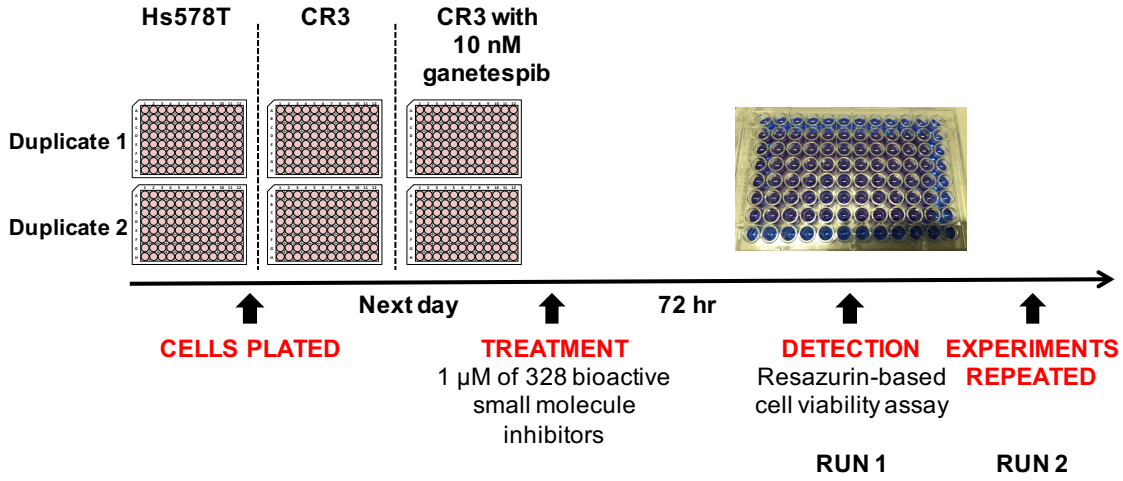


Figure 5.1: Schematic of the 96-well based bioactive small molecule screen

Parental Hs578T cells (800 cells/well) or HSP90i-resistant clone CR3 (1000 cells/well) were plated into 96-well plates. The next day, cells were treated with a fixed concentration (1 µM) of the individual 328 compounds for 72 hr. The CR3 was also treated in combination with 10 nM ganetespib. Each screen was performed twice in duplicate and resazurin-based cell viability assay was used as an end point. Cell viability (%) for each treatment was expressed relative to DMSO-treated controls.

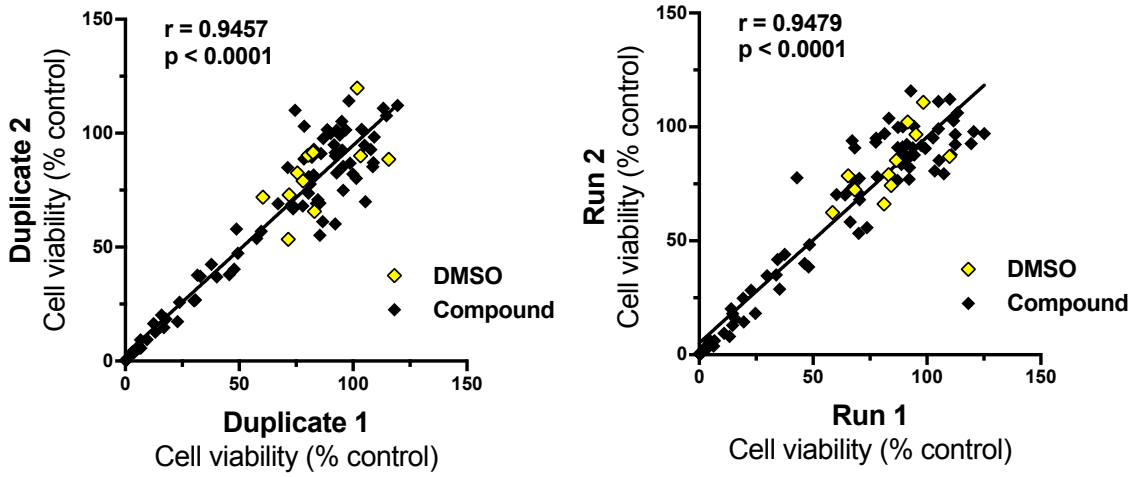


Figure 5.2: Correlation between duplicate samples and independent runs in the screen

Representative scatter plot for one 96-well plate showing the relationship between the cell viability of the compounds from the duplicate samples within each run (left panel), as well as, from the two independent runs (right panel). Pearson's correlation (r) was determined. Yellow symbols represent the DMSO-treated controls.

5.2.1. Identification of differentially active compounds in HSP90i-resistant clone CR3 compared with parental Hs578T cells

The cell viability of respective compounds in parental Hs578T cells and HSP90i-resistant clone CR3 was compared in order to determine their relative sensitivity (Z-score). CR3 did not show selective sensitivity (Z-score $\geq$ 2) to any compound, but showed selective resistance (Z-score $\leq$ -2) to 20/328 compounds compared with Hs578T cells **(Figure 5.3 and Table 5.1)**. As expected, CR3 showed resistance to ganetespib compared with Hs578T cells (Z-score of -1.90). The 20 compounds mainly consisted of inhibitors targeting proteins involved in proliferation and cell cycle checkpoints, such as topoisomerases, aurora kinase, CDK, PLK and CHEK. Of note, CR3 had a slower growth rate compared to Hs578T cells **(Figure 5.4)**. This suggests that compounds that are selectively cytotoxic to highly dividing cells would have decreased effects on the HSP90i-resistant clone CR3 compared with parental Hs578T cells.

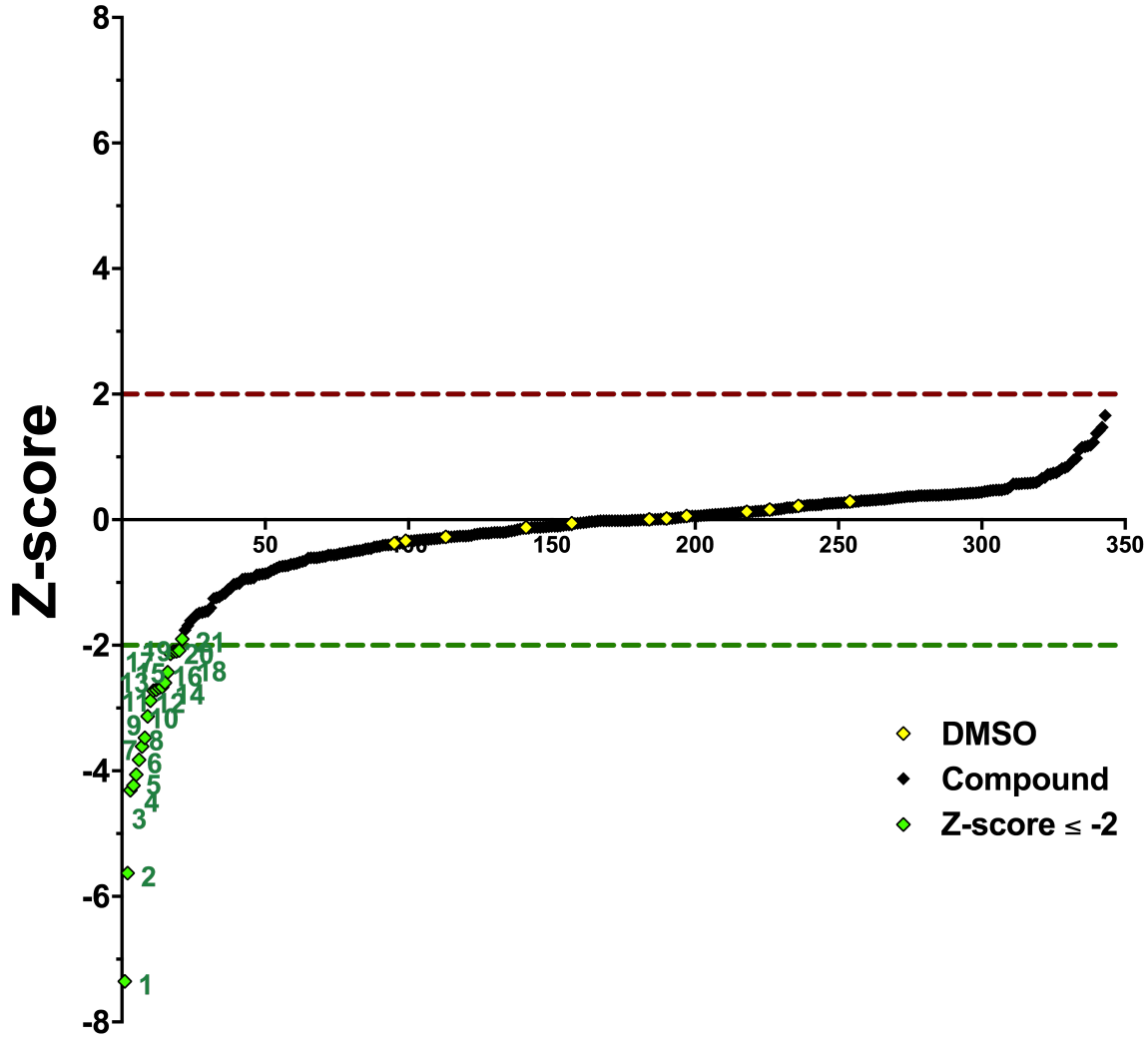


Figure 5.3: Z-scores of sensitivity to compounds comparing parental Hs578T cells and HSP90i-resistant clone CR3

The scatter plot of Z-scores calculated after comparing the sensitivity for the entire library of the small bioactive compounds in parental Hs578T cells and HSP90i-resistant clone CR3. The Z-scores were ranked from compound that was least sensitive to most sensitive in CR3 compared with Hs578T cells. Yellow symbols represent DMSO-treated controls. Green symbols represent compounds that were selectively cytotoxic to parental Hs578T cells compared with CR3 (Z-score ≤ -2).

Table 5.1: Compounds that were selectively cytotoxic to parental Hs578T cells compared with HSP90i-resistant clone CR3

	Compound	Target	Z-score
1	AT9283	BCR-ABL/JAK/Aurora Kinase	-7.35
2	Mitoxantrone	Topoisomerase	-5.63
3	Obatoclax Mesylate	BCL2	-4.31
4	Camptothecin	Topoisomerase	-4.23
5	SNS-032 (BMS-387032)	CDK	-4.06
6	AT7519	CDK	-3.82
7	PHA-739358 (Danusertib)	Aurora Kinase/BCR-ABL	-3.61
8	PHA-793887	CDK	-3.47
9	ZM-447439	Aurora Kinase	-3.13
10	2-Methoxyestradiol	HIF	-2.88
11	Adriamycin	Topoisomerase	-2.72
12	GSK461364	PLK	-2.71
13	GSK1059615	PI3K/MTOR	-2.68
14	AZD1152-HQPA (Barasertib)	Aurora Kinase	-2.67
15	PHA-680632	Aurora Kinase	-2.60
16	Deforolimus (MK-8669)	MTOR	-2.43
17	Topotecan Hydrochloride	Topoisomerase	-2.13
18	AZD7762	CHEK	-2.10
19	Dasatinib	SRC/ABL	-2.09
20	VX-680	Aurora Kinase	-2.08
21	Ganetespib	HSP90	-1.90

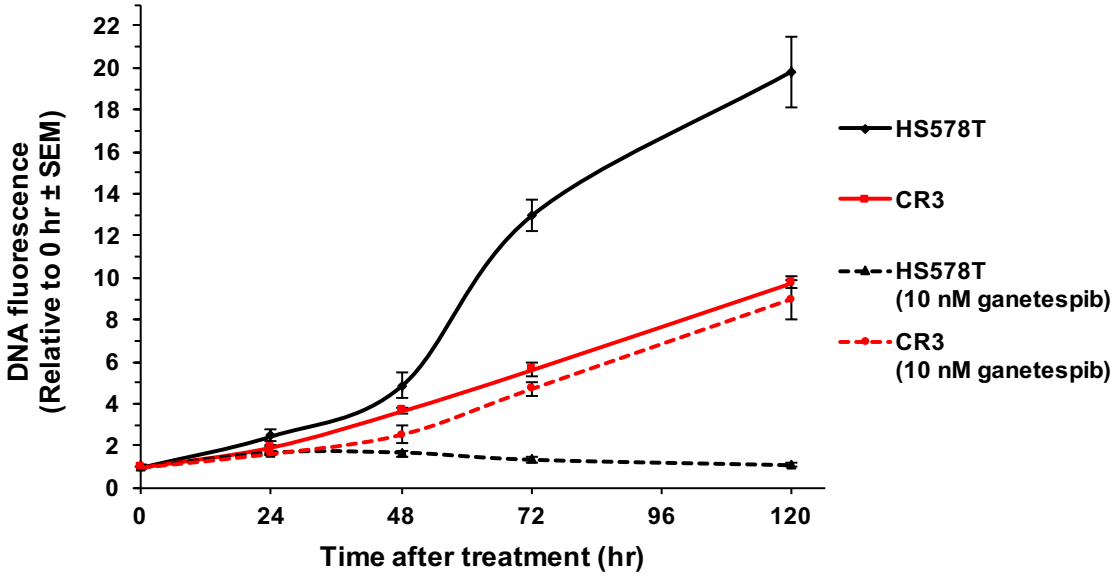


Figure 5.4: Growth curves of Hs578T cells and HSP90i-resistant clone CR3 upon ganetespib treatment

Parental Hs578T cells and HSP90i-resistant clone CR3 were plated into 96 well plates (300 cells/well). The next day, the cells were treated in the absence or presence of ganetespib (10 nM). The growth of Hs578T cells and CR3 was assessed using picogreen assay. Cells were lysed at indicated time points and the amount of DNA content was determined (as a surrogate measure of cell number). Mean relative DNA fluorescence was quantified relative to 0 hr from two independent experiments each performed with triplicates. Error bars indicate SEM.

5.2.2. Identification of differentially active compounds in HSP90i-resistant clone CR3 with the presence of ganetespib

A ganetespib concentration of 10 nM was selected for the combination screen as it had no significant effect on the growth of HSP90i-resistant clone CR3 **(Figure 5.4).** The Z-scores for the screen in combination with ganetespib for CR3 were determined by comparing the sensitivity of individual compound in the absence and presence of ganetespib. CR3 showed selective resistance (Z-score $\leq$ -2) to 5/328 compounds in the presence of ganetespib **(Figure 5.5 and Table 5.2)**. Interestingly, CR3 showed selective sensitivity (Z-score $\geq$ 2) to 10/328 compounds, only in the presence of ganetespib **(Figure 5.5 and Table 5.3)**. Therefore, although CR3 cells are resistant to HSP90i and their growth was unaffected in the presence of 10 nM ganetespib **(Figure 5.4)**, there was still a combination effect of ganetespib treatment on sensitivity to these 10 compounds **(Table 5.3)**.

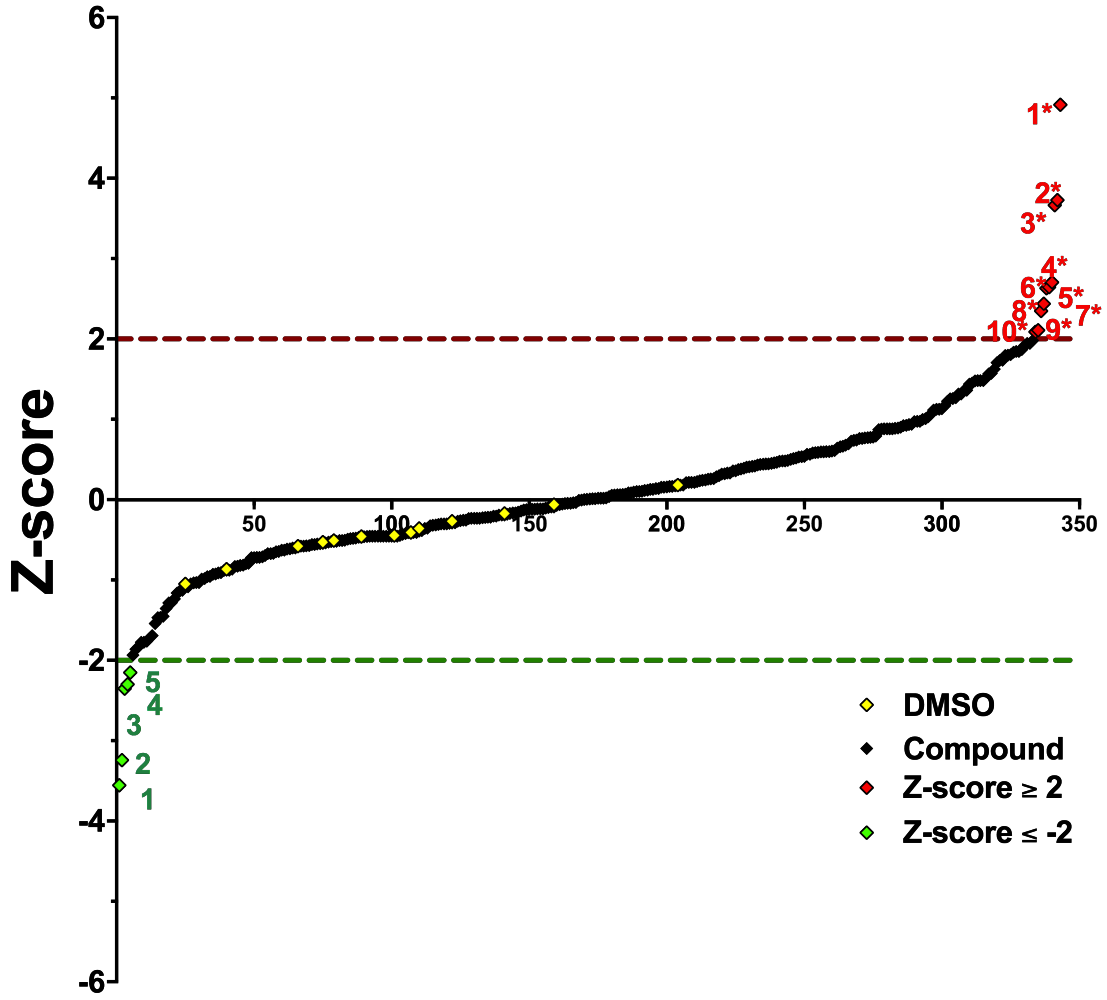


Figure 5.5: Z-scores of sensitivity to compounds comparing HSP90i-resistant clone CR3 in the absence and presence of ganetespib

The scatter plot of Z-scores calculated after comparing the sensitivity for the entire library of small bioactive compounds in HSP90i-resistant clone CR3 in the absence and presence of 10 nM ganetespib. The Z-scores were ranked from compound that was least sensitive to most sensitive in CR3 in the presence of ganetespib. Yellow dots represent DMSO-treated controls. Red symbols represent compounds that were selectively cytotoxic in CR3 with the presence of ganetespib (Z-score ≥ 2). Green symbols represent compounds that were selectively cytotoxic to CR3 with the absence of ganetespib (Z-score ≤ -2).

Table 5.2: Compounds that were selectively cytotoxic to HSP90i-resistant clone CR3 in the absence of ganetespib

	Compound	Target	Z-score
1	SB 743921	Kinesin spindle protein	-3.55
2	Ispinesib mesilate	Kinesin spindle protein	-3.24
3	ITF2357	HDAC	-2.35
4	NPI-2358	VDA	-2.30
5	BEZ235(NVP-BEZ235)	MTOR/PI3K	-2.15

Table 5.3: Compounds that were selectively cytotoxic to HSP90i-resistant clone CR3 in the presence of ganetespib

	Compound	Target	Z-score
1*	Aurora A Inhibitor I	Aurora Kinase	4.91
2*	MLN8237	Aurora	3.73
3*	LY2784544	JAK2	3.67
4*	LY2228820	p38 MAPK	2.71
5*	ENMD-2076	FLT/Aurora Kinase/SRC/VEGFR	2.64
6*	Tipifarnib	Farnesyltransferase (Ftase)	2.63
7*	Phleomycin	DNA	2.44
8*	U0126-EtOH	MEK	2.35
9*	SB 431542	ALK	2.11
10*	PHA-739358(Danusertib)	Aurora Kinase/BCR-ABL	2.09

5.2.3. Validation of positive hits from bioactive small molecule screen

Ten compounds that were selectively cytotoxic to HSP90i-resistant clone CR3 in the presence of ganetespib were re-tested to confirm their selectivity and the impact of ganetespib on drug sensitivity (IC_{50}). The selective effects of the compounds in the presence of ganetespib were mostly reproducible with differences in IC_{50} values reaching statistical significance for 5/10 of the compounds tested **(Figure 5.6 and Table 5.4)**. Although Aurora A Inhibitor I remained a significant hit upon retesting (Table 5.4), there was no difference in IC_{50} values for the other Aurora Kinase inhibitors (EMND-2076 and PHA-739358), suggesting that they were false positive hits **(Figure 5.7 and Table 5.4)**.

Table 5.4: Sensitivity to compounds from the screen that were selectively cytotoxic to HSP90i-resistant clone CR3

Compound	Target	IC_{50} ± SEM (μM)			p-value of IC_{50} comparison
		Hs578T	CR3	CR3 with 10 nM ganetespib	
LY2784544	JAK2	0.61 ± 0.09	1.09 ± 0.10	0.38 ± 0.03	**
U0126-EtOH	MEK	>3	>3	0.73 ± 0.13	**
LY2228820	p38 MAPK	>3	>3	1.35 ± 0.15	**
Aurora A Inhibitor I	Aurora Kinase	0.44 ± 0.07	0.46 ± 0.09	0.21 ± 0.03	*
MLN8237	Aurora	0.077 ± 0.009	0.095 ± 0.005	0.056 ± 0.004	*
Phleomycin[a]	DNA	0.17	0.60	0.27	
SB 431542[a]	ALK	>3	>3	0.42	
ENMD-2076[a]	FLT/Aurora Kinase/ SRC/VEGFR	0.40	0.43	0.37	
PHA-739358[a]	Aurora Kinase/ BCR-ABL	0.057	0.57	0.56	

IC_{50} of compound in CR3 in the absence or presence of ganetespib was compared. *, ** indicate p values ≤0.05, ≤0.01 respectively; by Student's t-test.

[a] IC_{50} was obtained from an individual experiment

Note: Tipifarnib did not show enough data points below 50% relative cell viability to fit the curve and calculate an IC_{50} value

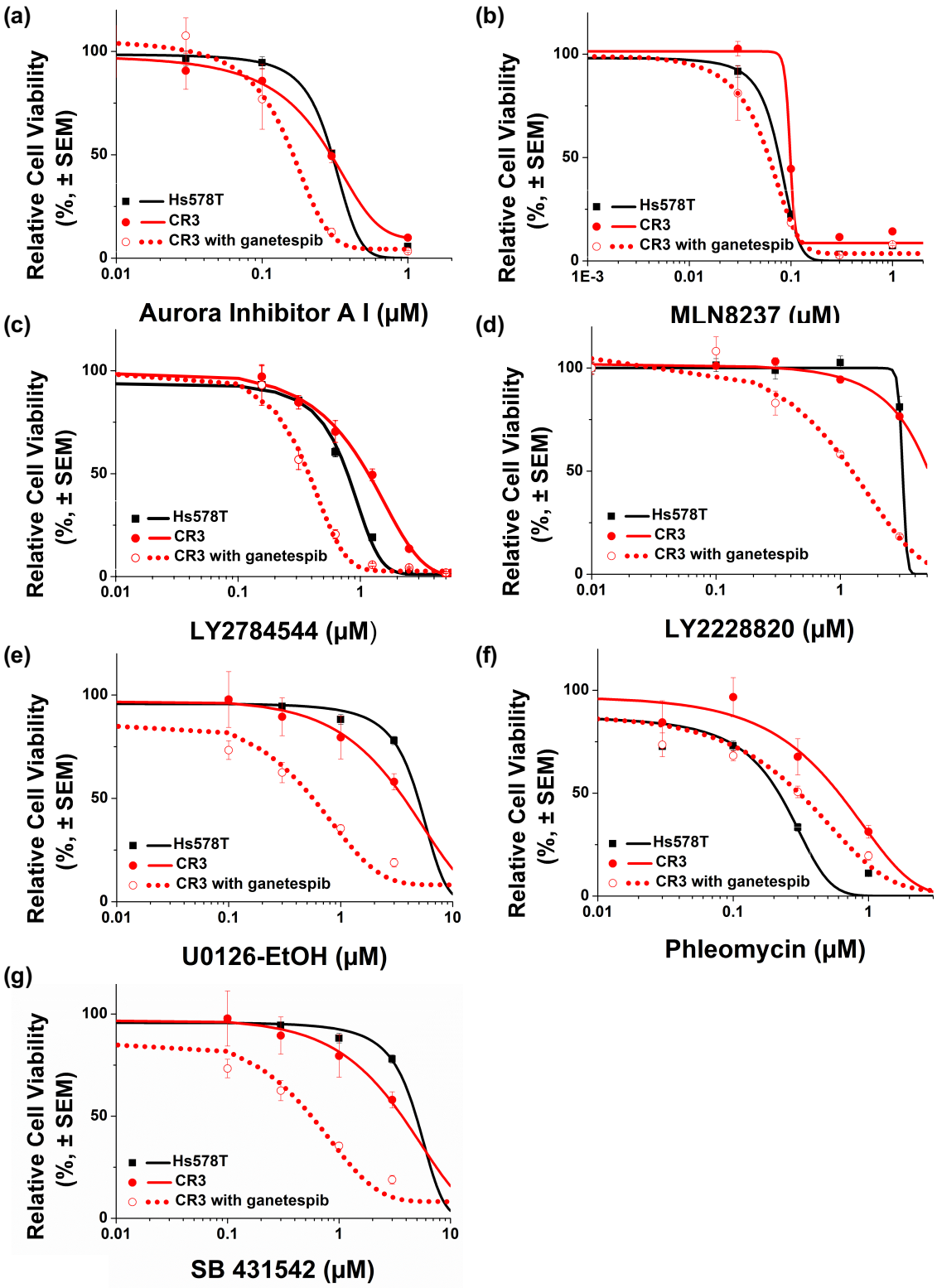


Figure 5.6: Dose-response of compounds from the screen that were selectively cytotoxic in HSP90i-resistant clone CR3

Parental Hs578T cells and HSP90i-resistant clone CR3 were treated with increasing concentration (0 - 3 μM) of **(a)** Aurora A Inhibitor I, **(b)** MLN8237, **(c)** LY2784544, **(d)** LY2228820, **(e)** U0126-EtOH, **(f)** Phleomycin and **(g)** SB 431542 for 72 hr and cell viability was assessed by a resazurin-based assay. CR3 was also treated in combination with 10 nM ganetespib. Cell viability (%) for each treatment was expressed relative to either DMSO-treated or ganetespib only-treated control for each combination. Representative graph from three independent experiments each performed in triplicates (except for phleomycin and SB 431542, each from a single experiment performed in triplicates). Error bars indicate SEM.

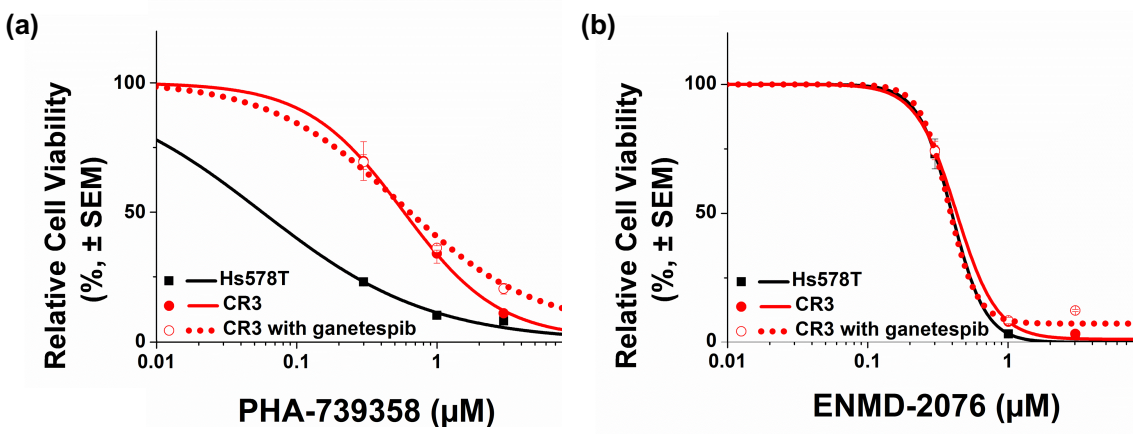


Figure 5.7: The effect of Aurora Kinase inhibitors in combination with ganetespib in HSP90i-resistant clone CR3

Parental Hs578T cells and HSP90i-resistant clone CR3 were treated with increasing concentration (0 - 3 μM) of Aurora kinase inhibitors **(a)** PHA-739358 and **(b)** ENMD-2076 for 72 hr and cell viability was assessed by a resazurin-based assay. CR3 was also treated in combination with 10 nM ganetespib. Cell viability for each treatment (%) was expressed relative to either DMSO-treated or ganetespib only-treated control for combination. Experiment was performed in triplicates and error bars indicate SEM.

LY2784544, a Janus Kinase 2 (JAK2) inhibitor, was among the most significant compounds from the validation that showed selective cytotoxicity to the HSP90i-resistant clone CR3 in the presence of ganetespib **(Table 5.4)**. The IC_{50} values of LY2784544 in CR3 decreased by three-fold with the presence of ganetespib; from 1.09 ± 0.10 nM to 0.38 ± 0.03 nM ($p \leq 0.01$). In addition, due to the JAK-STAT signalling pathway being among the most significantly altered pathways in the HSP90i-resistant clones **(Table 4.8)**, JAK2 inhibition was chosen for further investigation in our study.

Sensitivity to LY2784544 was tested in the other HSP90i-resistant clone CR2. CR2 also showed a significant increase in sensitivity to LY2784544, in the presence of 10 nM ganetespib. The IC_{50} values of LY2784544 in CR2 decreased by three-fold with the presence of ganetespib; from 1.63 ± 0.19 nM to 0.47 ± 0.02 nM ($p \leq 0.01$) **(Figure 5.8 and Table 5.5)**. The sensitivity of another JAK2 inhibitor (AZD1480) was then tested in the HSP90i-resistant clones **(Figure 5.9a)**. Interestingly, both CR2 and CR3 also showed significant

decrease in cell viability after treatment with 2 µM of AZD1480, in the presence of ganetespib **(Figure 5.9b)**. These observations suggest that the two HSP90i-resistant clones have increased sensitivity to JAK2 inhibition (JAK2i) in the presence of ganetespib.

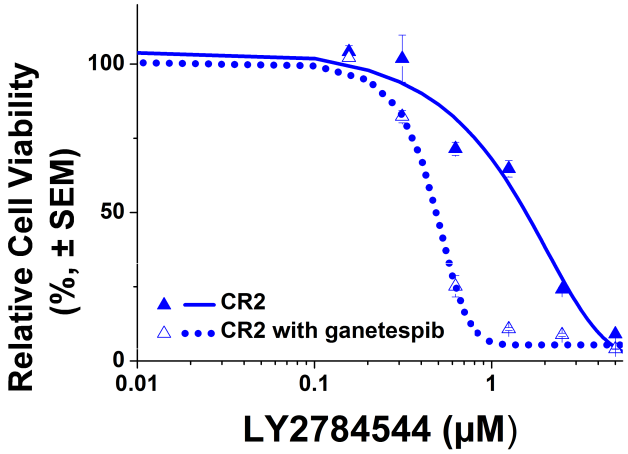


Figure 5.8: The effect of LY2784544 in combination with ganetespib in HSP90i-resistant clone CR2

HSP90i-resistant clone CR2 was treated with increasing concentrations (0.01 - 3 µM) of LY2784544 alone or in combination with 10 nM ganetespib for 72 hr and subjected to resazurin-based cell viability assay. Cell viability (%) for each treatment was quantified relative to either DMSO-treated or ganetespib only-treated control for combination. Representative graph from three independent experiments each performed in triplicates and error bars indicated SEM.

Table 5.5: Sensitivity to LY2784544 in combination with 10 nM ganetespib

Cells	LY2784544 (µM) IC_{50} ± SEM	LY2784544 (µM) IC_{50} ± SEM in combination with 10 nM ganetespib	p-value of IC_{50} comparison
Hs578T	0.61 ± 0.09	ND	
CR2	1.63 ± 0.19	0.47 ± 0.02	**
CR3[a]	1.09 ± 0.10	0.38 ± 0.03	**

IC_{50} of LY2784544 and in combination with ganetespib was compared.
** indicated p values ≤0.01; which was determined by Student's t-test.
ND: Not done, as 10 nM ganetespib is highly cytotoxic to Hs578T cells
[a] Values also shown in Table 5.4

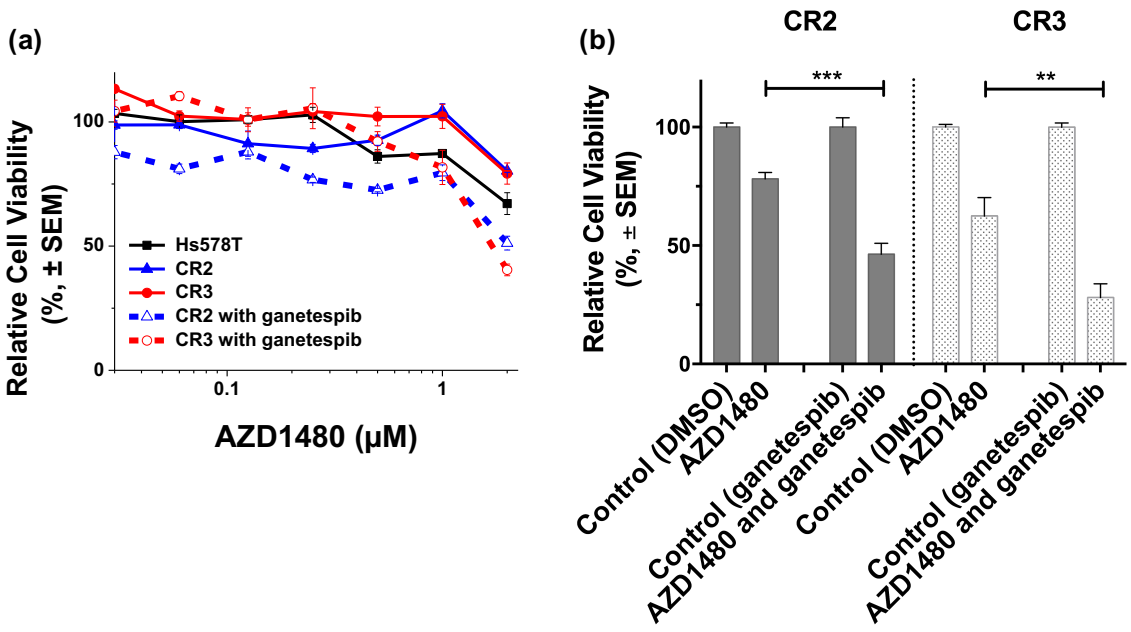


Figure 5.9: The effect of AZD1480 in combination with ganetespib in HSP90i-resistant clones CR2 and CR3

Hs578T cells and HSP90i-resistant clones CR2 and CR3 were treated with increasing concentration (0 - 3 μM) of the JAK2 inhibitor (AZD1480) for 72 hr and cell viability was assessed by resazurin-based assay. CR2 and CR3 were also treated in combination with 10 nM ganetespib. Cell viability (%) for each treatment was expressed relative to either DMSO-treated or ganetespib only-treated control for combination. **(a)** Representative graph from two independent experiments each performed in triplicates and error bars indicate SEM. **(b)** IC_{50} could not be calculated therefore cell viability was compared at the highest concentration of AZD1480 tested (2 μM). The graph represents the overall mean cell viability relative to DMSO-treated or ganetesib-treated control from two independent experiments each performed in triplicates. Error bars indicate SEM. The sensitivity of AZD1480; in the absence or presence of ganetespib were compared in the HSP90i-resistant clones. ** and *** indicate p values ≤0.01 and ≤0.001 respectively; by Student's t-test.

5.3. JAK2-STAT3 signalling pathway in HSP90i-resistant clones

JAK2 is activated by the binding of certain cytokines (e.g. IL6) to their receptor. Cytoplasmic signal transducer and activator of transcription 3 (STAT3) gets recruited to the receptor and phosphorylated, which in turn promotes its dimerisation (Heinrich et al., 1998). Dimerised pSTAT3 translocates to the nucleus, where it binds to specific DNA sequences promoting the transcription of target genes (Rawlings et al., 2004). JAK-STAT signalling pathways mediate several processes involved in cell survival and cancer progression (Yu et al., 2014).

Since HSP90i-resistant clones were more sensitive to JAK2i in the presence of ganetespib, JAK2-STAT3 signalling pathways might contribute to the mechanism of resistance to HSP90i. The expression of STAT3 was investigated in the parental Hs578T cells and HSP90i-resistant clones, in the presence of JAK2i (1 μM LY2784544), HSP90i (10 nM ganetespib) or in combination. The treatment of either JAK2i, HSP90i or in combination did not cause any changes in the expression of total STAT3 in the parental Hs578T cells, HSP90i-resistant clones CR2 and CR3. However, levels of pSTAT3 (Y705) were markedly reduced after LY2784544 treatment in Hs578T cells, CR2 and CR3 **(Figure 5.10a),** demonstrating that the compound was pharmacologically active at the concentration tested (1 μM). Interestingly, when compared to parental Hs578T cells, CR2 and CR3 expressed higher levels of pSTAT3 (Y705) in either absence or presence of ganetespib, but this did not reach statistical significance **(Figure 5.10a, b)**. This suggests that there might be an activation of the STAT3 signalling pathway in the HSP90i-resistant clones.

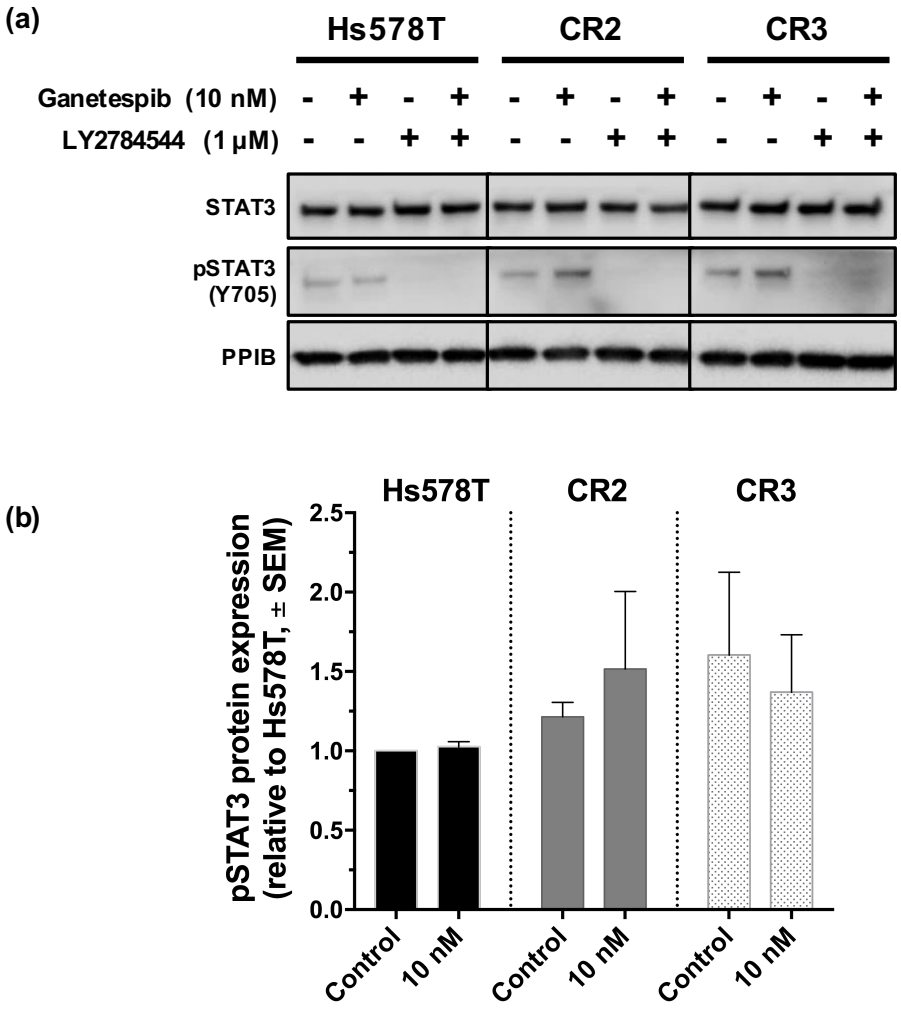


Figure 5.10: Inhibition of STAT3 activity in Hs578T cells and HSP90i-resistant clones

Parental Hs578T cells and HSP90i-resistant clones CR2 and CR3 cells were treated with ganetespib (10 nM), LY2784544 (1 µM) or in combination for 24 hr. **(a)** Lysates of treated cells were analysed by western blotting for the indicated proteins. PPIB was used as loading control. **(b)** Quantification of pSTAT3 protein expression was calculated (photon counts) after normalisation to its respective loading control and expressed relative to the protein band intensity in Hs578T cells. The graph represents the mean relative pSTAT3 protein expression of Hs578T cells, CR2 and CR3 from three independent experiments. Error bars indicate SEM.

5.3.1. Combined inhibition of JAK2 and HSP90 in HSP90i-resistant clones

The cytotoxic effect of JAK2i (1 μM LY2784544), HSP90i (10 nM ganetespib) or combination was investigated in parental Hs578T cells and HSP90i-resistant clones, in terms of induction of cell apoptosis and cell growth. In line with previous observations, ganetespib treatment alone did not cause an increase in apoptosis, as measured by cleaved PARP levels in the HSP90i-resistant clones CR2 and CR3. However, there was an increase in apoptosis after combination treatment with LY2784544 in both clones **(Figure 5.11)**. There was also an increase in apoptosis after combination treatment in parental Hs578T cells. Moreover, there was an increase in HSP70 expression in the combination treatment (most notably for CR3). This further suggests that the combined treatment with JAK2i causes an increase in the cytotoxic activity of HSP90i in HSP90i-resistant clones.

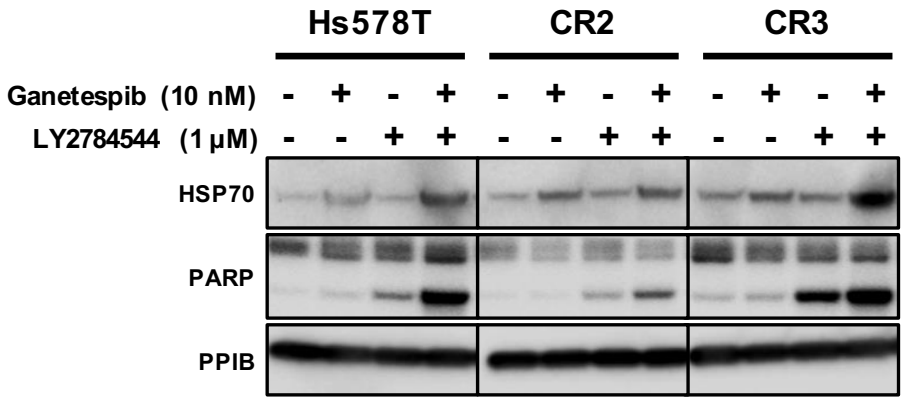


Figure 5.11: Induction of apoptosis in Hs578T cells and HSP90i-resistant clones after JAK2 and HSP90 inhibition

Parental Hs578T cells and HSP90i-resistant clones CR2 and CR3 were treated with ganetespib (10 nM), LY2784544 (1 μM) or in combination for 24 hr. Protein lysates were analysed by western blotting. Cleaved PARP was used to assess induction of apoptosis and HSP70 was used as a pharmacodynamic marker for inhibition of HSP90 activity. PPIB was used as loading control.

Sensitivity to ganetespib (IC_{50}) was assessed in parental Hs578T cells and HSP90i-resistant clones CR2 and CR3, in the absence or presence of LY2784544. As expected, there was a significant decrease in IC_{50} values of ganetespib in Hs578T, CR2 and CR3 cells with the presence of 1 µM LY2784544; 2.62 ± 0.18 nM, 4.50 ± 0.51 nM and 3.70 ± 0.25 nM respectively **(Figure 5.12 and Table 5.6)**.

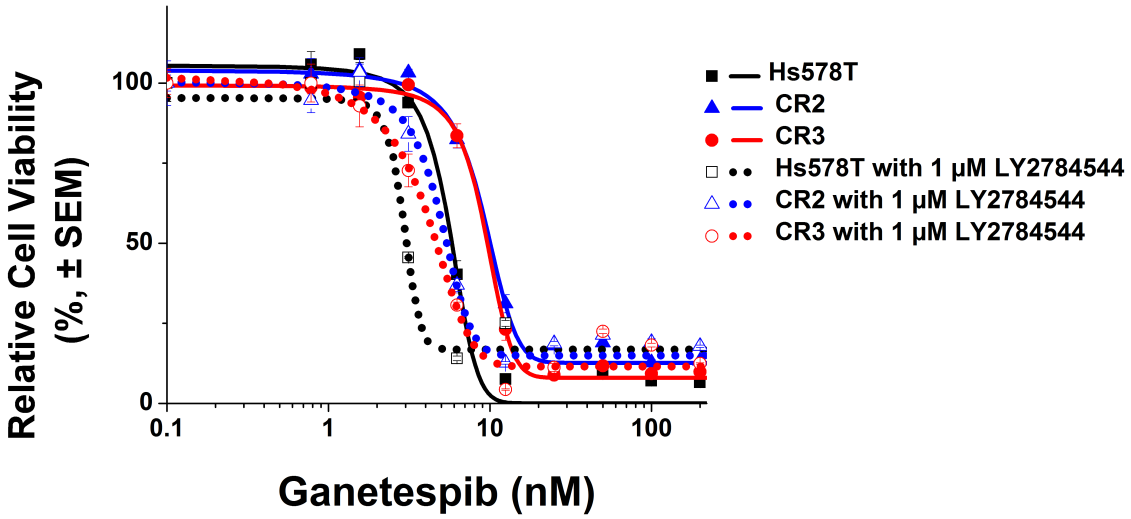


Figure 5.12: The effect of LY2784544 on sensitivity to ganetespib

Parental Hs578T cells and HSP90i-resistant clones CR2 and CR3 were treated with increasing concentration (0 - 200 nM) of ganetespib alone or in combination with 1 µM of LY2784544 for 72 hr and cell viability was assessed by resazurin-based assay. Cell viability (%) for each treatment was expressed relative to either DMSO-treated or LY2784544 only-treated controls. Representative graph from three independent experiments each performed in triplicates and error bars indicate SEM.

Table 5.6: Cytotoxicity of ganetespib alone and in combination with 1 µM LY2784544

Cell line	Ganetespib IC_{50} ± SEM (nM)	Ganetespib IC_{50} ± SEM in combination with 1 µM LY2784544 (nM)	p-value of IC_{50} comparison
Hs578T	5.53 ± 0.29	2.62 ± 0.18	**
CR2	10.16 ± 0.76	4.50 ± 0.51	**
CR3	10.06 ± 1.21	3.70 ± 0.25	**

IC_{50} of compound in HSP90i-resistant clones in the absence or presence of JAK2i was compared.
** p value ≤0.01; by Student's t-test.

5.3.2. Gene expression profiling of JAK-STAT signalling pathways

The expression of 92 genes involved in JAK-STAT signalling pathways (Table 2.5) was assessed in parental Hs578T cells and HSP90i-resistant clone CR3 using a RT-PCR JAK-STAT expression array and RNA-seq analysis. From the JAK-STAT expression array, the expression of 55/92 were upregulated in CR3 compared to Hs578T cells **(Figure 5.13)**. In addition, RNA-seq analysis showed that 20 genes were significantly differentially expressed in CR3 compared to Hs578T cells **(Figure 5.14)**. The differential gene expression analysis from each assay identified common upregulated genes including the cytokine IL6 and the oncogenic transcription factor MYC. The log2 FC of IL6 and MYC expression was 3.5 and 1.9, respectively in CR3 compared to Hs578T cells **(Supplementary Table 8)**. This further suggests that there is a significant activation of the JAK-STAT signalling pathways in HSP90i-resistant clones. This is consistent with the data obtained from the pathway enrichment analysis using Metacore^{TM}.

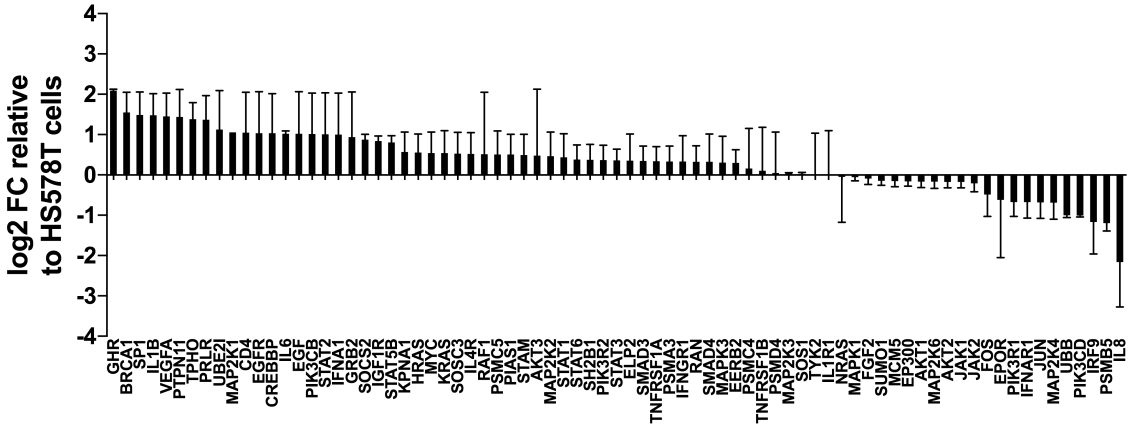


Figure 5.13: Expression of genes involved in JAK-STAT signalling pathways in HSP90i-resistant clone CR3

The expression of 92 genes associated with JAK-STAT signalling pathways were assessed in parental Hs578T cells and HSP90i-resistant clone CR3 by RT-PCR JAK-STAT array. The expression of each gene was normalised to an endogenous control gene (GAPDH) and compared between samples. The graph represents the mean log2 FC in gene expression in CR3 relative to HS578T cells from two independent experiments. Error bars indicate SEM.

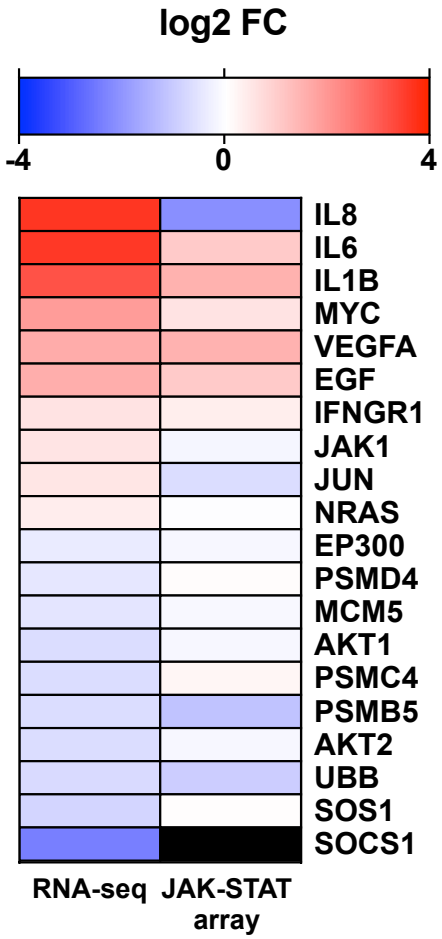


Figure 5.14: Differential expression of genes involved in JAK-STAT signaling pathways using RNA-seq and JAK-STAT array analysis.

Heatmap representing the gene expression of JAK-STAT signaling pathways in HSP90i-resistant clone CR3 compared to parental Hs578T cells obtained from RNA-seq and JAK-STAT array data. The colour scale indicates the log2 fold change in gene expression from blue (-4, downregulation) to red (+4, upregulation). Differential gene expression of genes that were significant (q-value ≤ 0.05) from the RNA-seq analysis are shown, and ranked from highest (upregulated) to lowest (downregulated) differential expression. A black box indicates that the gene expression level was below the detectable limit.

5.3.3. Autocrine-mediated JAK2-STAT3 signalling in HSP90i-resistant clones

Since JAK2 can be activated by the binding of IL6 to its receptor and initiates the JAK2-STAT3 signalling pathway (Heinrich et al., 1998), the expression of IL6 secreted into the cell culture medium by Hs578T cells and HSP90i-resistant clones CR2 and CR3 was determined using an ELISA assay **(Figure 5.15)**. Ganetespib treatment did not increase the levels of IL6 in media of these cells. Interestingly, when compared to the medium of untreated Hs578T cells, there were significantly higher levels of IL6 measured in the media of CR2 and CR3, either in the absence or presence of ganetespib. Together with previous observations, these results suggest that an activation of IL6-mediated JAK2-STAT3 signalling pathways in HSP90i-resistant clones might contribute to the mechanism of resistance to HSP90i in the cells.

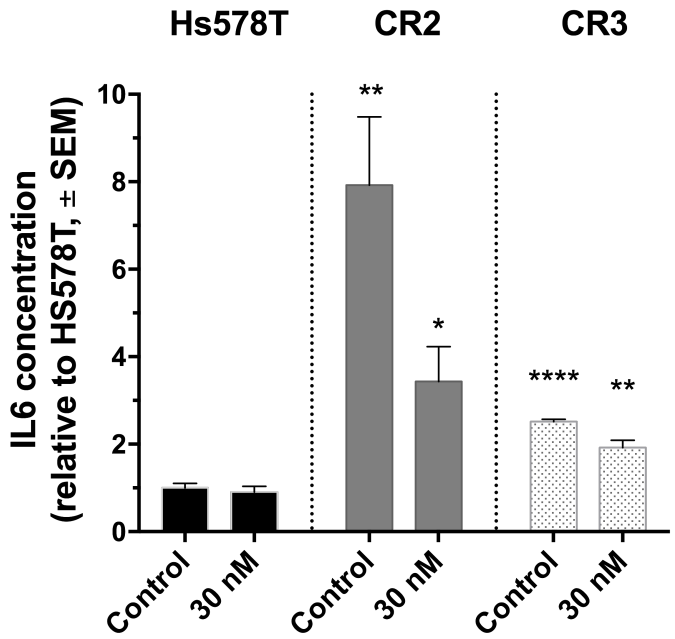


Figure 5.15: IL6 expression in Hs578T cells and HSP90i-resistant clones CR2 and CR3

Parental Hs578T cell and HSP90i-resistant clones CR2 and CR3 were treated with ganetespib (30 nM). After 24 hr treatment, the media was collected and subjected to the ELISA assay in order to measure the IL6 present in the media. The graph represents the mean IL6 concentration relative to Hs578T DMSO-treated cells from two independent experiments each performed in duplicate. Error bars indicate SEM. Individual HSP90i-resistant clones; in the absence and presence of ganetespib were compared to Hs578T DMSO-treated cells. *, **, **** indicate p value ≤0.05, ≤0.01 and ≤0.0001 respectively; by Student's t-test.

5.3.4. Correlation between pSTAT3 expression and sensitivity to HSP90i

Since activation of the JAK2-STAT3 signalling pathways might affect sensitivity to HSP90i in TNBC cells, the relationship between pSTAT3 expression and ganetespib sensitivity (IC_{50}) in a panel of TNBC cell lines was investigated. Different levels of pSTAT3 were observed among the TNBC cells. HCC1143 cells, being the least sensitive cell line to ganetespib, expressed the highest level of pSTAT3 and MDA-MB-453 cells expressed the lowest level of pSTAT3 **(Figure 5.16a)**. Despite the relatively small number of TNBC cell lines investigated (n=7), there was a positive trend ($r = 0.66$) correlating ganetespib IC_{50} values and pSTAT3 levels, although this did not reach statistical significance ($p = 0.1062$). The data suggest that higher pSTAT3 expression may be associated with increased resistance to HSP90i in TNBC cells **(Figure 5.16b)**.

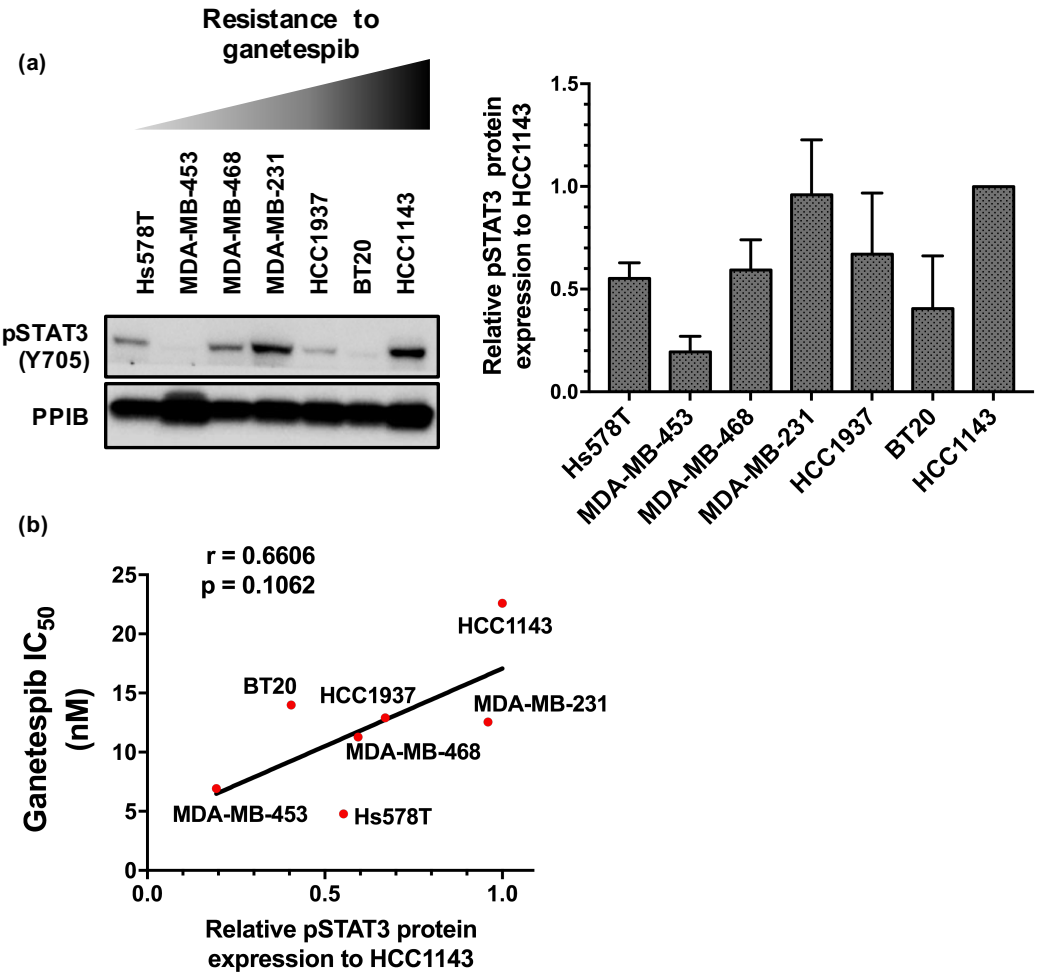


Figure 5.16: Correlation of pSTAT3 expression with ganetespib sensitivity (IC_{50})

(a) Lysates of TNBC cell lines (Hs578T, MDA-MB-453, MDA-MB-468, MDA-MB-231, HCC 1937, BT20 and HCC1143) were analysed by western blotting. PPIB was used as a loading control. Quantification of pSTAT3 protein band for each cell line was calculated (photon counts) after normalisation to its respective loading control and then expressed relative to the protein band intensity in HCC1143 cells. The graph represents the mean relative pSTAT3 protein expression of TNBC cell lines from three independent experiments. Error bars indicate SEM.

(b) The scatter plot displays the relationship between ganetespib sensitivity (IC_{50}) and mean relative pSTAT3 protein expression of TNBC cell lines to HCC1143 cells, determined by Pearson's correlation (r).

5.4. Biomarkers of intrinsic and acquired resistance to HSP90i in TNBC cells

Mechanisms of resistance to HSP90i have been reported in other cancer types. Reduced expression of NQO1 activity is associated with resistance to geldanamycin-based HSP90i in glioblastoma and melanoma cells (Gaspar et al., 2009). The expression of NQO1 protein was investigated in the parental Hs578T cells and HSP90i-resistant clones. In our study, the opposite trend in NQO1 expression was observed. There was an increase in NQO1 protein expression observed in the HSP90i-resistant clones when compared with parental Hs578T cells **(Figure 5.17a and b)**. The relationship between NQO1 protein expression and ganetespib sensitivity (IC_{50}) was also investigated in a panel of TNBC cells but there was no significant trend or correlation ($r = -0.1245$, $p = 0.7903$) **(Figure 5.18a and b)**. There is no further evidence in our study to demonstrate that reduced expression of NQO1 activity is associated with resistance to HSP90i in TNBC cells.

Downregulation of a pro-survival protein MCL1 is also associated with increased ganetespib sensitivity in several cancer cell lines, but combined treatment with inhibition of BCL family proteins (ABT737) is required to induce apoptosis in ganetespib-resistant lung cancer cells (Busacca et al., 2016). The expression of MCL protein was assessed in the parental Hs578T cells and the HSP90i-resistant clones. As expected, MCL1 expression in the Hs578T cells was significantly downregulated after 30 nM ganetespib treatment **(Figure 5.17a and c)**. However, there was no downregulation of MCL1 in the HSP90i-resistant clones CR2 or CR3 after ganetespib treatment. Interestingly, MCL1 expression in CR2 and CR3 was lower compared with the untreated Hs578T cells. This data suggest that the HSP90i-resistant clones are less dependent on MCL1 for their survival, in the absence or presence of ganetespib. The relationship between MCL1 expression and ganetespib sensitivity (IC_{50}) was

also investigated in the panel of TNBC cells. A positive correlation was observed but it did not reach statistical significance (r = 0.342, p = 0.4528) **(Figure 5.18a and c)**.

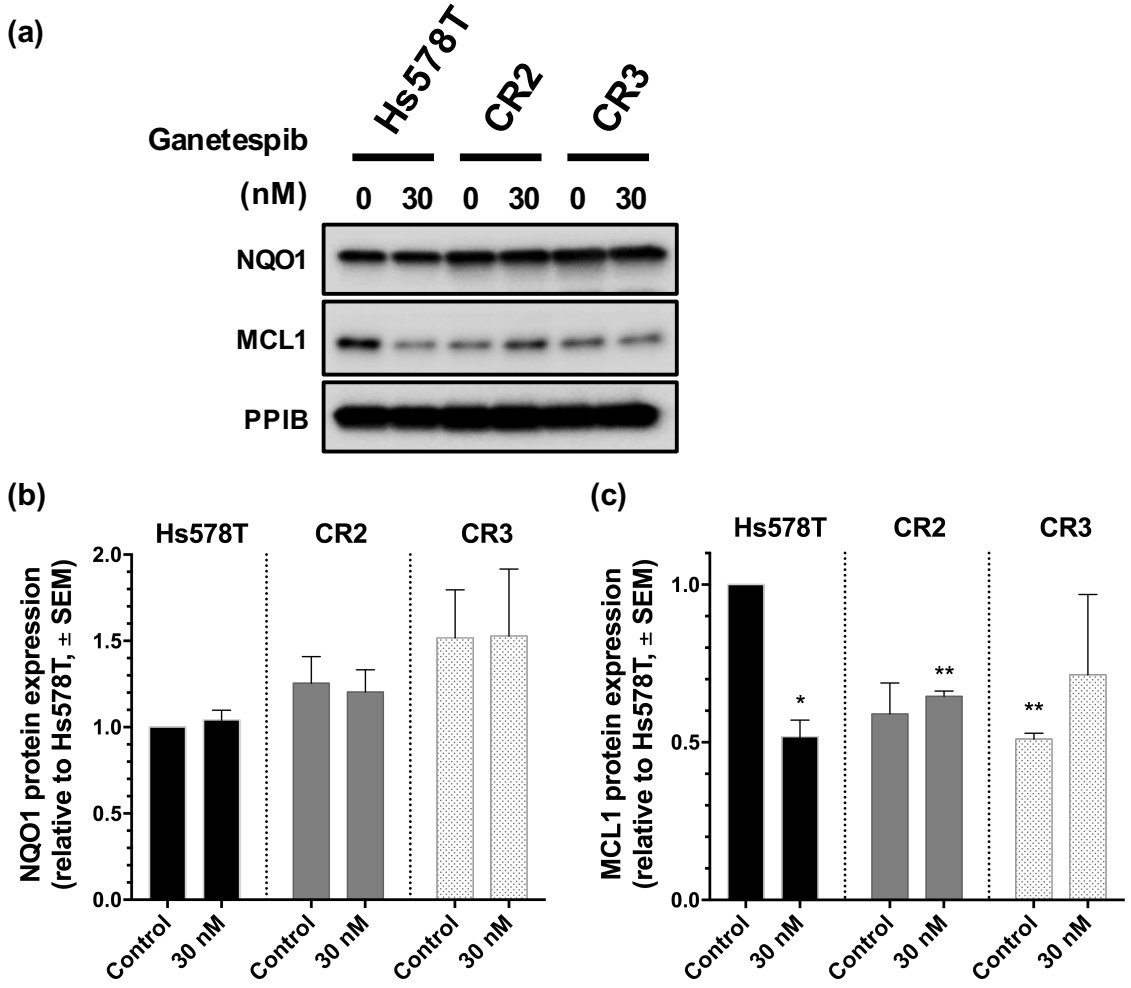


Figure 5.17: Expression of NQO1 and MCL1 in Hs578T cells and HSP90i-resistant clones

Parental Hs578Tcells and HSP90i-resistant clones CR2 and CR3 were treated with ganetespib (30 nM) for 24 hr. **(a)** Lysates of the treated cells were analysed by western blotting. PPIB was used as loading control. Quantification of NQO1 and MCL1 protein bands were calculated (photon counts) after normalisation to their respective loading controls and expressed relative to the protein band intensity in Hs578T cells. The graphs represent the mean relative **(b)** pSTAT3 and **(c)** MCL1 protein expression from three independent experiments. Error bars indicate SEM. The protein expression in the cells was compared to Hs578T DMSO-treated cells. * and ** indicate p value ≤0.05, and ≤0.01 respectively; by Student's t-test.

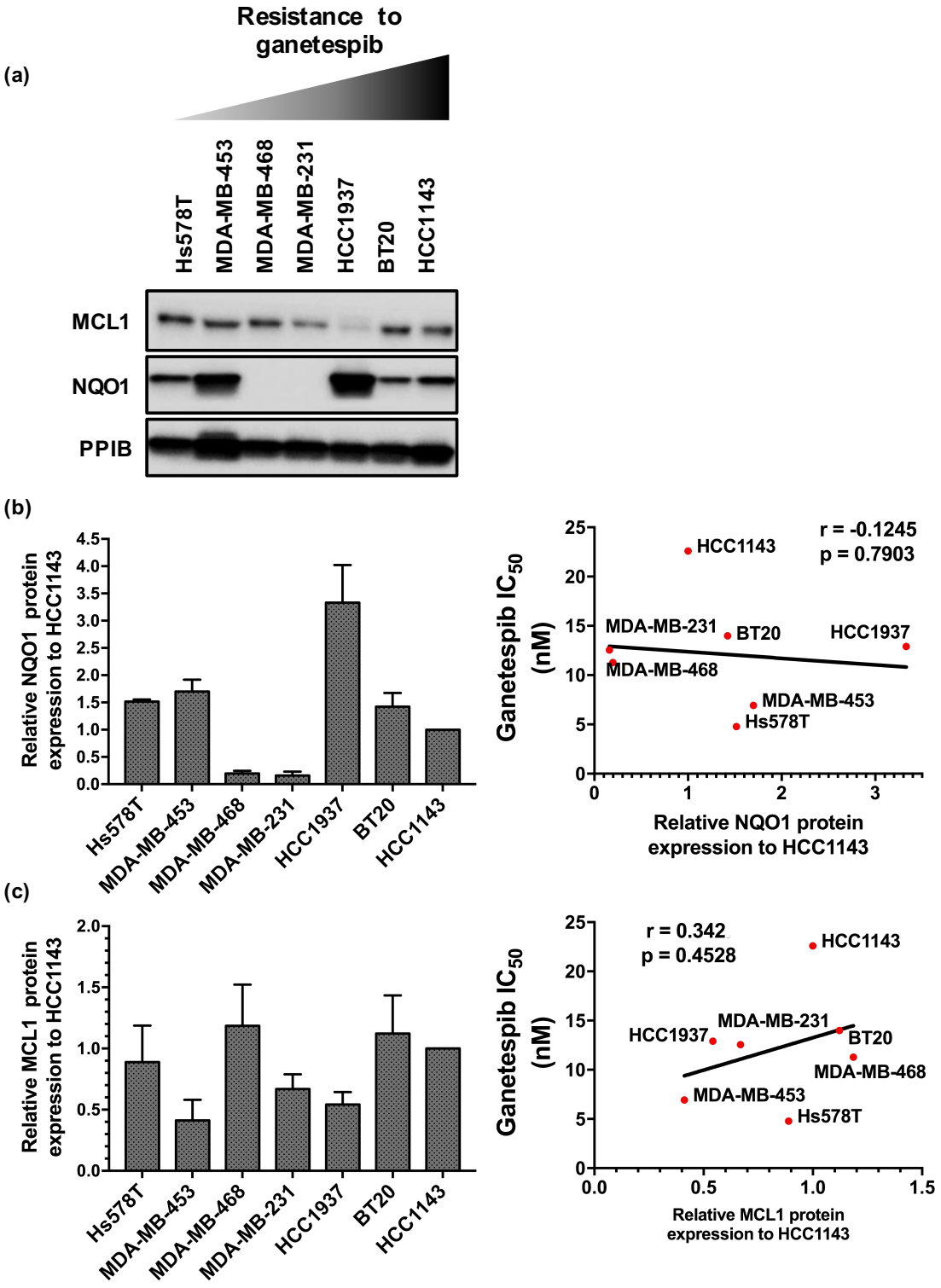


Figure 5.18: Correlation of NQO1 and MCL1 expression with ganetespib sensitivity

(a) Lysates of TNBC cell lines (Hs578T, MDA-MB-453, MDA-MB-468, MDA-MB-231, HCC 1937, BT20 and HCC1143) were analysed by western blotting. PPIB was used as loading control. Quantification of the protein band for each cell line was calculated (photon counts) after normalisation to their respective loading control, and then expressed relative to the protein band intensity in HCC1143 cells. The graphs represent the mean relative **(a)** NQO1 and **(b)** MCL1 protein expression of TNBC cell lines from three independent experiments. Error bars indicate SEM. The scatter plots display the relationship between ganetespib sensitivity (IC_{50}) and mean relative NQO1 and MCL1 protein expression in TNBC cell lines to HCC1143 cells, determined by Pearson's correlation (r).

5.4.1. The relationship of potential biomarkers to prognosis in breast cancer patients

In our study, differential expression of several proteins (UGT1A9, pSTAT3, NQO1 and MCL1) was observed in the HSP90i-resistant clones. Altered expression of these genes might also have an impact on tumour growth and progression in the clinic. Therefore, we investigated the association between the expression of these genes and breast cancer patients' survival. The hazard ratios (HR) for RNA expression of these genes were calculated by comparing the survival data (relapse-free survival) from 3554 breast cancer patients that were split based on median expression values **(Figure 5.19)**.

MKI67, a well-studied cellular marker for tumour cell proliferation was also included in the analysis. As expected, MKI67 RNA expression is a poor prognostic indicator for survival in breast cancer patients (HR = 1.42). MCL1 expression did not show clear association with survival. However, high expression of UGT1A9 showed a significant association with good prognosis while high expression of STAT3 and NQO1 showed a significant association with poor prognosis in breast cancer patients.

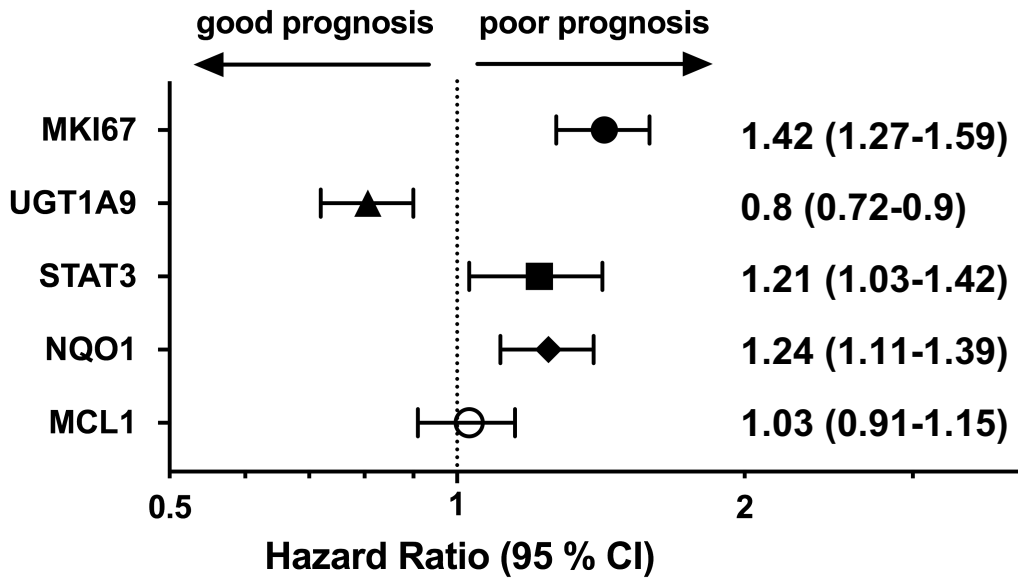


Figure 5.19: UGT1A9, STAT3, NQO1 and MCL1 expression and prognosis in breast cancer

Forest plot of hazard ratios (HR, with 95% confidence intervals) for relapse-free survival for UGT1A9, STAT3, NQO1 and MCL1 gene expression from 3554 breast cancer dataset (Kaplan-Meier Plotter) (http://kmplot.com/analysis, accessed August 2016). Median RNA expression levels were used to split patients into high/low expression groups. HR >1.0 poor prognosis (increased risk of relapse) for patients with tumour gene expression levels greater than the median value. HR <1 good prognosis (reduced risk of relapse) for patients with tumour gene expression levels greater than the median value.

5.5. Discussion

In order to identify potential novel targets for overcoming resistance to HSP90i in TNBC cells, we screened for the sensitivity of 328 bioactive small molecules in the HSP90i-resistant clone CR3. Our screen showed that, in addition to HSP90i, the CR3 clone was cross-resistant to a range of other compounds (20/328), mainly targeting proteins involved in proliferation and cell cycle checkpoints (topoisomerases, CDK and CHEK). Resistance to topoisomerase inhibitors is associated with the increased level of UGT activity in colon cancer cell lines and glucuronidation mediates the clearance of these inhibitors in the cells (Brangi et al., 1999). Since the HSP90i-resistant clones expressed high levels of UGT1A family members, glucuronidation might also contribute to the resistance to topoisomerase inhibitors in TNBC cells.

The screen also showed that several compounds (10/328) were selectively cytotoxic to the HSP90i-resistant clone CR3, with the presence of lower ganetespib concentration (10 nM). Among these compounds, the sensitivity of JAK2i was validated in both HSP90i-resistant clones. CR2 and CR3 showed increased sensitivity to JAK2i (LY2784544 and AZD1480), in the presence of ganetespib. The combined treatment also caused an upregulation of HSP70 (pharmacodynamic marker of HSP90i) and induction of apoptosis in HSP90i-resistant clones as well as the parental Hs578T cells. This suggests that JAK2i causes an increase in the cytotoxic activity of HSP90i in TNBC cells. Further studies with breast normal cell lines can be performed to assess whether this combined treatment is also toxic in normal cells. However, combined inhibition of JAK2 and HSP90 may still be a promising combination approach to overcome resistance to HSP90i in TNBC cells.

Ganetespib treatment causes downregulation of JAK-STAT signalling pathway proteins in pancreatic and erythroleukemia cells, including pSTAT3 (Nagaraju et al., 2016, Proia et al., 2011). In our study, ganetespib at 10 nM did not cause a downregulation of STAT3 and

pSTAT3 in parental Hs578T cells. However, higher concentrations of ganetespib did cause a downregulation of STAT3 and pSTAT3 in the parental Hs578T cells **(Supplementary Figure 3).** Consistent with previous studies (Proia et al., 2011), the JAK-STAT signalling pathway was also among the significantly enriched pathways with downregulated gene expression in parental Hs578T cells after ganetespib treatment **(Table 4.3)**.

The JAK-STAT signalling pathway was also altered in the HSP90i-resistant clones. The HSP90i-resistant clones expressed higher pSTAT3 when compared with the parental Hs578T cells, in the absence or presence of ganetespib. Several genes regulated by the JAK-STAT signalling pathway (IL6 and MYC) were also significantly upregulated in both clones. Moreover, there was a significantly higher level of cytokine IL6 in the culture media of these clones. These observations suggest that the HSP90i-resistant clones have an activation of JAK2-STAT3 signalling pathway, possibly through IL6. The IL6-mediated JAK2-STAT3 signalling pathway may be involved in the mechanism of acquired resistance to HSP90i in TNBC cells. Interestingly, there was a positive correlation between pSTAT3 expression and sensitivity to HSP90i in the panel of TNBC cells. Higher pSTAT3 expression was correlated with increased resistance to ganetespib in TNBC cells. However, the correlation did not reach statistical significance and this might be due to the limited number of cell lines used (n=7). Further studies with a larger panel of TNBC cell lines could determine whether pSTAT3 may be a potential biomarker of resistance to HSP90i in TNBC.

Reduced expression of NQO1 is a potential biomarker of resistance to geldanamycin-based HSP90i (17-AAG and 17-DMAG), but not to structurally unrelated HSP90i in glioblastoma and oesophageal cancer cells (Hadley and Hendricks, 2014, Gaspar et al., 2009). NQO1 is able to reduce geldanamycin-based HSP90i to an analogue with enhanced HSP90i activity in breast cancer cells (Guo et al., 2006). In our study, the HSP90i-resistant clones were more resistant to resorcinol-based HSP90i than geldanamycin-based HSP90i. Consistent with the

previous studies, there was also no evidence of correlation between reduced expression of NQO1 and increased resistance to ganetespib, a resorcinol-based HSP90i, in the TNBC cells.

MCL is an anti-apoptotic protein and its downregulation causes apoptosis in cells (Akgul, 2009). Downregulation of MCL1 is associated with increased sensitivity to ganetespib in lung cancer cell lines. However, ganetespib-resistant lung cancer cells have a loss in MCL1 dependency and they require a combined treatment with inhibition of BCL family proteins for induction of apoptosis (Busacca et al., 2016). We showed that ganetespib effectively caused the downregulation of MCL1 protein expression in TNBC cells (Hs578T cells). However, the HSP90i-resistant clones already expressed a reduced MCL1 expression, in the absence or presence of ganetespib, when compared with parental Hs578T cells. The clones had lost their dependency on MCL1 expression for survival. These data further suggest that there is an activation of alternative cell survival signalling pathways in the HSP90i-resistant clones, possibly the IL6-mediated JAK2-STAT3 signalling pathway.

There are several inhibitors targeting the IL6-mediated JAK2-STAT3 signalling pathway that are currently in clinical trials for several cancers, including Ruxolitinib in TNBC (clinicaltrials.gov). Upregulated IL6-mediated JAK2-STAT3 signalling pathway is involved in promoting oncogenesis, including cell proliferation, invasion, inflammation and immune function (Wang and Sun, 2014, Sansone and Bromberg, 2012). The activation of STAT3 plays a central role in mediating the cellular responses of this signalling pathway in cancer cells (Hirano et al., 2000, Guo et al., 2012). Feedback activation of STAT3 causes resistance to various targeted therapies (HER2, EGFR, MEK) and chemotherapies by restoring cell survival and proliferation (Lee et al., 2014, Zhao et al., 2016). Increased levels of IL6 induce the expression of anti-apoptotic proteins that inhibit apoptosis and promote proliferation in cancer cells. This have also been associated to mediate drug resistance including chemotherapy in prostate, breast and lung cancer cells (Pu et al., 2004, Guo et al., 2012, Yan

et al., 2014, Conze et al., 2001). The upregulated IL6-mediated JAK2-STAT3 signalling pathway observed in HSP90i-resistant clone CR3 might also be associated to the mechanism of resistance to chemotherapies in the cells, including Adriamycin and mitoxantrone.

In this study, we examined the prognostic effect of UGT1A9, STAT3, NQO1 and MCL1 gene expression in breast cancer patients. Interestingly, high expression of STAT3 is a poor prognosis indicator and UGT1A9 is a good prognosis indicator in breast cancer patients. Since activation of STAT3 is involved in cancer progression, expression of STAT3 and pSTAT3 are correlated with poor prognosis in breast and colorectal cancer patients (Kusaba et al., 2006, Chen et al., 2013, Diaz et al., 2006). The biological basis for better outcome with high expression of UGT1A9 in breast cancer patients is not known. UGT1A family members may be associated with preventing drug-induced toxicity in cancer patients. Germline polymorphisms in the UGT1A gene have been associated with increased toxicity to chemotherapy. As an example, UGT1A1*28 and UGT1A1*27 are correlated with severe irinotecan-induced toxicity in colon cancer patients (Carlini et al., 2005, Guillemette, 2003, Hertz and McLeod, 2013, Ando et al., 2000, Nagar and Remmel, 2006).

In this chapter, we demonstrate that the HSP90i-resistant clones were cross-resistant to chemotherapies and other targeted therapies, possibly due to the upregulated UGT1A family members, slower growth and upregulated IL-6 mediated JAK2-STAT3 signalling pathway. Combined inhibition of HSP90 and JAK2 can overcome the resistance to HSP90i in the HSP90i-resistant clones. In addition, expression of UGT1A9 and STAT3 might also be potential biomarkers of sensitivity to HSP90i and/or prognosis in TNBC patients.

6. Final discussion and conclusion

6.1. Final discussion

TNBC accounts for about 10% of all breast cancer cases and TNBC patients have a worse clinical outcome compared to other breast cancer patients (Reis-Filho and Tutt, 2008, Liedtke et al., 2008). It is still a major challenge to treat TNBC due to the lack of approved targeted therapies. Targeting HSP90 is a potentially promising approach for the development of novel therapeutics for TNBC as HSP90i has been shown to simultaneously inhibit several signalling pathways that are involved in the hallmarks of cancer (Garg et al., 2016, Neckers and Workman, 2012). HSP90i demonstrates anti-cancer activities in several cancers, including TNBC (Proia et al., 2014, Caldas-Lopes et al., 2009, Mehta et al., 2011). In this study, we demonstrate that TNBC cells are responsive to HSP90i, causing inhibition of cell viability, the downregulation of HSP90 client proteins (EGFR and AKT), induction of cell death by apoptosis, G2/M cell cycle arrest and inhibition of colony formation ability in several TNBC cell lines.

Despite promising tumour responses to HSP90i observed in TNBC patients, acquired and intrinsic resistance to HSP90i can arise. This resistance affects the efficacy of the therapy and allows disease progression in cancer patients (Awada et al., 2013). An understanding of the resistance mechanisms to targeted therapies might lead to the identification of predictive biomarkers for better selection of responsive patients to targeted therapies and/or alternative therapies after disease progression (Ellis and Hicklin, 2009). We established an in vitro model of HSP90i-resistant clones to identify potential mechanisms of resistance to HSP90i in TNBC. Two independent HSP90i-resistant clones were generated through prolonged exposure of a TNBC cell line (Hs578T cells) to HSP90i (ganetespib). Both clones showed cross-resistance to other HSP90i; most notably to resorcinol-based HSP90i. The degree of resistance in the clones compared to the parental cell line was not as high (4-fold) as other reported cell lines with acquired resistance to certain other targeted therapies (Engelman et

al., 2007). Nevertheless, we were able to use the HSP90i-resistant clones to detect genomic and proteomic changes that might contribute to the mechanisms of resistance to HSP90i.

Our study is the first to report potential mechanisms of acquired resistance to HSP90i in TNBC. The two independent HSP90i-resistant clones had similar patterns of genomic sequence variants that were not detectable in parental Hs578T cells. Thus, the clones might have derived from a small population of cells that were able to outgrow in the presence of HSP90i. This suggests that a pre-existing population of TNBC cells with intrinsic resistance to HSP90i existed within the parental Hs578T cell population, although we have no further evidence to support this. The presence of pre-existing resistant populations has been reported in other tumours, such as populations with secondary gatekeeper mutation in EGFR (T790M) in non-small cell lung cancer patients (Inukai et al., 2006, Su et al., 2012). The sequence variants identified in the HSP90i-resistant clones were heterozygous with wild-type gene sequences still present. However, we cannot eliminate the possibility of patterns of genomic mutations being associated with resistance to HSP90i in TNBC cells. Whole genome DNA sequencing could be carried out on the HSP90i-resistant clones (CR2, CR3 and the third clone CR6) to detect other genetic variants, including the ones in regulatory elements and non-expressed regions that might contribute to the resistance to HSP90i in TNBC cells.

Increased expression of HSP70 protein levels have been associated to reduced sensitivity to HSP90i in prostate and colon cancer cells (Powers et al., 2008, Guo et al., 2005). However, in our experimental settings, HSP70 expression does not appear to be associated with resistance to HSP90i in TNBC cells, although it does appear to be a pharmacodynamic marker of HSP90i. Another possible resistance mechanism to HSP90i, in particular geldanamycin-derived HSP90i, is the reduced protein expression of NQO1 in cancer cells, including glioblastoma and oesophageal cancer cells (Hadley and Hendricks, 2014, Gaspar

et al., 2009). However, in our study, there was no evidence of correlation between reduced NQO1 protein expression and decreased HSP90i sensitivity in TNBC cells. This might be due to the HSP90i-resistant clones being significantly resistant to resorcinol-based compounds, ganetespib and NVP-AUY922. The clones did not show a high degree of cross-resistance to other classes of HSP90i, including geldanamycin-based and purine-based HSP90i. This suggests that the mechanisms of resistance to HSP90i obtained from our studies might only be relevant to resorcinol-based HSP90i in TNBC.

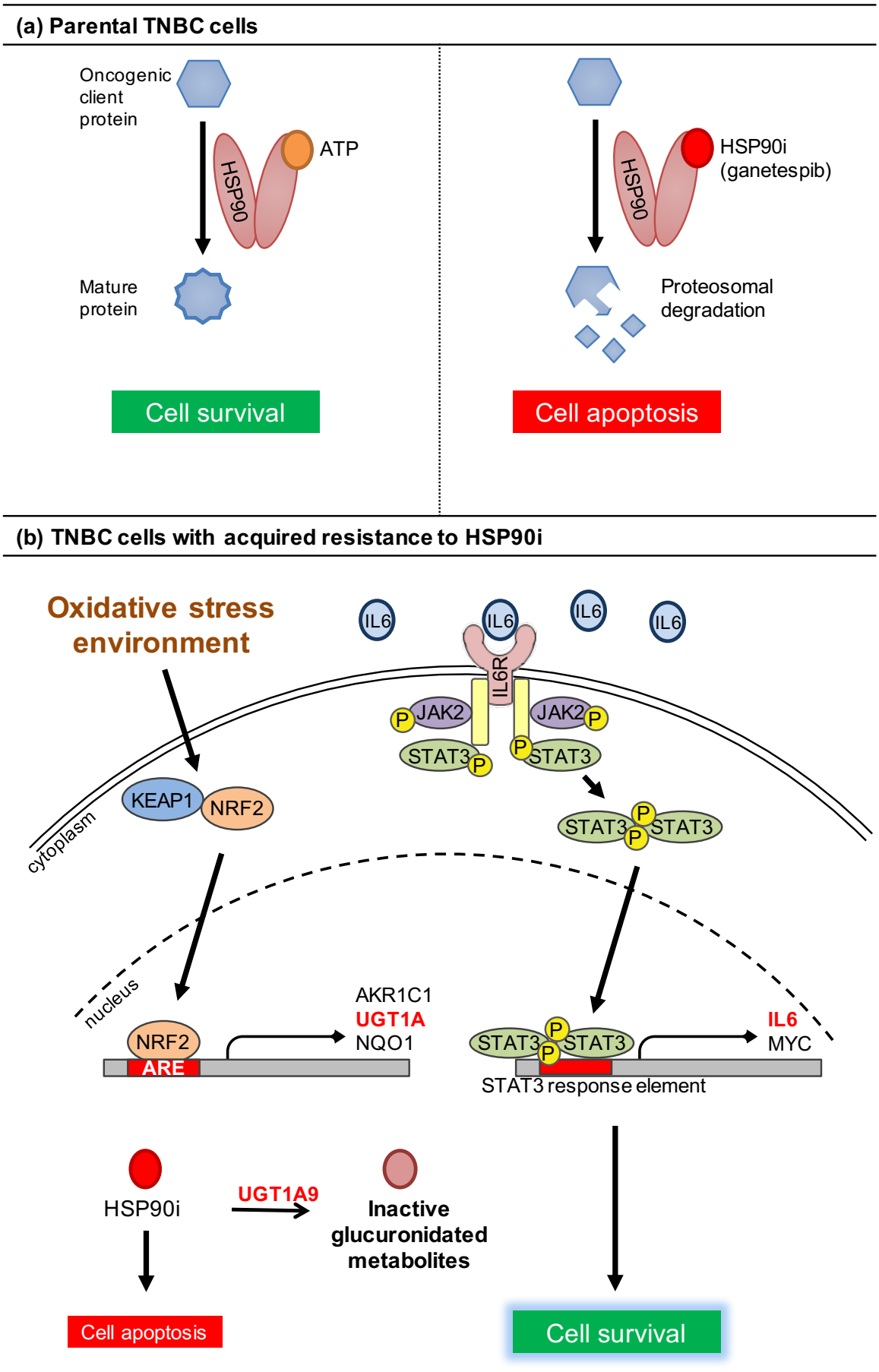
We demonstrate that increased expression of UGT1A family members, in particular UGT1A9, is associated with acquired resistance to resorcinol-based HSP90i in TNBC cells. This resistance can be overcome by a propofol, competitive inhibitor of UGT1A9. Our report is consistent with other studies, where UGT1A expression is shown to be associated with resistance to ganetespib and other resorcinol-based HSP90i in colorectal cancer cells. The HSP90i have been reported to undergo glucuronidation by UGT1A family members, and the glucuronidated metabolites are excreted from the cells. (Landmann et al., 2014, Acquaviva et al., 2014a). Therefore, resistance mechanism to resorcinol-based HSP90i in TNBC cells appears likely to be associated with increased glucuronidation via UGT1A9 proteins. The glucuronidation activity of UGT1A9 in the HSP90i-resistant clones can be further assessed in this study by measuring the level of ganetespib and its glucuronidated metabolite with HPLC-MS/MS (Donato et al., 2010).

Our data suggest that upregulation of UGT1A9 expression might be induced by the presence of intrinsic ROS in the HSP90i-resistant clones. The expression of other ARE-regulated genes, NQO1 protein and pATM were also upregulated in the clones, even in the absence of HSP90i. Further experiments still need to be performed to explore these findings, including the use of ROS-scavenger enzymes to investigate the effects of ROS on HSP90i sensitivity in TNBC cells. Redox homeostasis in cancer cells is important as excessive amounts of ROS

can cause cell death, but a moderate increase in ROS can promote cancer progression and confer resistance to anti-cancer drugs (Trachootham et al., 2009). The HSP90i-resistant clones in our study might have acquired the adaptive mechanisms to overcome the toxicity of elevated ROS levels in the cells and started to induce the activation of other survival pathways for maintaining cell survival.

The HSP90i-resistant clones in our study showed increased expression levels of IL6, pSTAT3 and JAK-STAT related genes. These data suggest that there is an upregulated IL6-mediated JAK2-STAT3 signalling pathway present in the HSP90i-resistant clones. We also demonstrate that inhibiting the JAK2-STAT3 signalling pathway is able to increase the cytotoxics effect of HSP90i on the HSP90i-resistant clones. This is consistent with another study of myeloproliferative neoplasmic cells. HSP90i (NVP-AUY922) was shown to have a combined cytotoxic effect with JAK2i (TG101209) by inducing downregulation of JAK2 signalling proteins and apoptosis in the cells (Fiskus et al., 2011).

We hypothesise that the upregulated IL6-mediated JAK2-STAT3 signalling pathway contributes to the mechanisms of resistance to HSP90i in TNBC cells, despite the presence of an elevated oxidative stress environment **(Figure 6.1)**. In this model, the oxidative stress environment in the cells induces the expression of ARE-dependent genes including UGT1A9. Upon exposure to HSP90i, the HSP90i is glucuronidated into its inactive metabolite by UGT1A9 whereupon it gets excreted out of the cells. A portion of HSP90i is still present in the cells and can induce apoptosis. However, the cells are able to overcome the cytotoxic effect of HSP90i due to the increased IL6-mediated JAK2-STAT3 survival signalling pathway. JAK2i is able to induce apoptosis in the cells. However, combined inhibition of JAK2 and HSP90 has a synergistic effect of increased cytotoxicity to the cells.


(a) Parental TNBC cells
Oncogenic client protein
ATP
HSP90
Mature protein
Cell survival
HSP90i (ganetespib)
HSP90
Proteosomal degradation
Cell apoptosis
(b) TNBC cells with acquired resistance to HSP90i
Oxidative stress environment
IL6
IL6R
JAK2
STAT3
KEAP1
NRF2
cytoplasm
nucleus
AKR1C1
UGT1A
NQO1
ARE
STAT3 response element
IL6
MYC
HSP90i
UGT1A9
Inactive glucuronidated metabolites
Cell apoptosis
Cell survival

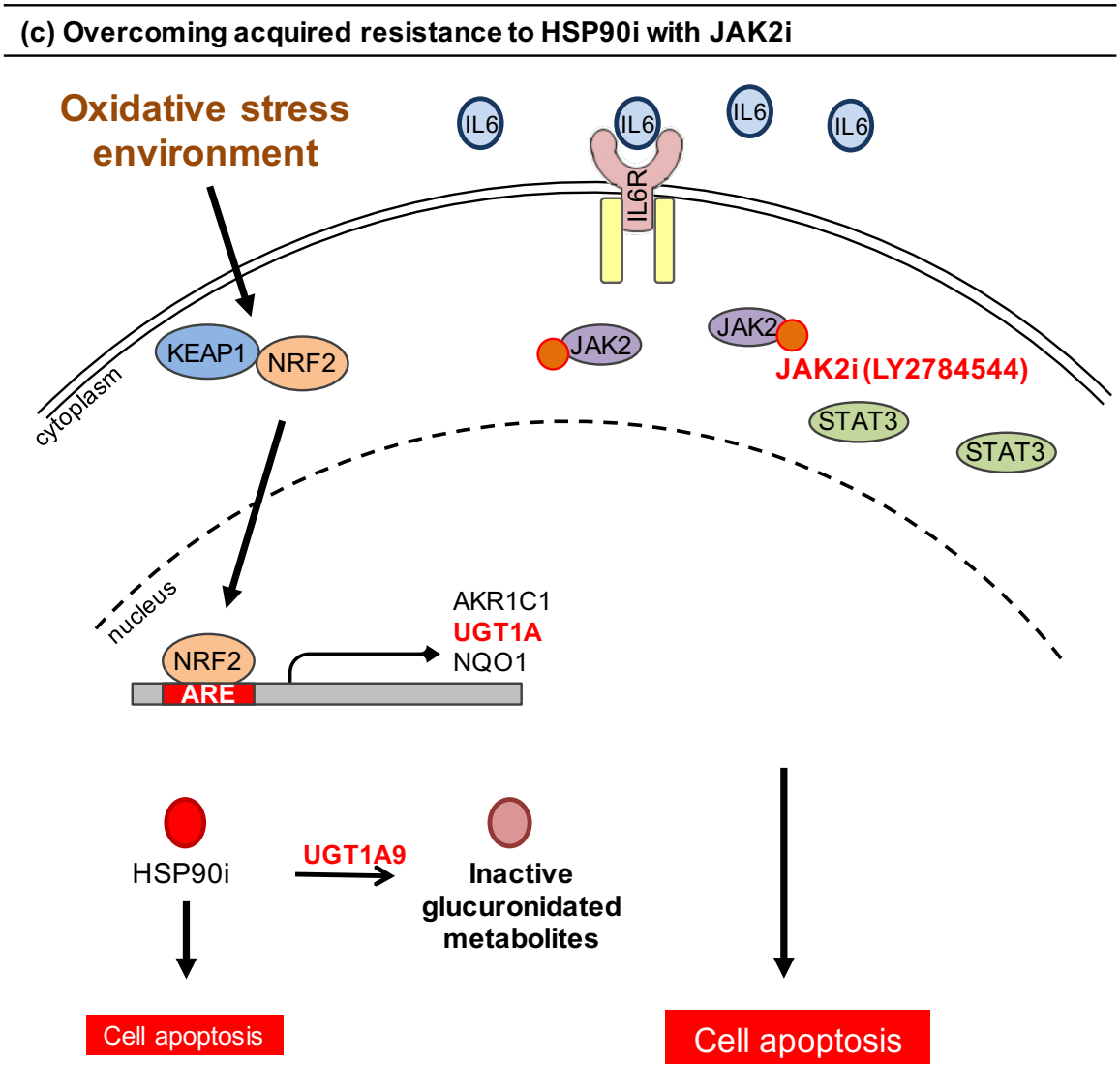


Figure 6.1: Proposed mechanisms of resistance to HSP90i in TNBC cells

(a) In parental TNBC cells, HSP90i (ganetespib) prevents the maturation of HSP90 oncogenic client proteins and directs them to ubiquitin-mediated proteosomal degradation. Since HSP90 client proteins are involved in many hallmarks of cancer including cell survival, HSP90i causes cell apoptosis in the cells.

(b) Due to the presence of endogenous oxidative stress in the TNBC cells with acquired resistance to HSP90i, there is an upregulated expression of NRF2 ARE-dependent genes including UGT1A9 in the cells. Upon exposure to resorcinol-based HSP90i (ganetespib), UGT1A9 proteins glucuronidate HSP90i, producing inactive glucuronidated metabolites. Most of the HSP90i gets metabolised but some is still present in the cells, which can induce apoptosis. However, the cells are able to overcome the cytotoxic effects of HSP90i through the increased activity of IL6-mediated JAK2-STAT3 survival signalling pathway. Binding of IL6 to its receptors causes the phosphorylation of JAK2. This leads to the recruitment and phosphorylation of STAT3. In turn, the pSTAT3 dimerises and translocates to the nucleus, which causes the transcription of genes involved in cell survival.

(c) JAK2i causes the downregulation of JAK2-STAT3 signalling, including the phosphorylation of STAT3 in TNBC cells. This causes the cells to undergo apoptosis. Combined inhibition of JAK2 and HSP90 is able to increase the cytotoxic effects and overcome the resistance of HSP90i in TNBC cells.

HSP90i has been reported to help overcome resistance to other targeted therapies in cancers, including resistance to BRAF inhibitor in melanoma and MEK or ALK inhibitor in non-small cell lung cancer (Acquaviva et al., 2012, Acquaviva et al., 2014b, Sang et al., 2013). This suggests that a combination approach of HSP90i with other targeted therapies could increase the efficacy of the therapy in cancer patients. Several HSP90i have successfully entered clinical trials as monotherapy and in combination with other therapies but they failed to progress further (clinaltrials.gov). One of the leading HSP90i, ganetespib entered Phase III clinical trial in lung cancer but showed lack of clinical benefit in combination with docetaxel compared to docetaxel alone (NCT01798485). Some of the challenges involved in the development of HSP90i are non-optimal safety profiles, lack of dose-limited clinical efficacy and absence of biomarkers for selection of patients that would benefit from the treatment (Wang et al., 2016).

UGT1A9 protein levels might be a potential biomarker of sensitivity to resorcinol-based HSP90i in TNBC cells. The expression of UGT1A9 protein in the panel of TNBC cells was assessed in our study but the levels were too low or undetected when compared to the HSP90i-resistant clones **(Supplementary Figure 4).** Even though we did not have enough evidence from our panel of TNBC cells, we cannot exclude the possibility that UGT1A9 might still be a predictive biomarker of response to resorcinol-based HSP90i in TNBC patients. Further studies need to be performed to explore these findings, including in other TNBC cell lines or assessing the effect of either overexpression or knockdown of UGT1A9 in HSP90i-sensitive or resistant cells.

Our data also suggest that breast cancer patients with low gene expression of UGT1A9 have poor prognosis. We hypothesise that a patient subgroup with low UGT1A9 expression in tumours might benefit from resorcinol-based HSP90i. Whereas, patients with high UGT1A9 expression tumours might benefit from non-resorcinol based HSP90i which would not

undergo glucuronidation by UGT1A9. However, UGT1A polymorphisms (UGT1A1*28 and UGT1A1*27) have been implicated with increased toxicity to chemotherapy in colon cancer patients (Carlini et al., 2005, Hertz and McLeod, 2013). This raises the question whether the presence of UGT1A polymorphisms might also induce toxicity to resorcinol-based HSP90i in cancer patients.

Another potential biomarker of sensitivity to HSP90i in TNBC cells is the expression of pSTAT3. We demonstrate that higher pSTAT3 expression might be associated with increased resistance to HSP90i in TNBC cell lines. However, the positive correlation in our analysis did not reach statistical significance. This might be due to the limited number of cell lines used (n=7). Further studies with a larger panel of TNBC cell lines or knockdown of STAT3 could be performed to explore these findings.

Feedback activation of STAT3 after inhibition of signalling pathways in cancer cells is able to restore cell survival and proliferation. This has been shown to cause resistance to various targeted therapies and chemotherapies, including resistance to MEK inhibitors in colorectal cancer or tyrosine kinase inhibitors in lung cancer (Lee et al., 2014, Zhao et al., 2016, Van Schaeybroeck et al., 2014). Elevated IL6 leads to the upregulation of anti-apoptotic proteins and this is also associated with increased chemotherapeutic resistance in breast and lung cancer cells (Yan et al., 2014, Conze et al., 2001). Increased expression of UGT1A family members and glucuronidation activity are associated with drug resistance in cancer cells, including resistance to topoisomerase inhibitors in colon cancer cells and methotrexate in breast cancer cells (Brangi et al., 1999, de Almagro et al., 2011). Interestingly, in our study, the HSP90i-resistant clones also showed cross-resistance to several chemotherapeutics (Adriamycin and mitoxantrone) and other targeted therapies. This might also be associated with the upregulated expression of UGT1A family members, slower growth and increased

activation of IL6-mediated JAK2-STAT3 survival signalling pathway observed in the HSP90i-resistant clones.

6.2. Limitations of study

One of the main limitations in our study is that we only focused on a single TNBC cell line, Hs578T cells. TNBC represents a heterogeneous disease and there are six TNBC subtypes (Lehmann et al., 2011). It is not known if our data could be applied to the other TNBC and breast cancer subtypes. Since TNBC has a low frequency of targetable oncogenic driver mutations, our data might be relevant to other cancers, such as advanced non-small cell lung cancer without known driver mutations (Chan and Hughes, 2015).

In order to translate the in vitro data in vivo, we attempted to grow the parental Hs578T cells and HSP90i-resistant clone CR3 in mice as tumour xenografts. Hs578T cells were used in other in vivo studies (Haupt et al., 2006), but unfortunately in our hands, the cells were unable to develop tumours. CR3 did manage to develop xenograft tumours but the growth rate was slow and variable, thus preventing us to continue with the in vivo studies. An alternative approach for the Hs578T cells and the resistant clones is to use in vitro 3D cultures including tumour spheroids that possess in vivo characteristics of tumours such as cell-cell interaction and hypoxia (Zanoni et al., 2016). Further studies with other TNBC cell lines that are able to grow tumours in mice can be performed to access potential biomarkers of sensitivity to resorcinol-based HSP90i (UGT1A9 and pSTAT3 expression) and the effects of combined inhibition (HSP90 and JAK2) in vivo. Immunohistochemistry staining (UGT1A9 and pSTAT3 expression) in tumours (tissue microarrays) obtained from cancer patients that have underwent treatment with resorcinol-based HSP90i in the clinical trials can also be performed to explore these findings.

The proteomic profiling of HSP90i-resistant clones using a phospho-RTK array is limited, as it only focuses on the phosphorylation activity of 49 RTKs. Whole proteomic profiling and/or phospho-proteome analysis such as using stable isotope labelling by amino acids in cell culture (SILAC) and MS can be performed to further identify differential expression and activity of proteins in the HSP90i-resistant clones compared with the parental Hs578T cells. This approach is highly sensitive as it directly quantifies and sequences the whole proteome including phosphopeptides simultaneously from different conditions (Mann, 2006, Ong et al., 2002).

Another limitation of our study is, for practical purposes, a fixed dose (1 μM) of the compounds was used in the small molecule screen. Potential hits with markedly lower or higher potency might have been undetected with this approach. Screens with a broader range of concentrations (10 nM -10 μM) could be performed to identify additional hits in the HSP90i-resistant clones.

6.3. Conclusion

We conclude that we can utilise the in vitro model of TNBC cells with acquired resistance to HSP90i, most notably resorcinol-based HSP90i, to investigate the potential mechanisms of resistance to HSP90i in TNBC. Based on our genetic profiling, the clones generated might have arisen from a pre-existing population of TNBC cells with resistance to the HSP90i. The mechanism of resistance to resorcinol-based HSP90i in TNBC cells is likely due to increased UGT1A9 expression and IL6-mediated JAK2-STAT3 survival signalling pathway. The HSP90i-resistant clones are also cross-resistant to other chemotherapies and targeted therapies, which might be associated with the slower growth, increased ROS and increased IL6-mediated JAK2-STAT3 signalling in the clones. Finally, we demonstrate that inhibition of the JAK2-STAT3 signalling pathway is able to increase the cytotoxic effect of HSP90i to

TNBC cells. A combined inhibition of HSP90 and JAK2 is a potential approach to improve the efficacy of HSP90i and overcome the resistance to HSP90i in TNBC. Since there are still no approved targeted therapies for TNBC, this combination treatment might be a novel approach to be explored for treating TNBC patients.

7. References

ACQUAVIVA, J., HE, S., ZHANG, C., JIMENEZ, J. P., NAGAI, M., SANG, J., SEQUEIRA, M., SMITH, D. L., OGAWA, L. S., INOUE, T., TATSUTA, N., KNOWLES, M. A., BATES, R. C. & PROIA, D. A. 2014a. FGFR3 translocations in bladder cancer: differential sensitivity to HSP90 inhibition based on drug metabolism. *Mol Cancer Res,* 12**,** 1042-54.

ACQUAVIVA, J., SMITH, D. L., JIMENEZ, J. P., ZHANG, C., SEQUEIRA, M., HE, S., SANG, J., BATES, R. C. & PROIA, D. A. 2014b. Overcoming acquired BRAF inhibitor resistance in melanoma via targeted inhibition of Hsp90 with ganetespib. *Mol Cancer Ther,* 13**,** 353-63.

ACQUAVIVA, J., SMITH, D. L., SANG, J., FRIEDLAND, J. C., HE, S., SEQUEIRA, M., ZHANG, C., WADA, Y. & PROIA, D. A. 2012. Targeting KRAS-mutant non-small cell lung cancer with the Hsp90 inhibitor ganetespib. *Mol Cancer Ther,* 11**,** 2633-43.

AKGUL, C. 2009. Mcl-1 is a potential therapeutic target in multiple types of cancer. *Cell Mol Life Sci,* 66**,** 1326-36.

ALLEGRA, C. J., JESSUP, J. M., SOMERFIELD, M. R., HAMILTON, S. R., HAMMOND, E. H., HAYES, D. F., MCALLISTER, P. K., MORTON, R. F. & SCHILSKY, R. L. 2009. American Society of Clinical Oncology provisional clinical opinion: testing for KRAS gene mutations in patients with metastatic colorectal carcinoma to predict response to anti-epidermal growth factor receptor monoclonal antibody therapy. *J Clin Oncol,* 27**,** 2091-6.

AN, W. G., SCHNUR, R. C., NECKERS, L. & BLAGOSKLONNY, M. V. 1997. Depletion of p185erbB2, Raf-1 and mutant p53 proteins by geldanamycin derivatives correlates with antiproliferative activity. *Cancer Chemother Pharmacol,* 40**,** 60-4.

ANDO, Y., SAKA, H., ANDO, M., SAWA, T., MURO, K., UEOKA, H., YOKOYAMA, A., SAITOH, S., SHIMOKATA, K. & HASEGAWA, Y. 2000. Polymorphisms of UDP-glucuronosyltransferase gene and irinotecan toxicity: a pharmacogenetic analysis. *Cancer Res,* 60**,** 6921-6.

ARTEAGA, C. L. 2011. Why is this effective HSP90 inhibitor not being developed in HER2+ breast cancer? *Clin Cancer Res,* 17**,** 4919-21.

ARTEAGA, C. L., SLIWKOWSKI, M. X., OSBORNE, C. K., PEREZ, E. A., PUGLISI, F. & GIANNI, L. 2012. Treatment of HER2-positive breast cancer: current status and future perspectives. *Nat Rev Clin Oncol,* 9**,** 16-32.

AUDEH, M. W., CARMICHAEL, J., PENSON, R. T., FRIEDLANDER, M., POWELL, B., BELL-MCGUINN, K. M., SCOTT, C., WEITZEL, J. N., OAKNIN, A., LOMAN, N., LU, K., SCHMUTZLER, R. K., MATULONIS, U., WICKENS, M. & TUTT, A. 2010. Oral poly(ADP-ribose) polymerase inhibitor olaparib in patients with BRCA1 or BRCA2 mutations and recurrent ovarian cancer: a proof-of-concept trial. *Lancet,* 376**,** 245-51.

AWADA, A., SPECTOR, N., EL-HARIRY, I., RODRIGUEZ, A., ERBAN, J., CORTES, J., GOMEZ, H., KONG, A., HICKISH, T., FEIN, L., VAHDAT, L., MACPHERSON, I., CANON, J.-L., MANSOOR, S., GIOVANNE, A., MCADAM, K.,

VUKOVIC, V., YALCIN, I., BRADLEY, R., PROIA, D., MANO, M., PEREZ, E. & CAMERON, D. 2013. Abstract P2-16-23: The ENCHANT-1 trial (NCT01677455): An open label multicenter phase 2 proof of concept study evaluating first line ganetespib monotherapy in women with metastatic HER2 positive or triple negative breast cancer (TNBC). *Cancer Research,* 73**,** P2-16-23-P2-16-23.

BANERJI, U., WALTON, M., RAYNAUD, F., GRIMSHAW, R., KELLAND, L., VALENTI, M., JUDSON, I. & WORKMAN, P. 2005. Pharmacokinetic-pharmacodynamic relationships for the heat shock protein 90 molecular chaperone inhibitor 17-allylamino, 17-demethoxygeldanamycin in human ovarian cancer xenograft models. *Clin Cancer Res,* 11**,** 7023-32.

BARBER, L. J., SANDHU, S., CHEN, L., CAMPBELL, J., KOZAREWA, I., FENWICK, K., ASSIOTIS, I., RODRIGUES, D. N., REIS FILHO, J. S., MORENO, V., MATEO, J., MOLIFE, L. R., DE BONO, J., KAYE, S., LORD, C. J. & ASHWORTH, A. 2013. Secondary mutations in BRCA2 associated with clinical resistance to a PARP inhibitor. *J Pathol,* 229**,** 422-9.

BARRETINA, J., CAPONIGRO, G., STRANSKY, N., VENKATESAN, K., MARGOLIN, A. A., KIM, S., WILSON, C. J., LEHAR, J., KRYUKOV, G. V., SONKIN, D., REDDY, A., LIU, M., MURRAY, L., BERGER, M. F., MONAHAN, J. E., MORAIS, P., MELTZER, J., KOREJWA, A., JANE-VALBUENA, J., MAPA, F. A., THIBAULT, J., BRIC-FURLONG, E., RAMAN, P., SHIPWAY, A., ENGELS, I. H., CHENG, J., YU, G. K., YU, J., ASPESI, P., JR., DE SILVA, M., JAGTAP, K., JONES, M. D., WANG, L., HATTON, C., PALESCANDOLO, E., GUPTA, S., MAHAN, S., SOUGNEZ, C., ONOFRIO, R. C., LIEFELD, T., MACCONAILL, L., WINCKLER, W., REICH, M., LI, N., MESIROV, J. P., GABRIEL, S. B., GETZ, G., ARDLIE, K., CHAN, V., MYER, V. E., WEBER, B. L., PORTER, J., WARMUTH, M., FINAN, P., HARRIS, J. L., MEYERSON, M., GOLUB, T. R., MORRISSEY, M. P., SELLERS, W. R., SCHLEGEL, R. & GARRAWAY, L. A. 2012. The Cancer Cell Line Encyclopedia enables predictive modelling of anticancer drug sensitivity. *Nature,* 483**,** 603-7.

BASELGA, J. & SWAIN, S. M. 2009. Novel anticancer targets: revisiting ERBB2 and discovering ERBB3. *Nat Rev Cancer,* 9**,** 463-75.

BENDELL, J. C., RODON, J., BURRIS, H. A., DE JONGE, M., VERWEIJ, J., BIRLE, D., DEMANSE, D., DE BUCK, S. S., RU, Q. C., PETERS, M., GOLDBRUNNER, M. & BASELGA, J. 2012. Phase I, dose-escalation study of BKM120, an oral pan-Class I PI3K inhibitor, in patients with advanced solid tumors. *J Clin Oncol,* 30**,** 282-90.

BIANCHINI, G., BALKO, J. M., MAYER, I. A., SANDERS, M. E. & GIANNI, L. 2016. Triple-negative breast cancer: challenges and opportunities of a heterogeneous disease. *Nat Rev Clin Oncol*.

BRANGI, M., LITMAN, T., CIOTTI, M., NISHIYAMA, K., KOHLHAGEN, G., TAKIMOTO, C., ROBEY, R., POMMIER, Y., FOJO, T. & BATES, S. E. 1999. Camptothecin resistance: role of the ATP-binding cassette (ABC), mitoxantrone-resistance half-transporter (MXR), and potential for glucuronidation in MXR-expressing cells. *Cancer Res,* 59**,** 5938-46.

BRYANT, H. E., SCHULTZ, N., THOMAS, H. D., PARKER, K. M., FLOWER, D., LOPEZ, E., KYLE, S., MEUTH, M., CURTIN, N. J. & HELLEDAY, T. 2005. Specific killing of BRCA2-deficient tumours with inhibitors of poly(ADP-ribose) polymerase. *Nature,* 434**,** 913-7.

BURRELL, R. A. & SWANTON, C. 2014. Tumour heterogeneity and the evolution of polyclonal drug resistance. *Mol Oncol,* 8**,** 1095-111.

BURROWS, F., ZHANG, H. & KAMAL, A. 2004. Hsp90 activation and cell cycle regulation. *Cell Cycle,* 3**,** 1530-6.

BUSACCA, S., LAW, E. W., POWLEY, I. R., PROIA, D. A., SEQUEIRA, M., LE QUESNE, J., KLABATSA, A., EDWARDS, J. M., MATCHETT, K. B., LUO, J. L., PRINGLE, J. H., EL-TANANI, M., MACFARLANE, M. & FENNELL, D. A. 2016. Resistance to HSP90 inhibition involving loss of MCL1 addiction. *Oncogene,* 35**,** 1483-92.

BUZDAR, A. U., IBRAHIM, N. K., FRANCIS, D., BOOSER, D. J., THOMAS, E. S., THERIAULT, R. L., PUSZTAI, L., GREEN, M. C., ARUN, B. K., GIORDANO, S. H., CRISTOFANILLI, M., FRYE, D. K., SMITH, T. L., HUNT, K. K., SINGLETARY, S. E., SAHIN, A. A., EWER, M. S., BUCHHOLZ, T. A., BERRY, D. & HORTOBAGYI, G. N. 2005. Significantly higher pathologic complete remission rate after neoadjuvant therapy with trastuzumab, paclitaxel, and epirubicin chemotherapy: results of a randomized trial in human epidermal growth factor receptor 2-positive operable breast cancer. *J Clin Oncol,* 23**,** 3676-85.

CALDAS-LOPES, E., CERCHIETTI, L., AHN, J. H., CLEMENT, C. C., ROBLES, A. I., RODINA, A., MOULICK, K., TALDONE, T., GOZMAN, A., GUO, Y., WU, N., DE STANCHINA, E., WHITE, J., GROSS, S. S., MA, Y., VARTICOVSKI, L., MELNICK, A. & CHIOSIS, G. 2009. Hsp90 inhibitor PU-H71, a multimodal inhibitor of malignancy, induces complete responses in triple-negative breast cancer models. *Proc Natl Acad Sci U S A,* 106**,** 8368-73.

CANCER GENOME ATLAS, N. 2012. Comprehensive molecular portraits of human breast tumours. *Nature,* 490**,** 61-70.

CAREY, L. A., RUGO, H. S., MARCOM, P. K., MAYER, E. L., ESTEVA, F. J., MA, C. X., LIU, M. C., STORNIOLO, A. M., RIMAWI, M. F., FORERO-TORRES, A., WOLFF, A. C., HOBDAY, T. J., IVANOVA, A., CHIU, W. K., FERRARO, M., BURROWS, E., BERNARD, P. S., HOADLEY, K. A., PEROU, C. M. & WINER, E. P. 2012. TBCRC 001: randomized phase II study of cetuximab in combination with carboplatin in stage IV triple-negative breast cancer. *J Clin Oncol,* 30**,** 2615-23.

CARLINI, L. E., MEROPOL, N. J., BEVER, J., ANDRIA, M. L., HILL, T., GOLD, P., ROGATKO, A., WANG, H. & BLANCHARD, R. L. 2005. UGT1A7 and UGT1A9 polymorphisms predict response and toxicity in colorectal cancer patients treated with capecitabine/irinotecan. *Clin Cancer Res,* 11**,** 1226-36.

CARLSON, J. J. & ROTH, J. A. 2013. The impact of the Oncotype Dx breast cancer assay in clinical practice: a systematic review and meta-analysis. *Breast Cancer Res Treat,* 141**,** 13-22.

CARLSON, R. W., ALLRED, D. C., ANDERSON, B. O., BURSTEIN, H. J., CARTER, W. B., EDGE, S. B., ERBAN, J. K., FARRAR, W. B., FORERO, A., GIORDANO, S. H., GOLDSTEIN, L. J., GRADISHAR, W. J., HAYES, D. F., HUDIS, C. A., LJUNG, B. M., MANKOFF, D. A., MARCOM, P. K., MAYER, I. A., MCCORMICK, B., PIERCE, L. J., REED, E. C., SACHDEV, J., SMITH, M. L., SOMLO, G., WARD, J. H., WOLFF, A. C., ZELLARS, R. & NATIONAL COMPREHENSIVE CANCER, N. 2011. Invasive breast cancer. *J Natl Compr Canc Netw,* 9**,** 136-222.

CHAN, B. A. & HUGHES, B. G. 2015. Targeted therapy for non-small cell lung cancer: current standards and the promise of the future. *Transl Lung Cancer Res,* 4**,** 36-54.

CHANG, J. C., WOOTEN, E. C., TSIMELZON, A., HILSENBECK, S. G., GUTIERREZ, M. C., ELLEDGE, R., MOHSIN, S., OSBORNE, C. K., CHAMNESS, G. C., ALLRED, D. C. & O'CONNELL, P. 2003. Gene expression profiling for the prediction of therapeutic response to docetaxel in patients with breast cancer. *Lancet,* 362**,** 362-9.

CHEANG, M. C., MARTIN, M., NIELSEN, T. O., PRAT, A., VODUC, D., RODRIGUEZ-LESCURE, A., RUIZ, A., CHIA, S., SHEPHERD, L., RUIZ-BORREGO, M., CALVO, L., ALBA, E., CARRASCO, E., CABALLERO, R., TU, D., PRITCHARD, K. I., LEVINE, M. N., BRAMWELL, V. H., PARKER, J., BERNARD, P. S., ELLIS, M. J., PEROU, C. M., DI LEO, A. & CAREY, L. A. 2015. Defining breast cancer intrinsic subtypes by quantitative receptor expression. *Oncologist,* 20**,** 474-82.

CHEN, B., PIEL, W. H., GUI, L., BRUFORD, E. & MONTEIRO, A. 2005. The HSP90 family of genes in the human genome: insights into their divergence and evolution. *Genomics,* 86**,** 627-37.

CHEN, Y., WANG, J., WANG, X., LIU, X., LI, H., LV, Q., ZHU, J., WEI, B. & TANG, Y. 2013. STAT3, a Poor Survival Predicator, Is Associated with Lymph Node Metastasis from Breast Cancer. *J Breast Cancer,* 16**,** 40-9.

CHENG, Q., CHANG, J. T., GERADTS, J., NECKERS, L. M., HAYSTEAD, T., SPECTOR, N. L. & LYERLY, H. K. 2012. Amplification and high-level expression of heat shock protein 90 marks aggressive phenotypes of human epidermal growth factor receptor 2 negative breast cancer. *Breast Cancer Res,* 14**,** R62.

CHIOSIS, G. & NECKERS, L. 2006. Tumor selectivity of Hsp90 inhibitors: the explanation remains elusive. *ACS Chem Biol,* 1**,** 279-84.

CINTRON, N. S. & TOFT, D. 2006. Defining the requirements for Hsp40 and Hsp70 in the Hsp90 chaperone pathway. *J Biol Chem,* 281**,** 26235-44.

CLARKE, P. A., HOSTEIN, I., BANERJI, U., STEFANO, F. D., MALONEY, A., WALTON, M., JUDSON, I. & WORKMAN, P. 2000. Gene expression profiling of human colon cancer cells following inhibition of signal transduction by 17-allylamino-17-demethoxygeldanamycin, an inhibitor of the hsp90 molecular chaperone. *Oncogene,* 19**,** 4125-33.

COMEN, E. A. & ROBSON, M. 2010. Poly(ADP-ribose) polymerase inhibitors in triple-negative breast cancer. *Cancer J,* 16**,** 48-52.

CONZE, D., WEISS, L., REGEN, P. S., BHUSHAN, A., WEAVER, D., JOHNSON, P. & RINCON, M. 2001. Autocrine production of interleukin 6 causes multidrug resistance in breast cancer cells. *Cancer Res,* 61**,** 8851-8.

COURT, M. H. 2005. Isoform-selective probe substrates for in vitro studies of human UDP-glucuronosyltransferases. *Methods Enzymol,* 400**,** 104-16.

CUMMINGS, J., ETHELL, B. T., JARDINE, L., BOYD, G., MACPHERSON, J. S., BURCHELL, B., SMYTH, J. F. & JODRELL, D. I. 2003. Glucuronidation as a mechanism of intrinsic drug resistance in human colon cancer: reversal of resistance by food additives. *Cancer Res,* 63**,** 8443-50.

DE ALMAGRO, M. C., SELGA, E., THIBAUT, R., PORTE, C., NOE, V. & CIUDAD, C. J. 2011. UDP-glucuronosyltransferase 1A6 overexpression in breast cancer cells resistant to methotrexate. *Biochem Pharmacol,* 81**,** 60-70.

DE BONT, R. & VAN LAREBEKE, N. 2004. Endogenous DNA damage in humans: a review of quantitative data. *Mutagenesis,* 19**,** 169-85.

DENAYER, T., STÖHR, T. & VAN ROY, M. 2014. Animal models in translational medicine: Validation and prediction. *New Horizons in Translational Medicine,* 2**,** 5-11.

DENT, R., TRUDEAU, M., PRITCHARD, K. I., HANNA, W. M., KAHN, H. K., SAWKA, C. A., LICKLEY, L. A., RAWLINSON, E., SUN, P. & NAROD, S. A. 2007. Triple-negative breast cancer: clinical features and patterns of recurrence. *Clin Cancer Res,* 13**,** 4429-34.

DIAZ, N., MINTON, S., COX, C., BOWMAN, T., GRITSKO, T., GARCIA, R., EWEIS, I., WLOCH, M., LIVINGSTON, S., SEIJO, E., CANTOR, A., LEE, J. H., BEAM, C. A., SULLIVAN, D., JOVE, R. & MURO-CACHO, C. A. 2006. Activation of stat3 in primary tumors from high-risk breast cancer patients is associated with elevated levels of activated SRC and survivin expression. *Clin Cancer Res,* 12**,** 20-8.

DICKLER, M. N., RUGO, H. S., EBERLE, C. A., BROGI, E., CARAVELLI, J. F., PANAGEAS, K. S., BOYD, J., YEH, B., LAKE, D. E., DANG, C. T., GILEWSKI, T. A., BROMBERG, J. F., SEIDMAN, A. D., D'ANDREA, G. M., MOASSER, M. M., MELISKO, M., PARK, J. W., DANCEY, J., NORTON, L. & HUDIS, C. A. 2008. A phase II trial of erlotinib in combination with bevacizumab in patients with metastatic breast cancer. *Clin Cancer Res,* 14**,** 7878-83.

DONATO, M. T., MONTERO, S., CASTELL, J. V., GOMEZ-LECHON, M. J. & LAHOZ, A. 2010. Validated assay for studying activity profiles of human liver UGTs after drug exposure: inhibition and induction studies. *Anal Bioanal Chem,* 396**,** 2251-63.

DUTTA, R. & INOUYE, M. 2000. GHKL, an emergent ATPase/kinase superfamily. *Trends Biochem Sci,* 25**,** 24-8.

EARLY BREAST CANCER TRIALISTS' COLLABORATIVE, G. 2005. Effects of chemotherapy and hormonal therapy for early breast cancer on recurrence and 15-year survival: an overview of the randomised trials. *Lancet,* 365**,** 1687-717.

EARLY BREAST CANCER TRIALISTS' COLLABORATIVE, G., DAVIES, C., GODWIN, J., GRAY, R., CLARKE, M., CUTTER, D., DARBY, S., MCGALE, P., PAN, H. C., TAYLOR, C., WANG, Y. C., DOWSETT, M., INGLE, J. & PETO, R. 2011. Relevance of breast cancer hormone receptors and other factors to the efficacy of adjuvant tamoxifen: patient-level meta-analysis of randomised trials. *Lancet,* 378**,** 771-84.

EISEMAN, J. L., LAN, J., LAGATTUTA, T. F., HAMBURGER, D. R., JOSEPH, E., COVEY, J. M. & EGORIN, M. J. 2005. Pharmacokinetics and pharmacodynamics of 17-demethoxy 17-[[(2-dimethylamino)ethyl]amino]geldanamycin (17DMAG, NSC 707545) in C.B-17 SCID mice bearing MDA-MB-231 human breast cancer xenografts. *Cancer Chemother Pharmacol,* 55**,** 21-32.

ELLEDGE, R. M., GREEN, S., PUGH, R., ALLRED, D. C., CLARK, G. M., HILL, J., RAVDIN, P., MARTINO, S. & OSBORNE, C. K. 2000. Estrogen receptor (ER) and progesterone receptor (PgR), by ligand-binding assay compared with ER, PgR and pS2,

by immuno-histochemistry in predicting response to tamoxifen in metastatic breast cancer: a Southwest Oncology Group Study. *Int J Cancer,* 89**,** 111-7.

ELLIS, I. O., GALEA, M., BROUGHTON, N., LOCKER, A., BLAMEY, R. W. & ELSTON, C. W. 1992. Pathological prognostic factors in breast cancer. II. Histological type. Relationship with survival in a large study with long-term follow-up. *Histopathology,* 20**,** 479-89.

ELLIS, L. M. & HICKLIN, D. J. 2009. Resistance to Targeted Therapies: Refining Anticancer Therapy in the Era of Molecular Oncology. *Clin Cancer Res,* 15**,** 7471-7478.

ELO, M. A., KAARNIRANTA, K., HELMINEN, H. J. & LAMMI, M. J. 2005. Hsp90 inhibitor geldanamycin increases hsp70 mRNA stabilisation but fails to activate HSF1 in cells exposed to hydrostatic pressure. *Biochim Biophys Acta,* 1743**,** 115-9.

ELSTON, C. W. & ELLIS, I. O. 2002. Pathological prognostic factors in breast cancer. I. The value of histological grade in breast cancer: experience from a large study with long-term follow-up. *Histopathology,* 41**,** 154-61.

ENGELMAN, J. A., ZEJNULLAHU, K., MITSUDOMI, T., SONG, Y., HYLAND, C., PARK, J. O., LINDEMAN, N., GALE, C. M., ZHAO, X., CHRISTENSEN, J., KOSAKA, T., HOLMES, A. J., ROGERS, A. M., CAPPUZZO, F., MOK, T., LEE, C., JOHNSON, B. E., CANTLEY, L. C. & JANNE, P. A. 2007. MET amplification leads to gefitinib resistance in lung cancer by activating ERBB3 signaling. *Science,* 316**,** 1039-43.

FARMER, H., MCCABE, N., LORD, C. J., TUTT, A. N., JOHNSON, D. A., RICHARDSON, T. B., SANTAROSA, M., DILLON, K. J., HICKSON, I., KNIGHTS, C., MARTIN, N. M., JACKSON, S. P., SMITH, G. C. & ASHWORTH, A. 2005. Targeting the DNA repair defect in BRCA mutant cells as a therapeutic strategy. *Nature,* 434**,** 917-21.

FERLAY, J., SOERJOMATARAM, I., DIKSHIT, R., ESER, S., MATHERS, C., REBELO, M., PARKIN, D. M., FORMAN, D. & BRAY, F. 2015. Cancer incidence and mortality worldwide: sources, methods and major patterns in GLOBOCAN 2012. *Int J Cancer,* 136**,** E359-86.

FERREIRA, D., ADEGA, F. & CHAVES, R. 2013. *The importance of cancer cell Lines as in vitro models in cancer methylome analysis and anticancer drugs testing*, INTECH Open Access Publisher.

FINN, R. S., CROWN, J. P., LANG, I., BOER, K., BONDARENKO, I. M., KULYK, S. O., ETTL, J., PATEL, R., PINTER, T., SCHMIDT, M., SHPARYK, Y., THUMMALA, A. R., VOYTKO, N. L., FOWST, C., HUANG, X., KIM, S. T., RANDOLPH, S. & SLAMON, D. J. 2015. The cyclin-dependent kinase 4/6 inhibitor palbociclib in combination with letrozole versus letrozole alone as first-line treatment of oestrogen receptor-positive, HER2-negative, advanced breast cancer (PALOMA-1/TRIO-18): a randomised phase 2 study. *Lancet Oncol,* 16**,** 25-35.

FISCHER, R., TRUDGIAN, D. C., WRIGHT, C., THOMAS, G., BRADBURY, L. A., BROWN, M. A., BOWNESS, P. & KESSLER, B. M. 2012. Discovery of candidate serum proteomic and metabolomic biomarkers in ankylosing spondylitis. *Mol Cell Proteomics,* 11**,** M111 013904.

FISKUS, W., VERSTOVSEK, S., MANSHOURI, T., RAO, R., BALUSU, R., VENKANNAGARI, S., RAO, N. N., HA, K., SMITH, J. E., HEMBRUFF, S. L.,

ABHYANKAR, S., MCGUIRK, J. & BHALLA, K. N. 2011. Heat shock protein 90 inhibitor is synergistic with JAK2 inhibitor and overcomes resistance to JAK2-TKI in human myeloproliferative neoplasm cells. *Clin Cancer Res,* 17**,** 7347-58.

FONG, P. C., BOSS, D. S., YAP, T. A., TUTT, A., WU, P., MERGUI-ROELVINK, M., MORTIMER, P., SWAISLAND, H., LAU, A., O'CONNOR, M. J., ASHWORTH, A., CARMICHAEL, J., KAYE, S. B., SCHELLENS, J. H. & DE BONO, J. S. 2009. Inhibition of poly(ADP-ribose) polymerase in tumors from BRCA mutation carriers. *N Engl J Med,* 361**,** 123-34.

FOULKES, W. D., STEFANSSON, I. M., CHAPPUIS, P. O., BEGIN, L. R., GOFFIN, J. R., WONG, N., TRUDEL, M. & AKSLEN, L. A. 2003. Germline BRCA1 mutations and a basal epithelial phenotype in breast cancer. *J Natl Cancer Inst,* 95**,** 1482-5.

FRIEDLAND, J. C., SMITH, D. L., SANG, J., ACQUAVIVA, J., HE, S., ZHANG, C. & PROIA, D. A. 2014. Targeted inhibition of Hsp90 by ganetespib is effective across a broad spectrum of breast cancer subtypes. *Invest New Drugs,* 32**,** 14-24.

FRUMAN, D. A. & ROMMEL, C. 2014. PI3K and cancer: lessons, challenges and opportunities. *Nat Rev Drug Discov,* 13**,** 140-56.

GARCIA-CARBONERO, R., CARNERO, A. & PAZ-ARES, L. 2013. Inhibition of HSP90 molecular chaperones: moving into the clinic. *Lancet Oncol,* 14**,** e358-69.

GARG, G., KHANDELWAL, A. & BLAGG, B. S. 2016. Anticancer Inhibitors of Hsp90 Function: Beyond the Usual Suspects. *Adv Cancer Res,* 129**,** 51-88.

GARNETT, M. J., EDELMAN, E. J., HEIDORN, S. J., GREENMAN, C. D., DASTUR, A., LAU, K. W., GRENINGER, P., THOMPSON, I. R., LUO, X., SOARES, J., LIU, Q., IORIO, F., SURDEZ, D., CHEN, L., MILANO, R. J., BIGNELL, G. R., TAM, A. T., DAVIES, H., STEVENSON, J. A., BARTHORPE, S., LUTZ, S. R., KOGERA, F., LAWRENCE, K., MCLAREN-DOUGLAS, A., MITROPOULOS, X., MIRONENKO, T., THI, H., RICHARDSON, L., ZHOU, W., JEWITT, F., ZHANG, T., O'BRIEN, P., BOISVERT, J. L., PRICE, S., HUR, W., YANG, W., DENG, X., BUTLER, A., CHOI, H. G., CHANG, J. W., BASELGA, J., STAMENKOVIC, I., ENGELMAN, J. A., SHARMA, S. V., DELATTRE, O., SAEZ-RODRIGUEZ, J., GRAY, N. S., SETTLEMAN, J., FUTREAL, P. A., HABER, D. A., STRATTON, M. R., RAMASWAMY, S., MCDERMOTT, U. & BENES, C. H. 2012. Systematic identification of genomic markers of drug sensitivity in cancer cells. *Nature,* 483**,** 570-5.

GASPAR, N., SHARP, S. Y., PACEY, S., JONES, C., WALTON, M., VASSAL, G., ECCLES, S., PEARSON, A. & WORKMAN, P. 2009. Acquired resistance to 17-allylamino-17-demethoxygeldanamycin (17-AAG, tanespimycin) in glioblastoma cells. *Cancer Res,* 69**,** 1966-75.

GELMON, K. A., TISCHKOWITZ, M., MACKAY, H., SWENERTON, K., ROBIDOUX, A., TONKIN, K., HIRTE, H., HUNTSMAN, D., CLEMONS, M., GILKS, B., YERUSHALMI, R., MACPHERSON, E., CARMICHAEL, J. & OZA, A. 2011. Olaparib in patients with recurrent high-grade serous or poorly differentiated ovarian carcinoma or triple-negative breast cancer: a phase 2, multicentre, open-label, non-randomised study. *Lancet Oncol,* 12**,** 852-61.

GONZALEZ-ANGULO, A. M., TIMMS, K. M., LIU, S., CHEN, H., LITTON, J. K., POTTER, J., LANCHBURY, J. S., STEMKE-HALE, K., HENNESSY, B. T., ARUN, B. K., HORTOBAGYI, G. N., DO, K. A., MILLS, G. B. & MERIC-BERNSTAM, F.

2011. Incidence and outcome of BRCA mutations in unselected patients with triple receptor-negative breast cancer. *Clin Cancer Res,* 17**,** 1082-9.

GORDON, V. & BANERJI, S. 2013. Molecular pathways: PI3K pathway targets in triple-negative breast cancers. *Clin Cancer Res,* 19**,** 3738-44.

GRANDIS, J. R. & SOK, J. C. 2004. Signaling through the epidermal growth factor receptor during the development of malignancy. *Pharmacol Ther,* 102**,** 37-46.

GROENENDIJK, F. H. & BERNARDS, R. 2014. Drug resistance to targeted therapies: deja vu all over again. *Mol Oncol,* 8**,** 1067-83.

GUILLEMETTE, C. 2003. Pharmacogenomics of human UDP-glucuronosyltransferase enzymes. *Pharmacogenomics J,* 3**,** 136-58.

GUO, F., ROCHA, K., BALI, P., PRANPAT, M., FISKUS, W., BOYAPALLE, S., KUMARASWAMY, S., BALASIS, M., GREEDY, B., ARMITAGE, E. S., LAWRENCE, N. & BHALLA, K. 2005. Abrogation of heat shock protein 70 induction as a strategy to increase antileukemia activity of heat shock protein 90 inhibitor 17-allylamino-demethoxy geldanamycin. *Cancer Res,* 65**,** 10536-44.

GUO, W., REIGAN, P., SIEGEL, D., ZIRROLLI, J., GUSTAFSON, D. & ROSS, D. 2006. The bioreduction of a series of benzoquinone ansamycins by NAD(P)H:quinone oxidoreductase 1 to more potent heat shock protein 90 inhibitors, the hydroquinone ansamycins. *Mol Pharmacol,* 70**,** 1194-203.

GUO, Y., XU, F., LU, T., DUAN, Z. & ZHANG, Z. 2012. Interleukin-6 signaling pathway in targeted therapy for cancer. *Cancer Treat Rev,* 38**,** 904-10.

GUO, Z., DESHPANDE, R. & PAULL, T. T. 2010a. ATM activation in the presence of oxidative stress. *Cell Cycle,* 9**,** 4805-11.

GUO, Z., KOZLOV, S., LAVIN, M. F., PERSON, M. D. & PAULL, T. T. 2010b. ATM activation by oxidative stress. *Science,* 330**,** 517-21.

HADLEY, K. E. & HENDRICKS, D. T. 2014. Use of NQO1 status as a selective biomarker for oesophageal squamous cell carcinomas with greater sensitivity to 17-AAG. *BMC Cancer,* 14**,** 334.

HAMMOND, M. E., HAYES, D. F., DOWSETT, M., ALLRED, D. C., HAGERTY, K. L., BADVE, S., FITZGIBBONS, P. L., FRANCIS, G., GOLDSTEIN, N. S., HAYES, M., HICKS, D. G., LESTER, S., LOVE, R., MANGU, P. B., MCSHANE, L., MILLER, K., OSBORNE, C. K., PAIK, S., PERLMUTTER, J., RHODES, A., SASANO, H., SCHWARTZ, J. N., SWEEP, F. C., TAUBE, S., TORLAKOVIC, E. E., VALENSTEIN, P., VIALE, G., VISSCHER, D., WHEELER, T., WILLIAMS, R. B., WITTLIFF, J. L., WOLFF, A. C., AMERICAN SOCIETY OF CLINICAL, O. & COLLEGE OF AMERICAN, P. 2010. American Society of Clinical Oncology/College of American Pathologists guideline recommendations for immunohistochemical testing of estrogen and progesterone receptors in breast cancer (unabridged version). *Arch Pathol Lab Med,* 134**,** e48-72.

HANAHAN, D. & WEINBERG, R. A. 2011. Hallmarks of cancer: the next generation. *Cell,* 144**,** 646-74.

HAUPT, L. M., THOMPSON, E. W., TREZISE, A. E., IRVING, R. E., IRVING, M. G. & GRIFFITHS, L. R. 2006. In vitro and in vivo MMP gene expression localisation by In

Situ-RT-PCR in cell culture and paraffin embedded human breast cancer cell line xenografts. *BMC Cancer,* 6**,** 18.

HAYES, J. D. & DINKOVA-KOSTOVA, A. T. 2014. The Nrf2 regulatory network provides an interface between redox and intermediary metabolism. *Trends Biochem Sci,* 39**,** 199-218.

HEATH, E. I., HILLMAN, D. W., VAISHAMPAYAN, U., SHENG, S., SARKAR, F., HARPER, F., GASKINS, M., PITOT, H. C., TAN, W., IVY, S. P., PILI, R., CARDUCCI, M. A., ERLICHMAN, C. & LIU, G. 2008. A phase II trial of 17-allylamino-17-demethoxygeldanamycin in patients with hormone-refractory metastatic prostate cancer. *Clin Cancer Res,* 14**,** 7940-6.

HEINRICH, P. C., BEHRMANN, I., MULLER-NEWEN, G., SCHAPER, F. & GRAEVE, L. 1998. Interleukin-6-type cytokine signalling through the gp130/Jak/STAT pathway. *Biochem J,* 334 (Pt 2)**,** 297-314.

HELLEDAY, T. 2011. The underlying mechanism for the PARP and BRCA synthetic lethality: clearing up the misunderstandings. *Mol Oncol,* 5**,** 387-93.

HERTZ, D. L. & MCLEOD, H. L. 2013. Use of pharmacogenetics for predicting cancer prognosis and treatment exposure, response and toxicity. *J Hum Genet,* 58**,** 346-52.

HIDALGO, M., AMANT, F., BIANKIN, A. V., BUDINSKA, E., BYRNE, A. T., CALDAS, C., CLARKE, R. B., DE JONG, S., JONKERS, J., MAELANDSMO, G. M., ROMAN-ROMAN, S., SEOANE, J., TRUSOLINO, L. & VILLANUEVA, A. 2014. Patient-derived xenograft models: an emerging platform for translational cancer research. *Cancer Discov,* 4**,** 998-1013.

HIRANO, T., ISHIHARA, K. & HIBI, M. 2000. Roles of STAT3 in mediating the cell growth, differentiation and survival signals relayed through the IL-6 family of cytokine receptors. *Oncogene,* 19**,** 2548-56.

INUKAI, M., TOYOOKA, S., ITO, S., ASANO, H., ICHIHARA, S., SOH, J., SUEHISA, H., OUCHIDA, M., AOE, K., AOE, M., KIURA, K., SHIMIZU, N. & DATE, H. 2006. Presence of epidermal growth factor receptor gene T790M mutation as a minor clone in non-small cell lung cancer. *Cancer Res,* 66**,** 7854-8.

ISHIKAWA, Y., KOZAKAI, T., MORITA, H., SAIDA, K., OKA, S. & MASUO, Y. 2006. Rapid detection of mycoplasma contamination in cell cultures using SYBR Green-based real-time polymerase chain reaction. *In Vitro Cell Dev Biol Anim,* 42**,** 63-9.

JHAVERI, K. & MODI, S. 2015. Ganetespib: research and clinical development. *Onco Targets Ther,* 8**,** 1849-58.

JHAVERI, K., TALDONE, T., MODI, S. & CHIOSIS, G. 2012. Advances in the clinical development of heat shock protein 90 (Hsp90) inhibitors in cancers. *Biochim Biophys Acta,* 1823**,** 742-55.

JOHNSON, B. D., SCHUMACHER, R. J., ROSS, E. D. & TOFT, D. O. 1998. Hop modulates Hsp70/Hsp90 interactions in protein folding. *J Biol Chem,* 273**,** 3679-86.

JUNG, K. A., CHOI, B. H., NAM, C. W., SONG, M., KIM, S. T., LEE, J. Y. & KWAK, M. K. 2013. Identification of aldo-keto reductases as NRF2-target marker genes in human cells. *Toxicol Lett,* 218**,** 39-49.

KALIMUTHO, M., PARSONS, K., MITTAL, D., LOPEZ, J. A., SRIHARI, S. & KHANNA, K. K. 2015. Targeted Therapies for Triple-Negative Breast Cancer: Combating a Stubborn Disease. *Trends Pharmacol Sci,* 36**,** 822-46.

KAMAL, A., THAO, L., SENSINTAFFAR, J., ZHANG, L., BOEHM, M. F., FRITZ, L. C. & BURROWS, F. J. 2003. A high-affinity conformation of Hsp90 confers tumour selectivity on Hsp90 inhibitors. *Nature,* 425**,** 407-10.

KARKOULIS, P. K., STRAVOPODIS, D. J., MARGARITIS, L. H. & VOUTSINAS, G. E. 2010. 17-Allylamino-17-demethoxygeldanamycin induces downregulation of critical Hsp90 protein clients and results in cell cycle arrest and apoptosis of human urinary bladder cancer cells. *BMC Cancer,* 10**,** 481.

KENSLER, T. W., WAKABAYASHI, N. & BISWAL, S. 2007. Cell survival responses to environmental stresses via the Keap1-Nrf2-ARE pathway. *Annu Rev Pharmacol Toxicol,* 47**,** 89-116.

KHANDELWAL, A., CROWLEY, V. M. & BLAGG, B. S. 2016. Natural Product Inspired N-Terminal Hsp90 Inhibitors: From Bench to Bedside? *Med Res Rev,* 36**,** 92-118.

KIM, G., ISON, G., MCKEE, A. E., ZHANG, H., TANG, S., GWISE, T., SRIDHARA, R., LEE, E., TZOU, A., PHILIP, R., CHIU, H. J., RICKS, T. K., PALMBY, T., RUSSELL, A. M., LADOUCEUR, G., PFUMA, E., LI, H., ZHAO, L., LIU, Q., VENUGOPAL, R., IBRAHIM, A. & PAZDUR, R. 2015. FDA Approval Summary: Olaparib Monotherapy in Patients with Deleterious Germline BRCA-Mutated Advanced Ovarian Cancer Treated with Three or More Lines of Chemotherapy. *Clin Cancer Res,* 21**,** 4257-61.

KUSABA, T., NAKAYAMA, T., YAMAZUMI, K., YAKATA, Y., YOSHIZAKI, A., INOUE, K., NAGAYASU, T. & SEKINE, I. 2006. Activation of STAT3 is a marker of poor prognosis in human colorectal cancer. *Oncol Rep,* 15**,** 1445-51.

LANDMANN, H., PROIA, D. A., HE, S., OGAWA, L. S., KRAMER, F., BEISSBARTH, T., GRADE, M., GAEDCKE, J., GHADIMI, M., MOLL, U. & DOBBELSTEIN, M. 2014. UDP glucuronosyltransferase 1A expression levels determine the response of colorectal cancer cells to the heat shock protein 90 inhibitor ganetespib. *Cell Death Dis,* 5**,** e1411.

LE DU, F., ECKHARDT, B. L., LIM, B., LITTON, J. K., MOULDER, S., MERIC-BERNSTAM, F., GONZALEZ-ANGULO, A. M. & UENO, N. T. 2015. Is the future of personalized therapy in triple-negative breast cancer based on molecular subtype? *Oncotarget,* 6**,** 12890-908.

LEE, H. J., ZHUANG, G., CAO, Y., DU, P., KIM, H. J. & SETTLEMAN, J. 2014. Drug resistance via feedback activation of Stat3 in oncogene-addicted cancer cells. *Cancer Cell,* 26**,** 207-21.

LEHMANN, B. D., BAUER, J. A., CHEN, X., SANDERS, M. E., CHAKRAVARTHY, A. B., SHYR, Y. & PIETENPOL, J. A. 2011. Identification of human triple-negative breast cancer subtypes and preclinical models for selection of targeted therapies. *J Clin Invest,* 121**,** 2750-67.

LI, J., SOROKA, J. & BUCHNER, J. 2012. The Hsp90 chaperone machinery: conformational dynamics and regulation by co-chaperones. *Biochim Biophys Acta,* 1823**,** 624-35.

LIEDTKE, C., MAZOUNI, C., HESS, K. R., ANDRE, F., TORDAI, A., MEJIA, J. A., SYMMANS, W. F., GONZALEZ-ANGULO, A. M., HENNESSY, B., GREEN, M., CRISTOFANILLI, M., HORTOBAGYI, G. N. & PUSZTAI, L. 2008. Response to neoadjuvant therapy and long-term survival in patients with triple-negative breast cancer. *J Clin Oncol,* 26**,** 1275-81.

LIEVRE, A., BACHET, J. B., LE CORRE, D., BOIGE, V., LANDI, B., EMILE, J. F., COTE, J. F., TOMASIC, G., PENNA, C., DUCREUX, M., ROUGIER, P., PENAULT-LLORCA, F. & LAURENT-PUIG, P. 2006. KRAS mutation status is predictive of response to cetuximab therapy in colorectal cancer. *Cancer Res,* 66**,** 3992-5.

LINDAHL, T. 1993. Instability and decay of the primary structure of DNA. *Nature,* 362**,** 709-15.

LIVRAGHI, L. & GARBER, J. E. 2015. PARP inhibitors in the management of breast cancer: current data and future prospects. *BMC Med,* 13**,** 188.

LOGUE, J. S. & MORRISON, D. K. 2012. Complexity in the signaling network: insights from the use of targeted inhibitors in cancer therapy. *Genes Dev,* 26**,** 641-50.

LORD, C. J. & ASHWORTH, A. 2013. Mechanisms of resistance to therapies targeting BRCA-mutant cancers. *Nat Med,* 19**,** 1381-8.

LORD, C. J. & ASHWORTH, A. 2016. BRCAness revisited. *Nat Rev Cancer,* 16**,** 110-20.

LUDWIG, J. A. & WEINSTEIN, J. N. 2005. Biomarkers in cancer staging, prognosis and treatment selection. *Nat Rev Cancer,* 5**,** 845-56.

MACKEEN, M. M., KRAMER, H. B., CHANG, K. H., COLEMAN, M. L., HOPKINSON, R. J., SCHOFIELD, C. J. & KESSLER, B. M. 2010. Small-molecule-based inhibition of histone demethylation in cells assessed by quantitative mass spectrometry. *J Proteome Res,* 9**,** 4082-92.

MAHALINGAM, D., SWORDS, R., CAREW, J. S., NAWROCKI, S. T., BHALLA, K. & GILES, F. J. 2009. Targeting HSP90 for cancer therapy. *Br J Cancer,* 100**,** 1523-9.

MALONEY, A., CLARKE, P. A., NAABY-HANSEN, S., STEIN, R., KOOPMAN, J. O., AKPAN, A., YANG, A., ZVELEBIL, M., CRAMER, R., STIMSON, L., AHERNE, W., BANERJI, U., JUDSON, I., SHARP, S., POWERS, M., DEBILLY, E., SALMONS, J., WALTON, M., BURLINGAME, A., WATERFIELD, M. & WORKMAN, P. 2007. Gene and protein expression profiling of human ovarian cancer cells treated with the heat shock protein 90 inhibitor 17-allylamino-17-demethoxygeldanamycin. *Cancer Res,* 67**,** 3239-53.

MANN, M. 2006. Functional and quantitative proteomics using SILAC. *Nat Rev Mol Cell Biol,* 7**,** 952-8.

MARIK, P. E. 2004. Propofol: therapeutic indications and side-effects. *Curr Pharm Des,* 10**,** 3639-49.

MARTY, M., COGNETTI, F., MARANINCHI, D., SNYDER, R., MAURIAC, L., TUBIANA-HULIN, M., CHAN, S., GRIMES, D., ANTON, A., LLUCH, A.,

KENNEDY, J., O'BYRNE, K., CONTE, P., GREEN, M., WARD, C., MAYNE, K. & EXTRA, J. M. 2005. Randomized phase II trial of the efficacy and safety of trastuzumab combined with docetaxel in patients with human epidermal growth factor receptor 2-positive metastatic breast cancer administered as first-line treatment: the M77001 study group. *J Clin Oncol,* 23**,** 4265-74.

MCLAUGHLIN, S. H., SOBOTT, F., YAO, Z. P., ZHANG, W., NIELSEN, P. R., GROSSMANN, J. G., LAUE, E. D., ROBINSON, C. V. & JACKSON, S. E. 2006. The co-chaperone p23 arrests the Hsp90 ATPase cycle to trap client proteins. *J Mol Biol,* 356**,** 746-58.

MEHTA, P. P., WHALEN, P., BAXI, S. M., KUNG, P. P., YAMAZAKI, S. & YIN, M. J. 2011. Effective targeting of triple-negative breast cancer cells by PF-4942847, a novel oral inhibitor of Hsp 90. *Clin Cancer Res,* 17**,** 5432-42.

MEYER, P., PRODROMOU, C., HU, B., VAUGHAN, C., ROE, S. M., PANARETOU, B., PIPER, P. W. & PEARL, L. H. 2003. Structural and functional analysis of the middle segment of hsp90: implications for ATP hydrolysis and client protein and cochaperone interactions. *Mol Cell,* 11**,** 647-58.

MIMNAUGH, E. G., CHAVANY, C. & NECKERS, L. 1996. Polyubiquitination and proteasomal degradation of the p185c-erbB-2 receptor protein-tyrosine kinase induced by geldanamycin. *J Biol Chem,* 271**,** 22796-801.

MINAMI, Y., KIMURA, Y., KAWASAKI, H., SUZUKI, K. & YAHARA, I. 1994. The carboxy-terminal region of mammalian HSP90 is required for its dimerization and function in vivo. *Mol Cell Biol,* 14**,** 1459-64.

MODI, S., STOPECK, A., LINDEN, H., SOLIT, D., CHANDARLAPATY, S., ROSEN, N., D'ANDREA, G., DICKLER, M., MOYNAHAN, M. E., SUGARMAN, S., MA, W., PATIL, S., NORTON, L., HANNAH, A. L. & HUDIS, C. 2011. HSP90 inhibition is effective in breast cancer: a phase II trial of tanespimycin (17-AAG) plus trastuzumab in patients with HER2-positive metastatic breast cancer progressing on trastuzumab. *Clin Cancer Res,* 17**,** 5132-9.

MODI, S., STOPECK, A. T., GORDON, M. S., MENDELSON, D., SOLIT, D. B., BAGATELL, R., MA, W., WHELER, J., ROSEN, N., NORTON, L., CROPP, G. F., JOHNSON, R. G., HANNAH, A. L. & HUDIS, C. A. 2007. Combination of trastuzumab and tanespimycin (17-AAG, KOS-953) is safe and active in trastuzumab-refractory HER-2 overexpressing breast cancer: a phase I dose-escalation study. *J Clin Oncol,* 25**,** 5410-7.

MORISHITA, A., GONG, J., NOMURA, T., YOSHIDA, H., IZUISHI, K., SUZUKI, Y., KUSHIDA, Y., HABA, R., D'ARMIENTO, J. & MASAKI, T. 2010. The use of protein array to identify targetable receptor tyrosine kinases for treatment of human colon cancer. *Int J Oncol,* 37**,** 829-35.

MORRIS, G. J., NAIDU, S., TOPHAM, A. K., GUILES, F., XU, Y., MCCUE, P., SCHWARTZ, G. F., PARK, P. K., ROSENBERG, A. L., BRILL, K. & MITCHELL, E. P. 2007. Differences in breast carcinoma characteristics in newly diagnosed African-American and Caucasian patients: a single-institution compilation compared with the National Cancer Institute's Surveillance, Epidemiology, and End Results database. *Cancer,* 110**,** 876-84.

MOTOHASHI, H. & YAMAMOTO, M. 2004. Nrf2-Keap1 defines a physiologically important stress response mechanism. *Trends Mol Med,* 10**,** 549-57.

NAGAR, S. & REMMEL, R. P. 2006. Uridine diphosphoglucuronosyltransferase pharmacogenetics and cancer. *Oncogene,* 25**,** 1659-72.

NAGARAJU, G. P., MEZINA, A., SHAIB, W. L., LANDRY, J. & EL-RAYES, B. F. 2016. Targeting the Janus-activated kinase-2-STAT3 signalling pathway in pancreatic cancer using the HSP90 inhibitor ganetespib. *Eur J Cancer,* 52**,** 109-19.

NECKERS, L. & WORKMAN, P. 2012. Hsp90 molecular chaperone inhibitors: are we there yet? *Clin Cancer Res,* 18**,** 64-76.

NGUYEN, T., NIOI, P. & PICKETT, C. B. 2009. The Nrf2-antioxidant response element signaling pathway and its activation by oxidative stress. *J Biol Chem,* 284**,** 13291-5.

NIEDERST, M. J. & ENGELMAN, J. A. 2013. Bypass mechanisms of resistance to receptor tyrosine kinase inhibition in lung cancer. *Sci Signal,* 6**,** re6.

NIELSEN, T. O., HSU, F. D., JENSEN, K., CHEANG, M., KARACA, G., HU, Z., HERNANDEZ-BOUSSARD, T., LIVASY, C., COWAN, D., DRESSLER, L., AKSLEN, L. A., RAGAZ, J., GOWN, A. M., GILKS, C. B., VAN DE RIJN, M. & PEROU, C. M. 2004. Immunohistochemical and clinical characterization of the basal-like subtype of invasive breast carcinoma. *Clin Cancer Res,* 10**,** 5367-74.

O'LEARY, B., FINN, R. S. & TURNER, N. C. 2016. Treating cancer with selective CDK4/6 inhibitors. *Nat Rev Clin Oncol,* 13**,** 417-30.

OLAYIOYE, M. A., NEVE, R. M., LANE, H. A. & HYNES, N. E. 2000. The ErbB signaling network: receptor heterodimerization in development and cancer. *EMBO J,* 19**,** 3159-67.

ONG, S. E., BLAGOEV, B., KRATCHMAROVA, I., KRISTENSEN, D. B., STEEN, H., PANDEY, A. & MANN, M. 2002. Stable isotope labeling by amino acids in cell culture, SILAC, as a simple and accurate approach to expression proteomics. *Mol Cell Proteomics,* 1**,** 376-86.

OTT, M., GOGVADZE, V., ORRENIUS, S. & ZHIVOTOVSKY, B. 2007. Mitochondria, oxidative stress and cell death. *Apoptosis,* 12**,** 913-22.

PARKER, J. S., MULLINS, M., CHEANG, M. C., LEUNG, S., VODUC, D., VICKERY, T., DAVIES, S., FAURON, C., HE, X., HU, Z., QUACKENBUSH, J. F., STIJLEMAN, I. J., PALAZZO, J., MARRON, J. S., NOBEL, A. B., MARDIS, E., NIELSEN, T. O., ELLIS, M. J., PEROU, C. M. & BERNARD, P. S. 2009. Supervised risk predictor of breast cancer based on intrinsic subtypes. *J Clin Oncol,* 27**,** 1160-7.

PEARL, L. H. & PRODROMOU, C. 2006. Structure and mechanism of the Hsp90 molecular chaperone machinery. *Annu Rev Biochem,* 75**,** 271-94.

PELICANO, H., CARNEY, D. & HUANG, P. 2004. ROS stress in cancer cells and therapeutic implications. *Drug Resist Updat,* 7**,** 97-110.

PEREZ, E. A., ROMOND, E. H., SUMAN, V. J., JEONG, J. H., DAVIDSON, N. E., GEYER, C. E., JR., MARTINO, S., MAMOUNAS, E. P., KAUFMAN, P. A. & WOLMARK, N. 2011. Four-year follow-up of trastuzumab plus adjuvant chemotherapy

for operable human epidermal growth factor receptor 2-positive breast cancer: joint analysis of data from NCCTG N9831 and NSABP B-31. *J Clin Oncol,* 29**,** 3366-73.

PEROU, C. M., SORLIE, T., EISEN, M. B., VAN DE RIJN, M., JEFFREY, S. S., REES, C. A., POLLACK, J. R., ROSS, D. T., JOHNSEN, H., AKSLEN, L. A., FLUGE, O., PERGAMENSCHIKOV, A., WILLIAMS, C., ZHU, S. X., LONNING, P. E., BORRESEN-DALE, A. L., BROWN, P. O. & BOTSTEIN, D. 2000. Molecular portraits of human breast tumours. *Nature,* 406**,** 747-52.

PICK, E., KLUGER, Y., GILTNANE, J. M., MOEDER, C., CAMP, R. L., RIMM, D. L. & KLUGER, H. M. 2007. High HSP90 expression is associated with decreased survival in breast cancer. *Cancer Res,* 67**,** 2932-7.

PIPER, P. W. & MILLSON, S. H. 2011. Mechanisms of Resistance to Hsp90 Inhibitor Drugs: A Complex Mosaic Emerges. *Pharmaceuticals (Basel),* 4**,** 1400-1422.

POWERS, M. V., CLARKE, P. A. & WORKMAN, P. 2008. Dual targeting of HSC70 and HSP72 inhibits HSP90 function and induces tumor-specific apoptosis. *Cancer Cell,* 14**,** 250-62.

PROIA, D. A. & BATES, R. C. 2014. Ganetespib and HSP90: translating preclinical hypotheses into clinical promise. *Cancer Res,* 74**,** 1294-300.

PROIA, D. A., FOLEY, K. P., KORBUT, T., SANG, J., SMITH, D., BATES, R. C., LIU, Y., ROSENBERG, A. F., ZHOU, D., KOYA, K., BARSOUM, J. & BLACKMAN, R. K. 2011. Multifaceted intervention by the Hsp90 inhibitor ganetespib (STA-9090) in cancer cells with activated JAK/STAT signaling. *PLoS One,* 6**,** e18552.

PROIA, D. A., ZHANG, C., SEQUEIRA, M., JIMENEZ, J. P., HE, S., SPECTOR, N., SHAPIRO, G. I., TOLANEY, S., NAGAI, M., ACQUAVIVA, J., SMITH, D. L., SANG, J., BATES, R. C. & EL-HARIRY, I. 2014. Preclinical activity profile and therapeutic efficacy of the HSP90 inhibitor ganetespib in triple-negative breast cancer. *Clin Cancer Res,* 20**,** 413-24.

PU, Y. S., HOUR, T. C., CHUANG, S. E., CHENG, A. L., LAI, M. K. & KUO, M. L. 2004. Interleukin-6 is responsible for drug resistance and anti-apoptotic effects in prostatic cancer cells. *Prostate,* 60**,** 120-9.

RAKHA, E. A., EL-SAYED, M. E., GREEN, A. R., LEE, A. H., ROBERTSON, J. F. & ELLIS, I. O. 2007. Prognostic markers in triple-negative breast cancer. *Cancer,* 109**,** 25-32.

RAKHA, E. A., EL-SAYED, M. E., LEE, A. H., ELSTON, C. W., GRAINGE, M. J., HODI, Z., BLAMEY, R. W. & ELLIS, I. O. 2008. Prognostic significance of Nottingham histologic grade in invasive breast carcinoma. *J Clin Oncol,* 26**,** 3153-8.

RAMENSKY, V., BORK, P. & SUNYAEV, S. 2002. Human non-synonymous SNPs: server and survey. *Nucleic Acids Res,* 30**,** 3894-900.

RAWLINGS, J. S., ROSLER, K. M. & HARRISON, D. A. 2004. The JAK/STAT signaling pathway. *J Cell Sci,* 117**,** 1281-3.

REIS-FILHO, J. S. & TUTT, A. N. 2008. Triple negative tumours: a critical review. *Histopathology,* 52**,** 108-18.

RETZLAFF, M., HAGN, F., MITSCHKE, L., HESSLING, M., GUGEL, F., KESSLER, H., RICHTER, K. & BUCHNER, J. 2010. Asymmetric activation of the hsp90 dimer by its cochaperone aha1. *Mol Cell,* 37**,** 344-54.

ROE, S. M., PRODROMOU, C., O'BRIEN, R., LADBURY, J. E., PIPER, P. W. & PEARL, L. H. 1999. Structural basis for inhibition of the Hsp90 molecular chaperone by the antitumor antibiotics radicicol and geldanamycin. *J Med Chem,* 42**,** 260-6.

ROMOND, E. H., PEREZ, E. A., BRYANT, J., SUMAN, V. J., GEYER, C. E., JR., DAVIDSON, N. E., TAN-CHIU, E., MARTINO, S., PAIK, S., KAUFMAN, P. A., SWAIN, S. M., PISANSKY, T. M., FEHRENBACHER, L., KUTTEH, L. A., VOGEL, V. G., VISSCHER, D. W., YOTHERS, G., JENKINS, R. B., BROWN, A. M., DAKHIL, S. R., MAMOUNAS, E. P., LINGLE, W. L., KLEIN, P. M., INGLE, J. N. & WOLMARK, N. 2005. Trastuzumab plus adjuvant chemotherapy for operable HER2-positive breast cancer. *N Engl J Med,* 353**,** 1673-84.

RONNEN, E. A., KONDAGUNTA, G. V., ISHILL, N., SWEENEY, S. M., DELUCA, J. K., SCHWARTZ, L., BACIK, J. & MOTZER, R. J. 2006. A phase II trial of 17-(Allylamino)-17-demethoxygeldanamycin in patients with papillary and clear cell renal cell carcinoma. *Invest New Drugs,* 24**,** 543-6.

ROSA, R., MONTELEONE, F., ZAMBRANO, N. & BIANCO, R. 2014. In vitro and in vivo models for analysis of resistance to anticancer molecular therapies. *Curr Med Chem,* 21**,** 1595-606.

ROWLAND, A., MINERS, J. O. & MACKENZIE, P. I. 2013. The UDP-glucuronosyltransferases: their role in drug metabolism and detoxification. *Int J Biochem Cell Biol,* 45**,** 1121-32.

SANG, J., ACQUAVIVA, J., FRIEDLAND, J. C., SMITH, D. L., SEQUEIRA, M., ZHANG, C., JIANG, Q., XUE, L., LOVLY, C. M., JIMENEZ, J. P., SHAW, A. T., DOEBELE, R. C., HE, S., BATES, R. C., CAMIDGE, D. R., MORRIS, S. W., EL-HARIRY, I. & PROIA, D. A. 2013. Targeted inhibition of the molecular chaperone Hsp90 overcomes ALK inhibitor resistance in non-small cell lung cancer. *Cancer Discov,* 3**,** 430-43.

SANSONE, P. & BROMBERG, J. 2012. Targeting the interleukin-6/Jak/stat pathway in human malignancies. *J Clin Oncol,* 30**,** 1005-14.

SCHNEEBERGER, K. 2014. Using next-generation sequencing to isolate mutant genes from forward genetic screens. *Nat Rev Genet,* 15**,** 662-76.

SCHULTE, T. W., AKINAGA, S., SOGA, S., SULLIVAN, W., STENSGARD, B., TOFT, D. & NECKERS, L. M. 1998. Antibiotic radicicol binds to the N-terminal domain of Hsp90 and shares important biologic activities with geldanamycin. *Cell Stress Chaperones,* 3**,** 100-8.

SHAH, S. P., ROTH, A., GOYA, R., OLOUMI, A., HA, G., ZHAO, Y., TURASHVILI, G., DING, J., TSE, K., HAFFARI, G., BASHASHATI, A., PRENTICE, L. M., KHATTRA, J., BURLEIGH, A., YAP, D., BERNARD, V., MCPHERSON, A., SHUMANSKY, K., CRISAN, A., GIULIANY, R., HERAVI-MOUSSAVI, A., ROSNER, J., LAI, D., BIROL, I., VARHOL, R., TAM, A., DHALLA, N., ZENG, T., MA, K., CHAN, S. K., GRIFFITH, M., MORADIAN, A., CHENG, S. W., MORIN, G. B., WATSON, P., GELMON, K., CHIA, S., CHIN, S. F., CURTIS, C., RUEDA, O. M., PHAROAH, P. D., DAMARAJU, S., MACKEY, J., HOON, K., HARKINS, T.,

TADIGOTLA, V., SIGAROUDINIA, M., GASCARD, P., TLSTY, T., COSTELLO, J. F., MEYER, I. M., EAVES, C. J., WASSERMAN, W. W., JONES, S., HUNTSMAN, D., HIRST, M., CALDAS, C., MARRA, M. A. & APARICIO, S. 2012. The clonal and mutational evolution spectrum of primary triple-negative breast cancers. *Nature,* 486**,** 395-9.

SHARMA, K., VABULAS, R. M., MACEK, B., PINKERT, S., COX, J., MANN, M. & HARTL, F. U. 2012. Quantitative proteomics reveals that Hsp90 inhibition preferentially targets kinases and the DNA damage response. *Mol Cell Proteomics,* 11**,** M111 014654.

SHIMAMURA, T., PERERA, S. A., FOLEY, K. P., SANG, J., RODIG, S. J., INOUE, T., CHEN, L., LI, D., CARRETERO, J., LI, Y. C., SINHA, P., CAREY, C. D., BORGMAN, C. L., JIMENEZ, J. P., MEYERSON, M., YING, W., BARSOUM, J., WONG, K. K. & SHAPIRO, G. I. 2012. Ganetespib (STA-9090), a nongeldanamycin HSP90 inhibitor, has potent antitumor activity in in vitro and in vivo models of non-small cell lung cancer. *Clin Cancer Res,* 18**,** 4973-85.

SHOEMAKER, R. H. 2006. The NCI60 human tumour cell line anticancer drug screen. *Nat Rev Cancer,* 6**,** 813-23.

SLAMON, D. J., CLARK, G. M., WONG, S. G., LEVIN, W. J., ULLRICH, A. & MCGUIRE, W. L. 1987. Human breast cancer: correlation of relapse and survival with amplification of the HER-2/neu oncogene. *Science,* 235**,** 177-82.

SOGA, S., AKINAGA, S. & SHIOTSU, Y. 2013. Hsp90 inhibitors as anti-cancer agents, from basic discoveries to clinical development. *Curr Pharm Des,* 19**,** 366-76.

SOLIT, D. B., ZHENG, F. F., DROBNJAK, M., MUNSTER, P. N., HIGGINS, B., VERBEL, D., HELLER, G., TONG, W., CORDON-CARDO, C., AGUS, D. B., SCHER, H. I. & ROSEN, N. 2002. 17-Allylamino-17-demethoxygeldanamycin induces the degradation of androgen receptor and HER-2/neu and inhibits the growth of prostate cancer xenografts. *Clin Cancer Res,* 8**,** 986-93.

SONG, C. H., PARK, S. Y., EOM, K. Y., KIM, J. H., KIM, S. W., KIM, J. S. & KIM, I. A. 2010. Potential prognostic value of heat-shock protein 90 in the presence of phosphatidylinositol-3-kinase overexpression or loss of PTEN, in invasive breast cancers. *Breast Cancer Res,* 12**,** R20.

SONG, D., CHAERKADY, R., TAN, A. C., GARCIA-GARCIA, E., NALLI, A., SUAREZ-GAUTHIER, A., LOPEZ-RIOS, F., ZHANG, X. F., SOLOMON, A., TONG, J., READ, M., FRITZ, C., JIMENO, A., PANDEY, A. & HIDALGO, M. 2008. Antitumor activity and molecular effects of the novel heat shock protein 90 inhibitor, IPI-504, in pancreatic cancer. *Mol Cancer Ther,* 7**,** 3275-84.

SORLIE, T., PEROU, C. M., TIBSHIRANI, R., AAS, T., GEISLER, S., JOHNSEN, H., HASTIE, T., EISEN, M. B., VAN DE RIJN, M., JEFFREY, S. S., THORSEN, T., QUIST, H., MATESE, J. C., BROWN, P. O., BOTSTEIN, D., LONNING, P. E. & BORRESEN-DALE, A. L. 2001. Gene expression patterns of breast carcinomas distinguish tumor subclasses with clinical implications. *Proc Natl Acad Sci U S A,* 98**,** 10869-74.

SORLIE, T., TIBSHIRANI, R., PARKER, J., HASTIE, T., MARRON, J. S., NOBEL, A., DENG, S., JOHNSEN, H., PESICH, R., GEISLER, S., DEMETER, J., PEROU, C. M., LONNING, P. E., BROWN, P. O., BORRESEN-DALE, A. L. & BOTSTEIN, D.

2003. Repeated observation of breast tumor subtypes in independent gene expression data sets. *Proc Natl Acad Sci U S A,* 100**,** 8418-23.

SU, K. Y., CHEN, H. Y., LI, K. C., KUO, M. L., YANG, J. C., CHAN, W. K., HO, B. C., CHANG, G. C., SHIH, J. Y., YU, S. L. & YANG, P. C. 2012. Pretreatment epidermal growth factor receptor (EGFR) T790M mutation predicts shorter EGFR tyrosine kinase inhibitor response duration in patients with non-small-cell lung cancer. *J Clin Oncol,* 30**,** 433-40.

SUPKO, J. G., HICKMAN, R. L., GREVER, M. R. & MALSPEIS, L. 1995. Preclinical pharmacologic evaluation of geldanamycin as an antitumor agent. *Cancer Chemother Pharmacol,* 36**,** 305-15.

TAIPALE, M., JAROSZ, D. F. & LINDQUIST, S. 2010. HSP90 at the hub of protein homeostasis: emerging mechanistic insights. *Nat Rev Mol Cell Biol,* 11**,** 515-28.

TOMLINSON, P. R., ZHENG, Y., FISCHER, R., HEIDASCH, R., GARDINER, C., EVETTS, S., HU, M., WADE-MARTINS, R., TURNER, M. R., MORRIS, J., TALBOT, K., KESSLER, B. M. & TOFARIS, G. K. 2015. Identification of distinct circulating exosomes in Parkinson's disease. *Ann Clin Transl Neurol,* 2**,** 353-61.

TRACHOOTHAM, D., ALEXANDRE, J. & HUANG, P. 2009. Targeting cancer cells by ROS-mediated mechanisms: a radical therapeutic approach? *Nat Rev Drug Discov,* 8**,** 579-91.

TRAPNELL, C., ROBERTS, A., GOFF, L., PERTEA, G., KIM, D., KELLEY, D. R., PIMENTEL, H., SALZBERG, S. L., RINN, J. L. & PACHTER, L. 2012. Differential gene and transcript expression analysis of RNA-seq experiments with TopHat and Cufflinks. *Nat Protoc,* 7**,** 562-78.

TREPEL, J., MOLLAPOUR, M., GIACCONE, G. & NECKERS, L. 2010. Targeting the dynamic HSP90 complex in cancer. *Nat Rev Cancer,* 10**,** 537-49.

TUKEY, R. H. & STRASSBURG, C. P. 2000. Human UDP-glucuronosyltransferases: metabolism, expression, and disease. *Annu Rev Pharmacol Toxicol,* 40**,** 581-616.

TUTT, A., ROBSON, M., GARBER, J. E., DOMCHEK, S. M., AUDEH, M. W., WEITZEL, J. N., FRIEDLANDER, M., ARUN, B., LOMAN, N., SCHMUTZLER, R. K., WARDLEY, A., MITCHELL, G., EARL, H., WICKENS, M. & CARMICHAEL, J. 2010. Oral poly(ADP-ribose) polymerase inhibitor olaparib in patients with BRCA1 or BRCA2 mutations and advanced breast cancer: a proof-of-concept trial. *Lancet,* 376**,** 235-44.

VAN SCHAEYBROECK, S., KALIMUTHO, M., DUNNE, P. D., CARSON, R., ALLEN, W., JITHESH, P. V., REDMOND, K. L., SASAZUKI, T., SHIRASAWA, S., BLAYNEY, J., MICHIELI, P., FENNING, C., LENZ, H. J., LAWLER, M., LONGLEY, D. B. & JOHNSTON, P. G. 2014. ADAM17-dependent c-MET-STAT3 signaling mediates resistance to MEK inhibitors in KRAS mutant colorectal cancer. *Cell Rep,* 7**,** 1940-55.

VERONESI, U., BOYLE, P., GOLDHIRSCH, A., ORECCHIA, R. & VIALE, G. 2005. Breast cancer. *Lancet,* 365**,** 1727-41.

VIALE, G. 2012. The current state of breast cancer classification. *Ann Oncol,* 23 Suppl 10**,** x207-10.

VIVANCO, I. & SAWYERS, C. L. 2002. The phosphatidylinositol 3-Kinase AKT pathway in human cancer. *Nat Rev Cancer,* 2**,** 489-501.

VON DER HEYDE, S., WAGNER, S., CZERNY, A., NIETERT, M., LUDEWIG, F., SALINAS-RIESTER, G., ARLT, D. & BEISSBARTH, T. 2015. mRNA profiling reveals determinants of trastuzumab efficiency in HER2-positive breast cancer. *PLoS One,* 10**,** e0117818.

VON MINCKWITZ, G., JONAT, W., FASCHING, P., DU BOIS, A., KLEEBERG, U., LUCK, H. J., KETTNER, E., HILFRICH, J., EIERMANN, W., TORODE, J. & SCHNEEWEISS, A. 2005. A multicentre phase II study on gefitinib in taxane- and anthracycline-pretreated metastatic breast cancer. *Breast Cancer Res Treat,* 89**,** 165-72.

WANG, M., SHEN, A., ZHANG, C., SONG, Z., AI, J., LIU, H., SUN, L., DING, J., GENG, M. & ZHANG, A. 2016. Development of Heat Shock Protein (Hsp90) Inhibitors To Combat Resistance to Tyrosine Kinase Inhibitors through Hsp90-Kinase Interactions. *J Med Chem,* 59**,** 5563-86.

WANG, S. W. & SUN, Y. M. 2014. The IL-6/JAK/STAT3 pathway: potential therapeutic strategies in treating colorectal cancer (Review). *Int J Oncol,* 44**,** 1032-40.

WANG, Z., GERSTEIN, M. & SNYDER, M. 2009. RNA-Seq: a revolutionary tool for transcriptomics. *Nat Rev Genet,* 10**,** 57-63.

WEIGELT, B. & REIS-FILHO, J. S. 2009. Histological and molecular types of breast cancer: is there a unifying taxonomy? *Nat Rev Clin Oncol,* 6**,** 718-30.

WHITESELL, L. & LINDQUIST, S. L. 2005. HSP90 and the chaperoning of cancer. *Nat Rev Cancer,* 5**,** 761-72.

WHITESELL, L., MIMNAUGH, E. G., DE COSTA, B., MYERS, C. E. & NECKERS, L. M. 1994. Inhibition of heat shock protein HSP90-pp60v-src heteroprotein complex formation by benzoquinone ansamycins: essential role for stress proteins in oncogenic transformation. *Proc Natl Acad Sci U S A,* 91**,** 8324-8.

WILDING, J. L. & BODMER, W. F. 2014. Cancer cell lines for drug discovery and development. *Cancer Res,* 74**,** 2377-84.

WOLFF, A. C., HAMMOND, M. E., HICKS, D. G., DOWSETT, M., MCSHANE, L. M., ALLISON, K. H., ALLRED, D. C., BARTLETT, J. M., BILOUS, M., FITZGIBBONS, P., HANNA, W., JENKINS, R. B., MANGU, P. B., PAIK, S., PEREZ, E. A., PRESS, M. F., SPEARS, P. A., VANCE, G. H., VIALE, G., HAYES, D. F., AMERICAN SOCIETY OF CLINICAL, O. & COLLEGE OF AMERICAN, P. 2013. Recommendations for human epidermal growth factor receptor 2 testing in breast cancer: American Society of Clinical Oncology/College of American Pathologists clinical practice guideline update. *J Clin Oncol,* 31**,** 3997-4013.

WU, W. S. 2006. The signaling mechanism of ROS in tumor progression. *Cancer Metastasis Rev,* 25**,** 695-705.

YAN, H. Q., HUANG, X. B., KE, S. Z., JIANG, Y. N., ZHANG, Y. H., WANG, Y. N., LI, J. & GAO, F. G. 2014. Interleukin 6 augments lung cancer chemotherapeutic resistance via ataxia-telangiectasia mutated/NF-kappaB pathway activation. *Cancer Sci,* 105**,** 1220-7.

YARDEN, Y. & SLIWKOWSKI, M. X. 2001. Untangling the ErbB signalling network. *Nat Rev Mol Cell Biol,* 2**,** 127-37.

YEWALE, C., BARADIA, D., VHORA, I., PATIL, S. & MISRA, A. 2013. Epidermal growth factor receptor targeting in cancer: a review of trends and strategies. *Biomaterials,* 34**,** 8690-707.

YING, W., DU, Z., SUN, L., FOLEY, K. P., PROIA, D. A., BLACKMAN, R. K., ZHOU, D., INOUE, T., TATSUTA, N., SANG, J., YE, S., ACQUAVIVA, J., OGAWA, L. S., WADA, Y., BARSOUM, J. & KOYA, K. 2012. Ganetespib, a unique triazolone-containing Hsp90 inhibitor, exhibits potent antitumor activity and a superior safety profile for cancer therapy. *Mol Cancer Ther,* 11**,** 475-84.

YONESAKA, K., ZEJNULLAHU, K., OKAMOTO, I., SATOH, T., CAPPUZZO, F., SOUGLAKOS, J., ERCAN, D., ROGERS, A., RONCALLI, M., TAKEDA, M., FUJISAKA, Y., PHILIPS, J., SHIMIZU, T., MAENISHI, O., CHO, Y., SUN, J., DESTRO, A., TAIRA, K., TAKEDA, K., OKABE, T., SWANSON, J., ITOH, H., TAKADA, M., LIFSHITS, E., OKUNO, K., ENGELMAN, J. A., SHIVDASANI, R. A., NISHIO, K., FUKUOKA, M., VARELLA-GARCIA, M., NAKAGAWA, K. & JANNE, P. A. 2011. Activation of ERBB2 signaling causes resistance to the EGFR-directed therapeutic antibody cetuximab. *Sci Transl Med,* 3**,** 99ra86.

YOUNG, J. C., OBERMANN, W. M. & HARTL, F. U. 1998. Specific binding of tetratricopeptide repeat proteins to the C-terminal 12-kDa domain of hsp90. *J Biol Chem,* 273**,** 18007-10.

YU, H., LEE, H., HERRMANN, A., BUETTNER, R. & JOVE, R. 2014. Revisiting STAT3 signalling in cancer: new and unexpected biological functions. *Nat Rev Cancer,* 14**,** 736-46.

ZAJAC, M., GOMEZ, G., BENITEZ, J. & MARTINEZ-DELGADO, B. 2010. Molecular signature of response and potential pathways related to resistance to the HSP90 inhibitor, 17AAG, in breast cancer. *BMC Med Genomics,* 3**,** 44.

ZANONI, M., PICCININI, F., ARIENTI, C., ZAMAGNI, A., SANTI, S., POLICO, R., BEVILACQUA, A. & TESEI, A. 2016. 3D tumor spheroid models for in vitro therapeutic screening: a systematic approach to enhance the biological relevance of data obtained. *Sci Rep,* 6**,** 19103.

ZHANG, M. & LUO, S. C. 2016. Gene expression profiling of epithelial ovarian cancer reveals key genes and pathways associated with chemotherapy resistance. *Genet Mol Res,* 15.

ZHANG, M. H., MAN, H. T., ZHAO, X. D., DONG, N. & MA, S. L. 2014. Estrogen receptor-positive breast cancer molecular signatures and therapeutic potentials (Review). *Biomed Rep,* 2**,** 41-52.

ZHAO, C., LI, H., LIN, H. J., YANG, S., LIN, J. & LIANG, G. 2016. Feedback Activation of STAT3 as a Cancer Drug-Resistance Mechanism. *Trends Pharmacol Sci,* 37**,** 47-61.

ZHAO, S., FUNG-LEUNG, W. P., BITTNER, A., NGO, K. & LIU, X. 2014. Comparison of RNA-Seq and microarray in transcriptome profiling of activated T cells. *PLoS One,* 9**,** e78644.

ZHOU, D., LIU, Y., YE, J., YING, W., OGAWA, L. S., INOUE, T., TATSUTA, N., WADA, Y., KOYA, K., HUANG, Q., BATES, R. C. & SONDERFAN, A. J. 2013. A rat retinal damage model predicts for potential clinical visual disturbances induced by Hsp90 inhibitors. *Toxicol Appl Pharmacol,* 273**,** 401-9.

ZOU, J., GUO, Y., GUETTOUCHE, T., SMITH, D. F. & VOELLMY, R. 1998. Repression of heat shock transcription factor HSF1 activation by HSP90 (HSP90 complex) that forms a stress-sensitive complex with HSF1. *Cell,* 94**,** 471-80.

8. Appendix

Supplementary Table 1: 326 compound bioactive small molecule library

Drug Name	Target(s)
17-AAG(Geldanamycin)	HSP90
17-DMAG	HSP90
2-Methoxyestradiol	HIF
ABT-263(Navitoclax)	Bcl-2
ABT-737	Bcl-2
ABT-751	Microtubule Formation
ABT-869	RTK | VEGFR | PDGFR | FGFR
ABT-888	PARP
AC-220	FLT
Acetaminophen(Tylenol)	COX
Adriamycin	Topoisomerase
AEE788	EGFR | HER1/2 | VEGFR | FGFR
AG-014699	PARP
AG14361	PARP
AG-490	JAK | EGFR
Alendronate Sodium	farnesyl diphosphate synthase
Allopurinol	xanthine oxidase
Amfebutamone hcl	norepinephrine-dopamine reuptake
Amisulpride	Dopamine Receptor
Amlodipine besylate	calcium channel
Anastrozole(Arimidex)	Aromatase
AP24534	VEGFR | FGFR | PDGFR | Flt
Apigenin	P450
Apixaban	Factor Xa
AS-605240	PI3K
AS703026	MEK
Asenapine maleate	5-HT | adrenergic receptor
AT7519	CDK
AT7867	Akt | S6 kinase
AT9283	Bcr-Abl| JAK | Aurora Kinase
Atazanavir(BMS-232632)	Proteasome
Atropine sulfate monohydrate	mAChRs
Aurora A Inhibitor I	Aurora Kinase
AV-951(Tivozanib)	VEGFR | c-Kit | PDGFR
Axitinib	VEGFR
AZD0530(Saracatinib)	SRC | Abl
AZD1152-HQPA(Barasertib)	Aurora Kinase
AZD1480	JAK
AZD2281(Olaparib)	PARP
AZD6244(Selumetinib)	MEK
AZD6482	PI3K
AZD7762	CHK
AZD8055	mTOR
AZD8330	MEK
Baicalin	prolyl endopeptidase |GABA receptor
BAY 73-4506(Regorafenib)	c-Kit | B-Raf | VEGFR
Belinostat(PXD101)	HDAC

Benazepril hydrochloride	RAAS
Benserazide hcl	Dopamine|AAAD
BEZ235(NVP-BEZ235)	mTOR | PI3K
BI 2536	PLK
BIBF1120(Vargatef)	VEGFR | PDGFR | FGFR
BIBR 953	thrombin
BIBR-1048	thrombin
BIBR1532	Telomerase
BIBW2992(Tovok)	EGFR | HER2
Bicalutamide(Casodex)	androgen receptor
BIIB021	HSP90
BIRB 796	p38 MAPK
Bisoprolol Fumarate	Adrenergic receptors
BIX 02188	MEK
BIX 02189	MEK
BMS 777607	c-Met
BMS 794833	c-Met | VEGFR | Met | Axl | Flt
BMS-599626	EGFR | HER2
BMS-707035	HIV-1 Integrase(IN)
BMS-708163	γ-secretase
BMS-790052	HCV protease
Bortezomib	proteasome
Bosutinib(SKI-606)	Src
BS-181 hydrochloride	CDK
BSI-201	PARP
Camptothecine	Topoisomerase
Capecitabine(Xeloda)	Antimetabolites
Carbamazepine(Carbatrol)	sodium channel
Carbidopa	aromatic-L-amino-acid decarboxylase
CCT129202	Aurora kinase
Cediranib(AZD2171)	VEGFR | FGFR
CHIR-99021	GSK-3
Chlorpromazine hcl	Dopamine | potassium channel
Chlorprothixene	5-HT | Dopamine receptor
CHR-2797	Aminopeptidase N(APN) | LAP
CI-1033(Canertinib)	EGFR | HER2
CI-1040 (PD184352)	MEK
Cilnidipine	calcium channe
Cilomilast(SB-207499)	PDE
Cilostazol	PDE
Cladribine	Antimetabolites
Clemastine fumarate	histamine H1 antagonist
Clofarabine	ribonucleotide reductase
Clopidogrel bisulfate	NULL
Clozapine	5-HT1C receptor
CP-724714	HER2
Cryptotanshinone	Stat
CUDC-101	HDAC | EGFR | HER2
CYC116	Aurora Kinase | VEGFR
Cyclopamine	Hedgehog
Cytarabine(Cytosar-U)	DNA polymerase
Danoprevir(ITMN-191)	Proteasome
Dasatinib	SRC | Abl
Decitabine	Antimetabolites

Deforolimus(MK-8669)	mTOR
Diclofenac sodium	COX
Diphenhydramine hcl	histamine H1
Dipyridamole	PDE
Docetaxel	Microtubule Formation
Donepezil hydrochloride	mAChRs
Dorzolamide HCL	carbonic anhydrase(CA)
Doxazosin mesylate	adrenergic receptor
Droxinostat	HDAC
Dutasteride(Avodart)	5α-reductase
Elvitegravir	HIV Integrase
Emtricitabine	nucleoside reverse transcriptase
Enalapril maleate	RAAS
Enalaprilat	RAAS
ENMD-2076	Flt | Aurora Kinase | Src | VEGFR
Enzastaurin	PKC
Eplerenone	RAAS
Epothilone A	Microtubule Formation
Epothilone B(EPO906)	Epothilone B
Erlotinib Hydrochloride	EGFR
Etoposide(Etopophos)	Topoisomerase
Everolimus(RAD001)	mTOR
EX 527	Sirtuin
Exemestane	aromatase enzyme
Fasudil HCl	ROCK
Febuxostat	XAO
Felodipine	calcium channel
Finasteride	5α-reductase
Flavopiridol(Alvocidib)	CDK
Flucytosine(Ancobon)	DNA/RNA synthesis
Fludarabine Phosphate	Antimetabolites
Fludarabine(Fludara)	Antimetabolites
Fluoxetine hydrochloride	5-HT
Fluvastatin Sodium	HMG-CoA reductase
Fulvestrant	estrogen receptor
GDC-0449(Vismodegib)	Hedgehog
GDC-0879	B-Raf
GDC-0941	PI3K
Gefitinib(Iressa)	EGFR | Akt
Gemcitabine Hydrochloride	Antimetabolites
Granisetron Hydrochloride	5-HT receptor
GSK1059615	PI3K | mTOR
GSK429286A	ROCK
GSK461364	PLK
Hesperadin	Aurora kinase
HMN-214	PLK
Ibuprofen	COX
IC-87114	PI3K
Icariin	PDE
Imatinib Mesylate	c-Kit | PDGFR
Imatinib(STI571)	PDGFR | c-Kit
Indirubin	CDK | GSK-3
INO-1001	PARP
Irbesartan(Avapro)	RAAS

Irinotecan	topoisomerase
Ispinesib(SB-715992)	Kinesin spindle protein
ITF2357	HDAC
JNJ 26854165	p53
JNJ-26481585	HDAC
JNJ-38877605	c-Met
JNJ-7706621	CDK | Aurora Kinase
Ketoprofen(Actron)	COX
Ketorolac Tromethamine	COX
Ki8751	VEGFR | c-Kit | PDGFR | FGFR
KRN 633	VEGFR | PDGFR | c-Kit
KU-0063794	mTOR
KU-55933	ATM
KU-60019	ATM
KW 2449	Flt | Abl | Aurora Kinase
Lapatinib Ditosylate	EGFR | HER2
LAQ824	HDAC
LBH-589(Panobinostat)	HDAC
LDE225	Smo
Lenalidomide	TNF-alpha
Letrozole	Aromatase
Linezolid	NULL
Luteolin(Luteolol)	PDE | Interleukin 6
LY2228820	p38 MAPK
LY2784544	JAK
LY294002	PI3K
LY500307	Erβ
Manidipine	calcium channel
Maraviroc(Selzentry)	CCR5(cellular coreceptor 5)
Masitinib(AB1010)	c-Kit | PDGFR | FGFR | VEGFR
MC1568	HDAC
MGCD0103(Mocetinostat)	HDAC
MGCD-265	c-Met | VEGFR | Tie-2
Mitoxantrone	Topoisomerase
Mizoribine	DNA/RNA synthesis
MK 3207 hydrochloride	CGRP
MK-2206	Akt
MLN2238	Proteasome
MLN8237	Aurora
MLN9708	Proteasome
Motesanib Diphosphate	VEGFR | PDGFR | c-Kit | Src
MP-470	c-Met | c-Kit | PDGFR | Flt3 | Src
MS-275	HDAC
Naftopidil	α1-adrenergic receptor
Naftopidil Dihydrochloride	adrenergic receptor
Nebivolol HCl	adrenergic receptor
Neratinib	HER2 | EGFR
Nilotinib	Bcr-Abl
Nisoldipine	calcium channel
Nizatidine	histamine H2-receptor
NPI-2358	VDA
NVP-ADW742	IGF-1R
NVP-AUY922	HSP90
NVP-BEP800	HSP90

NVP-TAE684	ALK
Obatoclax Mesylate	Bcl-2
ON-01910	PLK
OSI-930	c-Kit | VEGFR
Ozagrel	thromboxane A2 synthetase
Paclitaxel(Taxol)	Microtubule Formation
Pancuronium bromide	mAChRs
Pazopanib Hydrochloride	VEGFR
PD0325901	MEK
PD0332991	CDK
PD153035 hydrochloride	EGFR
PD318088	MEK
PD98059	MEK
Pelitinib	EGFR
Pemetrexed disodium	TS | DHFR | GARFT
Perindopril Erbumine	RAAS
PF-04217903	c-Met
PF-2341066	c-Met | ALK
PHA-680632	Aurora Kinase
PHA-739358(Danusertib)	Aurora Kinase | Bcr-Abl
PHA-793887	CDK
PI-103	PI3K | mTOR
PIK-293	PI3K
PIK-75 Hydrochloride	PI3K | DNA-PK
PIK-90	PI3K
PIK-93	PI3K
Pimobendan(Vetmedin)	PDE
Piroxicam	COX
PLX-4720	B-Raf
Pomalidomide	TNF-alpha
Pramipexole dihydrochloride monohydrate	NULL
Pyrimethamine	dihydrofolate reductase(DHFR)
Quercetin(Sophoretin)	PI3K | PKC | Src
R406	Syk
R406(free base)	Syk
RAF265	RAF | VEGFR
Raltegravir	HIV Integrase
Raltitrexed(Tomudex)	Antimetabolites
Ramipril	RAAS
Ranitidine Hydrochloride	histamine H2-receptor
Rapamycin(Sirolimus)	mTOR
Ritonavir	HIV protease
Rivaroxaban(Xarelto)	Factor Xa
RO4929097	Y-Secretase
Roscovitine(CYC202)	CDK
S-(+)-Rolipram	PDE
S31-201	STAT3
SB 202190	p38 MAPK
SB 203580	p38 MAPK
SB 216763	GSK-3
SB 431542	ALK
SB 525334	ALK
SB 743921	Kinesin spindle protein
SB939	HDAC

Selegiline hydrochloride	monoamine oxidase
Semagacestat	Y-Secretase
SGI-1776	Pim
SGX-523	c-Met | VEGFR
Sitagliptin phosphate	DPP-4
SNS-032(BMS-387032)	CDK
SNS-314 Mesylate	Aurora Kinase
Sodium valproate	HDAC
Sorafenib Tosylate	VEGFR | PDGFR | RAF | MEK
Sotalol hydrochloride	Beta-1 adrenergic receptor
SP600125	JNK
Stavudine	NART
SU11274(PKI-SU11274)	c-Met
Sulfamethoxazole	PABA
Sulfanilamide	PABA
Sunitinib Malate	FLT3 | PDGFR | VEGFR | Kit
Tadalafil(Cialis)	PDE
Tamoxifen Citrate	Estrogen receptor
Tamsulosin hydrochloride	hydroxysteroid dehydrogenase
Tandutinib (MLN518)	FLT-3 | PDGFR | KIT
Telmisartan	RAAS
Temsirolimus	mTOR
Tenofovir	NART
Terbinafine hydrochloride	COX
TG100-115	PI3K
TGX-221	PI3K
Tipifarnib	farnesyltransferase(Ftase)
Topotecan Hydrochloride	Topoisomerase
Trichostatin A	HDAC
Trilostane	hydroxysteroid dehydrogenase
Tropisetron hcl	5-HT receptor
TSU-68	VEGFR | PDGFR | FGFR
TW-37	Bcl-2
U0126-EtOH	MEK
Valsartan	RAAS
Vandetanib	VEGFR | EGFR | Src
Vardenafil(Vivanza)	PDE
Vatalanib	VEGFR | c-Kit | Flk | Flt | FGFR
Venlafaxine hcl	5-HT receptor
Vicriviroc Malate	CCR5(cellular coreceptor 5)
Vincristine Sulfate	Microtubule Formation
Vinorelbine(Navelbine)	p38 MAPK
Vorinostat	HDAC
VX-222	HCV protease
VX-680	Aurora Kinase
VX-702	p38 MAPK | IL-6 | IL-1β | TNFα
VX-745	p38 MAPK
VX-770	CFTR
WYE-354	mTOR
WZ3146	EGFR
WZ4002	EGFR
WZ8040	EGFR
XAV-939	Wnt
XL147	PI3K

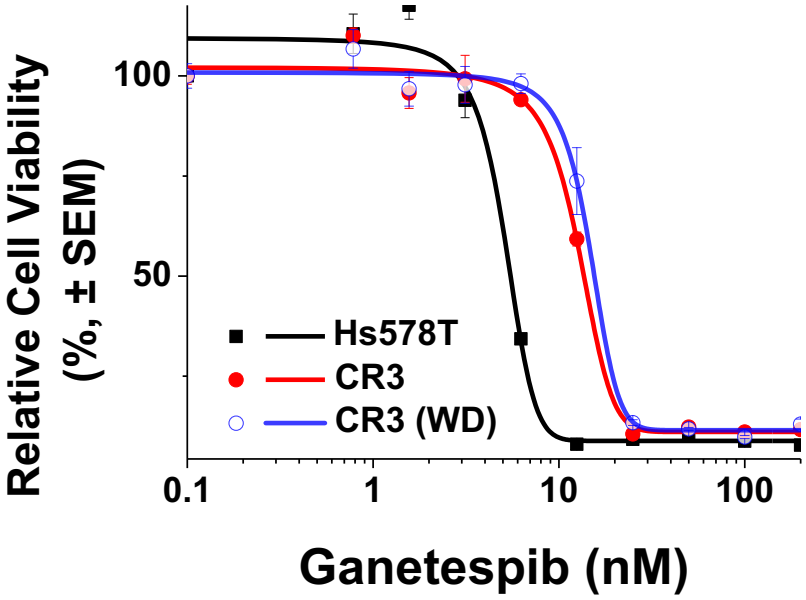
XL184	VEGFR | c-Met | Flt | Tie-2 | c-Kit
XL765	PI3K | mTOR
XL880(GSK1363089)	c-Met | VEGFR | FGFR
YM155	Survivin
Yohimbine hydrochloride	alpha 2-adrenergic receptors
Zalcitabine	NART
Zibotentan(ZD4054)	ETA-receptor
ZM-447439	Aurora Kinase
ZSTK474	PI3K

Supplementary Table 2: List of variants seen in both HSP90i-resistant clones

	SNP	Gene		Variants	PolyPhen
1	rs369712134	POLQ	Polymerase (DNA Directed), Theta	c.6850 G>A p.R2241*	
2		KCTD5	Potassium Channel Tetramerization Domain Containing 5	c.677 C>A p.F201L	0.999
3		DDX27	DEAD (Asp-Glu-Ala-Asp) Box Polypeptide 27	c.1393 T>G p.F462V	0.999
4		OTUD7B	OTU Deubiquitinase 7B	c.603 C>A p.S103I	0.997
5		RNF40	Ring Finger Protein 40, E3 Ubiquitin Protein Ligase	c.2480 A>T p.E682V	0.996
6	rs9814557	PPP2R3A	Protein Phosphatase 2, Regulatory Subunit B", Alpha	c.817 A>G p.D67G	0.989
7		CDH11	Cadherin 11, Type 2, OB-Cadherin (Osteoblast)	c.1193 T>G p.N193H	0.949
8		MANIA1	Mannosidase, Alpha, Class 1A, Member 1	c.1782 T>C p.H447R	0.872
9		MBD1	Methyl-CpG Binding Domain Protein 1	c.1543 G>C p.S1543W	0.79
10		EAPP	E2F-Associated Phosphoprotein	c.201 T>C p.Q40R	0.609
11		PLEC	Plectin	c.9675 C>G p.E3169Q	0.456
12		DIS3L2	DIS3 Like 3'-5' Exoribonuclease 2	c.1695 G>C p.E473D	0.2
13	rs3732410	GOLGB1	Golgin B1	c.3761 T>C p.Y1217C	0.162
14		AGGF1	Angiogenic Factor With G Patch And FHA Domains 1	c.1209 A>G p.K276R	0.124
15	rs3772219	ARHGEF3	Rho Guanine Nucleotide Exchange Factor (GEF) 3	c.1209 A>C p.L367V	0.086
16	rs13093808	PARP14	Poly (ADP-Ribose) Polymerase Family, Member 14	c.1948 C>A p.A561E	0.086
17		ROCK1	Rho-Associated, Coiled-Coil Containing Protein Kinase 1	c.4566 C>G p.D1209H	0.072
18	rs9843784	COMMD2	COMM Domain Containing 2	c.392 T>G p.I113L	0.03
19	rs2272962	BCAS4	Breast Carcinoma Amplified Sequence 4	c.268 G>T p.E56D	0.024
20	rs3732407	GOLGB1	Golgin B1	c.2858 G>C T916S	0.012

21	rs843358	EIF2B5	Eukaryotic Translation Initiation Factor 2B, Subunit 5 Epsilon	c.1881 A>G p.I587V	0.008
22	rs17429033	ADHD10	Abhydrolase Domain Containing 10	c.778 A>G p.I251V	0.004
23		LPCAT1	Lysophosphatidylcholine Acyltransferase 1	c.1676 C>G p.A515P	0.003
24		SLC25A26	Solute Carrier Family 25 Member 26	c.1106 G>T p.Q126H	0.002
25		YEATS2	YEATS Domain Containing 2	c.3214 G>C p.A1007P	0.002
26	rs1127412	GOLGB1	Golgin B1	c.5420 C>T p.G1770D	0.001
27	rs10935070	TOPBP1	Topoisomerase (DNA) II Binding Protein 1	c.3257 T>C p.N1042S	0.001
28	rs377527627	GMPS	Guanine Monphosphate Synthase	c.1276 A>G p.D314G	0.001
29	rs11719086	PARP14	Poly (ADP-Ribose) Polymerase Family, Member 14	c.1615 G>A p.R450K	0
30	rs9830734	VPS8	Vacuolar Protein Sorting 8 Homolog (S. Cerevisiae)	c.418 A>G p.I83V	0
31	rs11555405	VPS8	Vacuolar Protein Sorting 8 Homolog (S. Cerevisiae)	c.3664 C>T p.H1165Y	0
32	rs6762208	SENP2	SUMO1/Sentrin/SMT3 Specific Peptidase 2	c.1142 C>A p.T301K	0
33	rs17197552	PPP2R3A	Protein Phosphatase 2, Regulatory Subunit B'' Alpha	c.2541 A>G p.S642G	0
34**		FRRS1	Ferric-Chelate Reductase 1	c.2318 G>T p.F572L	0.801
35**		HPS5	Hermansky-Pudlak Syndrome 5	c.765 C>A p.A163S	0.026

**** Only seen in CR3**



Supplementary Figure 1: Sensitivity to ganetespib in HSP90i-resistant clone CR3

HSP90i-resistant clone CR3 was grown in culture for two weeks in complete medium without ganetespib. The sensitivity to ganetespib was assessed in the resistant clone after withdrawal and compared with the sensitivity in parental Hs578T cells and the resistant clone, which was grown in culture with 30 nM ganetespib. The cells were treated with increasing concentrations (0 - 200 nM) of ganetespib for 72 hr and cell viability was assessed using resazurin-based assay. Cell viability (%) for each treatment was expressed relative to the DMSO-treated control. Representative graph from two independent experiments, each performed in triplicates. Error bars indicate SEM.

Supplementary Table 3: Differentially expressed genes after ganetespib treatment in Hs578T cells

Gene		log2 FC	q-value
HSP90 chaperone complex and other HSP:			
HSP90AA1	HSP90-Alpha	1.78	2.59E-03
HSP90AB1	HSP90-Beta	0.96	8.01E-04
HSPA8	HSP70 member 8/HSC70	1.33	4.60E-03
HSPA1A	HSP70 member 1A/HSP72	3.81	8.01E-04
HSPA1B	HSP70 member 1B/HSP72	2.76	8.01E-04
HSPB1	HSP27 member 1	1.53	8.01E-04
HSPA4L	HSP70 member 4-like	1.26	8.01E-04
DNAJA1	HSP40 member A1	0.87	8.01E-04
DNAJA4	HSP40 member A4	1.63	8.01E-04
SERPINH1	HSP47 member 1	0.73	2.05E-03
HSPD1	HSP60 member 1	0.86	8.01E-04
AHSA1/AHA1	Activator Of Heat Shock 90kDa Protein ATPase	0.65	7.56E-03
Cell cycle regulations and checkpoints:			
CCNE2	cyclin E2	-1.56	3.13E-03
CCNF	cyclin F	-1.01	8.01E-04
DHFR	dihydrofolate reductase	-1.26	8.01E-04
DTL	denticleless E3 ubiquitin protein ligase homolog (Drosophila)	-0.93	8.01E-04
E2F1	E2F transcription factor 1	-0.65	1.46E-03
E2F7	E2F transcription factor 7	-0.89	8.01E-04
E2F8	E2F transcription factor 8	-1.69	8.01E-04
HELLS	helicase, lymphoid-specific	-1.52	8.01E-04
TAF15	TATA-Box Binding Protein Associated Factor 15	-0.70	1.46E-03
DNA replication:			
MCM10	minichromosome maintenance complex component 10	-1.07	8.01E-04
MCM2	minichromosome maintenance complex component 2	-0.66	8.01E-04
MCM5	minichromosome maintenance complex component 5	-0.95	8.01E-04
MCM6	minichromosome maintenance complex component 6	-0.85	8.01E-04
MCM8	minichromosome maintenance complex component 8	-0.86	8.01E-04
POLA1	polymerase (DNA directed), alpha 1, catalytic subunit	-0.73	8.01E-04
POLA2	polymerase (DNA directed), alpha 2, accessory subunit	-1.58	8.01E-04

RFC4	Replication Factor C Subunit 4	-1.50	7.13E-03
RMI1	RecQ mediated genome instability 1	-1.01	8.01E-04
RNASEH2A	ribonuclease H2, subunit A	-0.94	6.27E-03
WDHD1	WD repeat and HMG-box DNA binding protein 1	-0.71	1.46E-03
DNA repair:			
BRCA1	breast cancer 1, early onset	-0.80	2.66E-02
FANCD2	Fanconi anemia, complementation group D2	-0.86	3.13E-03
H2AFX	H2A histone family, member X	-0.57	8.01E-04
HMGB1	high mobility group box 1	-0.78	8.01E-04
KIAA0101	KIAA0101	-0.53	4.59E-02
LIG1	ligase I, DNA, ATP-dependent	-1.25	8.01E-04
PARP2	poly (ADP-ribose) polymerase 2	-0.85	8.01E-04
SMC6	structural maintenance of chromosomes 6	-0.91	1.46E-03
Chromosome condensation and segregation:			
CENPM	centromere protein M	-0.66	5.84E-03
ESPL1	extra spindle pole bodies homolog 1 (S. cerevisiae)	-1.18	8.01E-04
KIF20B	kinesin family member 20B	-0.47	4.14E-02
KIF22	kinesin family member 22	-0.66	1.46E-03
KIFC1	kinesin family member C1	-0.62	7.13E-03
KNTC1	kinetochore associated 1	-0.78	1.51E-02
CENPU	centromere protein U	-1.00	8.01E-04
NCAPG	non-SMC condensin I complex, subunit G	-0.79	8.01E-04
NCAPH	non-SMC condensin I complex, subunit H	-0.71	8.01E-04
NUF2	NUF2, NDC80 kinetochore complex component	-0.56	9.78E-03
PSRC1	proline/serine-rich coiled-coil 1	-0.63	2.05E-03
SPC24	SPC24, NDC80 kinetochore complex component	-1.68	3.64E-03
STMN1	stathmin 1	-0.57	2.09E-02
ZWINT	ZW10 interacting kinetochore protein	-0.84	8.01E-04
Histone exchange:			
ANP32E	acidic (leucine-rich) nuclear phosphoprotein 32 family, member E	-0.52	2.39E-02
ASF1B	anti-silencing function 1B histone chaperone	-0.76	8.01E-04
HIRIP3	HIRA interacting protein 3	-1.23	2.59E-03

Supplementary Table 4: The top 100 significantly upregulated genes in both HSP90i-resistant clones compared to Hs578T cells

Genes		CR2		CR3	
		log2 FC	q-value	log2 FC	q-value
UGT1A9	UDP Glucuronosyltransferase Family 1 Member A9	7.63	3.04E-02	7.16	1.98E-02
RYR2	Ryanodine Receptor 2	7.62	3.11E-02	8.64	2.42E-02
NLGN4X	Neuroligin 4, X-Linked	7.23	1.91E-02	7.02	1.36E-02
LINC01029	Long Intergenic Non-Protein Coding RNA 1029	7.15	4.84E-02	7.17	3.95E-02
RERG	RAS Like Estrogen Regulated Growth Inhibitor	6.88	4.27E-02	6.24	3.73E-02
NRG4	Neuregulin 4	6.57	5.58E-04	6.54	4.10E-04
UGT1A10	UDP Glucuronosyltransferase Family 1 Member A10	6.40	5.58E-04	6.73	4.10E-04
STK26	Serine/Threonine Protein Kinase 26	6.37	2.31E-03	6.61	1.71E-03
ANXA10	Annexin A10	6.12	5.58E-04	7.55	4.10E-04
NMNAT3	Nicotinamide Nucleotide Adenylyltransferase 3	6.09	7.87E-03	5.13	8.63E-03
PLCB1	Phospholipase C Beta 1	6.07	3.51E-02	5.99	2.95E-02
TGFA	Transforming Growth Factor Alpha	5.87	1.51E-02	6.04	7.33E-03
MAGEB2	MAGE Family Member B2	5.80	5.58E-04	5.59	4.10E-04
TMEM98	Transmembrane Protein 98	5.62	5.58E-04	5.37	4.10E-04
FBXL7	F-Box And Leucine-Rich Repeat Protein 7	5.62	3.57E-02	5.90	3.69E-02
AKR1C1	Aldo-Keto Reductase Family 1, Member C1	5.57	5.58E-04	5.84	4.10E-04
CFAP61	Cilia And Flagella Associated Protein 61	5.32	5.58E-04	5.58	4.10E-04
CXADR	Coxsackie Virus And Adenovirus Receptor	5.31	1.14E-02	3.93	3.73E-02
SLCO2B1	Solute Carrier Organic Anion Transporter Family Member 2B1	5.11	3.45E-03	5.92	2.56E-03
CDH7	Cadherin 7	5.10	5.58E-04	4.77	4.10E-04
RP11-775G23.1	ENSG00000265217	5.07	3.45E-03	4.21	2.56E-03
MSR1	Macrophage Scavenger Receptor 1	5.04	5.58E-04	5.14	4.10E-04
SPP1	Secreted Phosphoprotein 1	4.92	5.58E-04	6.11	4.10E-04
CEMIP	Cell Migration Inducing Hyaluronan Binding Protein	4.92	5.20E-03	6.15	4.10E-04
SVIP	Small VCP/P97-Interacting Protein	4.91	3.45E-03	5.07	1.41E-03
FIBIN	Fin Bud Initiation Factor Homolog (Zebrafish)	4.84	5.58E-04	1.47	1.17E-02
STK33	Serine/Threonine Kinase 33	4.80	7.59E-03	4.57	2.83E-03
EPHA6	EPH Receptor A6	4.78	3.71E-02	5.64	2.56E-02
ANGPTL4	Angiopoietin Like 4	4.70	1.79E-02	5.43	8.84E-03

NLRP4	NLR Family, Pyrin Domain Containing 4	4.68	3.34E-02	4.32	2.61E-02
THSD7A	Thrombospondin Type 1 Domain Containing 7A	4.68	5.20E-03	4.12	6.66E-03
PAGE2	PAGE Family Member 2	4.63	5.58E-04	4.64	4.10E-04
CCDC144NL-AS1	CCDC144NL Antisense RNA 1	4.63	9.01E-03	4.82	8.43E-03
PTER	Phosphotriesterase Related	4.61	5.58E-04	4.44	4.10E-04
MYO1D	Myosin ID	4.55	5.58E-04	4.62	4.10E-04
LRRC6	Leucine Rich Repeat Containing 6	4.54	2.59E-02	5.25	1.81E-02
AKR1C2	Aldo-Keto Reductase Family 1, Member C2	4.53	5.58E-04	4.68	4.10E-04
DHRS9	Dehydrogenase/Reductase (SDR Family) Member 9	4.50	5.58E-04	4.29	4.10E-04
RP11-13L2.4	ENSG00000261179	4.50	5.58E-04	4.76	4.10E-04
EDNRB	Endothelin Receptor Type B	4.50	8.47E-03	4.53	6.22E-03
LOC101928697	Uncharacterized LOC101928697	4.47	3.80E-02	3.98	3.11E-02
LIN28B	Lin-28 Homolog B	4.43	3.93E-02	4.23	3.18E-02
CLSTN2	Calsyntenin 2	4.33	5.58E-04	4.38	4.10E-04
PASD1	PAS Domain Containing 1	4.32	5.58E-04	3.09	4.10E-04
RARRES2	Retinoic Acid Receptor Responder 2	4.32	5.58E-04	3.76	4.10E-04
ABCB1	ATP Binding Cassette Subfamily B Member 1	4.30	2.68E-02	5.63	1.63E-02
PLBD1	Phospholipase B Domain Containing 1	4.30	5.58E-04	4.20	4.10E-04
EDARADD	EDAR-Associated Death Domain	4.26	4.03E-02	4.76	2.76E-02
GUSBP2	Glucuronidase, Beta Pseudogene 2	4.26	9.50E-03	4.66	3.37E-03
LOC344887	NmrA-Like Family Domain Containing 1 Pseudogene	4.25	1.91E-02	4.60	1.42E-02
MSL3P1	Male-Specific Lethal 3 Homolog (Drosophila) Pseudogene 1	4.22	5.58E-04	3.70	4.10E-04
ZNF91	Zinc Finger Protein 91	4.16	1.72E-02	3.50	2.65E-02
LINC01139	Long Intergenic Non-Protein Coding RNA 1139	4.10	4.76E-02	3.08	4.36E-02
TUBA3C	Tubulin Alpha 3c	4.04	5.58E-04	3.88	4.10E-04
OLFML1	Olfactomedin Like 1	4.03	5.58E-04	2.93	4.10E-04
ANKRD20A19P	Ankyrin Repeat Domain 20 Family Member A19, Pseudogene	4.03	4.05E-02	3.41	4.03E-02
TDRKH	Tudor And KH Domain Containing	4.02	3.36E-02	3.56	3.18E-02
GRID2	Glutamate Ionotropic Receptor Delta Type Subunit 2	4.01	5.58E-04	3.78	4.10E-04
TRDN	Triadin	4.01	5.58E-04	2.49	2.83E-03
ABCA1	ATP Binding Cassette Subfamily A Member 1	3.92	5.58E-04	4.17	4.10E-04
NEO1	Neogenin 1	3.92	5.58E-04	4.05	4.10E-04
NRCAM	Neuronal Cell Adhesion Molecule	3.91	5.58E-04	4.63	4.10E-04

ZNF43	Zinc Finger Protein 43	3.90	5.58E-04	3.41	1.41E-03
GABARAPL1	GABA Type A Receptor Associated Protein Like 1	3.89	1.47E-03	5.13	4.10E-04
LINC00200	Long Intergenic Non-Protein Coding RNA 200	3.86	4.54E-03	2.46	2.88E-02
SBSN	Suprabasin	3.84	5.58E-04	3.68	7.59E-04
WDR72	WD Repeat Domain 72	3.83	5.58E-04	3.85	4.10E-04
AKR1C3	Aldo-Keto Reductase Family 1, Member C3	3.81	5.58E-04	3.73	4.10E-04
F2RL2	Coagulation Factor II Thrombin Receptor Like 2	3.79	5.20E-03	3.83	4.37E-03
AC003092.1	ENSG00000236453	3.79	9.25E-03	4.98	6.66E-03
HCN1	Hyperpolarization Activated Cyclic Nucleotide Gated Potassium Channel 1	3.79	3.07E-03	4.31	2.29E-03
LINC01579	Long Intergenic Non-Protein Coding RNA 1579	3.79	4.49E-02	4.28	3.09E-02
PCDHB3	Protocadherin Beta 3	3.78	8.76E-03	3.86	6.66E-03
LINC00619	Long Intergenic Non-Protein Coding RNA 619	3.77	5.58E-04	1.67	2.51E-02
PCDHB2	Protocadherin Beta 2	3.76	8.76E-03	3.51	8.01E-03
TUBA4A	Tubulin Alpha 4a	3.72	5.58E-04	3.14	4.10E-04
CHI3L1	Chitinase 3 Like 1	3.68	5.58E-04	3.62	4.10E-04
VWA5A	Von Willebrand Factor A Domain Containing 5A	3.62	5.58E-04	3.87	4.10E-04
ERO1B	Endoplasmic Reticulum Oxidoreductase Beta	3.60	2.72E-02	3.24	3.27E-02
SHC3	SHC (Src Homology 2 Domain Containing) Transforming Protein 3	3.57	5.58E-04	3.72	1.09E-03
MUC13	Mucin 13, Cell Surface Associated	3.56	5.58E-04	4.92	4.10E-04
BHLHE41	Basic Helix-Loop-Helix Family Member E41	3.55	1.04E-03	3.61	7.59E-04
GAGE1	G Antigen 1	3.54	5.58E-04	3.40	4.10E-04
ZNF334	Zinc Finger Protein 334	3.53	5.53E-03	3.32	5.77E-03
SLC2A12	Solute Carrier Family 2 Member 12	3.50	5.58E-04	3.29	4.10E-04
GAGE4	G Antigen 4	3.47	1.68E-02	2.70	2.47E-02
AKR1B10	Aldo-Keto Reductase Family 1, Member B10 (Aldose Reductase)	3.45	5.58E-04	3.50	4.10E-04
PLXDC2	Plexin Domain Containing 2	3.45	5.58E-04	3.71	4.10E-04
LIPH	Lipase H	3.43	1.49E-02	2.74	3.44E-02
SEZ6L2	Seizure Related 6 Homolog Like 2	3.40	5.58E-04	3.05	4.10E-04
CDH10	Cadherin 10	3.39	5.58E-04	5.00	4.10E-04
KCNK13	Potassium Two Pore Domain Channel Subfamily K Member 13	3.37	8.76E-03	2.63	1.55E-02
CREB5	CAMP Responsive Element Binding Protein 5	3.34	5.58E-04	2.29	9.05E-03
LOC105374670	Uncharacterized LOC105374670	3.33	9.78E-03	3.24	9.68E-03

CADM2	Cell Adhesion Molecule 2	3.33	5.58E-04	3.47	4.10E-04
MXRA5	Matrix-Remodelling Associated 5	3.31	5.58E-04	4.05	4.10E-04
CALN1	Calneuron 1	3.26	5.58E-04	2.79	4.12E-03
BEX2	Brain Expressed X-Linked 2	3.21	1.08E-02	2.63	2.15E-02
GALNT13	Polypeptide N-Acetylgalactosaminyltransferase 13	3.21	7.04E-03	2.98	1.07E-02
KYNU	Kynureninase	3.20	5.58E-04	4.13	4.10E-04

Supplementary Table 5: The top 100 significantly downregulated genes in both HSP90i-resistant clones compared to Hs578T cells

Genes		CR2		CR3	
		log2 FC	q-value	log2 FC	q-value
EMILIN1	Elastin Microfibril Interfacer 1	-6.22	5.58E-04	-8.13	4.10E-04
NPAS3	Neuronal PAS Domain Protein 3	-5.84	3.71E-02	-3.44	8.43E-03
NXN	Nucleoredoxin	-5.71	5.58E-04	-6.09	4.10E-04
CSPG4	Chondroitin Sulfate Proteoglycan 4	-5.63	5.58E-04	-8.32	2.83E-02
NCAM1	Neural Cell Adhesion Molecule 1	-5.46	5.58E-04	-4.28	4.10E-04
SFRP2	Secreted Frizzled-Related Protein 2	-5.42	5.58E-04	-3.31	4.10E-04
HHIP	Hedgehog Interacting Protein	-5.42	5.58E-04	-3.50	4.10E-04
BAIAP2L2	BAI1 Associated Protein 2 Like 2	-5.00	1.46E-02	-4.10	1.87E-02
PKP2	Plakophilin 2	-4.84	3.66E-02	-2.81	4.10E-04
ANXA3	Annexin A3	-4.73	5.58E-04	-5.35	4.10E-04
NOS3	Nitric Oxide Synthase 3	-4.45	1.70E-02	-5.17	4.62E-03
ATP11A	ATPase Phospholipid Transporting 11A	-4.45	3.07E-03	-4.71	4.10E-04
ZNF702P	Zinc Finger Protein 702, Pseudogene	-4.34	9.25E-03	-5.40	2.50E-02
GALNT14	Polypeptide N-Acetylgalactosaminyltransferase 14	-4.30	5.58E-04	-4.33	4.10E-04
SLITRK5	SLIT And NTRK Like Family Member 5	-4.25	5.20E-03	-4.77	2.89E-02
PLPPR4	Phospholipid Phosphatase Related 4	-4.18	1.16E-02	-1.96	4.10E-04
SLITRK6	SLIT And NTRK Like Family Member 6	-4.09	5.58E-04	-1.96	4.10E-04
NFE4	Nuclear Factor, Erythroid 4	-4.07	1.16E-02	-4.37	7.33E-03
COL8A1	Collagen Type VIII Alpha 1	-4.05	5.58E-04	-3.18	4.10E-04
C1QTNF6	C1q And Tumor Necrosis Factor Related Protein 6	-3.92	5.58E-04	-3.98	4.03E-02
HHIPL1	HHIP Like 1	-3.86	5.58E-04	-3.50	5.57E-03
SFRP1	Secreted Frizzled-Related Protein 1	-3.86	5.58E-04	-0.84	2.00E-03
PADI2	Peptidyl Arginine Deiminase 2	-3.84	1.00E-02	-3.42	1.38E-02
MX2	MX Dynamin Like GTPase 2	-3.84	5.58E-04	-3.38	4.10E-04
PTPRC	Protein Tyrosine Phosphatase, Receptor Type C	-3.83	5.58E-04	-4.72	4.10E-04
POU3F2	POU Class 3 Homeobox 2	-3.79	5.58E-04	-3.15	4.10E-04
OXTR	Oxytocin Receptor	-3.73	1.37E-02	-4.12	1.09E-03
AFF3	AF4/FMR2 Family Member 3	-3.72	5.58E-04	-2.51	4.10E-04
OLFML3	Olfactomedin Like 3	-3.69	5.58E-04	-4.11	4.10E-04
GDA	Guanine Deaminase	-3.68	5.58E-04	-5.25	4.10E-04
TINAGL1	Tubulointerstitial Nephritis Antigen Like 1	-3.65	5.58E-04	-6.19	4.10E-04
TENM4	Teneurin Transmembrane Protein 4	-3.63	5.58E-04	-1.83	2.01E-02

KCNK2	Potassium Two Pore Domain Channel Subfamily K Member 2	-3.63	5.84E-03	-5.06	2.99E-02
UNC13D	Unc-13 Homolog D	-3.60	5.58E-04	-2.50	6.66E-03
CPT1C	Carnitine Palmitoyltransferase 1C	-3.59	5.58E-04	-6.64	4.10E-04
MEST	Mesoderm Specific Transcript	-3.57	5.58E-04	-6.73	4.10E-04
SH3RF3	SH3 Domain Containing Ring Finger 3	-3.55	5.58E-04	-3.86	4.10E-04
FARP1	FERM, ARH/RhoGEF And Pleckstrin Domain Protein 1	-3.55	5.58E-04	-3.85	4.10E-04
SNCA	Synuclein Alpha	-3.44	4.32E-02	-2.38	4.13E-02
TM7SF2	Transmembrane 7 Superfamily Member 2	-3.42	1.89E-03	-2.92	3.87E-03
PRTFDC1	Phosphoribosyl Transferase Domain Containing 1	-3.41	6.44E-03	-4.32	3.37E-03
SCAR	Scavenger Receptor Protein Family Member	-3.35	1.81E-02	-4.87	5.77E-03
KCNN4	Potassium Calcium-Activated Channel Subfamily N Member 4	-3.34	5.58E-04	-1.45	4.10E-04
FHAD1	Forkhead-Associated (FHA) Phosphopeptide Binding Domain 1	-3.34	5.58E-04	-2.81	4.10E-04
DMKN	Dermokine	-3.33	5.58E-04	-5.31	4.10E-04
CLDN11	Claudin 11	-3.33	1.04E-03	-3.61	7.59E-04
CYP1B1	Cytochrome P450 Family 1 Subfamily B Member 1	-3.31	5.58E-04	-3.68	4.10E-04
AMPH	Amphiphysin	-3.27	5.58E-04	-0.91	4.10E-04
LPAR1	Lysophosphatidic Acid Receptor 1	-3.24	5.58E-04	-2.53	4.10E-04
ARHGDIB	Rho GDP Dissociation Inhibitor Beta	-3.23	5.58E-04	-3.53	4.10E-04
PLXDC1	Plexin Domain Containing 1	-3.15	9.01E-03	-5.87	4.10E-04
HIC1	Hypermethylated In Cancer 1	-3.13	5.58E-04	-3.79	3.62E-03
TBX15	T-Box 15	-3.08	5.58E-04	-2.82	4.10E-04
FZD8	Frizzled Class Receptor 8	-3.07	1.16E-02	-3.31	8.43E-03
FAM149A	Family With Sequence Similarity 149 Member A	-3.01	1.04E-03	-3.54	7.59E-04
SEPT3	Septin 3	-3.00	5.58E-04	-4.26	7.59E-04
LOC101927417	Uncharacterized LOC101927417	-3.00	1.04E-03	-2.94	5.77E-03
COLEC12	Collectin Subfamily Member 12	-2.95	5.58E-04	-3.78	4.10E-04
CCDC88C	Coiled-Coil Domain Containing 88C	-2.94	1.06E-02	-3.92	2.83E-03
BANK1	B-Cell Scaffold Protein With Ankyrin Repeats 1	-2.92	3.63E-02	-2.91	1.17E-02
CALHM2	Calcium Homeostasis Modulator 2	-2.89	5.58E-04	-3.49	4.10E-04
CDC42EP1	CDC42 Effector Protein 1	-2.88	5.58E-04	-4.25	4.10E-04
RNF150	Ring Finger Protein 150	-2.85	3.51E-02	-4.06	5.36E-03
FAM101B	Family With Sequence Similarity 101 Member B	-2.85	5.58E-04	-3.47	4.10E-04
PLAC8	Placenta Specific 8	-2.82	5.58E-04	-3.39	4.10E-04
COL9A2	Collagen Type IX Alpha 2	-2.82	1.91E-02	-3.44	5.36E-03

BGN	Biglycan	-2.80	5.58E-04	-6.63	4.10E-04
ANK1	Ankyrin 1	-2.80	5.58E-04	-3.02	4.10E-04
TCF7L1	Transcription Factor 7 Like 1	-2.78	5.58E-04	-1.26	2.00E-03
SEMA5A	Semaphorin 5A	-2.77	5.58E-04	-2.21	4.10E-04
GRIK2	Glutamate Ionotropic Receptor Kainate Type Subunit 2	-2.76	5.58E-04	-0.93	4.10E-04
ADGRG6	Adhesion G Protein-Coupled Receptor G6	-2.72	5.58E-04	-2.59	4.10E-04
LYPD1	LY6/PLAUR Domain Containing 1	-2.71	5.58E-04	-3.35	4.10E-04
NCALD	Neurocalcin Delta	-2.71	5.58E-04	-3.77	4.10E-04
ENOX1	Ecto-NOX Disulfide-Thiol Exchanger 1	-2.70	3.63E-02	-3.23	4.23E-02
KLHL13	Kelch Like Family Member 13	-2.70	5.58E-04	-3.45	4.10E-04
CIB2	Calcium And Integrin Binding Family Member 2	-2.67	2.86E-02	-2.71	1.72E-02
SERPINB7	Serpin Family B Member 7	-2.67	5.58E-04	-1.90	4.10E-04
THBS3	Thrombospondin 3	-2.67	5.58E-04	-2.27	2.29E-03
TLX2	T-Cell Leukemia Homeobox 2	-2.65	8.47E-03	-2.00	3.11E-03
TOR4A	Torsin Family 4 Member A	-2.63	5.58E-04	-2.75	4.10E-04
FADS2	Fatty Acid Desaturase 2	-2.63	1.47E-03	-3.25	4.10E-04
HYAL1	Hyaluronoglucosaminidase 1	-2.61	3.50E-02	-3.47	2.56E-02
MN1	Meningioma (Disrupted In Balanced Translocation) 1	-2.60	5.58E-04	-3.96	4.10E-04
DNAH2	Dynein Axonemal Heavy Chain 2	-2.59	5.58E-04	-3.03	4.10E-04
ABCA3	ATP Binding Cassette Subfamily A Member 3	-2.58	5.58E-04	-2.82	4.10E-04
FBLN1	Fibulin 1	-2.58	5.58E-04	-3.39	4.10E-04
PRSS21	Protease, Serine 21	-2.58	5.58E-04	-2.26	4.10E-04
TFAP2C	Transcription Factor AP-2 Gamma	-2.57	5.58E-04	-2.22	4.10E-04
LHFP	Lipoma HMGIC Fusion Partner	-2.56	5.58E-04	-0.84	4.10E-04
SCD5	Stearoyl-CoA Desaturase 5	-2.55	5.58E-04	-2.06	4.10E-04
LZTS1	Leucine Zipper, Putative Tumor Suppressor 1	-2.50	5.58E-04	-3.22	4.10E-04
ABI3	ABI Family Member 3	-2.48	2.82E-02	-3.00	2.34E-02
LOC643201	Centrosomal Protein 192kDa Pseudogene	-2.43	5.58E-04	-3.29	4.10E-04
TMEFF2	Transmembrane Protein With EGF Like And Two Follistatin Like Domains 2	-2.42	5.58E-04	-1.09	4.10E-04
CFH	Complement Factor H	-2.41	5.58E-04	-0.66	1.09E-03
GNGT2	G Protein Subunit Gamma Transducin 2	-2.41	2.08E-02	-1.76	2.20E-02
IL20RB	Interleukin 20 Receptor Subunit Beta	-2.41	8.47E-03	-2.24	6.00E-03
SLIT2	Slit Guidance Ligand 2	-2.40	5.58E-04	-1.71	4.10E-04
CHAC1	ChaC Glutathione-Specific Gamma-Glutamylcyclotransferase 1	-2.39	5.58E-04	-0.87	2.29E-03

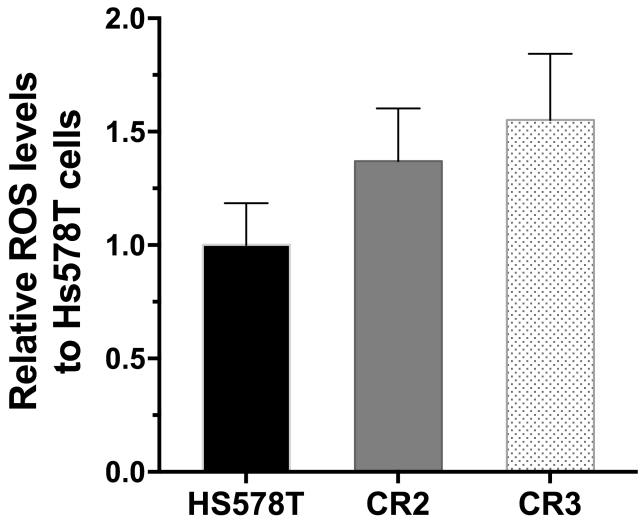
Supplementary Table 6: Differential gene expression of AKR1C family members in Hs578T (30 nM ganetespib), CR2 and CR3 cells compared to DMSO-treated Hs578T cells

Genes		Hs578T 30 nM		CR2		CR3	
		log2 FC	q-value	log2 FC	q-value	log2 FC	q-value
AKR1C1	Aldo-keto reductase family 1 member C1	2.53	8.01E-04	5.57	5.58E-04	5.84	4.10E-04
AKR1C2	Aldo-keto reductase family 1 member C2	1.52	8.01E-04	4.53	5.58E-04	4.68	4.10E-04
AKR1C3	Aldo-keto reductase family 1 member C3	1.97	8.01E-04	3.81	5.58E-04	3.73	4.10E-04
AKR1C4	Aldo-keto reductase family 1 member C4	NA	NA	NA	NA	NA	NA

Supplementary Table 7: Differential expression of ARE genes in Hs578T (30 nM ganetespib), CR2 and CR3 cells compared to DMSO-treated Hs578T cells

Genes		Hs578T 30 nM		CR2		CR3	
		log2 FC	q-value	log2 FC	q-value	log2 FC	q-value
Detoxification:							
ABCC2	ATP Binding Cassette Subfamily C Member 2	0.58	1.46E-03	0.77	8.47E-03	1.24	4.10E-04
ABCC3	ATP Binding Cassette Subfamily C Member 3	-1.71	8.01E-04	2.05	5.58E-04	1.87	4.10E-04
AKR1B1	Aldo-Keto Reductase Family 1, Member B1 (Aldose Reductase)	0.79	8.01E-04	2.04	5.58E-04	2.26	4.10E-04
AKR1C1	Aldo-Keto Reductase Family 1, Member C1	2.53	8.01E-04	5.57	5.58E-04	5.84	4.10E-04
CBR1	Carbonyl Reductase 1	-0.54	8.73E-03	0.39	0.052 (ns)	0.43	1.68E-02
EPHX1	Epoxide Hydrolase 1	0.41	0.063 (ns)	1.40	5.58E-04	1.33	4.10E-04
MGST1	Microsomal Glutathione S-Transferase 1	-0.05	0.874 (ns)	0.27	0.201 (ns)	0.97	4.10E-04
NQO1	NAD(P)H Quinone Dehydrogenase 1	-0.14	0.653 (ns)	0.50	2.13E-02	1.00	4.10E-04
PTGR1	Prostaglandin Reductase 1	0.98	8.01E-04	-0.35	0.097 (ns)	-0.72	4.10E-04
Antioxidant(GSH):							
GCLC	Glutamate-Cysteine Ligase Catalytic Subunit	-0.05	0.914 (ns)	0.61	0.121 (ns)	0.78	3.17E-02
GSR	Glutathione Reductase	0.35	0.079 (ns)	0.57	1.89E-03	0.91	4.10E-04
SLC7A11	Solute Carrier Family 7 Member 11	0.52	2.29E-02	0.58	1.24E-02	1.56	4.10E-04
Antioxidant(TXN):							
PRDX1	Peroxiredoxin 1	0.45	1.58E-02	0.03	0.919 (ns)	0.16	0.448 (ns)
SRXN1	Sulfiredoxin 1	-0.10	0.721 (ns)	0.88	5.58E-04	1.01	4.10E-04
TXNRD1	Thioredoxin Reductase 1	0.81	1.51E-02	0.39	0.262 (ns)	0.76	1.81E-02
NADPH regeneration:							
G6PD	Glucose-6-Phosphate Dehydrogenase	-0.27	0.339 (ns)	0.78	5.58E-04	0.76	4.10E-04
ME1	Malic Enzyme 1	0.59	2.05E-03	0.63	5.58E-04	0.59	7.59E-04
TALDO1	Transaldolase 1	-0.08	0.785 (ns)	0.34	0.072 (ns)	0.49	5.36E-03

Iron metabolism:							
BLVRB	Biliverdin Reductase B	0.04	0.926 (ns)	0.97	5.58E-04	1.30	4.10E-04
FTH1	Ferritin, Heavy Polypeptide 1	0.23	0.415 (ns)	0.26	0.330 (ns)	0.47	3.76E-02
FTL	Ferritin, Light Polypeptide	0.85	8.01E-04	0.20	0.389 (ns)	0.15	0.513 (ns)
HMOX1	Heme Oxygenase 1	0.09	0.749 (ns)	0.17	0.447 (ns)	0.38	2.98E-02
Transcription factors:							
MAFG	V-Maf Avian Musculoaponeurotic Fibrosarcoma Oncogene Homolog G	0.14	0.696 (ns)	0.86	5.58E-04	1.04	4.10E-04
PPARG	Peroxisome Proliferator Activated Receptor Gamma	-1.35	8.01E-04	1.54	5.58E-04	1.25	4.10E-04
RXRA	Retinoid X Receptor Alpha	0.62	5.00E-03	-0.15	0.609 (ns)	-0.38	0.087 (ns)

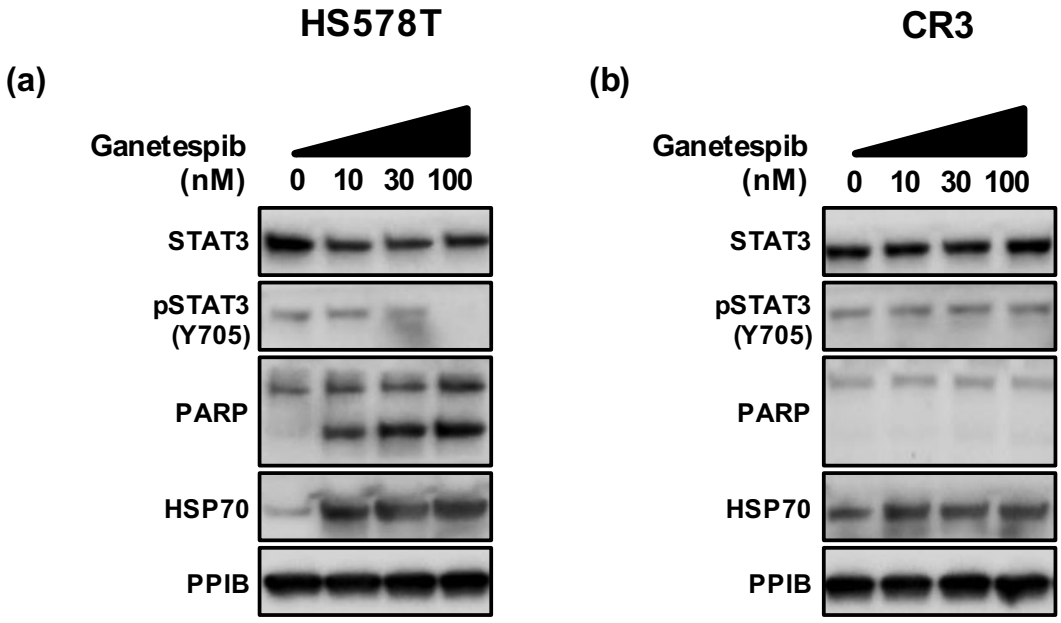


Supplementary Figure 2: ROS levels in Hs578T cells and HSP90i-resistant clones CR2 and CR3

In order to measure ROS levels, parental Hs578T cells and HSP90i-resistant clones CR2 and CR3 were subjected to a ROS-Glo^{TM} H_2O_2 assay. The cells were seeded in 96-well plate (10^4 cells). After overnight incubation, the media was removed from all wells and fresh media containing a ROS substrate was added. The cells were incubated for 2 hr to allow the substrate to react with any ROS present in the cells, and converted it to a luciferin substrate. After treatment, ROS-Glo^{TM} detection solution was added to the wells and incubated for another 20 min at room temperature. The luciferin substrate reacted with the detection solution to produce a luminescent signal. The luminescence intensity (excitation at 485 nm) was measured using a plate reader. After subtracting the average luminesce intensity of blank (medium, no cells) from the wells, the luminescence intensity for each well was proportional to the ROS levels in the media. The graph represents the mean ROS levels in each cell line relative to parental Hs578T cells from two independent experiments each performed in duplicates. Error bars indicate SEM. Student's t-test was performed to compare between cell lines but the analysis did not reach statistical significance.

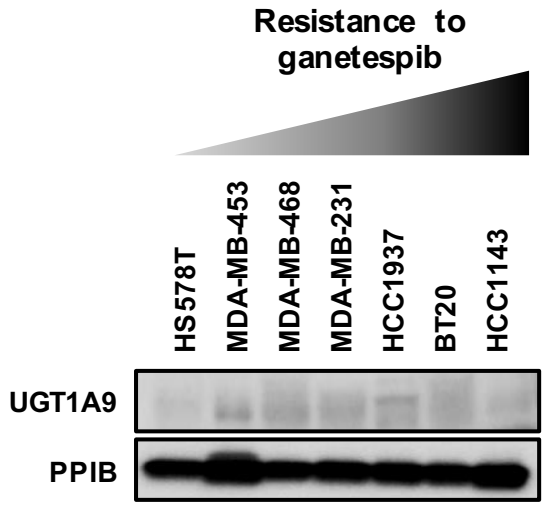
Supplementary Table 8: Differential gene expression of genes associated to JAK-STAT signaling pathway in HSP90i-resistant clone CR3 compared to DMSO-treated Hs578T cells

Genes		RNA-seq		JAK-STAT array	
		log2 FC	q-value	log2 FC	SEM
IL8	Interleukin 8	3.57	4.10E-04	-2.16	1.12
IL6	Interleukin 6	3.53	4.10E-04	1.02	0.07
IL1B	Interleukin 1 Beta	3.11	4.10E-04	1.48	0.53
MYC	V-Myc Avian Myelocytomatosis Viral Oncogene Homolog	1.88	4.10E-04	0.54	0.52
VEGFA	Vascular Endothelial Growth Factor A	1.57	4.10E-04	1.45	0.58
EGF	Epidermal Growth Factor	1.54	2.56E-03	1.02	1.04
IFNGR1	Interferon Gamma Receptor 1	0.54	6.43E-03	0.34	0.64
JAK1	Janus Kinase 1	0.52	8.01E-03	-0.18	0.15
JUN	Jun Proto-Oncogene	0.50	2.56E-03	-0.68	0.40
NRAS	Neuroblastoma RAS Viral Oncogene Homolog	0.35	4.19E-02	-0.05	1.13
EP300	E1A Binding Protein P300	-0.42	1.77E-02	-0.16	0.12
PSMD4	Proteasome 26S Subunit, Non-ATPase 4	-0.47	4.37E-03	0.05	1.02
MCM5	Minichromosome Maintenance Complex Component 5	-0.53	8.43E-03	-0.15	0.14
AKT1	V-Akt Murine Thymoma Viral Oncogene Homolog 1	-0.68	4.10E-04	-0.16	0.15
PSMC4	Proteasome 26S Subunit, ATPase 4	-0.69	4.10E-04	0.16	1.00
PSMB5	Proteasome Subunit Beta 5	-0.69	4.10E-04	-1.19	0.20
AKT2	V-Akt Murine Thymoma Viral Oncogene Homolog 2	-0.70	3.37E-03	-0.17	0.15
UBB	Ubiquitin B	-0.75	4.10E-04	-1.00	0.05
SOS1	SOS Ras/Rac Guanine Nucleotide Exchange Factor 1	-0.85	4.10E-04	0.03	0.04
SOCS1	Suppressor Of Cytokine Signaling 1	-2.44	4.10E-02	-2.16	1.12



Supplementary Figure 3: The effect of ganetespib treatment on JAK2-STAT3 signalling pathway in TNBC cells

(a) Parental Hs578T cells and (b) HSP90i-resistant clone CR3 were treated with ganetespib (0 - 100 nM) for 24 hr. Protein lysates were analysed by western blotting. Expression of STAT3 and pSTAT3 (Y705) were examined in order to assess the effects of HSP90i on the activation of JAK2-STAT3 signalling pathway. Cleaved PARP was used to assess the induction of apoptosis and HSP70 was used as a pharmacodynamic marker for inhibition of HSP90 activity. PPIB was used as loading control.



Supplementary Figure 4: Expression of UGT1A9 in TNBC cells

Lysates of TNBC cell lines (Hs578T, MDA-MB-453, MDA-MB-468, MDA-MB-231, HCC1937, BT20 and HCC1143) were analysed by western blotting. PPIB was used as loading control.